THE EXAMINATION OF CHIRAL X-TYPE LIGANDS IN Pd(II)-CATALYZED ENANTIOSELECTIVE OXDIATATIVE TRANSFORMATIONS

by

Andrew Henry Aebly

A dissertation submitted in partial fulfillment
of the requirements for the degree

of

Doctor of Philosophy

in

Chemistry

MONTANA STATE UNIVERSITY
Bozeman, Montana

July 2015

DEDICATION

To my wife Angela—my best friend and my constant support

ACKNOWLEDGEMENTS

I am so grateful to the many mentors, friends and colleagues who have challenged and encouraged me throughout this process. A special thank you to my advisor, Dr. Trevor Rainey for your unique insight and problem solving ability. I would like to express my gratitude to Dr. Mary Cloninger and Dr. T. Nicholas Jones who believed in my abilities and sparked my independent research career. Also thank you to the members of my committee, Dr. Tom Livinghouse for your wisdom and jest, Dr. Valerie Copie for your generosity of spirit and Doralyn Rossmann for being my advocate. I appreciate the time and expertise you have given me.

TABLE OF CONTENTS

TABLE OF CONTENTS - CONTINUED

LIST OF TABLES

Table Page

LIST OF FIGURES

Figure Page

LIST OF SCHEMES

Scheme Page

LIST OF SCHEMES - CONTINUED

Scheme Page

LIST OF SCHEMES - CONTINUED

Scheme Page

ABSTRACT

Palladium catalysis has been utilized extensively in organic chemistry for the synthesis of complex molecules. Despite its abundant use and many successful applications, there remain challenging transformations, specifically with developing new chiral centers. The aim of this research was to explore the underdeveloped, weakly coordinating X-type ligands and their applicability in enantioselective reactions. The electrophilic catalyst, generated by the coordination of sulfonic or phosphoric acid ligands, was utilized to explore underfunctionalized starting materials, such as unactivated alkenes and aryl C-H bonds.

Herein we report two Pd^{II}-catalyzed enantioselective transformations: oxidative amination and 1,2-carboamination. The Wacker-type oxidative amination was accomplished with good yields and modest enantioselectivity in the synthesis of chiral indolines and a cyclic carbamate. Substantial loss in enantioselectivity was seen with *ortho*-substituted anilines. The 1,2-carboamination coupled a mild, directing group facilitated C-H activation on a series of aryl ureas with a subsequent chiral C-N bond formation. Electron-rich, *para*-substituted aryl ureas provided the highest consistent yields and enantioselectivities. Electron deficient substrates provided little reactivity and substitutions at the *ortho*- and *meta*-positions gave inconsistent results. To our knowledge these transformations mark the first enantioselective examples of Pd^{II}-catalyzed oxidative transformations utilizing chiral sulfonic acid ligands.

CHAPTER 1: INTRODUCTION TO PALLADIUM(II) CATALYSIS AND TYPES OF LIGANDS

In the last 50 years, palladium catalysis has emerged as a versatile means of bond formation, continually challenging the paradigms of organic synthesis. This organometallic reagent has been utilized to develop new C-C and C-heteroatom bonds and has been utilized extensively in natural product total synthesis.[1] The applicability of palladium as a catalyst is due to the facile, two-electron interconversion of two stable oxidation states, Pd^0 (d^{10}) and Pd^{II} (d^8).[2] Despite the stability of both oxidation states, Pd^0 has received considerably more attention in the literature, culminating in the awarding of the 2010 Nobel Prize for the Pd^0 cross-coupling work of Heck, Negishi, and Suzuki.[3] Another popular Pd^0-catalyzed reaction in organic synthesis is the Tsuji-Trost reaction which utilizes the Pd^0 catalyst to facilitate nucleophilic attack on an allylic substrate with a good leaving group, X (i.e. acetate, halogens, carbonate, etc.) (Figure 1.1). After coordinating to the alkene, oxidative addition occurs with the departure of X to form a Pd^{II}-π-allyl intermediate. This complex is then attacked by a suitable nucleophile to generate a new C-C, C-O, C-S or C-N bond. Considerable progress in the asymmetric version of this allyation has led to its application in many natural product total syntheses.[4]

One potential reason for the underdevelopment of Pd^{II} catalysis is the necessity for a reoxidant to convert the in situ generated Pd^0 (created by reductive elimination) to Pd^{II} in order to turnover the catalytic cycle. Numerous reoxidants, from the ubiquitous O_2 to organic compounds such as benzoquinone (BQ) to heavy metal salts (Cu^{II}) to harsh

peracids, such as *tert*-butyl hydroperoxide (TBHP), have been utilized to regenerate Pd^{II} within the reaction.[5]

Figure 1.1: Tsuji-Trost Catalytic Cycle

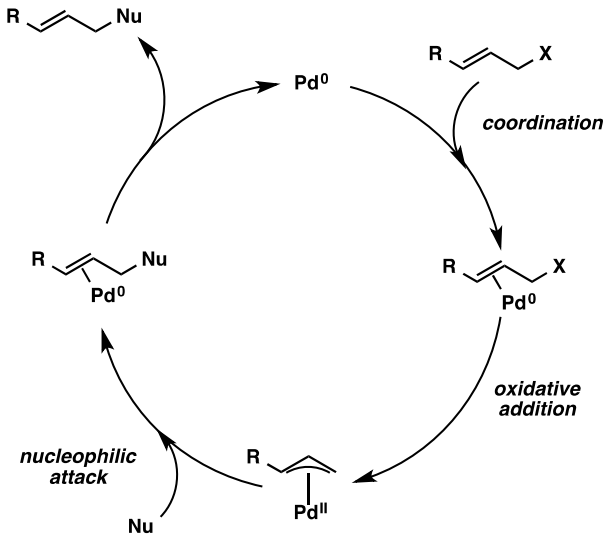

The conditions needed for reoxidation can limit the substrate scope, precluding compounds sensitive to oxidation. Furthermore, if the reoxidation to Pd^{II} does not occur efficiently the aggregation of inactive palladium black can occur, irreversibly removing the catalyst from the reaction.

Despite this limitation, many Pd^{II} catalyzed reactions have been developed for the formation of C-C, C-O and C-N bonds.[6] As an electrophilic catalyst, Pd^{II} is prone to two distinct reaction pathways early in the catalytic cycle: 1) formation of a π–alkene complex (Wacker-type reaction) or 2) formation of σ-aryl complex (Oxidative Heck/C-H Activation reactions) (Figure 1.2). Beginning with the Wacker-type reaction, the formation of the Pd^{II}- π-alkene complex delocalizes the electron density of the alkene into

an empty *d*-orbital of the metal, making the alkene susceptible to nucleophilic attack. The nucleophile can approach either inter- or intramolecularly, and in a Markovnikov or anti-Markovnikov fashion, depending on the ligand and reaction conditions. Subsequent β–hydride elimination of the transient σ-Pd^{II}-C bond leads to a Pd^{II}-hydride species, which quickly proceeds through reductive elimination to give Pd^{0}. Reoxidation of the catalyst to Pd^{II} then allows the catalytic cycle to repeat.

Figure 1.2: Pd^{II} Oxidative Catalytic Cycles

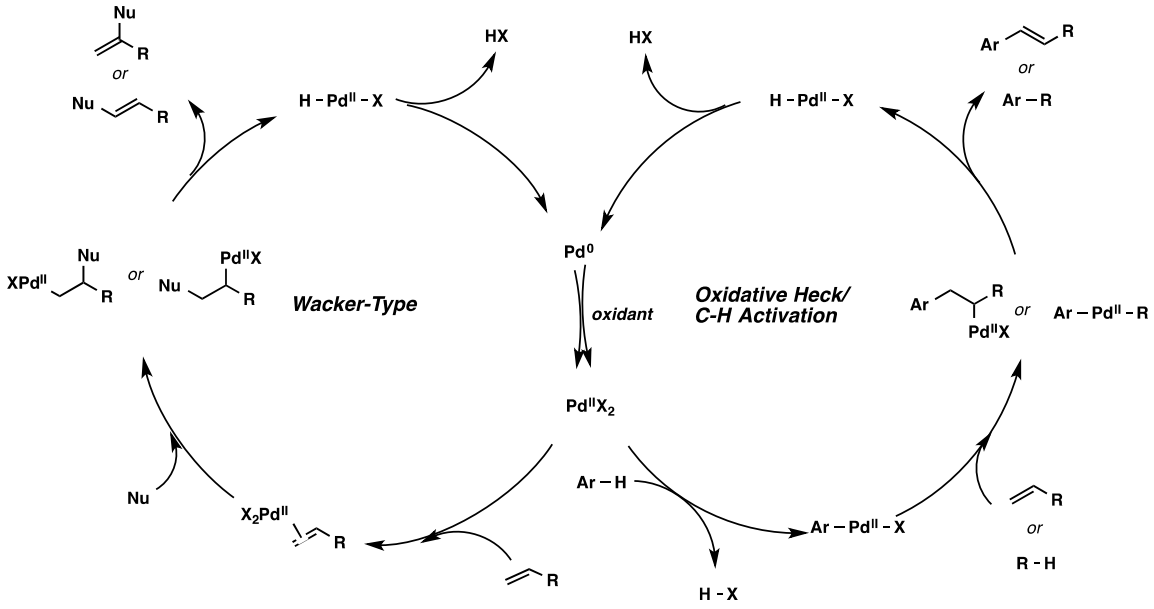

The catalytic cycle of the Oxidative Heck/C-H activation pathway begins with C-H insertion into an aryl C-H bond through electrophilic substitution. This σ-Pd^{II}-aryl intermediate can then either a) complex with an alkene and upon migratory insertion and β–hydride elimination give alkene products (Oxidative Heck) or b) can go through another C-H insertion, which upon reductive elimination gives a dehydrogenative cross-

coupling product. Again at the end of these catalytic cycles a reoxidant is needed to efficiently convert Pd^0 back to Pd^{II}.

A distinct advantage of Pd^{II} catalysis over its Pd^0 counterpart is the utilization of less functionalized substrates for analogous bond formations. For example, the Pd^0-catalyzed Tsuji-Trost reaction requires an activated alkene (a suitable leaving group X in the allylic position to the alkene) in order to generate the Pd-π-allyl intermediate needed for reaction. In contrast, the Wacker-type reaction can occur with simple alkenes. Similarly, the Pd^0 catalyzed Heck reaction, as well as other cross-coupling reactions, require an aryl halide (or pseudo-halide) to form the aryl-palladium intermediate, while the oxidative version can utilize simple hydrocarbons to generate same intermediate through C-H insertion.

Types of Ligands

Ligands play a key role in the reactivity and stability of a catalyst. Therefore, in the development of any transition metal catalyzed reaction, especially an asymmetric transformation, selection of a ligand is of paramount importance. Two types of ligand classes exist: L-type (formally neutral) and X-type (formally anionic).[7] L-type ligands act as dative, two-electron donors to a vacant *d*-orbital on the metal center, analogous to a Lewis base in classical organic chemistry. Examples of common L-type ligands include phosphines, trialkylamines and *N*-heterocyclic carbenes. Conversely, X-type ligands act as single-electron donors to the metal center which also contributes an electron to form a

bond, analogous to a covalent bond in classical organic chemistry. Examples of X-type ligands include alkoxides, halides and alkyl groups.

The bulk of palladium catalysis, including enantioselective reactions, has utilized chiral L-type ligands almost exclusively.[8] The appeal of these strongly coordinating ligands is they are tightly bound to the metal center, stabilizing the catalyst. In asymmetric catalysis, this tight ligand coordination is advantageous for imparting the chirality of the ligand in the transition state of the developing chiral center. However, the possible side effect of these strongly coordinating ligands is the buildup of electron density on the metal center, potentially making the catalyst less reactive. In contrast, we seek to explore the utility of X-type ligands, which through weak coordination to the metal provides a catalyst that is more electrophilic. Our aim is to apply chiral X-type ligands to asymmetric, oxidative Pd^{II}-catalyzed transformations that have historically suffered from a lack of reactivity and/or stereoinduction.

Examination of Chiral X-Type Ligands in Catalysis

Many new potential X-type ligands have emerged from the organocatalysis literature, notably chiral phosphoric acids derived from the BINOL scaffold. Pioneering research by a number of groups has combined these chiral compounds in the same reaction with numerous transition metals, including palladium.[9] However, the role of these chiral phosphoric acids is not always as a formal ligand to the metal center.[10,11] Some of these alternative approaches include a) one pot catalysis, in which two separate catalytic cycles (organocatalysis and transition metal catalysis) occur in the same

reaction,[12] and b) ion-paired chiral catalysis, in which the chiral counterion forms a tight-ion pair with a separate ligand bound to the transition metal.[13]

In terms of palladium-catalyzed reactions that utilize an X-type chiral phosphoric acid ligand, most of the enantioselective examples proceed through a π–allyl intermediate.[14] Work by Gong[15] and Beller[16] incorporated two different chiral compounds – the chiral phosphoric acid and a strongly coordinating chiral phosphoramidite to promote stereoinduction for the alkylation and amination of allylic alcohols (Figure 1.3).

Figure 1.3: Pd^{II}-π-allyl Intermediate Utilizing Chiral Phosphoric Acids

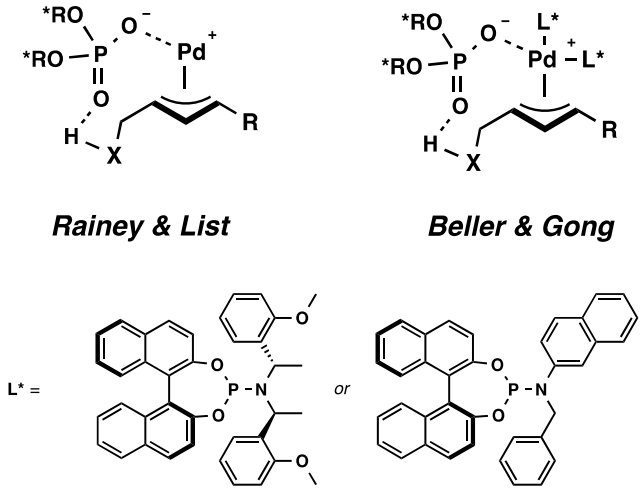

Enantioselective reactions by List[17] and our group[18] utilized the chiral phosphoric acid as the sole source of chirality for the transformation (Figure 1.3). Notably, the semipinacol rearrangement developed in our lab was a Pd^{II}-catalyzed oxidative transformation (Scheme 1.1). The success of this reaction served as the inspiration to explore other enantioselective versions of Pd^{II}-catalyzed oxidative reactions with chiral X-type ligands.

Scheme 1.1: Pd^{II}-Catalyzed Semipinacol Rearrangement

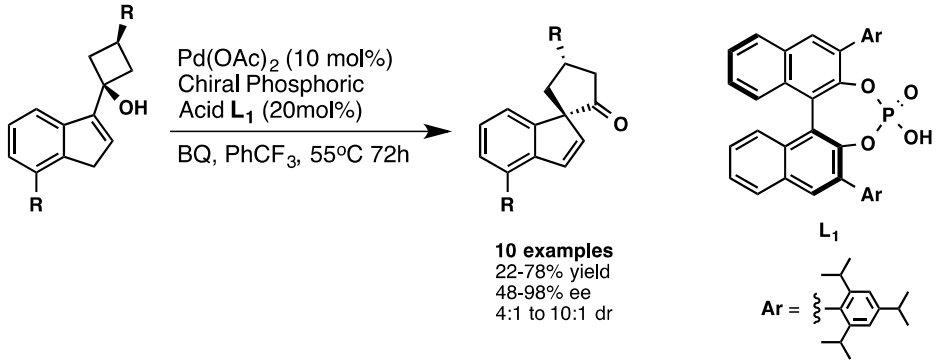

Conclusion

Recent breakthroughs in the application of chiral X-type ligands in palladium-catalyzed enantioselective transformations have shown the potential for this unique ligand class. In contrast to the much more prevalent, strongly coordinating chiral L-type ligands, the weak bond between the metal center and the X-type ligand has the potential to create a more electrophilic catalyst suitable for asymmetric Pd^{II}-catalyzed oxidative reactions.

CHAPTER 2: ENANTIOSELECTIVE OXIDATIVE AMINATION WITH CHIRAL X-TYPE LIGANDS

The Wacker Reaction

The Wacker process was initially discovered by a group of chemists at Wacker-Chemie in Germany in 1959 as a means of converting ethylene to acetaldehyde with catalytic amounts of $PdCl_2$.[19,20] The catalytic cycle was turned-over with molecular oxygen and copper chloride, oxidizing Pd^0 back to the active Pd^{II} catalyst (Scheme 2.1).

Scheme 2.1: General Catalytic Cycle for the Wacker Process

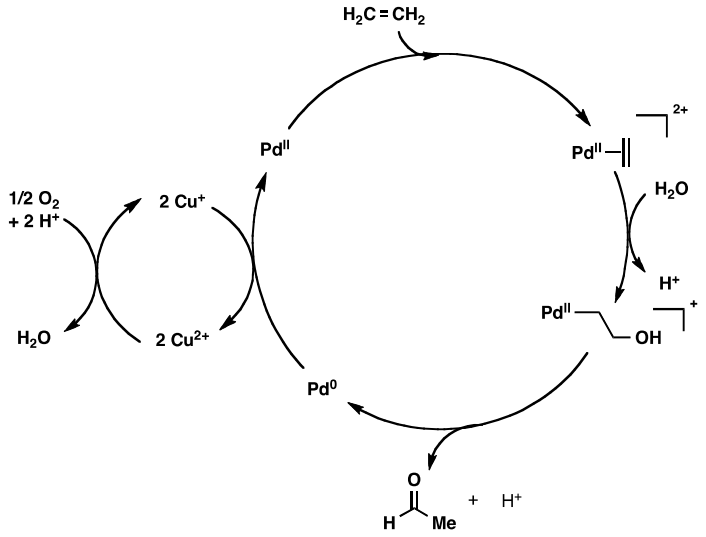

Upon formation of the new bond, the transient Pd^{II}-C bond is prone to multiple transformations: a) protodepalladation (hydroamination); b) subsequent attack by an additional nucleophile; or c) β–hydride elimination (Wacker-type oxidation) (Scheme 2.2.). All of these transformations have the potential to create a stereogenic center that can be enriched through an enantioselective transformation. Unique to the Wacker-type

oxidation is the retention of the alkene for further reactivity. Existing enantioselective transition metal-catalyzed reactions can yield similar products (most notably the Tsjui-Trost reaction), however these transformations utilize more reactive alkenes (i.e. allylic to a labile leaving group) starting materials. The Wacker-type oxidative reaction employs unactivated alkenes but in turn presents the unique challenge of reoxidizing the catalyst.

Scheme 2.2: Nucleopalladation Step of Wacker-Type Reaction

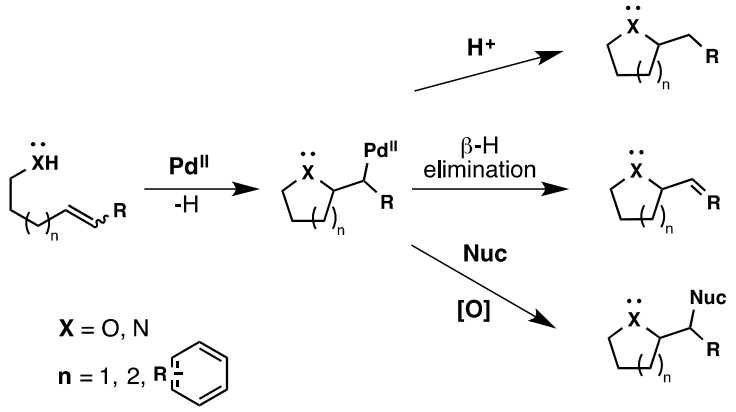

Initial success for the enantioselective version of the Wacker-type oxidation was accomplished with oxygen nucleophiles.[21] Despite this breakthrough, few enantioselective reactions utilizing nitrogen based nucleophiles (Wacker-type oxidative amination or Aza-Wacker oxidation) existed until recently. Recognizing the gap in the literature, we sought to utilize chiral X-type ligands to accomplish this transformation beginning with the intramolecular version of the reaction.

Integral to the reactivity of the Wacker-type reaction is the formation of the Pd-π-alkene complex. This type of coordination is described through the Dewar-Chatt-Duncanson model (Figure 2.1).[22] The alkene π-electrons act as σ-donor to a vacant *d*-

orbital on the metal, delocalizing the electron density from the alkene. Depending on the metal, its oxidation state, and the ligands used, a second mode of bonding, called back bonding can occur in which a filled *d*-orbital on the metal mixes with a vacant π* on the alkene.

Figure 2.1: Dewar-Chatt-Duncanson Model from Metal-π-Alkene Complex[22]

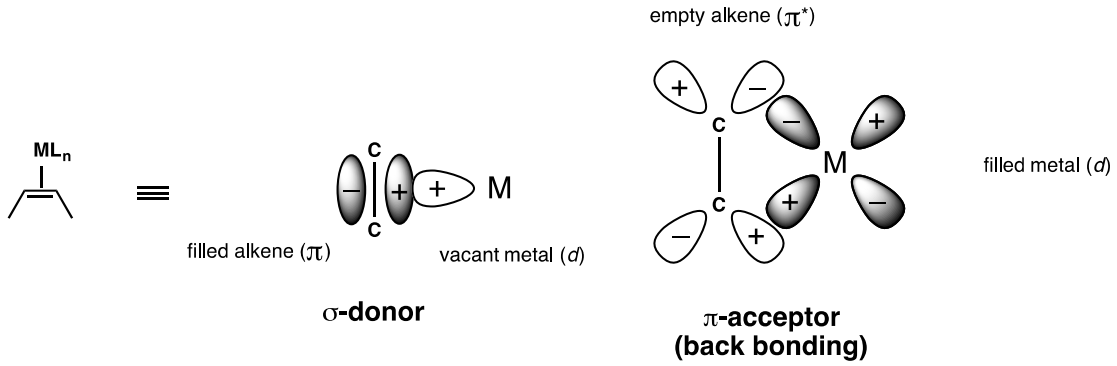

Due to the higher oxidation state of Pd^{II} little back bonding occurs, rendering the alkene electrophilic and susceptible to nucleophilic attack.[23] In an effort to maintain the electrophilicity of the complex, we sought to introduce chirality through weakly coordinating X-type ligands as opposed to strongly Lewis basic chiral L-type ligands for the asymmetric transformation.

Racemic Intramolecular Oxidative Amination

The first example of an intramolecular oxidative amination was published by Hegedus in 1978 using stoichiometric bis(acetonitrile)palladium(II) chloride for the conversion of o-allylanilines to indoles.[24] Shortly thereafter a catalytic version of the

reaction was applied to the cyclization of tosyl-protected amino olefins utilizing benzoquinone as a stoichiometric reoxidant (Scheme 2.3).[25]

Scheme 2.3: Oxidative Cyclization of Tosylamides

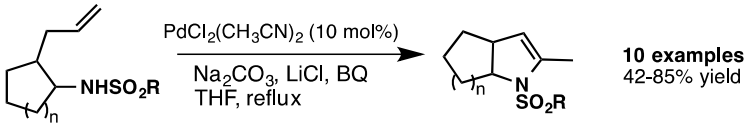

The groups of Larock[26] and Andersson[27] furthered this research by using molecular oxygen as the reoxidant in dimethyl sulfoxide (DMSO), eliminating benzoquinone and its oxidative byproduct from the reaction. Both used tosylamides, further expanding the substrate scope to acyclic and benzyl olefinic tosylamides (Scheme 2.4). Using the same O_2/DMSO system, Hiemstra[28] converted aminals to mono- and bicyclic imidazolidines in good to excellent yields (Scheme 2.5).

Scheme 2.4: $Pd(OAc)_2$/DMSO Catalyzed Oxidative Cyclization of Tosylamides

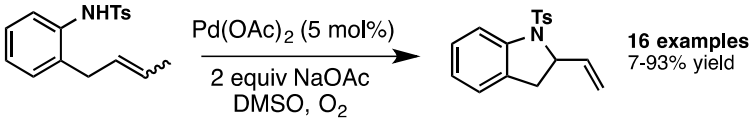

Scheme 2.5: $Pd(OAc)_2$/DMSO Catalyzed Oxidative Cyclization of Aminals

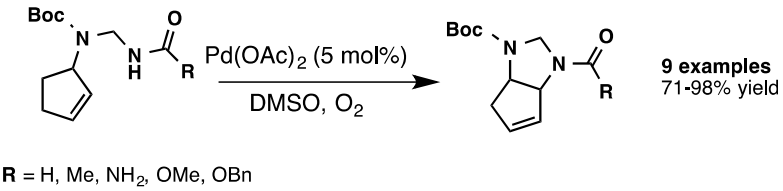

Recognizing that the turnover limiting step of the catalytic cycle was the oxidation of Pd(0) to Pd(II) by molecular oxygen, Stahl applied a palladium(II) acetate/pyridine system[29] to more efficiently re-oxidize the palladium(0) to the active catalyst.[30] The pyridine ligands help to stabilize the Pd(0) intermediate, reducing the formation of inactive palladium black by allowing O_2 to more efficiently re-oxidize the catalyst. This catalyst system increased the turnover rate by 10-100 times relative to that of the $Pd(OAc)_2$/DMSO conditions.[31] Furthermore, this catalyst system proved applicable in a wide range of solvents with varying degrees of polarity, achieving the greatest success in a non-polar medium as the catalyst loading could be reduced to 0.2% $Pd(OAc)_2$ and 0.4% pyridine in *p*-xylenes (Scheme 2.6).

Scheme 2.6: $Pd(OAc)_2$/pyridine Catalyzed Oxidative Cyclization of Tosylamides

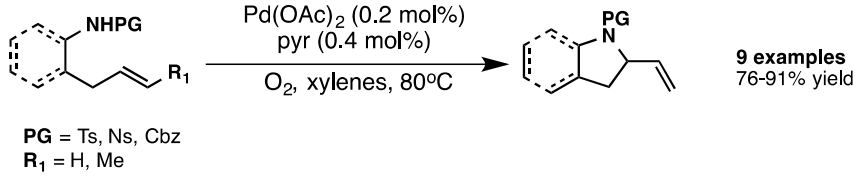

Yang further expanded the scope of the reaction with a tandem oxidative cyclization in the formation of indolines in good to excellent yields with a 4:1 pyridine to catalyst ratio (Scheme 2.7).[32]

Scheme 2.7: $Pd(OAc)_2$/pyridine Catalyzed Oxidative Cascade Cyclization

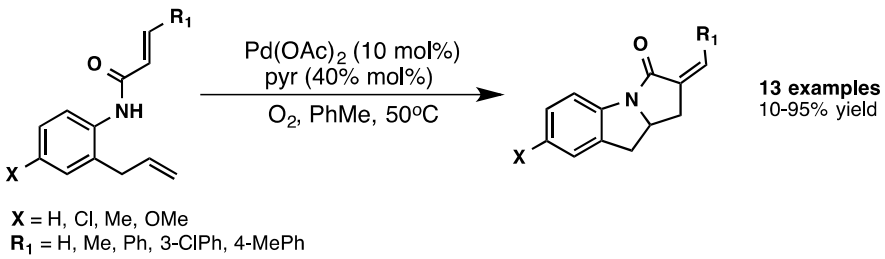

Mechanistic Considerations

In order to develop an asymmetric version of this transformation, consideration of the mechanism must be explored. Numerous studies have been performed in order to elucidate the mechanism of the Wacker-type oxidative amination. Whether the catalytic cycle goes through *cis*- or *trans*-aminopalladation is highly dependent upon the substrate, ligand and additives used in the reaction (Scheme 2.8).[33] As the chiral center is formed in this step of the catalytic cycle a thorough understanding of both pathways, and the conditions that favor them, is vital.[34] In *cis*-aminopalladation the amine initially coordinates with the palladium catalyst via ligand substitution and subsequent alkene insertion into the Pd-N bond results in the creation of the new C-N bond and a transient Pd^{II}-C bond on the same face of the molecule. Conversely, *trans*-aminopalladation begins with the formation of a Pd^{II}-π–alkene complex followed by nucleophilic attack by the amine from the opposite face, resulting in the opposite stereochemistry of the C-N bond relative to *cis*-aminopalladation.

Scheme 2.8: *cis*- and *trans*-Aminopalladation Catalytic Cycles

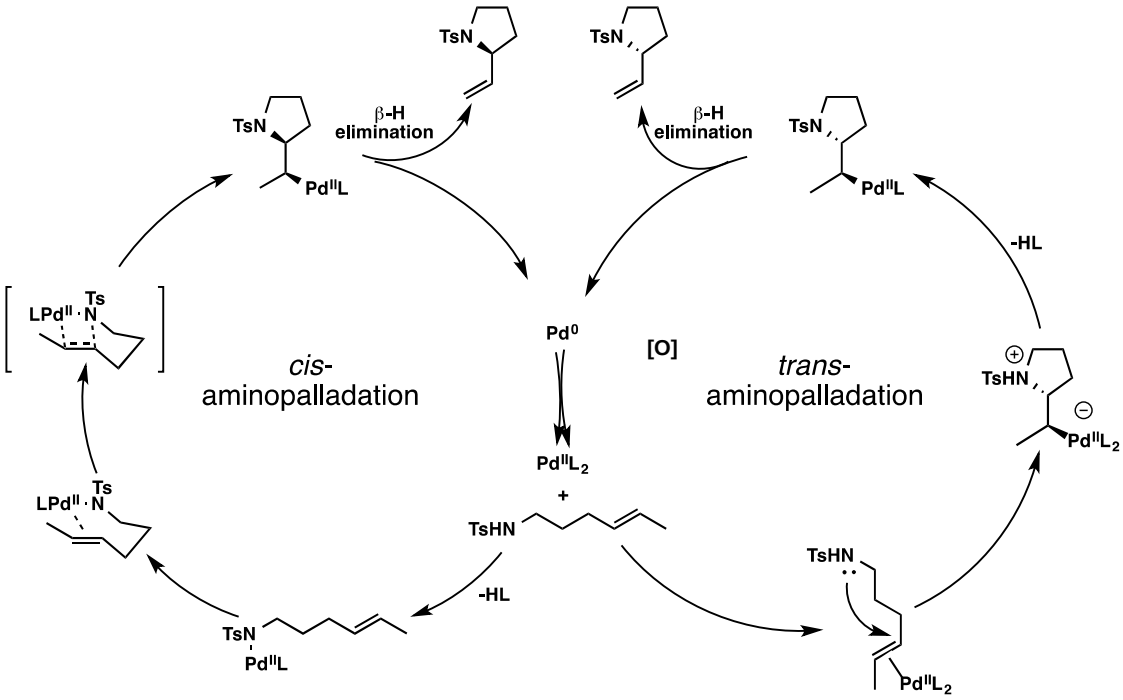

Enantioselective Intramolecular Oxidative Amination

The first enantioselective intramolecular oxidative amination was accomplished by Yang in moderate yields with good enantioselectivity (75-93% ee) substituting the chiral (–)-sparteine for pyridine (Scheme 2.9). Despite the success of (-)-sparteine as a ligand in this enantioselective transformation and others,[35] the opposite enantiomer, (+)-sparteine, is not commercially available and is non-trivial to synthesize.[36] Therefore, other ligand systems were explored.

Scheme 2.9: $Pd(OAc)_2$/(-)-Sparteine Catalyzed Oxidative Cascade Cyclization

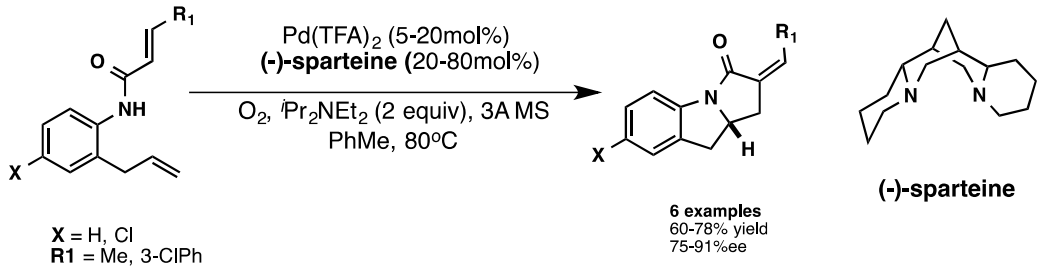

Building off of the successful application of a novel *N*-heterocyclic carbene (NHC)-coordinated Pd^{II} catalysts for the racemic synthesis of tosylamides,[37] Stahl synthesized a chiral version of the ligand (^{7}NHC) and tested its viability on two substrates.[38] The oxidative cyclization cascade achieved moderate enantioselectivity (63% ee) in a low yield (35%) while the reaction of an aromatic tosylamide gave almost no enantioselectivity (up to 9% ee) in a poor yield (12-63%) (Scheme 2.10).

Scheme 2.10: $Pd^{II}/^7$NHC Catalyzed Oxidative Cyclizations

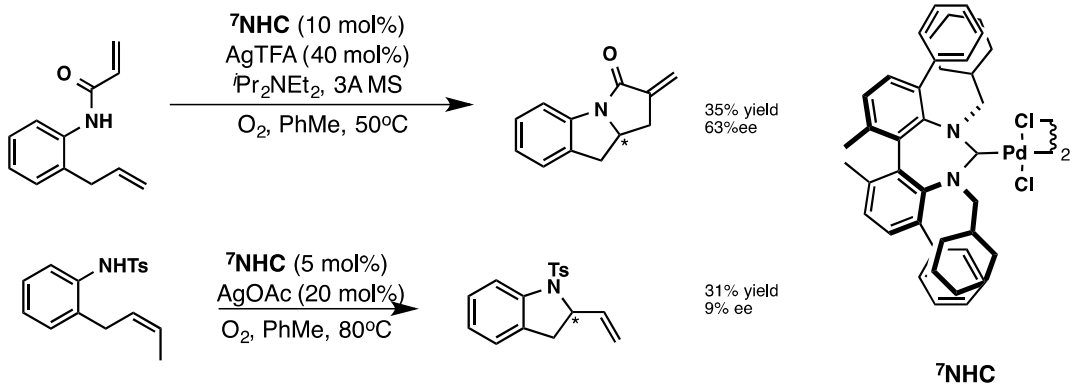

To further test the applicability of NHC complexes in this oxidative transformation Stahl utilized a previously synthesized chiral five-membered Pd-NHC complex, ^{5}NHC.[39]

However, neither substrate tested cyclized with good levels of stereoindction in either acidic or basic conditions (Scheme 2.11).

Scheme 2.11: $Pd^{II}/^{5}$NHC Catalyzed Oxidative Cyclizations

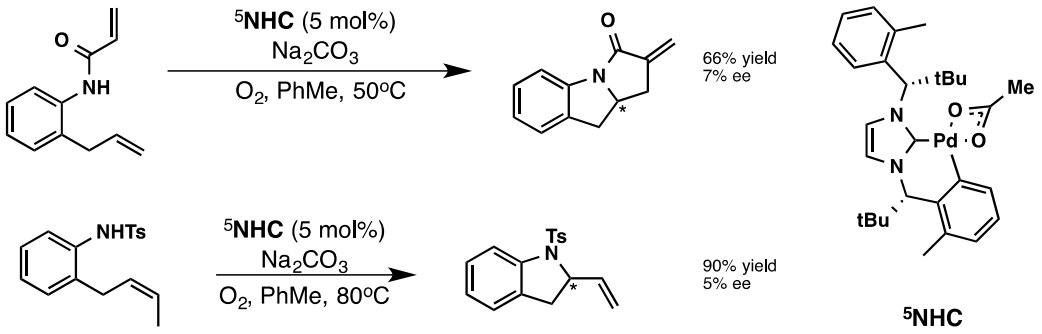

More closely mirroring the successful (-)-sparteine ligand, Yang attempted to develop a catalyst system for the oxidative cascade cyclization. After screening a variety of nitrogenous bases, quinoline and isoquinoline proved to be the most diastereoselective (dr > 24:1).[40] Coupling the quinolone with an oxazoline moiety gave a chelating, chiral ligand that is readily tunable and synthesized in a few steps. After screening a series of these quinolone-oxazoline (quinox) ligands, ^{t}Bu-quinox gave the highest enantioselectivity (93% ee). Further optimization of the reaction conditions gave cyclization products of disubstituted olefins in good yields (45-82%) with excellent enantioselectivities (80-98% ee) and diasterioselectivities (dr > 24:1) (Scheme 11).[41] Lastly, the aminopalladation step in the catalytic cycle was determined to be exclusively *cis.*

Scheme 2.12: $Pd(OAc)_2$/^{t}Bu-quinox Catalyzed Oxidative Cascade Cyclization

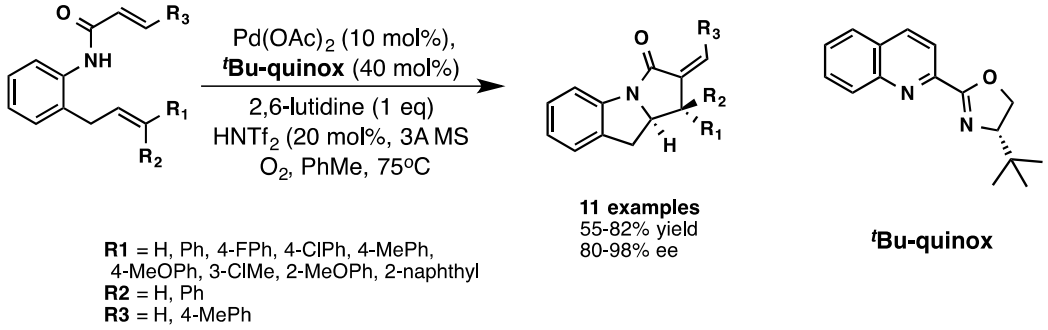

Using the same quinox ligand system, Zhang applied the ^{i}Pr-quinox ligand for the enantioselective cyclization of benzyl olefinic tosylamides (Scheme 2.13).[42] This system found good success with *p*-substituted substrates giving good yields (75-94%) and moderate enantioselectivity (69-74% ee). However, *o*-substituted substrates gave poor yields (4-37%) and significantly reduced enantioselectivity (-8 to -35% ee).

Scheme 2.13: $Pd(OAc)_2$/^{i}Pr-quinox Catalyzed Oxidative Cyclization of Tosylamides

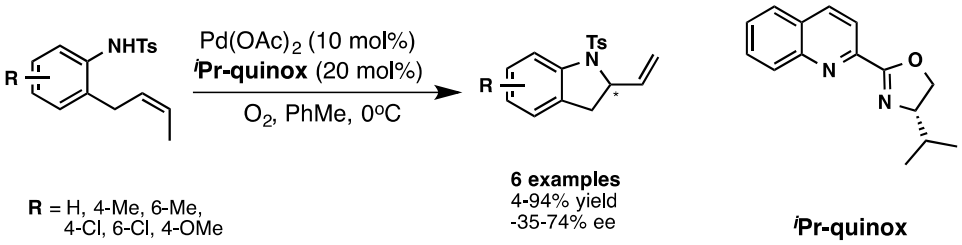

Stahl evaluated a series of quinox and pyridine-oxazoline (pyrox) ligands for the enantioselective oxidative amination of acyclic olefinic tosylamides.[43] The pyrox ligand proved to be more enantioselective and optimization of the conditions (with 3Å molecular sieves in toluene) gave moderate to excellent yields (52-98%) with excellent

enantioselectivities (76-98% ee) with lower catalyst loadings than the previous examples (Scheme 2.14). However, the substrate scope was limited to *cis*-olefins as *trans*-substrates gave lower yields (51%) and significantly lower enantioselectivities (50% ee).

Scheme 2.14: $Pd(TFA)_2$/Pyrox Catalyzed Oxidative Cyclization of Tosylamides

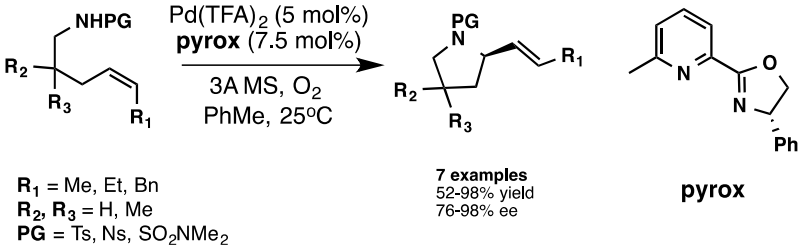

The rate-limiting step of the catalytic cycle was the determined to be *cis*-aminopalladation. Computational analysis on the pyrox ligand showed the small electronic differences of the two nitrogens in the chelating ligand plays a significant role in the asymmetric transformation. The more basic oxazoline nitrogen exhibits a *trans* influence (with respect to the tosylamide), allowing the chiral phenyl group of the oxazoline to establish the stereocenter of the substrate (Figure 2.2).

Figure 2.2: The Stereochemistry-Inducing Transition State of the Pyrox Catalytic Cycle

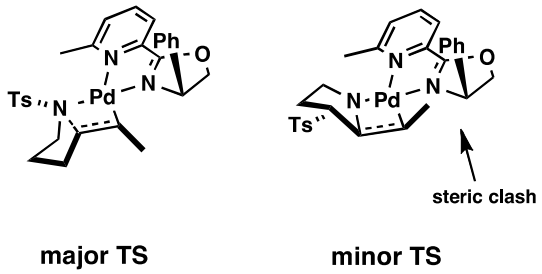

Utilizing a very similar catalyst/ligand system Zhang synthesized isoindoinones in high yields and enantioselectivies (Scheme 2.15). [44]

Scheme 2.15: $Pd(TFA)_2$/^{t}Bu-Pyrox Catalyzed Oxidative Cyclization of Tosylamides

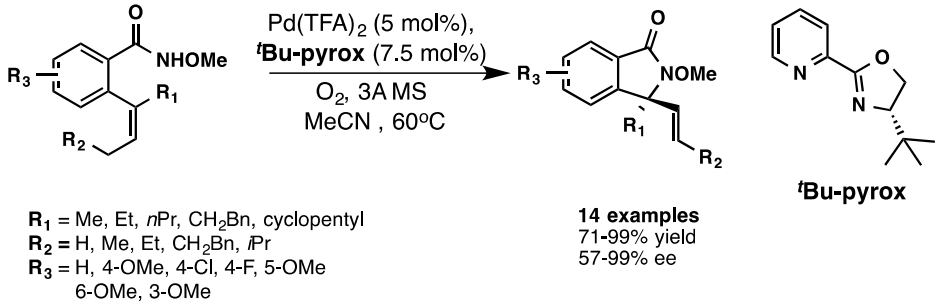

Chiral X-Type Ligands

Despite the successful application of bidenate nitrogenous ligands in the enantioselective oxidative amination, our approach sought to maintain the electrophilicity of Pd^{II}-π-alkene complex through weakly coordinating X-type ligands. Through two acid-promoted ligand exchanges with a commercially available Pd^{II} species the chiral catalyst is generated in situ (Figure 2.3).

Figure 2.3: Ligand Exchange of Chiral X-Type Ligands

With the previous success of a Pd^{II}-chiral phosphate complex in our group[45] and the proliferation of chiral phosphoric acids in the literature,[46] this ligand class was first explored. In order to develop suitable conditions for the reaction, the achiral conditions

were optimized using diphenylphosphate (DPP), and then screened with multiple chiral phosphate ligands (Figure 2.5). Also several substrates, both aromatic and acyclic olefinic tosylamides, were screened under these conditions (Figure 2.4).

Figure 2.4: Substrates Tested

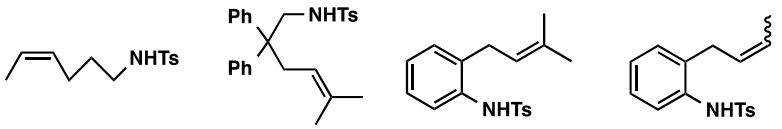

Figure 2.5: Chiral Phosphoric Acid Ligands

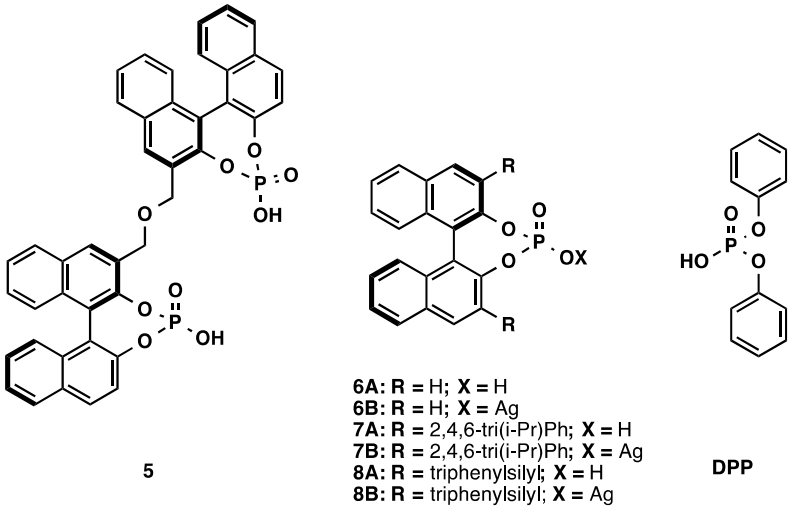

Chiral Phosphoric Acid Ligands

Tri-substituted tosylaniline **3** proved to be the model substrate, while substrates **1** and **2** suffered from lack of conversion which prohibited enantioselective study. Substrate **3** benefits from the conformational rigidity of the aniline core in comparison to the

germinal di-substituted **2** and linear **1**. Also, the increased acidity of the tosylamine in **3** may play a role in the efficacy of the nucleopalladation.

The initial conditions of the reaction utilized $Pd(OAc)_2$ (10 mol%) as the palladium source with a phosphate ligand (20 mol%) and benzoquinone as the reoxidant in toluene. Under achiral conditions **3** proceeded with excellent conversion (Table 2, entry 1). However, when subjected to chiral phosphate **5**, a good conversion but low enantioselectivity was evidenced (entry 2).

Table 2.1: Oxidative Amination of 3 with Phosphate Ligands

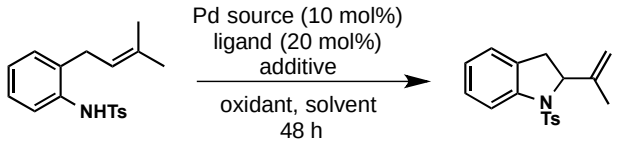

Entry	Ligand	Catalyst	Additive	Oxidant	Conversion (%)	ee(%)
1	**DPP**	$Pd(OAc)_2$		BQ	>95	n.d.
2	**5**	$Pd(OAc)_2$		BQ	60	17
3	no ligand	$Pd(OAc)_2$		BQ	30	n.d.
4	**6B**	$(CH_3CN)_2PdCl_2$		BQ	33	2
5	**7B**	$(CH_3CN)_2PdCl_2$		BQ	30	17
6	no ligand	$(CH_3CN)_2PdCl_2$		BQ	50	n.d.
7	**6B**	$(CH_3CN)_2PdCl_2$		O_2	9	n.d.
8	**6B**	$(CH_3CN)_2PdCl_2$	Cs_2CO_3	O_2	83	n.d.
9	**7B**	$(CH_3CN)_2PdCl_2$	Cs_2CO_3	O_2	44	11
10	**8B**	$(CH_3CN)_2PdCl_2$	Cs_2CO_3	O_2	87	6
11	no ligand	$(CH_3CN)_2PdCl_2$	Cs_2CO_3	O_2	>95	n.d
12	**DPP**	$(CH_3CN)_4Pd(BF_4)_2$		O_2	11	n.d.
13	**6A**	$(CH_3CN)_4Pd(BF_4)_2$	Cs_2CO_3	O_2	59	2
14	**7A**	$(CH_3CN)_4Pd(BF_4)_2$	Cs_2CO_3	O_2	71	1
15	no ligand	$(CH_3CN)_4Pd(BF_4)_2$	Cs_2CO_3	O_2	67	n.d.
16	**DPP**	Pd_2dba_3	Cs_2CO_3	O_2	83	n.d.
17	**7A**	Pd_2dba_3	Cs_2CO_3	O_2	23	1

Disappointed in the lack of stereoinduction, a control reaction was screened (omitting the phosphate ligand) in order to probe the background reactions. A clear enhancement with the phosphate ligand is seen as the control gave a low conversion (entry 3). With the lack of success of $Pd(OAc)_2$ as a palladium source, $(CH_3CN)_2PdCl_2$ was attempted. In order to promote coordination of the ligand to the catalyst, silver salts of the phosphate ligands were explored (Figure 2.3, **6B**, **7B** and **8B**). Precipitation of AgCl would favor coordination in the ligand exchange equilibrium and subsequently remove the inhibitory chloride ligands from the system. Using ligand **6B** to optimize conditions, benzoquinone was the first oxidant screened. For the cyclization of **3**, using ligands **6B** and **7B**, conversions were moderate with low enantioselectivities (entries 4-5). In an attempt to simplify the system, O_2 was tested as an oxidant. It was discovered that a base (Cs_2CO_3) was necessary to achieve the transformation (entries 8). Subsequent examination with chiral ligands **7B** and **8B** gave good conversions but poor enantioselectivities (entries 9-10). A control reaction showed excellent conversion without the addition of a phosphoric acid ligand (entry 11).

The last Pd^{II} source tested was tetrakis(acetonitrile)palladium(II) tetrafluoroborate. Reactions under racemic conditions showed the necessity Cs_2CO_3 with the O_2 oxidant, as the conversion was low without the basic additive (entry 12). Ligands **6A** and **7A** were producing good conversions, but essentially racemic products (entries 13-14). Yet again, a control reaction showed considerable reactivity without the phosphoric acid ligand (entry 15).

Lastly $Pd_2(dba)_3$ was explored. Good conversion was seen using DPP, but the asymmetric transformation proved unsuccessful, resulting in both a low conversion and no enantioselectivity using ligand **7A** (entry 17).

The use of phosphoric acid ligands in the stereoselective intramolecular oxidative amination was largely unsuccessful, reaching a maximum enantioselectivity of 17% ee. A rationale for the poor stereoselectivity is the existence of other pathways for cyclization that do not include the chiral phosphate ligand. With the control experiments showing substantial conversion, it appears as if the ligand-coordinated complex is not the lowest energy pathway.

Chiral Sulfonic Acid Ligands

With the lack of success of chiral phosphoric acids, a new class of ligand was explored, specifically sulfonic acids. In order to test the viability of this ligand class, camphorsulfonic acid was chosen. As a chiral, inexpensive and commercially available in both enantiomers, it is an ideal model ligand. To our gratification the use of (+)-camphorsulfonic acid ((+)-CSA) provided greater conversion and better enantioselectivity than any of the previous trials with chiral phosphoric acids. A screen of various palladium sources showed $Pd(OAc)_2$ gave the best combination of yield and enantioselectivity (Table 2.2). Exploration of the in situ generated AcOH, upon proposed acid-promoted ligand exchange with (+)-CSA, was explored with the synthesis of $Pd[(+)\text{-}CSA]_2$ complex. Nearly identical results were seen when comparing the reactions utilizing the preformed complex (entry 5) versus combining (+)-CSA and $Pd(OAc)_2$ in the reaction flask. This gives evidence to $Pd[(+)\text{-}CSA]_2$ being the active catalyst and that

AcOH plays no detrimental role in the catalytic cycle. The in situ generated catalyst was therefore utilized in further reactions. No appreciable background reactions occurred upon omission of the palladium source (entry 6) and the addition of the sulfonic acid ligand proved essential for reactivity (entry 7).

Table 2.2: Palladium Source Screen for Oxidative Amination of 3 with (+)-CSA

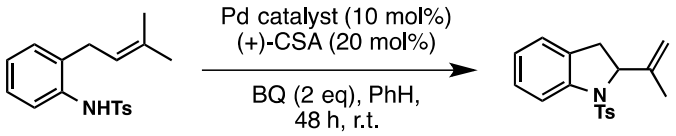

Entry	Pd source	Conversion (%)[b]	Yield(%)[c]	ee(%)[d]
1	$Pd(CH_3CN)_2Cl_2$	81	73	11
2	$Pd_2(dba)_3$	69	40	38
3	$Pd(TFA)_2$	59	53	24
4	$Pd(OAc)_2$	60	55	40
5	$Pd[(+)\text{-}CSA]_2$	64	56	41
6	none	<5	n.d.	n.d.
7	$Pd(OAc)_2$/no L	8	n.d.	n.d.

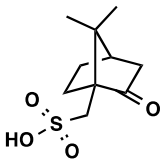

(+)-CSA

[a] 0.05 mmol scale in 0.1 M PhH. [b] Based on crude ^{1}H-NMR. [c] Isolated yield after column chromatography. [d] Determined by chiral HPLC.

In order to increase conversion, additives were explored in this reaction. The sodium salt of (+)-CSA ((+)-NaCSA) increased the yield of the transformation at 10 mol% (Table 2.3, entry 2). However, (+)-NaCSA is not acting as a ligand whereupon removal of (+)-CSA gives no reaction (entry 3). Increasing the ligand/catalyst ratio did not prove beneficial for the yield (entry 4).

Table 2.3: Additive Screen for Oxidative Amination of 3 with (+)-CSA

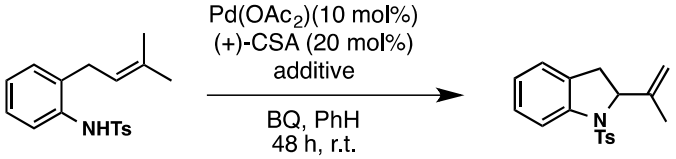

Entry	Additive	Conversion (%)[a]	Yield(%)[b]	ee(%)[c]
1	no additive	60	55	40
2	(+)-NaCSA (10 mol%)	91	64	50
3[x]	(+)-NaCSA (10 mol%)	8	n.d.	n.d.
4[y]	(+)-NaCSA (10 mol%)	65	38	41

[a] Based on crude ^{1}H-NMR. [b] Isolated yield after column chromatography. [c] Determined by chiral HPLC. [x] No (+)-CSA. [y] 1 equiv (+)-CSA

Next the reoxidant and solvent were examined. While product was formed with O_2 as the sole oxidant, benzoquinone (2 equiv) proved most efficient (Table 2.4, entry 6) and benzene was determined to be the optimal solvent (entry 6).[47]

Table 2.4: Reoxidant and Solvent Screen for Oxidative Amination of 3 with (+)-CSA

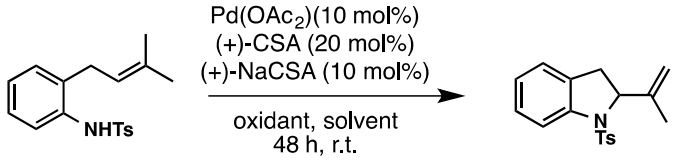

Entry	Oxidant	Solvent	Conversion (%)[a]	Yield(%)[b]	ee(%)[c]
1	O_2	PhH	63	34	50
2	MnO_2	PhH	16	12	10
3	BQ (1 equiv)	PhH	67	52	50
4	O_2/BQ (20 mol%)	PhH	49	32	n.d.
5	O_2/Cu(piv)$_2$ (1.1 equiv)	PhH	15	n.d.	n.d.
6	BQ (2 equiv)	PhH	95	65	50
7	BQ (2 equiv)	PhMe	95	54	48
8	BQ (2 equiv)	DCM	55	40	44

[a] Based on crude ^{1}H-NMR. [b] Isolated yield after column chromatography. [c] Determined by chiral HPLC.

With the optimized reaction conditions in hand, a number of substrates were synthesized to explore the scope and limitations of the catalyst system. A series of di- and tri-substituted tosylanilines (**3a-f**, **4a-f**) were synthesized in four steps from commercially available starting materials. The carboxylic acid was reduced to the primary alcohol with $LiAlH_4$, the aniline was protected with pTsCl or MsCl,[48] and the benzyl alcohol was converted to the chloride with $SOCl_2$,[49] all in excellent yields. The alkene was introduced via a Grignard to give corresponding alkene substrate.[50]

Scheme 2.16: Synthesis of Di- and Tri-Substituted Tosylanilines 3a-f and 4a-f

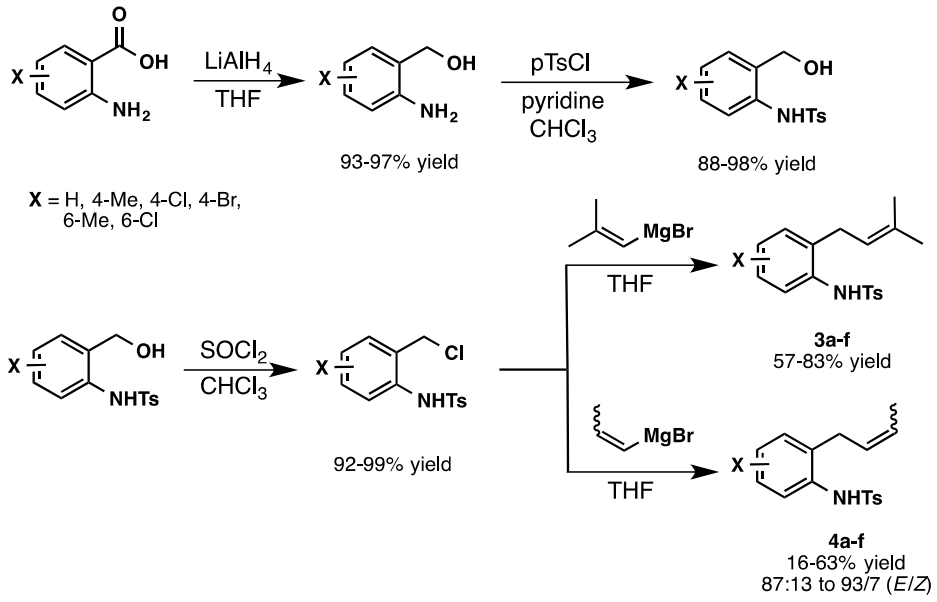

Other amine nucleophiles were analyzed with the synthesis of tosylcarbamate **9** (Scheme 2.17). Reduction of tiglic acid with $LiAlH_4$[51] and nucleophilic attack of the allylic alcohol on p-toluenesulfonyl isocyanate gave **9** in a 48% yield over two steps. Lastly, exploration of larger ring cyclizations was examined with the synthesis of **10** which upon oxidative

amination forms a morpholine product. The substrate was made in three steps beginning with the allylic alkylation of 2-nitrophenol (Scheme 2.18). Subsequent reduction of the nitro group[52] and tosylation of the aniline[53] gave **10** in a 63% yield over three steps.

Scheme 2.17: Synthesis of Tosylcarbamate 9

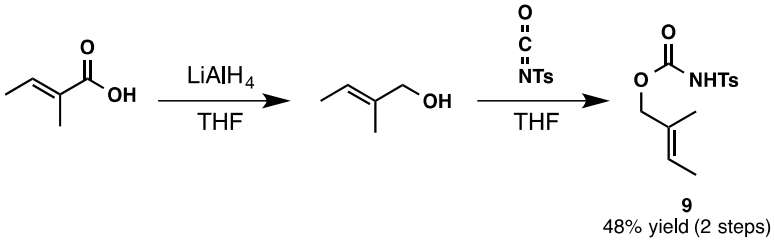

Scheme 2.18: Synthesis of 10

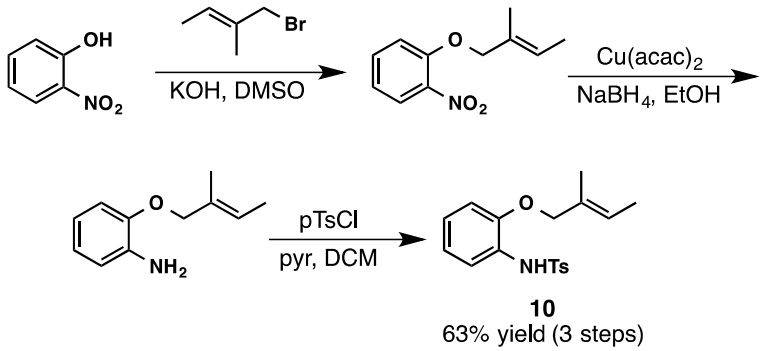

Examination of Substrate Scope

Many substrates effectively cyclized to produce indolines with varying levels of stereoselectivity (Table 2.5). The tosyl-protecting group proved to be superior in reactivity and enantioselectivity in comparison to the mesylate (entries 1 and 2). While requiring longer reaction times the tri-substituted substrates gave higher yields and increased enantioselectivity. *Para*-substituted substrates (entries 4-9) proceeded smoothly to give good yields and moderate enantioselectivity. However, upon subjecting

ortho-substituted substrates to the reaction conditions, complete loss of enantioselectivity occurred. These findings are consistent with the literature.[42]

Table 2.5: Substrate Scope of Enantioselective Oxidative Amination with (+)-CSA

entry		substrate	product			yield (%)[b]	% ee
1[c]	**3a**	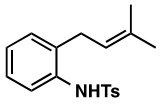	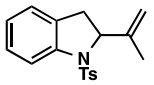	**11a**		74	44
2[c]	**3aa**	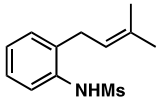	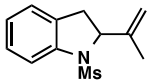	**11aa**		55	38
3[d]	**4a**	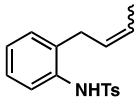	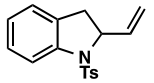	**12a**		54	29
4[d]	**3b**	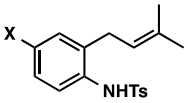	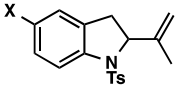	**11b**	X = Me	76	43
5[d]	**3c**			**11c**	X = Cl	70	42
6[d]	**3d**			**11d**	X = Br	67	45
7[c]	**4b**	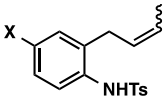	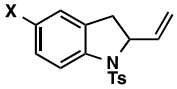	**12b**	X = Me	55	27
8[c]	**4c**			**12c**	X = Cl	62	27
9[c]	**4d**			**12d**	X = Br	68	27
10[d]	**3e**	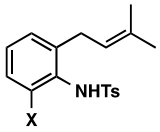	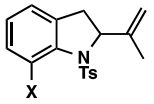	**11e**	X = Me	66	13
11[f]	**3f**			**11f**	X = Cl	53	0
12[e]	**4e**	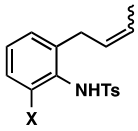	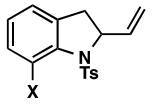	**12e**	X = Me	66	0
13[g]	**4f**			**12f**	X = Cl	46	0
14[g]	**9**	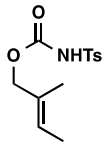	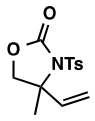	**13**		52[g]	44
15[h]	**10**	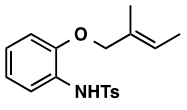	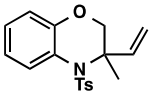	**14**		44[h]	0

[a] Conditions: Substrate (0.1 mmol), $Pd(OAc)_2$ (0.01 mmol), (+)-CSA (0.02 mmol), (+)-NaCSA (0.01 mmol), BQ (0.2 mmol),1 mL benzene.[b] Isolated yield. [c] 60 h, r.t. [d] 5 h, r.t. [e] 18 h, r.t., [f] 60 h, 50 °C. [g] 24 h, 50 °C. [h] 72 h, 50 °C.

The formation of tosylcarbamate **13** (entry 14) occurred with similar enantioselectivity to indoline derivatives **11**. The creation of a chiral six-membered ring proved unfeasible as morpholine **14** was shown to be racemic.

Mechanistic Considerations

As the utilization of X-type ligands in this reaction is novel and previous mechanistic studies focused on the role of L-type ligands, trends in conditions that favor *cis*- vs. *trans*-aminopalladation are difficult to extrapolate. The closest mechanistic analysis to the (+)-CSA ligand is Stahl's examination of "ligand-free" $Pd(TFA)_2$. Through NMR and chiral HPLC analysis, Stahl determined the *trans*- to *cis*- ratio to be 16:84 (Scheme 2.19).[54] Furthermore, of the enantioselective reactions that have utilized deuterium labeling studies to unambiguously establish the mechanism of the reaction, all have exhibited *cis*-aminopalladation.[41,55]

Scheme 2.19: Mechanistic Examination of "Ligand Free" $Pd(TFA)_2$

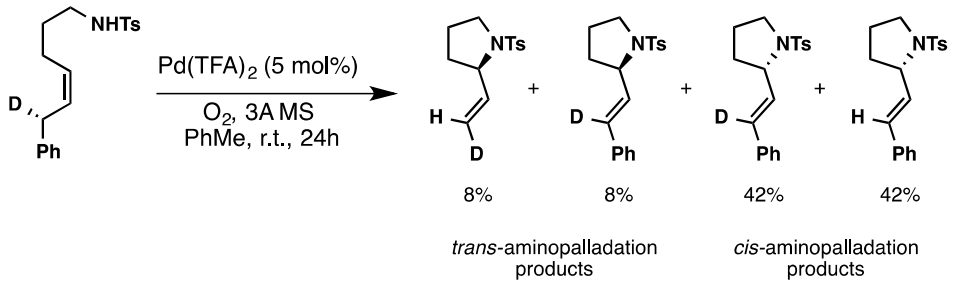

Despite the ambiguity in the mechanism, both *cis*- and *trans*-aminopalladation transition states can be analyzed to assess the efficacy of (+)-CSA as a chiral ligand. A key limitation of the (+)-CSA ligand is the methylene between the coordinated sulfonate and the chiral camphor core. This rotational freedom allows the chiral portion of the

molecule to adopt a conformation distant from the developing stereocenter. Even with this limitation, as a model ligand (+)-CSA gave modest levels of enantioselectivity and further rational design could be implemented in the future examination of this asymmetric transformation.

Scheme 2.20: Proposed *cis*- and *trans*-Aminpalladation Pathways with (+)-CSA

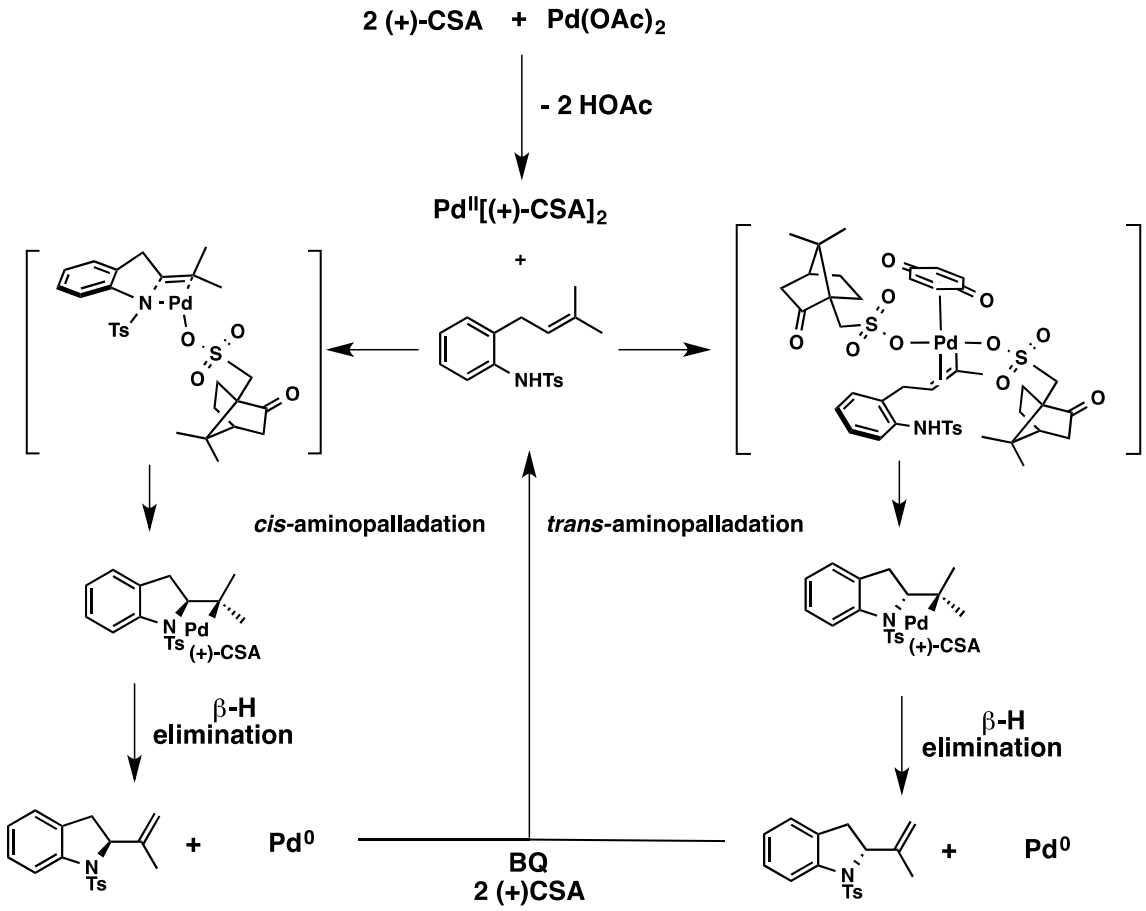

Intermolecular Oxidative Amination

With the success of the intramolecular oxidative amination using the Pd^{II}/(+)-CSA catalyst a brief exploration of the intermolecular version of the reaction was attempted. Inherent in the intermolecular Wacker-type oxidative amination is the issue of regioselectivity. Lacking a symmetrical alkene the addition of the nitrogen nucleophile can occur via Markovnikov or anti-Markovnikov aminopalladation.[56] An additional concern, especially with chiral X-type ligands, is the competitive coordination of the amine as a ligand to the catalyst, potentially poisoning the catalyst and rendering it achiral or unreactive.

With these limitations in mind, styrene was chosen as the model alkene and variety of nitrogen nucleophiles were tested. Upon exploration of these conditions no reaction occurred without the addition of camphorsulfonic acid and only Markovnikov products were evident. Phthalamide showed the most promise as a nucleophile, while saccharin and methyl tosylamine gave no reaction. However low yields precluded further examination of this reaction (Scheme 2.21).

Scheme 2.21: Intermolecular Oxidative Amination of Styrene

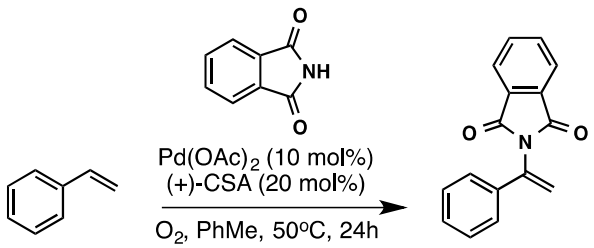

15
(44% yield)

In an attempt to exploit the chiral nature of the catalyst an asymmetric version of an existing racemic 2,2-difunctionalization of alkenes was explored.[57] Initial intermolecular oxidative amination and β–hydride elimination would leave the substrate prone to asymmetric intramolecular oxypalladation. Butyl acrylate was reacted with N-(2-hydroxyethyl)-4-methylbenzenesulfonamide to produce oxazolidine **16** in a moderate yield. Unfortunately, upon examination of the resulting stereocenter, the reaction proved to be racemic. Presumably, after initial intermolecular oxidative amination the resulting ring closure proceeds through a Bronsted acid-catalyzed Michael addition resulting in no stereoinduction.

Scheme 2.22: Difunctionalization of Butyl Acrylate

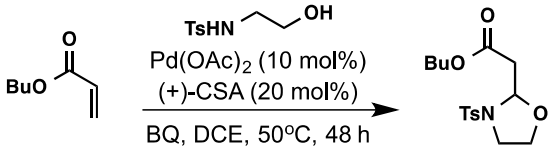

16
(63% yield)

Also, attempted cyclizations with *trans*-crotonic acid and acrylic acid did not give any desired products.

Conclusion

Chiral X-type ligands have proven applicable for the Pd^{II}-catalyzed enantioselective intramolecular oxidative amination. To our knowledge, this is the first application of a chiral sulfonic acid as a ligand in an asymmetric palladium catalyzed

reaction. As a model ligand, (+)-CSA provided good yields (up to 76%) and moderate levels of enantioselectivity (up to 45% ee) in the synthesis of chiral indolines and a cyclic carbamate.

Experimental

General Information

Commercial reagents were purified prior to use following the guidelines of Perrin and Armarego.[58] Et_2O and THF were distilled from sodium benzophenone ketyl under a positive pressure of argon. All other solvents were obtained from commercial vendors and used as received unless otherwise noted. $Pd(CH_3CN)_2Cl_2$, $Pd(TFA)_2$, $Pd(OAc)_2$, $Pd(CH_3CN)_4(BF_4)_2$ (Strem), and $Pd_2(dba)_3$ (Aldrich) were purchased from commercial vendors and used as received. Organic solutions were concentrated under reduced pressure on a Büchi rotary evaporator. Chromatographic purification of products was accomplished using forced-flow chromatography on Silicycle SiliaFlash® F60 40–63 μm, 60 Å silica gel according to the method described by Still.[59] Thin-layer chromatography (TLC) was performed on Silicycle SiliaPlate® G, 250 μm plates. Visualization of the developed chromatogram was performed by fluorescence quenching or staining with $KMnO_4$ stain.

^1H NMR spectra (300 or 500 MHz) and ^{13}C NMR (75 or 125 MHz) spectra were recorded on Bruker DPX 300 or AVANCE-500 spectrometers in $CDCl_3$ and are internally referenced to residual solvent signals (δ 7.26 and δ 77.16, respectively). Data for ^1H NMR are reported as follows: chemical shift (δ ppm), multiplicity (s = singlet, d =

doublet, t = triplet, q = quartet, m = multiplet, b = broad, app = apparent), integration, coupling constant (Hz) and assignment. Data for ^{13}C NMR are reported in terms of chemical shift. IR spectra were recorded on a JASCO 4100 spectrometer as thin films on a NaCl plate and are reported in terms of frequency of absorption (cm^{-1}). Mass spectra were obtained from the Montana State University Mass Spectral facility using a Bruker micrOTOF (ESI-TOF). High performance liquid chromatography (HPLC) was performed on a DIONEX UltiMate 3000 chromatograph using a Daicel Chiralcel® AD-H column (25 x 0.46 cm) and AD-H guard cartridge (0.4 x 1 cm), a Daicel Chiralcel® AS-H column (25 x 0.46 cm) and AS-H guard cartridge (0.4 x 1 cm), Daicel Chiralcel® OD-H column (25 x 0.46 cm) and OD-H guard cartridge (0.4 x 1 cm) or Daicel Chiralcel® OJ-H column (25 x 0.46 cm) and OJ-H guard cartridge (0.4 x 1 cm) as noted.

Synthesis of Amino Carboxylic Acids

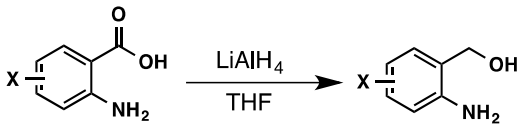

To a suspension of lithium aluminum hydride (20.4 mmol) in THF (10 mL) was added benzoic acid (8.5 mmol) dissolved in THF (24 mL) dropwise over 20 minutes at room temperature. The reaction continued to stir at room temperature for 3.5 h, and then was quenched at 0 ^{o}C with H_2O (10 mL). The suspension was filtered through a Celite plug with EtOAc (100 mL), washed with brine (30 mL), dried with $MgSO_4$ and concentrated *in vacuo*.

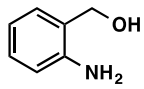

(2-aminophenyl)methanol: 94% yield (light brown solid). Characterization is consistent with commercially available material. **^{1}H NMR** (500 MHz, $CDCl_3$) δ 7.17-7.12 (m, 1H), 7.09-7.05 (m, 1H), 6.75-6.73 (m, 2H), 4.68 (s, 2H), 3.41 (s, 2H). **^{13}C NMR** (75 MHz, $CDCl_3$) δ 146.02, 129.50, 129.32, 124.99, 118.37, 116.21, 64.46.

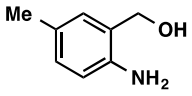

(2-amino-5-methylphenyl)methanol: 93% yield (yellow solid). **^{1}H NMR** (500 MHz, $CDCl_3$) δ 6.93 (dd, *J* = 7.9, 2.1 Hz, 1H), 6.88 (d, *J* = 2.0 Hz, 1H), 6.62 (d, *J* = 7.9 Hz, 1H), 4.63 (s, 2H), 3.11 (bs, 3H), 2.22 (s, 3H). **^{13}C NMR** (126 MHz, $CDCl_3$) δ 143.40, 129.94, 127.74, 125.23, 116.46, 64.51, 20.47.

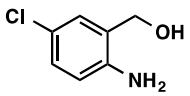

(2-amino-5-chlorophenyl)methanol: 93% yield (light yellow solid). **^{1}H NMR** (500 MHz, $CDCl_3$) δ 7.10 – 7.04 (m, 2H), 6.62 (d, *J* = 8.3 Hz, 1H), 4.65 – 4.60 (s, 2H), 4.40-3.95 (bs, 2H). **^{13}C NMR** (126 MHz, $CDCl_3$) δ 144.74, 129.11, 128.90, 126.25, 122.72, 117.23, 63.99.

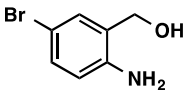

(2-amino-5-bromophenyl)methanol: 96% yield (light brown solid). Characterization consistent with the literature.[60] **^{1}H NMR** (500 MHz, $CDCl_3$) δ 7.24 – 7.16 (m, 2H), 6.58 (d, *J* = 8.4 Hz, 1H), 4.62 (s, 2H), 4.17 (bs, 2H). **^{13}C NMR** (75 MHz, $CDCl_3$) δ 145.19, 131.99, 131.70, 126.70, 117.65, 109.69, 63.91.

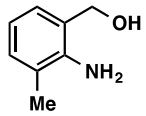

(2-amino-3-methylphenyl)methanol: 97% yield (light brown solid). **^{1}H NMR** (500 MHz, $CDCl_3$) δ 7.05 (d, *J* = 7.4 Hz, 1H), 6.95 (d, *J* = 7.3 Hz, 1H), 6.66 (app t, *J* = 7.4 Hz, 1H), 4.67 (s, 2H), 3.35 (bs, 3H), 2.19 (s, 3H). **^{13}C NMR** (126 MHz, $CDCl_3$) δ 144.31, 130.71, 127.25, 124.30, 122.80, 117.74, 64.69, 17.39.

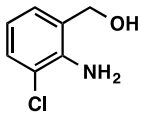

(2-amino-3-chlorophenyl)methanol: 93% yield (light brown solid). Characterization is consistent with the literature[61] **^{1}H NMR** (500 MHz, $CDCl_3$) δ 7.23 (dd, *J* = 8.0, 1.5 Hz, 1H), 6.96 (dd, *J* = 7.4, 1.5 Hz, 1H), 6.63 (app t, *J* = 7.7 Hz, 1H), 4.67 (s, 2H), 3.91 – 3.49 (bs, 2H). **^{13}C NMR** (126 MHz, $CDCl_3$) δ 142.73, 129.44, 127.57, 125.88, 120.15, 118.05, 64.52.

<u>Tosylamino Alcohol Synthesis</u>

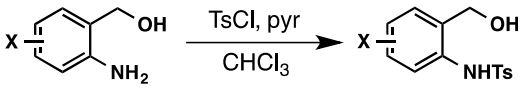

The amino alcohol was tosylated according to literature procedure and used in the next step without further purification.[62]

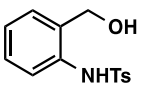

N-(2-hydroxymethyl-phenyl)-4 methyl-benzenesulfonamide: 96% yield. Characterization is consistent with the literature.[48] **^{1}H NMR** (500 MHz, $CDCl_3$) δ 7.67 – 7.62 (m, 2H), 7.44 (d, *J* = 8.0 Hz, 1H), 7.22 (d, *J* = 8.1 Hz, 3H), 7.12 – 7.06 (m, 2H), 4.39 (s, 2H), 2.38 (s, 3H).

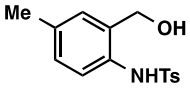

N-(2-Hydroxymethyl-4-methyl-phenyl)-4-methyl-benzenesulfonamide: 98% yield. Characterization is consistent with the literature[37]. **^{1}H NMR** (500 MHz, $CDCl_3$) δ 7.72 (s, 1H), 7.61 (d, *J* = 8.3 Hz, 2H), 7.24 – 7.19 (m, 3H), 7.02 (dd, *J* = 8.1, 2.1 Hz, 1H), 6.91 (d, *J* = 2.1 Hz, 1H), 4.32 (s, 2H), 2.38 (s, 3H), 2.26 (s, 3H).

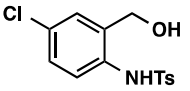

N-(4-chloro-2-hydroxymethyl-phenyl)-4-methyl-benzenesulfonamide: 98% yield. Characterization is consistent with the literature.[37] **^{1}H NMR** (500 MHz,$CDCl_3$) δ 7.84 (s, 1H), 7.63 (d, *J* = 8.2 Hz, 2H), 7.37 (d, *J* = 8.6 Hz, 1H), 7.24 – 7.20 (m, 3H), 7.09 (d, *J* = 2.5 Hz, 1H), 4.33 (s, 2H), 2.39 (s, 3H).

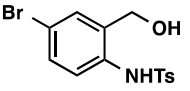

N-(4-bromo-2-(hydroxymethyl)phenyl)-4-methylbenzenesulfonamide: 95% yield. Characterization is consistent with the literature.[63] **^{1}H NMR** (300 MHz, $CDCl_3$) δ 7.87 (s, 1H), 7.64 (d, *J* = 8.3 Hz, 2H), 7.47 – 7.30 (m, 3H), 7.26 – 7.20 (m, 3H), 4.34 (s, 2H), 2.39 (s, 3H).

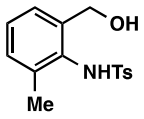

N-(2-hydroxymethyl-6-methyl-phenyl)-4-methyl-benzenesulfonamide: 94% yield. Characterization is consistent with the literature.[37] **^{1}H NMR** (500 MHz, $CDCl_3$) δ 7.55 (d, *J* = 8.3 Hz, 2H), 7.23 (d, *J* = 8.1 Hz, 2H), 7.19 – 7.14 (m, 2H) , 7.10 (dd, *J* = 7.1, 2.1 Hz, 1H), 6.70 (bs, 1H), 4.38 (s, 2H), 2.41 (s, 3H), 1.96 (s, 3H).

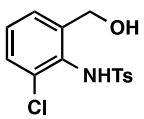

N-(6-chloro-2-hydroxymethylphenyl)-4-methylbenzenesulfonamide: 88% yield Characterization is consistent with the literature.[64] **^{1}H NMR** (500

MHz, $CDCl_3$) δ 7.53 (d, *J* = 7.7 Hz, 1H), 7.50 (d, *J* = 8.3 Hz, 2H), 7.24 – 7.19 (m, 4H) , 6.47 (s, 1H), 4.85 (s, 2H), 2.42 (s, 3H).

The amino alcohol was mesylated according to the same procedure, substituting MsCl for TsCl and increasing the reaction time to 12 h.

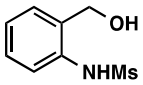

N-(2-(hydroxymethyl)phenyl)methanesulfonamide: 87% yield. **^{1}H NMR** (500 MHz, $CDCl_3$) δ 7.79 (s, 1H), 7.56 (d, *J* = 8.2 Hz, 1H), 7.35 (t, *J* = 7.9 Hz, 1H), 7.25 – 7.21 (m, 1H), 7.14 (t, *J* = 7.4 Hz, 1H), 4.78 (s, 2H), 3.06 (s, 3H).

<u>Tosylamino Chloride Synthesis</u>

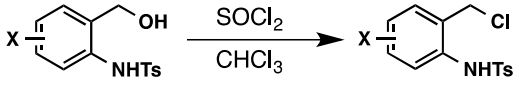

The following tosylamino chloride compounds were synthesized according to a literature procedure. [65]

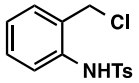

N-(2-(chloromethyl)phenyl)-4-methylbenzenesulfonamide: 96% yield (white solid), mp 96-98°C. **^{1}H NMR** (500 MHz, $CDCl_3$) δ 7.65 (d, *J* = 8.3 Hz, 2H), 7.36 (dd, *J* = 8.1, 1.4 Hz, 1H), 7.30 (td, *J* = 7.7, 1.7 Hz, 2H), 7.25 (m, 2H), 7.16 (td, *J* = 7.5, 1.4 Hz, 1H), 6.74 (s, 1H), 4.30 (s, 2H), 2.40 (s, 3H). **^{13}C NMR** (126 MHz, $CDCl_3$) δ 144.21, 136.70, 135.26, 131.09, 130.52, 130.15, 129.88, 127.27, 126.63, 125.44, 43.30, 21.68. **IR** (thin film) 3268, 3065, 2976, 2924, 1598, 1495, 1333, 1160,

1092 cm^{-1}. **TLC**: R_f = 0.18 (10% EtOAc/hex, UV & $KMnO_4$ visualization). **HRMS** (ESI) calculated for $C_{14}H_{14}ClNO_2S$ ($[M+H]^+$): 296.0507, found: 296.0507.

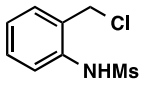

N-(2-(chloromethyl)phenyl)methanesulfonamide:[66] 92% yield (light brown solid), mp 82-85°C. **^{1}H NMR** (500 MHz, $CDCl_3$) δ 7.56 (d, *J* = 7.9 Hz, 1H), 7.42 – 7.37 (m, 2H), 7.22 (td, *J* = 7.5, 1.2 Hz, 1H), 6.67 (s, 1H), 4.68 (s, 2H), 3.10 (s, 3H). **^{13}C NMR** (126 MHz, $CDCl_3$) δ 135.40, 131.10, 130.47, 130.31, 126.48, 123.63, 43.31, 40.31. **IR** (thin film) 3278, 3067, 3024, 2932, 1605, 1587, 1497, 1399, 1326, 1152, 974. **TLC**: R_f = 0.10 (10% EtOAc/hex, UV & $KMnO_4$ visualization).

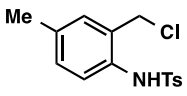

N-(2-Chloromethyl-4-methyl-phenyl)-4-methyl-benzenesulfonamide: 95% yield (white solid), mp 93-96°C. **^{1}H NMR** (500 MHz, $CDCl_3$) δ 7.62 (d, *J* = 8.4 Hz, 2H), 7.24 (d, *J* = 8.1 Hz, 2H), 7.19 (d, *J* = 8.2 Hz, 1H), 7.11 – 7.05 (m, 2H), 6.58 (s, 1H), 4.24 (s, 2H), 2.40 (s, 3H), 2.30 (s, 3H). **^{13}C NMR** (126 MHz, $CDCl_3$) δ 144.09, 137.01, 136.84, 132.41, 131.72, 131.10, 130.74, 129.85, 127.29, 126.30, 43.35, 21.70, 20.95. **IR** (CH_2Cl_2, film) 3267, 3030, 2923, 1598, 1503, 1332, 1161, 1092 cm^{-1}. **TLC**: R_f = 0.23 (10% EtOAc/hex, UV & $KMnO_4$ visualization). **HRMS** (ESI) calculated for $C_{15}H_{16}ClNO_2S$ ($[M+H]^+$): 310.0663, found: 310.0675.

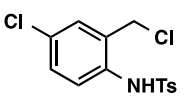

N-(4-Chloro-2-chloromethyl-phenyl)-4-methyl-benzenesulfonamide: 99% yield (white solid), mp 99-102°C. **^{1}H NMR** (500 MHz, $CDCl_3$) δ 7.63 (d, *J* = 8.3 Hz, 2H), 7.30 – 7.26 (m, 5H), 6.76 (s, 1H), 4.25 (s, 2H), 2.41 (s, 3H). **^{13}C**

NMR (126 MHz, $CDCl_3$) δ 144.48, 136.38, 133.65, 133.26, 132.24, 130.39, 130.19, 130.01, 127.30, 127.14, 42.39, 21.72. **IR** (thin film) 3261, 3064, 2977, 1598, 1488, 1332, 1162, 1092 cm^{-1}. **TLC**: R_f = 0.17 (10% EtOAc/hex, UV & $KMnO_4$ visualization). **HRMS** (ESI) calculated for $C_{14}H_{13}Cl_2NO_2S$ ($[M+H]^+$): 330.0117, found: 330.0123.

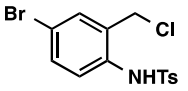

N-(4-bromo-2-(chloromethyl)phenyl)-4-methylbenzenesulfonamide: 83% yield (tan solid), mp 108-110°C. **^{1}H NMR** (500 MHz, $CDCl_3$) δ 7.64 (d, *J* = 8.2 Hz, 2H), 7.44-7.36 (m, 2H), 7.27-7.20 (m, 3H), 6.76 (bs, 1H), 4.24 (s, 2H), 2.41 (s, 3H). **^{13}C NMR (**126 MHz, $CDCl_3$) δ 144.52, 136.33, 134.27, 133.29, 133.17, 133.05, 130.03, 127.28, 127.12, 119.84, 42.34, 21.73. **IR** (thin film) 3268, 3064, 2979, 1597, 1486, 1332, 1162, 1092 cm^{-1}. **TLC**: R_f = 0.17 (10% EtOAc/hex, UV & $KMnO_4$ visualization). **HRMS** (ESI) calculated for $C_{14}H_{13}ClBrNO_2S$ ($[M+H]^+$): 373.9612, found: 373.9607.

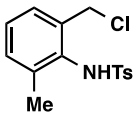

N-(2-Chloromethyl-6-methyl-phenyl)-4-methyl-benzenesulfonamide[2]: 92% yield (white solid), mp 119-122°C. **^{1}H NMR** (500 MHz, $CDCl_3$) δ 7.60 (d, *J* = 8.2 Hz, 2H), 7.27-7.21 (m, 5H), 6.25 (s, 1H), 4.40 (s, 2H), 2.44 (s, 3H), 2.04 (s, 3H). **^{13}C NMR** (126 MHz, $CDCl_3$) δ 144.24, 138.64, 137.42, 136.99, 132.64, 131.91, 129.95, 128.63, 128.39, 127.26, 43.95, 21.73, 18.59. **IR** (thin film) 3250, 3062, 2979, 2928, 1597, 1467, 1398, 1330, 1160, 1092 cm^{-1}. **TLC**: R_f = 0.20 (10% EtOAc/hex, UV & $KMnO_4$ visualization). **HRMS** (ESI) calculated for $C_{15}H_{16}ClNO_2S$ ($[M+H]^+$): 310.0663, found: 310.0683.

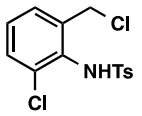

N-(2-chloro-6-(chloromethyl)phenyl)-4-methylbenzenesulfonamide: 95% yield (orange solid), mp 115-117^{o}C. **^{1}H NMR** (500 MHz, $CDCl_3$) δ 7.57 (dd, *J* = 7.6, 1.7 Hz, 1H), 7.49 (d, *J* = 8.3 Hz, 2H), 7.27-7.21 (m, 4H), 6.38 (s, 1H), 4.99 (s, 2H), 2.42 (s, 3H). **^{13}C NMR** (126 MHz, $CDCl_3$) δ 144.54, 139.72, 136.11, 132.66, 130.97, 129.92, 129.72, 129.47, 128.99, 127.71, 43.01, 21.77. **IR** (thin film) 3294, 3065, 2978, 2924, 1598, 1574, 1446, 1399, 1334, 1163, 1091cm^{-1}. **TLC**: R_f = 0.20 (10% EtOAc/hex, UV & $KMnO_4$ visualization). **HRMS** (ESI) calculated for $C_{14}H_{13}Cl_2NO_2S$ ($[M+H]^+$): 330.0117, found: 330.0168.

Synthesis of Tri-substituted Substrates[67]

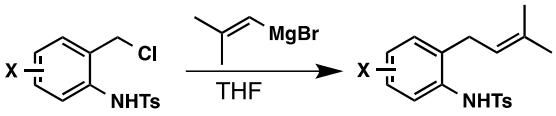

To the commercially available 2-methyl-1-propenylmagnesium bromide solution (Aldrich, 0.5 M, 3 eq) was added the corresponding benzenesulfonamide (1 eq) dropwise over 30 minutes in THF (0.2 M). The solution was stirred at room temperature for 6 h, then quenched at 0 ^{o}C with H_2O, extracted with Et_2O (3 x 30 mL), washed with brine (30 mL), dried with $MgSO_4$, and concentrated *in vacuo*. The crude product was purified by silica flash column chromatography (10-15% EtOAc/Hex).

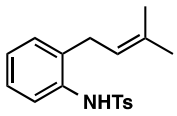

4-methyl-*N*-(2-(3-methylbut-2-en-1-yl)phenyl)benzenesulfonamide (**3a**): 83% (white solid), mp 69-71°C. **^{1}H NMR** (500 MHz, $CDCl_3$) δ 7.58 (d, *J* = 8.3 Hz, 2H), 7.45 (d, *J* = 7.8, 1H), 7.24 – 7.15 (m, 3H), 7.10 – 7.03 (m, 2H), 6.51 (s, 1H), 4.97-4.95 (m, 1H), 2.95 (d, *J* = 7.1 Hz, 2H), 2.38 (s, 3H), 1.74 (d, *J* = 1.5 Hz, 3H), 1.71 (s, 3H). **^{13}C NMR** (126 MHz, $CDCl_3$) δ 143.86, 136.94, 135.17, 134.88, 133.62, 130.05, 129.66, 127.41, 127.23, 126.00, 123.76, 121.38, 31.20, 25.78, 21.65, 17.96. **IR** (thin film) 3276, 2972, 2923, 2856, 1492, 1333, 1161, 1091 cm^{-1}. **TLC**: R_f = 0.29 (4:1 hex/Et_2O, UV & $KMnO_4$ visualization). **HRMS** (ESI) calculated for $C_{18}H_{21}NO_2S$ ($[M+H]^+$): 316.1366, found: 316.1452.

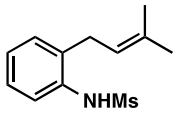

N-(2-(3-methylbut-2-en-1-yl)phenyl)methanesulfonamide (**3aa**): 57% yield (white solid), mp 75-78°C. **^{1}H NMR** (500 MHz, $CDCl_3$) δ 7.50 (d, *J* = 7.9 Hz, 1H), 7.23 (ddd, *J* = 12.8, 7.7, 1.7 Hz, 2H), 7.13 (td, *J* = 7.5, 1.3 Hz, 1H), 6.44 (s, 1H), 5.17 (tdd, *J* = 6.9, 2.8, 1.4 Hz, 1H), 3.36 (d, *J* = 7.1 Hz, 2H), 2.99 (s, 3H), 1.82 (s, 4H), 1.80 – 1.76 (m, 6H). **^{13}C NMR** (75 MHz, $CDCl_3$) δ 135.46, 135.24, 132.60, 130.60, 127.84, 125.88, 122.00, 121.35, 39.83, 31.75, 25.84, 18.04. **IR** (thin film) 3277, 2970, 2925, 2857, 1492, 1325, 1153, 973, 748 cm^{-1}. **TLC**: R_f = 0.10 (4:1 hexanes/Et_2O, UV & $KMnO_4$ visualization). **HRMS** (ESI) calculated for $C_{12}H_{17}NO_2S$ ($[M+H]^+$): 240.1105, found: 240.1053.

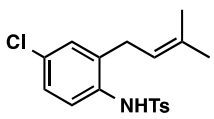

N-(4-chloro-2-(3-methylbut-2-en-1-yl)phenyl)-4-methylbenzenesulfonamide (**3c**): 63% yield (pale yellow solid), mp

79-81°C. **^{1}H NMR** (500 MHz, $CDCl_3$) δ 7.57 (d, *J* = 8.3 Hz, 2H), 7.38 (d, *J* = 8.6 Hz, 1H), 7.23 (d, *J* = 8.0 Hz, 2H), 7.15 (dd, *J* = 8.6, 2.5 Hz, 1H), 7.04 (d, *J* = 2.5 Hz, 1H), 6.44 (s, 1H), 4.93 (t, *J* = 7.2 Hz, 1H), 2.90 (d, *J* = 7.1 Hz, 2H), 2.40 (s, 3H), 1.74 (s, 3H), 1.68 (s, 3H). **^{13}C NMR** (126 MHz, $CDCl_3$) δ 144.17, 136.68, 135.77, 135.68, 133.74, 131.49, 129.91, 129.82, 127.45, 127.25, 125.30, 120.44, 30.99, 25.82, 21.70, 18.00. **IR** (thin film) 3277, 2970, 2917, 2857, 1484, 1332, 1162, 1092 cm^{-1}. **TLC**: R_f = 0.24 (4:1 hexanes/Et_2O, UV & $KMnO_4$ visualization). **HRMS** (ESI) calculated for $C_{18}H_{20}ClNO_2S$ ($[M+H]^+$): 350.0976, found: 350.0991.

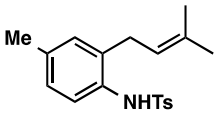

4-methyl-*N*-(4-methyl-2-(3-methylbut-2-en-1-yl)phenyl)benzenesulfonamide (**3b**): 65% yield (pale yellow solid), mp 81-82 °C. **^{1}H NMR** (500 MHz, $CDCl_3$) δ 7.56 (dd, *J* = 8.5, 2.2 Hz, 2H), 7.29 (d, *J* = 8.1 Hz, 1H), 7.21 (d, *J* = 8.2 Hz, 2H), 6.97 (d, *J* = 8.2 Hz, 1H), 6.86 (d, *J* = 2.0 Hz, 1H), 6.38 (s, 1H), 4.96 – 4.93 (m, 1H), 2.89 (d, *J* = 7.1 Hz, 2H), 2.39 (s, 3H), 2.27 (s, 3H), 1.72 (s, 3H), 1.69 (s, 3H). **^{13}C NMR** (126 MHz, $CDCl_3$) δ 143.73, 137.06, 136.04, 134.56, 134.14, 132.40, 130.72, 129.64, 128.01, 127.28, 124.50, 121.62, 31.16, 25.81, 21.67, 21.05, 17.98. **IR** (thin film) 3280, 2970, 2920, 2857, 1497, 1332, 1163, 1092 cm^{-1}. **TLC**: R_f = 0.31 (4:1 hexanes/Et_2O, UV & $KMnO_4$ visualization). **HRMS** (ESI) calculated for $C_{19}H_{23}NO_2S$ ($[M+H]^+$): 330.1522, found: 330.1594.

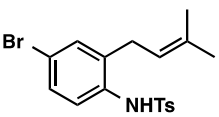

N-(4-bromo-2-(3-methylbut-2-en-1-yl)phenyl)-4-methylbenzenesulfonamide (**3d**): 60% yield (white solid), mp 90-

92°C. **^{1}H NMR** (500 MHz, $CDCl_3$) δ 7.58 (d, *J* = 8.4 Hz, 2H), 7.34 – 7.28 (m, 2H), 7.23 (d, *J* = 8.1 Hz, 2H), 7.19 (d, *J* = 2.2 Hz, 1H), 6.48 (s, 1H), 4.96 – 4.89 (m, 1H), 2.91 (d, *J* = 7.1 Hz, 2H), 2.40 (s, 3H), 1.74 (s, 3H), 1.68 (s, 3H). **^{13}C NMR** (126 MHz, $CDCl_3$) δ 144.20, 136.65, 135.81, 135.76, 134.34, 132.84, 130.45, 129.84, 127.25, 125.35, 120.43, 119.30, 30.99, 25.83, 21.70, 18.01. **IR** (thin film) 3276, 2970, 2915, 1597, 1482, 1384, 1332, 1162, 1092 cm^{-1}. **TLC**: R_f = 0.20 (4:1 hexanes/Et_2O, UV & $KMnO_4$ visualization). **HRMS** (ESI) calculated for $C_{18}H_{20}BrNO_2S$ ($[M+H]^+$): 394.0471, found: 394.075.

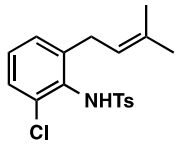

N-(2-chloro-6-(3-methylbut-2-en-1-yl)phenyl)-4-methylbenzenesulfonamide (**3f**) 63% yield (pale yellow solid), mp 52-56 °C. **^{1}H NMR** (500 MHz, $CDCl_3$) δ 7.54 (d, *J* = 8.3 Hz, 2H), 7.20 (d, *J* = 8.0 Hz, 2H), 7.17 (dd, *J* = 7.5, 1.8 Hz, 1H), 7.11 (app. t, *J* = 7.7 Hz, 1H), 7.07 (dd, *J* = 7.9, 1.8 Hz, 1H), 6.19 (s, 1H), 5.23-5.20 (m, 1H), 3.62 (d, *J* = 7.3 Hz, 2H), 2.40 (s, 3H), 1.75 (s, 3H), 1.71 (s, 3H). **^{13}C NMR** (126 MHz, $CDCl_3$) δ 144.22, 144.07, 136.97, 133.89, 132.86, 131.19, 129.59, 129.19, 128.62, 127.76, 127.24, 122.37, 31.32, 25.90, 21.75, 18.14. **IR** (thin film) 3253, 2970, 2922, 2856, 1444, 1333, 1164, 1092 cm^{-1}. **TLC**: R_f = 0.39 (4:1 hexanes/Et_2O, UV & $KMnO_4$ visualization). **HRMS** (ESI) calculated for $C_{18}H_{20}ClNO_2S$ ($[M+H]^+$): 350.0976, found: 350.0999.

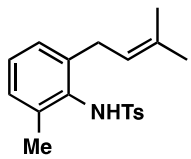

4-methyl-*N*-(2-methyl-6-(3-methylbut-2-en-1-yl)phenyl)benzenesulfonamide (**3e**): 68% yield (pale yellow solid), mp 69-74 °C. **^{1}H NMR** (500 MHz, $CDCl_3$) δ 7.57 (d, *J* = 8.3 Hz, 2H), 7.24

(d, *J* = 8.1 Hz, 2H), 7.11 (t, *J* = 7.5 Hz, 1H), 7.06 (d, *J* = 7.5 Hz, 1H), 6.97 (dd, *J* = 7.6, 1.7 Hz, 1H), 5.97 (s, 1H), 4.97 – 4.93 (m, 1H), 2.94 (d, *J* = 7.0 Hz, 2H), 2.42 (s, 3H), 2.17 (s, 3H), 1.70 – 1.68 (s, 3H), 1.59 (s, 3H). **^{13}C NMR** (126 MHz, $CDCl_3$) δ 143.81, 140.63, 138.28, 137.75, 133.89, 132.64, 129.69, 129.40, 128.00, 127.75, 127.43, 122.25, 31.05, 25.81, 21.70, 19.22, 18.03. **IR** (thin film) 3264, 2968, 2924, 2858, 1463, 1327, 1159, 1092 cm^{-1}. **TLC**: R_f = 0.26 (4:1 hexanes/Et_2O, UV & $KMnO_4$ visualization). **HRMS** (ESI) calculated for $C_{19}H_{23}NO_2S$ ($[M+H]^+$): 330.1522, found: 330.1584.

Typical Procedure for the Gringard Reaction
of Tri-substituted Alkene Substrates[6]

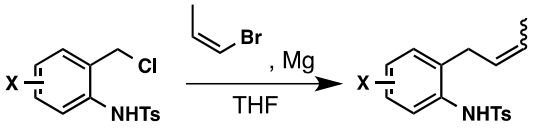

To magnesium turnings (3 eq, stirred vigorously overnight under Ar), was added cis-1-bromo-1-propene (3 eq) in THF and heated at 50 ^oC for 1.5 h. After cooling to r.t. the corresponding benzenesulfonamide (1 eq) was added dropwise over 30 minutes in THF (0.15 M) and continued to stir at r.t. for 6 h. The reaction was quenched at 0 ^oC with H_2O, extracted with Et_2O (3 x 30 mL), washed with brine (30 mL), dried with $MgSO_4$, filtered and concentrated *in vacuo*. The crude product was purified by silica column chromatography (10-15% EtOAc/Hex).

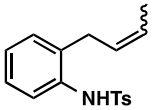

N-(2-(but-2-en-1-yl)phenyl)-4-methylbenzenesulfonamide (**4a**): 60% yield

(white solid, 87:13 *Z/E* isomer). **^{1}H NMR** (500 MHz, $CDCl_3$) *Z*-isomer δ 7.59 (d, *J* = 8.4 Hz, 2H), 7.41 (d, *J* = 7.9 Hz, 5H), 7.20 (m, 3H), 7.11 – 7.07 (m, 2H), 6.47 (s, 1H), 5.68 – 5.61 (m, 1H), 5.28-5.22 (m, 1H), 3.03 (d, *J* = 7.2 Hz, 12H), 2.39 (s, 3H), 1.71 (d, *J* = 6.8, 3H). *E*-isomer identical (or unseen) as *Z*-isomer except for δ 6.60 (s, 1H), 5.39 – 5.37 (m, 1H), 2.92 (d, *J* = 4.7 Hz, 2H), 1.68 – 1.65 (m, 2H). **^{13}C NMR** (75 MHz, $CDCl_3$) mixture of isomers δ 143.92, 136.91, 135.14, 133.39, 130.48, 130.13, 129.73, 129.70, 128.36, 127.99, 127.71, 127.57, 127.25, 127.22, 126.93, 126.23, 126.14, 124.20, 124.14, 35.35, 30.02, 21.70, 18.01, 13.04. **HRMS** (ESI) calculated for $C_{17}H_{19}NO_2S$ ($[M+H]^+$): 302.1209, found: 302.1284.

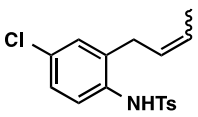

N-(2-(but-2-en-1-yl)-4-chlorophenyl)-4-methylbenzenesulfonamide (**4c**): 58% yield (light brown solid, 93:7 *Z/E* isomer). **^{1}H NMR** (500 MHz, $CDCl_3$) *Z*-isomer δ 7.58 (d, *J* = 8.2 Hz, 2H), 7.34 (d, *J* = 8.5 Hz, 1H), 7.24 (d, *J* = 8.1 Hz, 2H), 7.15 (dd, *J* = 8.5, 2.5 Hz, 2H), 7.07 (d, *J* = 2.5 Hz, 2H), 6.41 (s, 1H), 5.70 – 5.65 (m, 1H), 5.23 – 5.20 (m, 1H), 2.98 (d, *J* = 7.3 Hz, 2H), 2.40 (s, 3H), 1.68 (d, *J* = 6.9, 3H). *E*-isomer identical (or unseen) as *Z*-isomer except for δ 7.03 (d, *J* = 2.5 Hz, 1H), 6.52 (s, 1H), 5.38 (d, *J* = 6.3 Hz, 1H), 2.87 (d, *J* = 5.8 Hz, 2H). **^{13}C NMR** (126 MHz, $CDCl_3$) mixture of isomers δ 144.20, 136.69, 135.56, 133.67, 131.77, 130.31, 129.96, 129.84, 128.72, 127.70, 127.67, 127.57, 127.48, 127.27, 127.22, 126.30, 125.79, 125.72, 35.06, 29.71, 21.70, 13.04. **HRMS** (ESI) calculated for $C_{17}H_{18}ClNO_2S$ ($[M+H]^+$): 336.0820, found: 336.0838.

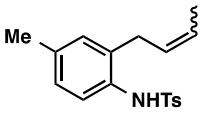

N-(2-(but-2-en-1-yl)-4-methylphenyl)-4-methylbenzenesulfonamide (**4b**): 63% yield (white solid, 91:9 *Z/E* isomer). **^{1}H NMR** (500 MHz, $CDCl_3$) *Z*-isomer δ 7.57 (d, *J* = 8.3 Hz, 2H), 7.25 – 7.19 (m, 3H), 6.98 (dd, *J* = 8.1, 2.1 Hz, 1H), 6.89 (s, 1H), 6.33 (s, 1H), 5.65 – 5.58 (m, 1H), 5.28 – 5.17 (m, 1H), 2.97 (d, *J* = 7.2 Hz, 2H), 2.39 (s, 3H), 2.27 (s, 3H), 1.69 (d, *J* = 6.9, 3H). *E*-isomer identical (or unseen) as *Z*-isomer except for δ 6.45 (s, 1H), 5.36 (t, *J* = 5.4 Hz, 1H), 2.85 (d, *J* = 4.5 Hz, 2H), 1.66 (dd, *J* = 4.9, 1.6 Hz, 3H). **^{13}C NMR** (126 MHz, $CDCl_3$) δ 143.77, 137.09, 136.32, 134.03, 132.35, 130.77, 129.66, 128.11, 127.48, 127.31, 126.60, 124.97, 29.91, 21.69, 21.07, 13.04. **HRMS** (ESI) calculated for $C_{18}H_{21}NO_2S$ ($[M+H]^+$): 316.1366, found: 316.1406.

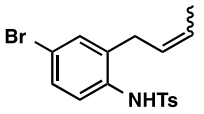

N-(4-bromo-2-(but-2-en-1-yl)phenyl)-4-methylbenzenesulfonamide (**4d**): 55% yield (brown solid, 91:9 *Z/E* isomer). **^{1}H NMR** (500 MHz, $CDCl_3$) *Z*-isomer δ 7.58 (d, *J* = 8.3 Hz, 2H), 7.32 – 7.28 (m, 2H), 7.25 – 7.21 (m, 3H), 6.41 (s, 1H), 5.71 – 5.65 (m, 1H), 5.24 – 5.18 (m, 1H), 2.98 (d, *J* = 7.2 Hz, 2H), 2.40 (s, 3H), 1.69 (d, *J* = 6.5 Hz, 3H). *E*-isomer identical (or unseen) as *Z*-isomer except for δ 6.53 (s, 1H), 5.38 (app t, *J* = 6.0 Hz, 1H), 5.34 (d, *J* = 6.1 Hz, 1H), 2.87 (d, *J* = 5.8 Hz, 2H). **^{13}C NMR** (126 MHz, $CDCl_3$) mixture of isomers) δ 144.22, 136.65, 135.72, 134.23, 133.21, 132.86, 130.65, 130.53, 129.84, 127.67, 127.46, 127.25, 127.21, 126.27, 125.88, 125.79, 119.59, 34.98, 29.63, 21.69, 13.03 **HRMS** (ESI) calculated for $C_{17}H_{18}BrNO_2S$ ($[M+H]^+$): 380.0314, found: 380.0310.

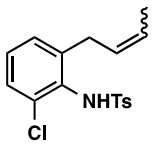

N-(2-(but-2-en-1-yl)-6-chlorophenyl)-4-methylbenzenesulfonamide (**4f**): 16% yield (white solid, 93:7 *Z/E* isomer). **^{1}H NMR** (500 MHz, $CDCl_3$) *Z*-isomer δ 7.55 (d, *J* = 8.3 Hz, 2H), 7.22 (m, 3H), 7.14 (app t, *J* = 7.7 Hz, 1H), 7.10 (dd, *J* = 7.9, 1.8 Hz, 1H), 6.24 (s, 1H), 5.67 – 5.60 (m, 1H), 5.53 – 5.46 (m, 1H), 3.73 (d, *J* = 7.3 Hz, 2H), 2.42 (s, 3H), 1.73 (d, *J* = 6.9, 3H). *E*-isomer identical (or unseen) as *Z*-isomer except for δ 7.64 (d, *J* = 8.2 Hz, 2H), 3.61 (d, *J* = 5.7 Hz, 2H), 1.70 (d, *J* = 5.4 Hz, 3H). **^{13}C NMR** (75 MHz, $CDCl_3$) δ 144.12, 143.64, 136.79, 132.82, 131.22, 129.60, 129.18, 128.67, 128.26, 127.74, 127.33, 126.10, 30.11, 21.77, 13.15. **HRMS** (ESI) calculated for $C_{17}H_{18}ClNO_2S$ ($[M+H]^+$): 336.0820, found: 336.0839.

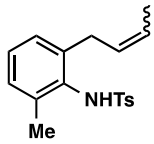

N-(2-(but-2-en-1-yl)-6-methylphenyl)-4-methylbenzenesulfonamide (**4e**): 63% yield (white solid, 90:10 Z/E isomer). **^{1}H NMR** (500 MHz, $CDCl_3$) *Z*-isomer ^{1}H NMR (500 MHz, $CDCl_3$) δ 7.58 (d, *J* = 8.3 Hz, 2H), 7.25 (d, *J* = 8.0 Hz, 2H), 7.13 (app t, *J* = 7.5 Hz, 1H), 7.06 (d, *J* = 7.5 Hz, 1H), 7.01 (d, *J* = 7.4 Hz, 1H), 5.97 (s, 1H), 5.61 – 5.49 (m, 1H), 5.29 – 5.21 (m, 1H), 3.07 (d, *J* = 7.1 Hz, 2H), 2.42 (s, 3H), 2.12 (s, 3H), 1.61 (d, *J* = 6.8, 3H). *E*-isomer identical (or unseen) as *Z*-isomer except for δ 6.12 (d, *J* = 19.7 Hz, 1H), 5.34 – 5.30 (m, 1H), 2.87 (s, 1H), 2.30 (s, 2H), 2.20 (s, 1H). **^{13}C NMR** (126 MHz, $CDCl_3$) mixture of isomers δ 143.85, 140.30, 138.22, 137.77, 132.64, 129.76, 129.72, 129.43, 129.18, 128.23, 128.10, 127.98, 127.80, 127.77, 127.43, 127.31, 127.16, 126.00, 29.89, 21.70, 19.11, 18.03, 13.71, 13.07, 11.90, 11.56. **HRMS** (ESI) calculated for $C_{18}H_{21}NO_2S$ ($[M+H]^+$): 316.1366, found: 316.1427.

Synthesis of Tosylcarbamate 9

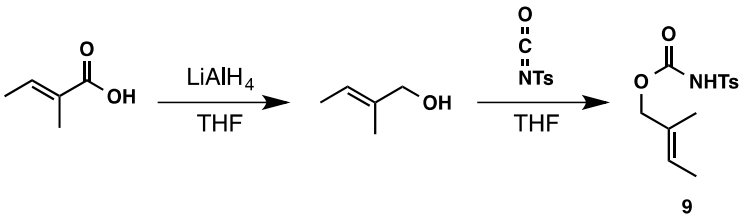

(*E*)-2-methyl-2-butenyl alcohol synthesized according to literature[68] and reacted without further purification with p-toluenesulfonyl isocyanate (1 eq) by dropwise addition at 0 ^{o}C in THF (0.5 M) and stirring at r.t. for 1.5 h. The crude solution was concentrated *in vaccuo* and purified by silica column chromatography (20% EtOAc/Hex). (*E*)-2-methylbut-2-en-1-yl tosylcarbamate (**9**): 48% yield over two steps (clear oil). **^{1}H NMR** (500 MHz,$CDCl_3$) δ 7.92 (d, *J* = 8.4 Hz, 2H), 7.52 (bs, 1H), 7.33 (d, *J* = 8.1 Hz, 3H), 5.55 – 5.45 (m, 1H), 4.45 (s, 2H), 2.45 (s, 3H), 1.60 (d, *J* = 7.0 Hz, 3H), 1.56 (s, 3H). **^{13}C NMR** (75 MHz, $CDCl_3$) δ 150.61, 145.12, 135.65, 129.77, 129.69, 128.50, 128.43, 125.80, 72.94, 21.80, 13.59, 13.38. **IR** (thin film) 3242, 3070, 2984, 2921, 1749, 1495, 1348, 1225, 1161, 1091 cm^{-1}. **TLC**: R_f = 0.29 (20% EtOAc/hexanes, UV & $KMnO_4$ visualization).

Synthesis of 10

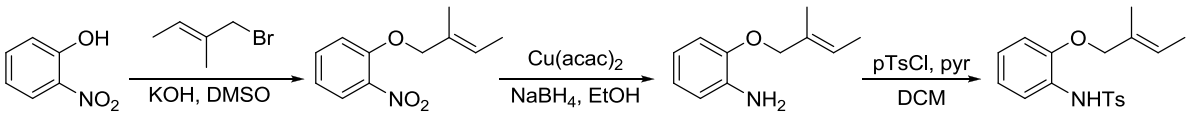

(*E*)-4-methyl-*N*-(2-((2-methylbut-2-en-1-yl)oxy)phenyl)benzenesulfonamide (**10**) was synthesized in three steps from 2-nitrophenol according to literature procedures,[69] 63%

yield (tan solid), mp 76-77 °C. **^{1}H NMR** (500 MHz, $CDCl_3$) δ 7.63 (d, *J* = 8.0 Hz, 2H), 7.55 (dd, *J* = 8.0, 1.7 Hz, 1H), 7.17 (d, *J* = 8.0 Hz, 2H), 7.04 – 6.96 (m, 2H), 6.88 (app t, *J* = 7.6 Hz, 1H), 6.72 (d, *J* = 8.0 Hz, 1H), 5.46 – 5.42 (m, 1H), 4.20 (s, 2H), 2.35 (s, 3H), 1.64 (d, *J* = 6.8 Hz, 3H), 1.58 (s, 3H). **^{13}C NMR** (126 MHz, $CDCl_3$) δ 148.88, 143.68, 136.54, 130.95, 129.49, 127.33, 126.31, 125.26, 124.18, 121.20, 121.10, 111.96, 74.68, 21.61, 13.63, 13.36. **IR** (thin film) 3337, 3270, 2981, 2920, 2861, 1599, 1497, 1340, 1166 cm^{-1}. **TLC**: R_f = 0.33 (10% EtOAc/hexanes, UV & $KMnO_4$ visualization). **HRMS** (ESI) calculated for $C_{18}H_{21}NO_3S$ ($[M+H]^+$): 332.1315, found: 332.1319.

Typical Procedure for Oxidative Amination

To a flame-dried 2-dram vial was added $Pd(OAc)_2$ (2.2 mg, 0.01 mmol) and (+)-CSA (4.6 mg, 0.02 mmol) and stirred under Ar for 20 min at r.t. with PhH* (0.4 mL). To the reaction flask was added the substrate (0.1 mmol), benzoquinone (21.8 mg, 0.2 mmol) and (+)-CSA^-Na^+ (2.5 mg, 0.01 mmol) with PhH (0.6 mL). The vial was capped and stirred the corresponding time and temperature as listed in Table 2.5. The crude product was diluted with EtOAc (3 mL) and stirred vigorously with sat. $Na_2S_2O_3$ (4 mL). The organic layer was washed with sat. $Na_2S_2O_3$ (2 x 5 mL), sat. K_2CO_3 (2 x 5 mL), and water (5 mL), dried with $MgSO_4$ and concentrated *in vacuo*. The crude product was purified by silica column chromatography (4:1 hexanes/Et_2O or 10-20% EtOAc/Hex).

***Note**: It was discovered the use of anhydrous PhH gave lower conversions in comparison to PhH containing a trace amounts of H_2O. As such, PhH was washed with

H_2O (v/v = 1:1) and dried with Na_2SO_4 (1.0g/10 mL PhH) for at least 5 hours. This observation and procedure are consistent with previous results in our laboratory.[18] Racemic products for the HPLC assay were synthesized by an identical procedure omitting (+)-CSA^-Na^+ and utilizing (+/-)-CSA in exchange for the chiral ligand.

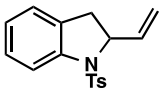

1-tosyl-2-vinylindoline (**12a**): 54% yield (white solid), mp 99-102 °C. **^{1}H NMR** (500 MHz, $CDCl_3$) δ 7.66 (d, *J* = 8.1 Hz, 1H), 7.59 (d, *J* = 8.0 Hz, 2H), 7.20 (dd, *J* = 19.5, 7.9 Hz, 3H), 7.06 – 6.98 (m, 2H), 5.91 (ddd, *J* = 16.8, 10.2, 6.2 Hz, 1H), 5.39 (d, *J* = 16.9 Hz, 1H), 5.15 (d, *J* = 10.3 Hz, 1H), 4.79 – 4.69 (m, 1H), 2.95 (dd, *J* = 16.0, 9.7 Hz, 1H), 2.65 (dd, *J* = 16.0, 3.2 Hz, 1H), 2.36 (s, 3H). **^{13}C NMR** (126 MHz, $CDCl_3$) δ 143.97, 141.59, 137.76, 135.59, 131.37, 129.69, 127.93, 127.25, 125.19, 124.63, 117.01, 115.89, 63.97, 35.14, 21.65. **IR** (thin film) 3067, 2984, 2921, 2853, 1599, 1477, 1460, 1355, 1168 cm^{-1}. **TLC**: R_f = 0.46 (4:1 hexanes/Et_2O, UV & $KMnO_4$ visualization). **HRMS** (ESI) calculated for $C_{17}H_{17}NO_2S$ ($[M+H]^+$): 300.1053, found: 300.1175. **HPLC**: Daicel CHIRALCEL AD-H column, 2% IPA in hexanes, 1.0 mL/min, λ=254 nm: t_R(major) = 14.9 min, t_R(minor) = 22.9 min.

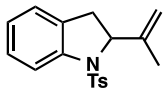

2-(prop-1-en-2-yl)-1-tosylindoline (**11a**): 74% yield (white solid), mp 83-86 °C. **^{1}H NMR** (500 MHz, $CDCl_3$) δ 7.68 (d, *J* = 8.1 Hz, 1H), 7.60 (d, *J* = 8.2 Hz, 2H), 7.23 – 7.15 (m, 3H), 7.05 – 6.97 (m, 2H), 5.07 (s, 1H), 4.86 (s, 1H), 4.66 (dd, *J* = 10.1, 3.8 Hz, 1H), 2.98 (dd, *J* = 16.3, 10.1 Hz, 1H), 2.69 (dd, *J* = 16.2, 3.8 Hz, 1H), 2.36 (s, 3H), 1.70 (s, 3H). **^{13}C NMR** (126 MHz, $CDCl_3$) δ 144.53, 143.94, 142.17,

135.34, 131.53, 129.67, 127.91, 127.31, 124.95, 124.45, 116.54, 112.38, 66.93, 34.49, 21.66, 17.85. **IR** (thin film) 2920, 2852, 1478, 1461, 1355, 1169, 1091 cm^{-1}. **TLC**: R_f = 0.23 (4:1 hexanes/Et_2O, UV & $KMnO_4$ visualization). **HRMS** (ESI) calculated for $C_{18}H_{19}NO_2S$ ($[M+H]^+$): 314.1209, found: 314.1277. **HPLC**: Daicel CHIRALCEL AS-H column, 10% IPA in hexanes, 1.0 mL/min, λ＝254 nm: t_R(major) = 11.6 min, t_R(minor) = 14.5 min.

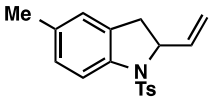

5-methyl-1-tosyl-2-vinylindoline (**12b**): 55% yield (white solid). **^{1}H NMR** (500 MHz, $CDCl_3$) δ 7.57 (d, *J* = 8.3 Hz, 2H), 7.54 (d, *J* = 8.2 Hz, 1H), 7.17 (d, *J* = 8.1 Hz, 2H), 7.01 (d, *J* = 8.1 Hz, 1H), 6.85 (s, 1H), 5.90 (ddd, *J* = 16.6, 10.3, 6.1 Hz, 1H), 5.38 (app dt, *J* = 17.0, 1.4 Hz, 1H), 5.14 (app dt, *J* = 10.2, 1.3 Hz, 1H), 4.76 – 4.66 (m, 1H), 2.87 (dd, *J* = 16.0, 9.6 Hz, 1H), 2.58 (dd, *J* = 16.0, 3.1 Hz, 1H), 2.36 (s, 3H), 2.27 (s, 3H). **^{13}C NMR** (126 MHz, $CDCl_3$) δ 137.79, 129.66, 128.52, 127.27, 125.81, 116.97, 115.74, 64.03, 35.07, 21.65, 21.10. **IR** ($CHCl_3$, film) 2921, 2862, 1598, 1486, 1353, 1166 cm^{-1}. **TLC**: R_f = 0.48 (4:1 hexanes/Et_2O, UV & $KMnO_4$ visualization). **HRMS** (ESI) calculated for $C_{18}H_{19}NO_2S$ ($[M+H]^+$): 314.1209, found: 314.1324. **HPLC**: Daicel CHIRALCEL AS-H column, 10% IPA in hexanes, 1.0 mL/min, λ＝254 nm: t_R(major) = 10.4 min, t_R(minor) = 21.7 min.

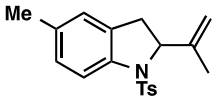

5-methyl-2-(prop-1-en-2-yl)-1-tosylindoline (**11b**): 76% yield (white solid) , 88-90 ^oC. **^{1}H NMR** (500 MHz, $CDCl_3$) δ 7.58 (d, *J* = 8.3 Hz, 2H), 7.55 (d, *J* = 8.2 Hz, 1H), 7.18 (d, *J* = 8.1 Hz, 2H), 7.00 (d, *J* = 8.1 Hz, 1H), 6.83 (s,

1H), 5.06 (s, 1H), 4.85 (s, 1H), 4.62 (dd, *J* = 10.0, 3.7 Hz, 1H), 2.90 (dd, *J* = 16.2, 10.0 Hz, 1H), 2.63 (dd, *J* = 16.2, 3.7 Hz, 1H), 2.36 (s, 3H), 2.27 (s, 3H), 1.70 (s, 3H). **^{13}C NMR** (126 MHz, $CDCl_3$) δ 144.58, 143.81, 139.77, 135.28, 134.23, 131.73, 129.63, 128.48, 127.32, 125.58, 116.47, 112.22, 67.01, 34.41, 21.65, 21.07, 17.94. **IR** (CH_2Cl_2,film) 3076, 2921, 2860, 1487, 1355, 1168, 1091, 816 cm^{-1}. **TLC**: R_f = 0.47 (4:1 hexanes/Et_2O, UV & $KMnO_4$ visualization). **HRMS** (ESI) calculated for $C_{18}H_{21}NO_2S$ ($[M+H]^+$): 328.1366, found: 328.1409. **HPLC**: Daicel CHIRALCEL AD-H column, 2% IPA in hexanes, 1.0 mL/min, λ＝254 nm: t_R(major) = 12.8 min, t_R(minor) = 25.6 min.

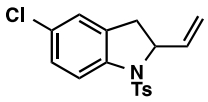

5-chloro-1-tosyl-2-vinylindoline (**12c**): 62% yield (white solid), mp 68-71°C. **^{1}H NMR** (500 MHz, $CDCl_3$ δ 7.59 – 7.57 (m, 3H), 7.21 – 7.17 (m, 3H), 7.01 (s, 1H), 5.89 (ddd, *J* = 16.7, 10.3, 6.1 Hz, 1H), 5.38 (app dt, *J* = 17.0, 1.3 Hz, 1H), 5.17 (app dt, *J* = 10.3, 1.2 Hz, 1H), 4.78 – 4.66 (m, 1H), 2.91 (dd, *J* = 16.2, 9.7 Hz, 1H), 2.62 (dd, *J* = 16.2, 3.3 Hz, 1H), 2.37 (s, 3H). **^{13}C NMR** (126 MHz, $CDCl_3$) δ 144.28, 140.36, 137.30, 135.27, 133.35, 129.91, 129.85, 128.03, 127.23, 125.42, 117.97, 116.21, 64.22, 34.94, 21.68. **IR** (film) 3087, 2954, 2922, 2851, 1597, 1470, 1357, 1166, 1091cm^{-1}. **TLC**: R_f = 0.40 (4:1 hexanes/Et_2O, UV & $KMnO_4$ visualization). **HRMS** (ESI) calculated for $C_{17}H_{17}NO_2S$ ($[M+H]^+$): 334.0663, found: 334.0705. **HPLC**: Daicel CHIRALCEL AD-H column, 2% IPA in hexanes, 1.0 mL/min, λ＝254 nm: t_R(major) = 16.7 min, t_R(minor) = 23.4 min.

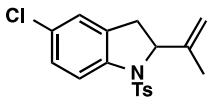

5-chloro-2-(prop-1-en-2-yl)-1-tosylindoline (**11c**): 70% yield (white solid), mp 88-90 ^{o}C. **^{1}H NMR** (500 MHz, $CDCl_3$) δ 7.63 – 7.53 (m, 3H), 7.21 (d, *J* = 8.1 Hz, 2H), 7.17 (dd, *J* = 8.6, 2.2 Hz, 1H), 7.00 (s, 1H), 5.06 (s, 1H), 4.87 (s, 1H), 4.65 (dd, *J* = 10.2, 3.8 Hz, 1H), 2.95 (dd, *J* = 16.5, 10.1 Hz, 1H), 2.67 (dd, *J* = 16.5, 3.8 Hz, 1H), 2.38 (s, 3H), 1.69 (s, 3H). **^{13}C NMR** (126 MHz, $CDCl_3$) δ 144.27, 133.51, 129.82, 127.98, 127.26, 125.18, 117.46, 112.71, 67.19, 34.23, 21.68, 17.80. **IR** (film) 2921, 1598, 1470, 1357, 1167, 1091cm^{-1}. **TLC**: R_f = 0.43 (4:1 hexanes/Et_2O, UV & $KMnO_4$ visualization). **HRMS** (ESI) calculated for $C_{18}H_{18}ClNO_2S$ ($[M+H]^+$): 348.0820, found: 348.0861. **HPLC**: Daicel CHIRALCEL AS-H column, 10% IPA in hexanes, 1.0 mL/min, λ＝254 nm: t_R(major) = 12.5 min, t_R(minor) = 14.9 min.

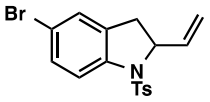

5-bromo-1-tosyl-2-vinylindoline (**11d**): 68% yield (white solid). mp 87-89 ^{o}C **^{1}H NMR** (500 MHz,$CDCl_3$) δ 7.58 (d, *J* = 8.3 Hz, 2H), 7.53 (d, *J* = 8.6 Hz, 1H), 7.32 (dd, *J* = 8.6, 2.0 Hz, 1H), 7.21 (d, *J* = 8.0 Hz, 2H), 7.16 (s, 1H), 5.89 (ddd, *J* = 16.7, 10.3, 6.1 Hz, 1H), 5.38 (app dt, *J* = 16.9, 1.2 Hz, 1H), 5.17 (app d, *J* = 10.3 Hz, 1H), 4.78 – 4.69 (m, 1H), 2.93 (dd, *J* = 16.3, 9.7 Hz, 1H), 2.63 (dd, *J* = 16.2, 3.3 Hz, 1H), 2.37 (s, 3H). **^{13}C NMR** (126 MHz, $CDCl_3$) δ 144.29, 140.87, 137.28, 135.25, 133.69, 130.91, 129.85, 128.31, 127.20, 118.31, 117.39, 116.21, 64.16, 34.87, 21.67. **IR** (thin film) 2921, 2851, 1595, 1468, 1355, 1165 cm^{-1}. **TLC**: R_f = 0.24 (4:1 hexanes/Et_2O, UV & $KMnO_4$ visualization). **HRMS** (ESI) calculated for $C_{17}H_{16}BrNO_2S$ ($[M+H]^+$): 380.0138, found: 380.0172. **HPLC**: Daicel CHIRALCEL AD-H column, 2% IPA in hexanes, 1.0 mL/min, λ＝254 nm: t_R(major) = 17.8 min, t_R(minor) = 26.6 min.

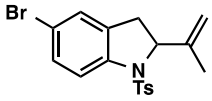

5-bromo-2-(prop-1-en-2-yl)-1-tosylindoline (**12d**): 67% yield (white solid). mp 101-102°C. **^{1}H NMR** (500 MHz, $CDCl_3$) δ 7.59 (d, *J* = 8.3 Hz, 2H), 7.55 (d, *J* = 8.6 Hz, 1H), 7.32 (dd, *J* = 8.6, 2.0 Hz, 1H), 7.21 (d, *J* = 8.1 Hz, 2H), 7.15 (s, 1H), 5.05 (s, 1H), 4.87 (s, 1H), 4.65 (dd, *J* = 10.1, 3.8 Hz, 1H), 2.97 (dd, *J* = 16.5, 10.1 Hz, 1H), 2.68 (dd, *J* = 16.5, 3.9 Hz, 1H), 2.38 (s, 3H), 1.69 (s, 3H). **^{13}C NMR** (126 MHz, $CDCl_3$) δ 144.28, 144.06, 141.46, 135.03, 133.86, 130.89, 129.83, 128.09, 127.27, 117.84, 117.18, 112.74, 67.17, 34.21, 21.69, 17.77. **IR** ($CHCl_3$, film) 3080, 2920, 1652, 1597, 1469, 1357, 1156 cm^{-1}. **TLC**: R_f = 0.30 (4:1 hexanes/Et_2O, UV & $KMnO_4$ visualization). **HRMS** (ESI) calculated for $C_{18}H_{18}BrNO_2S$ ($[M+H]^+$): 392.0314, found: 392.0394. **HPLC**: Daicel CHIRALCEL AD-H column, 2% IPA in hexanes, 1.0 mL/min, λ＝254 nm: t_R(major) = 14.3 min, t_R(minor) = 28.5 min.

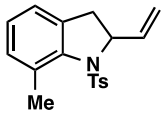

7-methyl-1-tosyl-2-vinylindoline (**12e**): 66% yield (white solid), mp 106-108°C. **^{1}H NMR** (500 MHz, $CDCl_3$) δ 7.39 (d, *J* = 8.2 Hz, 2H), 7.15 (d, *J* = 8.1 Hz, 2H), 7.10 (d, *J* = 7.7 Hz, 1H), 7.04 (app t, *J* = 7.5 Hz, 1H), 6.85 (d, *J* = 7.3 Hz, 1H), 5.70 (ddd, *J* = 17.0, 10.3, 5.0 Hz, 1H), 5.33 (app dt, *J* = 16.9, 1.5 Hz, 1H), 5.05 (app dt, *J* = 10.3, 1.5 Hz, 1H), 4.83 – 4.74 (m, 1H), 2.60 (s, 3H), 2.39 (s, 3H), 2.28 (dd, *J* = 15.7, 7.8 Hz, 1H), 2.22 (d, *J* = 15.5 Hz, 1H). **^{13}C NMR** (126 MHz, $CDCl_3$) δ 144.03, 140.74, 136.53, 136.02, 135.11, 132.90, 130.43, 129.51, 127.73, 126.74, 122.29, 115.75, 64.94, 34.64, 21.72, 20.08. **IR** (CH_2Cl_2, film) 3020, 2923, 2851, 1597, 1458, 1355, 1164 cm^{-1}. **TLC**: R_f = 0.50 (4:1 hexanes/Et_2O, UV & $KMnO_4$ visualization **HRMS** (ESI) calculated for $C_{18}H_{19}NO_2S$ ($[M+H]^+$): 314.1209, found: 314.1351. **HPLC**: Daicel

CHIRALCEL AS-H column, 10% IPA in hexanes, 1.0 mL/min, λ=254 nm: t_R(major) = 10.4 min, t_R(minor) = 21.7 min.

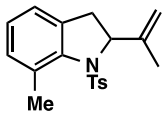

7-methyl-2-(prop-1-en-2-yl)-1-tosylindoline (**11e**): 66% yield (white solid). **^{1}H NMR** (500 MHz, $CDCl_3$) δ 7.42 – 7.35 (m, 2H), 7.15 (d, *J* = 8.0 Hz, 2H), 7.10 (d, *J* = 7.6 Hz, 1H), 7.03 (app t, *J* = 7.5 Hz, 1H), 6.84 (d, *J* = 7.3 Hz, 1H), 4.92 (s, 1H), 4.77 (s, 1H), 4.67 (d, *J* = 8.2 Hz, 1H), 2.59 (s, 3H), 2.39 (s, 3H), 2.34 (d, *J* = 15.8 Hz, 1H), 2.24 (dd, *J* = 16.0, 8.2 Hz, 1H), 1.65 (s, 3H). **^{13}C NMR** (126 MHz, $CDCl_3$) δ 143.98, 143.03, 141.09, 136.54, 134.88, 132.59, 130.38, 129.49, 127.74, 126.68, 121.98, 112.05, 67.69, 33.32, 21.72, 20.05, 19.42. **IR** (CH_2Cl_2, film) 3050, 2922, 1597, 1458, 1444, 1353, 1167, 1091 cm^{-1}. **TLC**: R_f = 0.51 (4:1 hexanes/Et_2O, UV & $KMnO_4$ visualization). **HRMS** (ESI) calculated for $C_{18}H_{21}NO_2S$ ($[M+H]^+$): 328.1366, found: 328.1430. **HPLC**: Daicel CHIRALCEL AS-H column, 10% IPA in hexanes, 1.0 mL/min, λ=254 nm: t_R(major) = 7.0 min, t_R(minor) = 8.3 min.

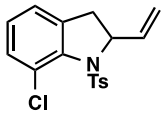

7-chloro-1-tosyl-2-vinylindoline (**12f**): 46% yield (white solid), mp 100-101°C. **^{1}H NMR** (500 MHz, $CDCl_3$) δ 7.61 (d, *J* = 8.3 Hz, 2H), 7.27 (d, *J* = 8.2 Hz, 1H), 7.23 (d, *J* = 8.0 Hz, 2H), 7.06 (app t, *J* = 7.7 Hz, 1H), 7.00 (d, *J* = 7.4 Hz, 1H), 5.69 (ddd, *J* = 16.9, 10.3, 5.0 Hz, 1H), 5.34 – 5.30 (m, 1H), 5.06 (app dt, *J* = 10.4, 1.4 Hz, 1H), 4.98 (m, 1H), 2.76 (dd, *J* = 15.7, 8.2 Hz, 1H), 2.42 – 2.39 (m, 4H). **^{13}C NMR** (126 MHz, $CDCl_3$) δ 144.22, 139.41, 138.21, 135.88, 135.77, 129.66, 129.59, 127.73, 127.66, 127.58, 123.50, 116.18, 65.46, 35.66, 21.73. **IR** ($CHCl_3$, film) 3066,

2954, 2851, 1596, 1458, 1443, 1431, 1362, 1169 cm^{-1}. **TLC**: R_f = 0.33 (10% EtOAc/hexanes, UV & $KMnO_4$ visualization). **HRMS** (ESI) calculated for $C_{17}H_{16}ClNO_2S$ ($[M+H]^+$): 334.0663, found: 334.0699. **HPLC**: Daicel CHIRALCEL AD-H column, 2% IPA in hexanes, 1.0 mL/min, λ＝254 nm: t_R(major) = 20.5 min, t_R(minor) = 22.4 min.

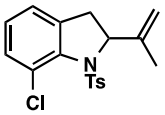

7-chloro-2-(prop-1-en-2-yl)-1-tosylindoline (**11f**): 53% yield (white solid), mp 121-123 ^oC. **^{1}H NMR** (500 MHz, $CDCl_3$) δ 7.60 (d, *J* = 8.4 Hz, 2H), 7.26 (d, *J* = 7.9 Hz, 1H), 7.22 (d, *J* = 8.0 Hz, 2H), 7.05 (app t, *J* = 7.7 Hz, 1H), 6.98 (d, *J* = 7.3 Hz, 1H), 4.93 (s, 1H), 4.87 (d, *J* = 8.3 Hz, 1H), 4.77 (s, 1H), 2.72 (dd, *J* = 16.0, 8.4 Hz, 1H), 2.51 (d, *J* = 16.1 Hz, 1H), 2.41 (s, 3H), 1.62 (s, 3H). **^{13}C NMR** (126 MHz, $CDCl_3$) δ 144.14, 142.45, 139.86, 138.72, 135.89, 129.64, 129.57, 127.79, 127.58, 127.31, 123.16, 112.53, 68.24, 34.41, 21.74, 19.16. **IR** (film) 3085, 3066, 2972, 2921, 2852, 1458, 1442, 1361, 1172 cm^{-1}. **TLC**: R_f = 0.32 (4:1 hexanes/Et_2O, UV & $KMnO_4$ visualization). **HRMS** (ESI) calculated for $C_{18}H_{18}ClNO_2S$ ($[M+H]^+$): 348.0820, found: 348.0871. **HPLC**: Daicel CHIRALCEL AD-H column, 2% IPA in hexanes, 1.0 mL/min, λ＝254 nm: t_R(major) = 17.9 min, t_R(minor) = 19.8 min.

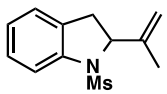

1-(methylsulfonyl)-2-(prop-1-en-2-yl)indoline (**3aa**): 55% yield (white solid), mp 100-104^oC. **^{1}H NMR** (500 MHz, $CDCl_3$) δ 7.42 (d, *J* = 8.0 Hz, 1H), 7.23 – 7.16 (m, 2H), 7.04 (app t, *J* = 7.3 Hz, 2H), 5.07 (s, 1H), 4.88 (s, 1H), 4.82 (dd, *J* = 10.3, 4.0 Hz, 1H), 3.53 – 3.47 (m, 2H), 2.91 – 2.88 (m, 4H), 1.72 (s, 3H). **^{13}C**

NMR (126 MHz, $CDCl_3$) δ 144.34, 142.02, 130.58, 128.20, 125.33, 124.17, 114.75, 112.79, 67.11, 37.07, 34.83, 17.57. **IR** ($CHCl_3$, film) 3078, 3016, 2925, 2853, 1653, 1061, 1479, 1460, 1348, 1159 cm^{-1}. **TLC**: R_f = 0.17 (10% EtOAc/hexanes, UV & $KMnO_4$ visualization). **HRMS** (ESI) calculated for $C_{12}H_{15}NO_2S$ ($[M+H]^+$): 238.0896, found: 238.0897. **HPLC**: Daicel CHIRALCEL AS-H column, 10% IPA in hexanes, 1.0 mL/min, λ=254 nm: t_R(major) = 11.2 min, t_R(minor) = 12.9 min.

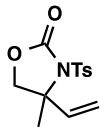

4-methyl-3-tosyl-4-vinyloxazolidin-2-one (**13**): 52% yield (clear oil). **^{1}H NMR** (500 MHz, $CDCl_3$) δ 7.95 (d, *J* = 8.4 Hz, 2H), 7.33 (d, *J* = 8.1 Hz, 2H), 6.10 (dd, *J* = 17.4, 10.7 Hz, 1H), 5.42 (d, *J* = 17.4 Hz, 1H), 5.40 (d, *J* = 10.7 Hz, 1H), 4.12, 4.00 (ABq, 2H, *J* = 8.7 Hz), 2.44 (s, 3H), 1.83 (s, 3H). **^{13}C NMR** (126 MHz, $CDCl_3$) δ 152.34, 145.50, 138.28, 135.76, 129.72, 129.61, 129.22, 129.11, 117.30, 74.63, 66.13, 23.52, 21.82. **IR** ($CHCl_3$, film) 3094, 3071, 2978, 2923, 2852, 1779, 1597, 1367, 1246, 1175, 1146, 1089, 1073 cm^{-1}. **TLC**: R_f = 0.28 (20% EtOAc/hexanes, UV & $KMnO_4$ visualization). **HRMS** (ESI) calculated for $C_{13}H_{15}NO_4S$ ($[M+H]^+$): 282.0795, found: 282.0861. **HPLC**: Daicel CHIRALCEL AD-H column, 20% IPA in hexanes, 1.0 mL/min, λ=220 nm: t_R(major) = 15.7 min, t_R(minor) = 11.9 min.

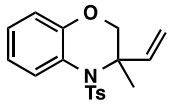

3-methyl-4-tosyl-3-vinyl-3,4-dihydro-2*H*-benzo[*b*][1,4]oxazine (**14**): 44% yield (clear oil). **^{1}H NMR** (500 MHz, $CDCl_3$) δ 7.66 (d, *J* = 8.2 Hz, 1H), 7.47 (d, *J* = 7.9 Hz, 2H), 7.23 (d, *J* = 8.0 Hz, 2H), 7.09 (t, *J* = 7.7 Hz, 1H), 6.91 (t, *J* = 7.8 Hz, 1H), 6.78 (d, *J* = 8.2 Hz, 1H), 5.94 (dd, *J* = 17.6, 10.9 Hz, 1H), 5.11 (d, *J* = 17.5

Hz, 1H), 5.07 (d, *J* = 10.9 Hz, 1H), 3.85, 3.64 (ABq, 2H, *J* = 11.0 Hz), 2.40 (s, 3H), 1.53 (s, 3H). **^{13}C NMR** (126 MHz, $CDCl_3$) δ 148.13, 143.81, 139.59, 137.81, 129.64, 128.05, 127.66, 126.72, 124.65, 120.41, 116.34, 114.74, 70.31, 60.08, 23.69, 21.52. **IR** (film) 3085, 2985, 2923, 2852, 1491, 1352, 1252, 1170, 1089 cm^{-1}. **TLC**: R_f = 0.30 (10% EtOAc/hexanes, UV & $KMnO_4$ visualization). **HRMS** (ESI) calculated for $C_{18}H_{19}NO_3S$ ($[M+H]^+$): 330.1158, found: 330.1288. **HPLC**: Daicel CHIRALCEL AD-H column, 10% IPA in hexanes, 1.0 mL/min, λ＝254 nm: t_R(major) = 8.6 min, t_R(minor) = 8.2 min.

Intramolecular Oxidative Amination of Styrene

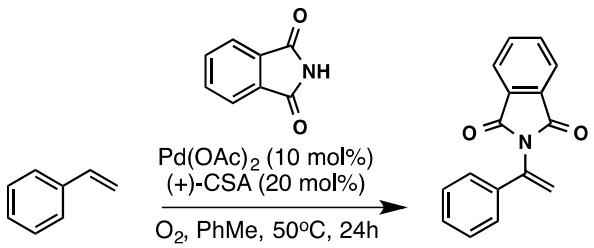

15

To a flame-dried 2-dram vial was added $Pd(OAc)_2$ (0.01 mmol) and (+)-CSA (0.02 mmol) and stirred under Ar with PhMe (0.4 mL) for 20 min. Styrene (0.2 mmol) and phthalamide (0.1 mmol) were added to the reaction with PhMe (0.6 mL) which was flushed with O_2. The reaction was stirred at 50°C under 1 atm O_2 for 24h and purified directly by silica column chromatography (10% EtOAc/Hex) to give 2-(1-phenyl-vinyl-)-isoindole-1,3-dione (**15**): 44% yield (white solid). Characterization is consistent with the literature.[70] **^{1}H NMR** (500 MHz, $CDCl_3$) δ 8.00 – 7.88 (m, 2H), 7.84 – 7.75 (m, 2H), 7.42 – 7.29 (m, 5H), 6.01 (s, 1H), 5.45 (s, 1H). **^{13}C NMR** (75 MHz, $CDCl_3$) δ 167.27, 137.35,

135.54, 134.54, 132.01, 129.08, 128.79, 125.53, 123.99, 116.26. **HRMS** (ESI) calculated for $C_{16}H_{11}NO_2$ ($[M+H]^+$): 250.0862, found: 250.0928.

Difunctionalization of Butyl Acrylate

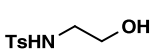

N-(2-hydroxyethyl)-4-methylbenzenesulfonamide: Synthesized according to literature procedure[71] and consistent with literature characterization. [72] **^{1}H NMR** (500 MHz, $CDCl_3$) δ 7.76 (d, *J* = 8.0 Hz, 2H), 7.32 (d, *J* = 8.0 Hz, 2H), 5.00 (t, *J* = 6.2 Hz, 1H), 3.70 (q, *J* = 5.1 Hz, 2H), 3.09 (q, *J* = 5.5 Hz, 2H), 2.43 (s, 3H), 2.01 (t, *J* = 5.3 Hz, 1H). **^{13}C NMR** (75 MHz, $CDCl_3$) δ 143.77, 136.71, 129.94, 127.25, 61.44, 45.33, 21.67.

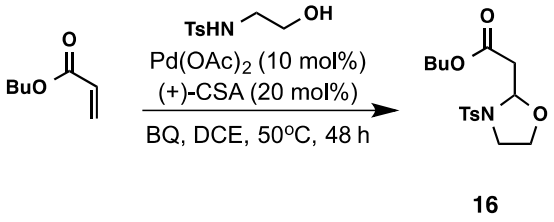

16

To a flame-dried 2-dram vial was added $Pd(OAc)_2$ (0.01 mmol) and (+)-CSA (0.02 mmol) and stirred under Ar with DCE (0.4 mL) for 20 min. Butyl acrylate (0.1 mmol), N-(2-hydroxyethyl)-4-methylbenzenesulfonamide (0.1 mmol) and BQ (0.1 mmol) were added to the reaction with DCE and the reaction was stirred at 50°C for 72h and purified directly by silica column chromatography (25% EtOAc/Hex) to give butyl 2-(3-tosyloxazolidin-2-yl)acetate (**16**): 63% yield (yellow oil). Characterization consistent with the literature.[56] **^{1}H NMR** (500 MHz, $CDCl_3$) δ 7.75 (d, *J* = 8.1 Hz, 2H), 7.35 (d, *J* = 8.0 Hz, 2H), 5.43 (dd, *J* = 8.5, 3.2 Hz, 1H), 4.11 (t, *J* = 6.7 Hz, 2H), 3.94 – 3.86 (m, 1H),

3.50 – 3.37 (m, 3H), 2.99 (dd, *J* = 15.8, 3.2 Hz, 1H), 2.69 (dd, *J* = 15.8, 8.5 Hz, 1H), 2.44 (s, 3H), 1.66 – 1.59 (m, 2H), 1.42 – 1.34 (m, 2H), 0.93 (t, *J* = 7.4 Hz, 3H). **^{13}C NMR** (75 MHz, $CDCl_3$) δ 169.65, 144.58, 133.64, 130.16, 128.01, 88.18, 65.66, 64.87, 46.83, 41.51, 30.68, 21.72, 19.23, 13.84. **HPLC**: Daicel CHIRALCEL AD-H column, 20% IPA in hexanes, 1.0 mL/min, λ＝254 nm: t_R = 9.9 min, 13.5 min.

CHAPTER 3: OXIDATIVE HECK REACTION WITH BORONIC ACIDS AND CHIRAL X-TYPE LIGANDS

Background

The Nobel Prize winning Heck reaction (or Mizoroki-Heck) has garnered significant attention in the literature since its discovery by Heck and Mizoroki in the early 1970s, becoming the most efficient means of creating a C-C bond with an alkene.[73] This Pd^0 catalyzed coupling reaction has been widely studied both mechanistically and in its applications in synthesis (Figure 3.1).[74] However, in a publication that predates his seminal coupling work Heck described an oxidative version of the transformation utilizing substoichiometric amounts of Pd^{II}, copper or mercury salts as reoxidants and arylmercury reagents as coupling partners.[75]

Figure 3.1: Classical Heck Catalytic Cycle

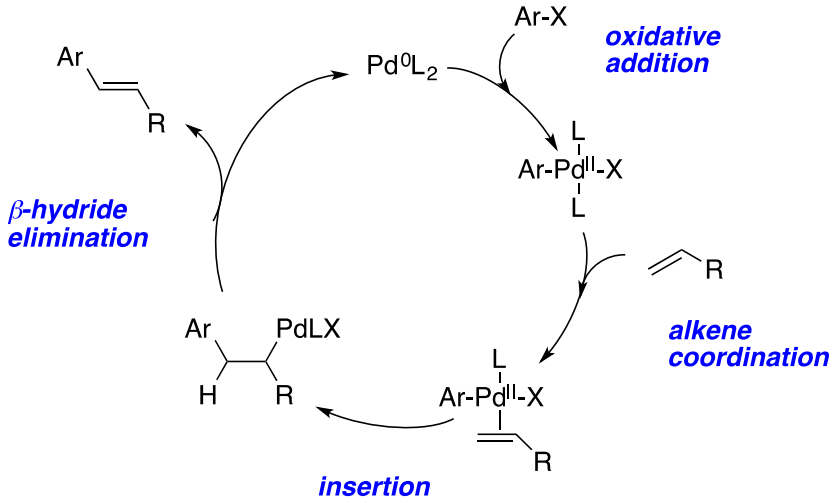

This Oxidative Heck reaction utilizes a transmetallation in the first step of the catalytic cycle, as opposed to an oxidative addition in the classic Heck and proceeds through an

identical catalytic pathway, but upon β–hydride elimination requires a reoxidant to convert Pd^0 back to the active Pd^{II} (Figure 3.2). Furthermore, the oxidative variant of the Heck reaction allows for potential arene-alkene coupling to occur in the presence of complex substrates that contain halides or pseudo-halides.

Figure 3.2: Oxidative Heck with Arylboronic Acid

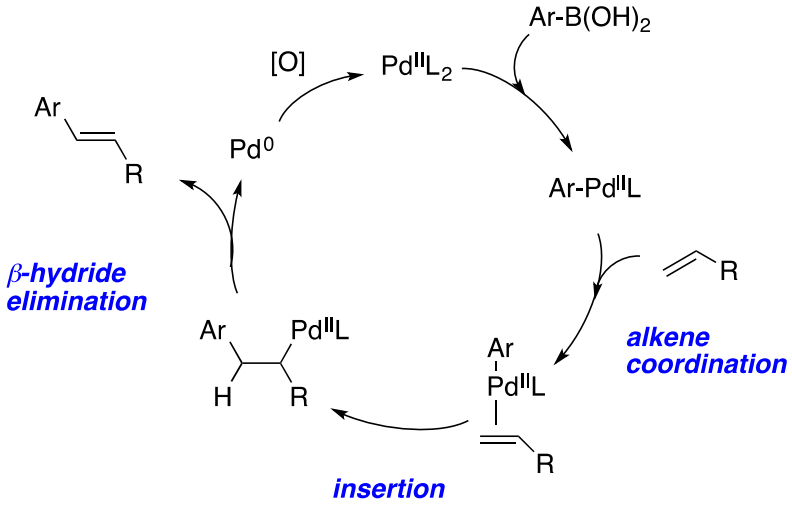

While there are many suitable reagents to generate the arylpalladium species (including but not limited to stannates, silanols, and carboxylic acids), boron derivatives, and specifically boronic acids, have seen the most application for the oxidative Heck due to their commercial availability and functional group tolerance.[76] Coupling with boronic acids is efficient, does not require harsh reaction conditions and does not produce a heavy metal byproduct.

The oxidative Heck reaction with boronic acids has utilized a variety of ligand systems including commercially available palladium salts (so called “ligandless” reactions), bidentate nitrogenous ligands (1,10-phenanthroline and its derivatives), and

NHC ligands.[77] Historically the substrate scope has been limited to electron-deficient alkenes, which are biased towards addition to the terminal end of the alkene both sterically and electronically (the β-carbon is more electron-deficient, resulting in reactivity analogous to a Michael addition). Reactions with nonbiased alkenes suffer from a lack of regioselectivity (mixtures of α- and β-addition), as well as unpredictable β–hydride elimination (Scheme 3.1).[78]

Scheme 3.1: Potential Oxidative Heck Products of Unbiased Alkenes

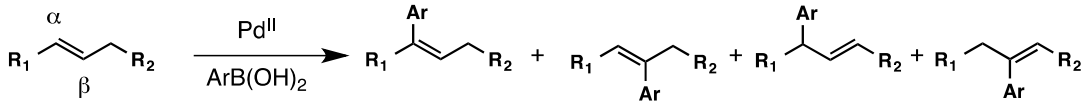

Our aim in applying X-type ligands to this transformation is to exploit the electrophilicity of the Pd-π-alkene complex,[79] facilitating the creation a new C-C bond under mild conditions for unbiased alkene substrates. Also, the steric bulk of the (+)-CSA ligand could be harnessed to promote a single regioisomer. Lastly, with the chiral (+)-CSA ligand we explored the viability of the underdeveloped enantioselective oxidative Heck.

Racemic Oxidative Heck with Boronic Acids

Initial interest in the oxidative Heck with boronic acids began with an attempted expansion of the tosylcarbamate substrate scope in the oxidative amination reaction. Despite having good success with the formation of **13**, other tosylcarbamate substrates proved unreactive. Recognizing the similar conditions between the oxidative Heck and

the oxidative amination reactions (both Pd^{II}-catalyzed oxidative transformations) we sought to utilize the active, in situ generated Pd[(+)-CSA]$_2$ catalyst (still present after the oxidative amination reaction) and further functionalize the alkene product in the same reaction flask. This sequential one-pot reaction would not only expedite the derivatization of chiral cyclic tosylcarbamate products, but effectively eliminate the work-up for the oxidative amination reaction while economically recycling the palladium catalyst.

After **13** was subjected to the optimized oxidative amination conditions, benzeneboronic acid was added and allowed to further react. Gratifyingly, the oxidative Heck reaction occurred adding the aryl group to the terminal end of the alkene and giving exclusively the *trans*-isomer (Scheme 3.2). The reaction occurred without affecting the newly formed stereocenter, but with a reduction in the overall yield (relative to the oxidative amination product). While this example proved the viability of the Pd[(+)-CSA]$_2$ complex for the one-pot transformation, isolation of the corresponding Heck product proved difficult with other boronic acids, limiting further examination of this sequence.

Scheme 3.2: One-Pot Amination-Oxidative Heck with Phenylbornic Acid

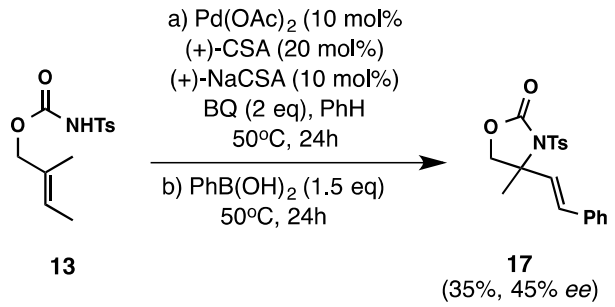

13 **17** (35%, 45% *ee*)

To further explore the viability and scope of the Pd^{II}/(+)-CSA catalyst for the oxidative Heck, electron-deficient alkenes were next explored. Examination of these model, biased alkenes provided a benchmark to compare the effectiveness of (+)-CSA as a ligand to existing ligands in the literature. The reaction of alkylacrylates gave exclusively *trans*-products in good to excellent yields with O_2 (1 atm) as the reoxidant at room temperature (Table 3.1). The reaction was enhanced with the addition of (+)-CSA as a ligand and only acrylic acid provided low yields under optimized conditions. The reaction proved intolerant of additional substitution on the alkene as methyl crotonate gave no reaction. Also, attempts to promote a second oxidative Heck reaction to produce a tri-substituted product were unsuccessful.

Table 3.1: Oxidative Heck with Acrylates and Arylboronic Acids

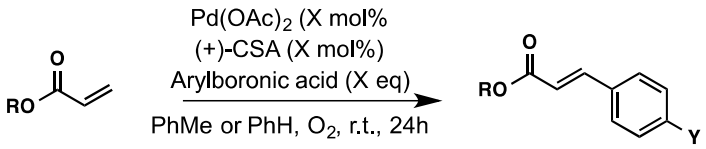

Entry	R	Y	Catalyst/Ligand (mol%)	Boronic Acid (eq)	Yield(%)
1	nBu	H	10/20	$PhB(OH)_2$ (1.05)	93
2	nBu	H	5/10	$PhB(OH)_2$ (1.2)	32
3	*n*Bu	H	10/no ligand	$PhB(OH)_2$ (1.05)	26
4	nBu	Me	10/20	4-$MePhB(OH)_2$ (1.05)	83
5	nBu	OMe	10/20	4-$MeOPhB(OH)_2$ (1.05)	67
6	Me	OMe	10/20	4-$MeOPhB(OH)_2$ (1.5)	64
7	Et	OMe	10/20	4-$MeOPhB(OH)_2$ (1.5)	82
8	H	H	10/20	$PhB(OH)_2$ (1.5)	18

Styrene was next examined as a substrate. While also an electron-deficient alkene, often the transformation requires heating to completion.[80] The reaction proceeded with

excellent yields under very mild conditions (room temperature with a balloon of air as the reoxidant) to give exclusively the *trans*-product (Table 3.2). The addition of (+)-CSA again dramatically improved the reactivity. Reduction of the catalyst loading corresponded with reduced yields (even at slightly elevated temperatures). The reaction was tolerant of other boronic acids, albeit a lower yield for the electron-donating 4-methoxyphenyl boronic acid.

Table 3.2: Oxidative Heck with Styrene and Arylboronic Acids

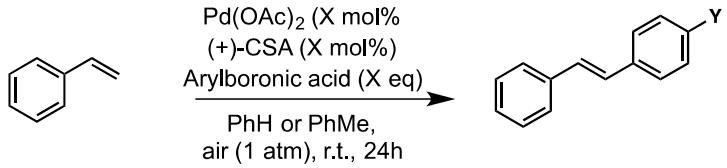

Entry	Y	Catalyst/Ligand (mol%)	Boronic Acid (eq)	Yield(%)
1	H	10/20	$PhB(OH)_2$ (1.05)	98
2	H	10/no ligand	$PhB(OH)_2$ (1.05)	15
3	H	7.5/15	$PhB(OH)_2$ (1.05)	97
4	Me	6/12	$PhB(OH)_2$ (1.05)	71
5	H	5/10	$PhB(OH)_2$ (1.05)	39
6*	H	5/10	$PhB(OH)_2$ (1.05)	54
7	Me	10/20	$PhB(OH)_2$ (1.5)	quant
8	OMe	10/20	$PhB(OH)_2$ (1.05)	57

***Trial at 35°C**

Attempts to react further functionalized sytrenes (α-bromostyrene and β–nitrosytrene) gave no oxidative Heck products.

While the yields for the oxidative Heck reactions of styrene and alkyl acrylates are good, the catalyst loadings for these reactions are high in comparison to existing procedures in the literature.[81] With this in mind, attention was turned towards more complex alkenes. Unfortunately, other electron-deficient α,β-unsaturated ketones,

including cyclohexeone and benzylideneacetone did not give oxidative Heck products. Instead only saturated ketones, as a result of conjugate additions, were seen in poor conversions.

Next, indole was explored to see if the catalyst could preferentially favor addition to either the 2 or 3 position of the molecule. The ability to preferentially arylate an unprotected indole would be not only be synthetically useful, but demonstrate regioselectivity in a less electronically biased alkene (Scheme 3.3). Unfortunately, no difference in the conversion ratios was seen when comparing trials with and without (+)-CSA.

Scheme 3.3: Oxidative Heck with Indole and Phenylboronic Acid

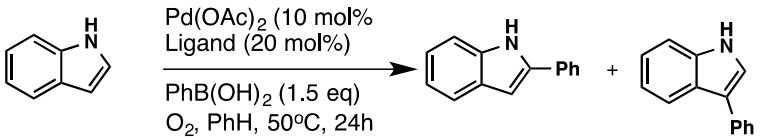

(+)-CSA	77	23
no ligand	74	22

Asymmetric Oxidative Heck with Boronic Acids

In recent years asymmetric variants of the oxidative Heck with boronic acids have emerged utilizing a variety of different chiral ligands. Initial studies began with bidentate chiral phosphine ligands. Successful asymmetric examples of the classical Heck reaction have shown this to be successful ligand class, citing the formation of a chiral cationic Pd^{II}-alkene complex as the key stereoinducing intermediate.[82] Gelman utilized two commercially available ligands for the enantioselective synthesis of 2-aryl-2,3-

dihydrofurans.[83] With a few exceptions, (*R*)-MeOBiphep provided better enantioselectivities (0-82% ee) versus (*R*)-BINAP (21-86% ee) with similar yields for identical substrates.

Scheme 3.4: Enantioselective Oxidative Heck of 2,3-Dihydrofuran

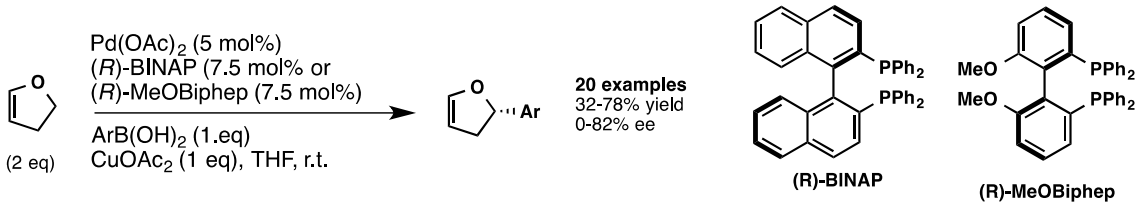

Concurrent work by Mikami found (*S*,*S*)-Chiraphos to be the most successful ligand screened for both the inter- and intramolecular variants of the reaction.[84,85] The oxidative Heck reaction of cyclic carboxylates with 4-trifluoromethylphenyl boronic acid gave good yields and moderate enantioselectivity. The reaction scope was not tolerant of electron-rich boronic acids (4-Me, 4-OMe) and was limited to cyclopentenyl substrates.

Scheme 3.5: Enantioselective Oxidative Heck of Cyclic Alkenes with (*S*,*S*)-Chiraphos

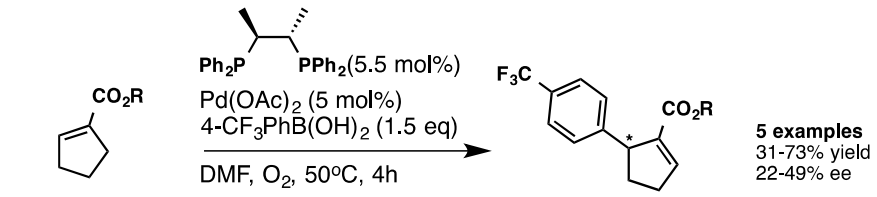

R = Me, Et, iPr, Ph, Bn

The intramolecular version of the reaction produced five and six-membered heterocycles in good yields with variable levels of enantioselectivity of the developing quaternary

center. Furthermore, attack of the in situ generated Pd^{II}-H species on the resulting alkene produced mixtures of alkene and alkane products (56/44 to 87/13).

Scheme 3.6: Enantioselective Intramolecular Oxidative Heck with (*S*,*S*)-Chiraphos

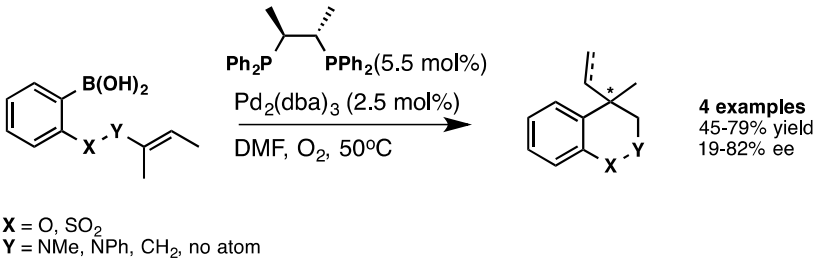

Chelating nitrogenous ligands have also proven to be successful for this transformation. Initial work by Jung utilized a premade Pd^{II}-pyridine-oxazoline complex (Pd-PyOx) to achieve an asymmetric reaction with *trans*-2-methyl-2-butenal and methyl tiglate in good yields and enantioselectivities.[86]

Scheme 3.7: Enantioselective Oxidative Heck of Acyclic Alkenes Pd-PyOx Catalyst

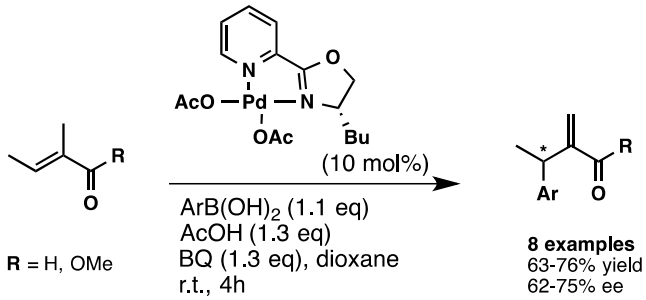

Sigman also found success with a similar PyOx ligand in an enantioselective redox-relay reaction. After stereoselective addition of the aryl ring the double bond migrated to the

homoallylic racemic alcohol and oxidized it to the corresponding aldehyde or ketone. Excellent enantioselectivities and good regioselectivity was seen for the γ–product.[87]

Scheme 3.8: Enantioselective Redox-Relay Oxidative Heck

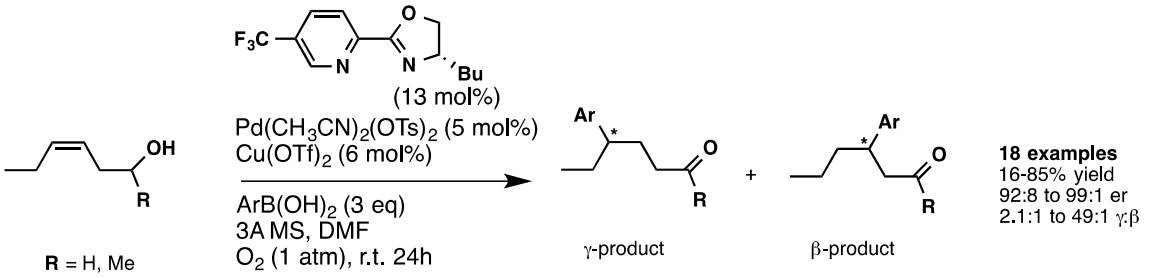

Jung improved the stereoselectivity and expanded the substrate scope to cyclic alkenes with a novel tridentate NHC-Pd complex,[88] synthesized as the dimer in seven steps from L-leucine or L-phenylalanine.[89]

Scheme 3.9: Enantioselective Oxidative Heck of Cyclic & Acyclic Alkenes with NHC-Pd Catalyst

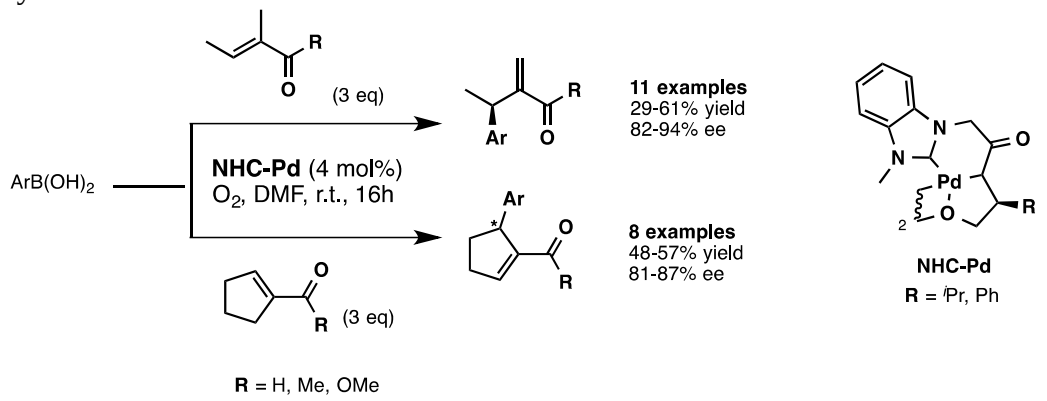

All of the successful enantioselective examples utilized bidentate (or tridentate) dative L-type complexes to generate stereoselectivity. The coordination of the alkene is

sterically directed by the chiral moiety of the ligand and the orientation is well defined through the strongly coordinating chelating complex (Figure 3.3). In contrast, we sought to develop enantioselectivity by replacing the dative chiral L-type ligands with a chiral X-type ligand. While the more electrophilic nature of the Pd^{II}-alkene complex may lead to a more reactive intermediate, the weak coordination of the X-type ligand may not be suitable for imparting chirality. In order to bias the coordination of the alkene, (+)-CSA must be *trans*- with respect to the aryl group in the square planar complex.

Figure 3.3: Proposed Pd^{II}-Alkene Complexes with L-Type Ligand vs (+)-CSA Ligand

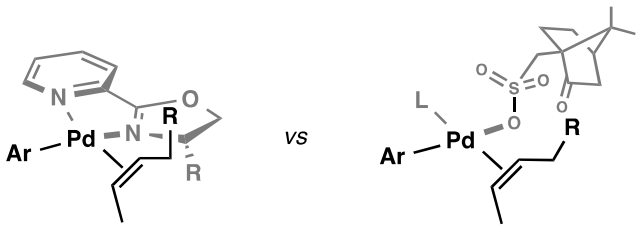

Initial efforts to achieve enantioselectivity with our catalyst began with tiglic acid. Despite significant optimization of the reaction conditions, conversions remained low. Next, methyl tiglate was synthesized and examined. A complex mixture of products containing both a single oxidative Heck product **18** and double oxidative Heck product **19** in approximately equal ratios were seen in the crude ^{1}H-NMR. Increasing the temperature and the amount of benzeneboronic acid appeared to favor the double oxidative product, but the ratio of the two products still made the reaction synthetically nonviable.

Table 3.3: Enantioselective Oxidative Heck of Acyclic Alkenes with (+)-CSA

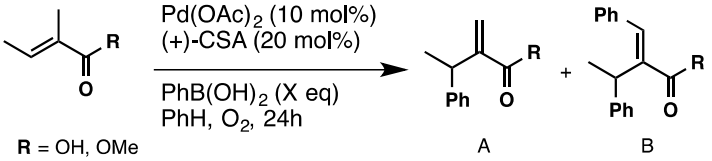

Entry	R	X	Conversion (A/B)(%)[a]
1	OH	1.05 eq	24/0
2	OH	1.50 eq	28/0
3	OMe	1.05 eq	68/32
4	OMe	1.00 eq	53/47
5	OMe	2.20 eq	40/60

[a]Based on crude ^{1}H-NMR. [b]Trial at 45°C

With the lack of success with acyclic products, attention was turned to the cyclic 2,3-dihydrofuran. Again, issues with complex products mixtures were seen rendering further examination unwarranted. Conversely, 1-acetyl-1-cyclohexene did not react under established conditions.

Conclusion

The application of (+)-CSA as a ligand for the oxidative Heck with boronic acids proved effective in the racemic form of the reaction, albeit with moderately high catalyst loadings. Transformations with styrene and alkylacrylates occurred in good to excellent yields. The reaction conditions proved amenable to a one-pot reaction with the previously established asymmetric oxidative amination. Unfortunately the use of (+)-CSA as a ligand was not applicable for electronically unbiased alkenes and the chiral nature of the catalyst could not be harnessed in an enantioselective transformation.

Experimental

Oxidative Heck with Acrylates

To a flame-dried 2-dram vial was added $Pd(OAc)_2$ and (+)-CSA with PhMe or PhH (0.4 mL) and stirred at r.t. for 20 min. The corresponding acrylate (1 eq) and boronic acid were added with additional solvent (0.6 mL), the vial was evacuated with O_2, and the reaction was stirred at r.t. under O_2 (1 atm) for 24h. The reaction was purified directly by silica column chromatography (7:1 hexanes/EtOAc). The corresponding equivalence for $Pd(OAc)_2$, (+)-CSA, and boronic acid are found in Table 3.1.

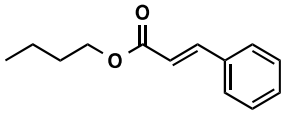

butyl cinnamate: 93% yield (yellow oil). Characterization is consistent with the literature[90] **^{1}H NMR** (500 MHz, $CDCl_3$) δ 7.69 (d, *J* = 16.0 Hz, 1H), 7.53 (dd, *J* = 6.5, 2.9 Hz, 2H), 7.42 – 7.36 (m, 3H), 6.45 (d, *J* = 16.0 Hz, 1H), 4.21 (t, *J* = 6.7 Hz, 2H), 1.73 – 1.66 (m, 2H), 1.48 – 1.41 (m, 2H), 0.97 (t, *J* = 7.3 Hz, 3H). **^{13}C NMR** (75 MHz, $CDCl_3$) δ 167.24, 144.68, 134.60, 130.33, 128.99, 128.17, 118.42, 64.57, 30.91, 19.34, 13.89.

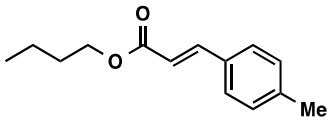

(E)-butyl 3-p-tolylacrylate: 83% yield (yellow oil). Characterization is consistent with the literature.[89] **^{1}H NMR** (500 MHz, $CDCl_3$) δ 7.66 (d, *J* = 16.0 Hz, 1H), 7.43 (d, *J* = 7.9 Hz, 2H), 7.19 (d, *J* = 7.9 Hz, 2H), 6.40 (d, *J* = 16.0 Hz, 1H), 4.20 (t, *J* = 6.7 Hz, 2H), 2.37 (s, 3H), 1.71-1.66 (m,

2H), 1.47-1.40 (m, 2H), 0.97 (t, *J* = 7.4 Hz, 3H). **^{13}C NMR** (75 MHz, $CDCl_3$) δ 167.43, 144.68, 140.73, 131.87, 129.73, 128.17, 117.32, 64.48, 30.93, 21.60, 19.35, 13.90.

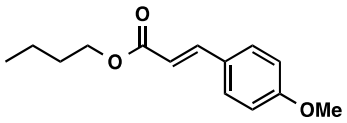

(E)-butyl 3-(4-methoxyphenyl)acrylate: 67% yield (yellow oil). Characterization is consistent with the literature.[89] ^{1}H NMR (500 MHz, $CDCl_3$) δ 7.64 (d, *J* = 15.9 Hz, 1H), 7.48 (d, *J* = 8.6 Hz, 2H), 6.90 (d, *J* = 8.6 Hz, 2H), 6.31 (d, *J* = 15.9 Hz, 1H), 4.20 (t, *J* = 6.7 Hz, 2H), 3.84 (s, 3H), 1.71-1.65 (m, 2H), 1.47-1.39 (m, 2H), 0.96 (t, *J* = 7.4 Hz, 3H). **^{13}C NMR** (75 MHz, $CDCl_3$) δ 167.58, 161.45, 144.33, 129.82, 127.35, 115.92, 114.43, 64.41, 55.51, 30.96, 19.36, 13.91.

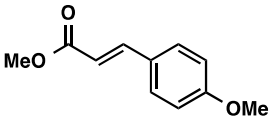

(E)-methyl 3-(4-methoxyphenyl)acrylate: 64% yield (white solid). Characterization is consistent with the literature[91] ^{1}H NMR (500 MHz, $CDCl_3$) δ 7.65 (d, *J* = 16.0 Hz, 1H), 7.47 (d, *J* = 8.6 Hz, 2H), 6.90 (d, *J* = 8.6 Hz, 2H), 6.31 (d, *J* = 16.0 Hz, 1H), 3.83 (s, 3H), 3.79 (s, 3H). ^{13}C NMR (126 MHz, $CDCl_3$) δ 167.90, 161.52, 144.66, 129.86, 127.24, 115.39, 114.45, 55.51, 51.72.

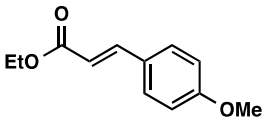

(E)-ethyl 3-(4-methoxyphenyl)acrylate: 82% yield (colorless oil). Characterization is consistent with the literature[92] **^{1}H NMR** (500 MHz, $CDCl_3$) δ 7.64 (d, *J* = 16.0 Hz, 1H), 7.47 (d, *J* = 8.5 Hz, 2H), 6.95 – 6.86 (m, 2H), 6.31 (d, *J* = 16.0 Hz, 1H), 4.25 (q, *J* = 7.1 Hz, 2H), 3.83 (s, 3H), 1.33 (t, *J* = 7.1 Hz, 3H).

^{13}C NMR (75 MHz, $CDCl_3$) δ 167.47, 161.45, 144.37, 129.81, 127.33, 115.88, 114.43, 60.46, 55.50, 14.50.

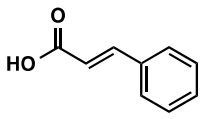

trans-cinnamic acid. 18% yield (white solid). Characterization consistent with commercially available product. **^{1}H NMR** (500 MHz, $CDCl_3$) δ 7.79 (d, *J* = 16.0 Hz, 1H), 7.61 – 7.53 (m, 2H), 7.47 – 7.37 (m, 3H), 6.46 (d, *J* = 16.0 Hz, 1H). **^{13}C NMR** (75 MHz, $CDCl_3$) δ 171.84, 147.22, 134.19, 130.90, 129.12, 128.51, 117.31.

Oxidative Heck with Styrene

To a flame-dried 2-dram vial was added $Pd(OAc)_2$ and (+)-CSA with PhH (0.4 mL) and stirred at r.t. for 20 min. Styrene (1 eq) and corresponding boronic acid were added with additional PhH (0.6 mL) and the reaction was stirred at r.t. under air (1 atm) for 24h. The reaction was purified directly by silica column chromatography (7:1 hexanes/EtOAc). The corresponding equivalence for $Pd(OAc)_2$, (+)-CSA, and boronic acid are found in Table 3.2.

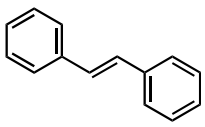

(E)-1,2-diphenylethene: Characterization is consistent with the literature.[89] **^{1}H NMR** (500 MHz, $CDCl_3$) δ 7.53 (d, *J* = 7.5 Hz, 4H), 7.37 (t, *J* = 7.6 Hz, 4H), 7.29 – 7.26 (m, 2H), 7.12 (s, 2H). **^{13}C NMR** (75 MHz, $CDCl_3$) δ 137.46, 128.82, 127.76, 126.65.

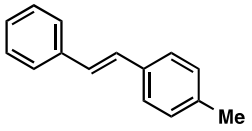

(E)-1-methyl-4-styrylbenzene: Characterization is consistent with the literature.[89] **^{1}H NMR** (500 MHz, $CDCl_3$) δ 7.53 (d, *J* = 7.7 Hz, 2H), 7.44 (d, *J* = 7.9 Hz, 2H), 7.37 (t, *J* = 7.5 Hz, 2H), 7.28-7.25 (m, 1H), 7.19 (d, *J* = 7.8 Hz, 2H), 7.10 (d, *J* = 3.7 Hz, 2H), 2.38 (s, 3H). **^{13}C NMR** (75 MHz, $CDCl_3$) δ 137.66, 134.69, 129.53, 128.79, 128.76, 127.84, 127.54, 126.56, 126.53, 21.41.

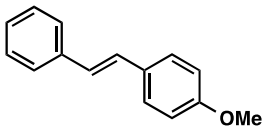

(E)-1-methoxy-4-styrylbenzene: Characterization is consistent with the literature.[93] **^{1}H NMR** (500 MHz, $CDCl_3$) δ 7.55 – 7.46 (m, 4H), 7.36 (d, *J* = 6.9 Hz, 2H), 7.28 (s, 1H), 7.10 (d, *J* = 16.3 Hz, 1H), 7.00 (d, *J* = 16.3 Hz, 1H), 6.93 (d, *J* = 8.0 Hz, 2H), 3.86 (s, 3H). **^{13}C NMR** (75 MHz, $CDCl_3$) δ 159.44, 137.79, 130.29, 128.78, 128.35, 127.86, 127.35, 126.76, 126.39, 114.27, 55.48.

<u>One-Pot Oxidative Amination/Oxidative Heck</u>

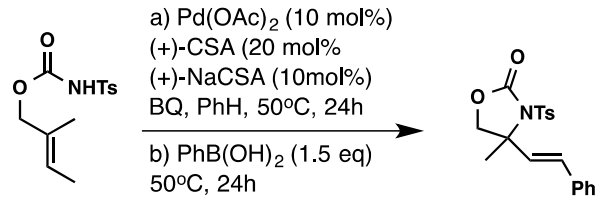

9 **17**

To a flame-dried 2-dram vial was added $Pd(OAc)_2$ (0.01 mmol) and (+)-CSA (0.02 mmol) with PhH (0.4 mL) and stirred at r.t. for 20 min. Tosylcarbamate **9** (0.1 mmol), (+)-NaCSA (0.01 mmol) and benzoquinone (0.2 mmol) were added with PhH (0.6 mL) and the reaction was stirred at 50^{o}C 24h. Benzenboronic acid (0.15 mmol) was added and

the reaction continued to stir for 24h at 50°C. The crude product was diluted with EtOAc, washed with sat. K_2CO_3 (4 x 5 mL), H_2O (5 mL), dried with $MgSO_4$, and concentrated *in vaccuo*. The reaction was purified by silica column chromatography (20% EtOAc/hexanes) to give (*E*)-4-methyl-4-styryl-3-tosyloxazolidin-2-one (**17**): 35% yield (colorless oil). **^{1}H NMR** (500 MHz, $CDCl_3$) δ 7.89 (d, *J* = 8.4 Hz, 2H), 7.38 – 7.30 (m, 5H), 7.23 (d, *J* = 8.1 Hz, 2H), 6.68 (d, *J* = 16.2 Hz, 1H), 6.29 (d, *J* = 16.2 Hz, 1H), 4.21, 4.10 (ABq, 2H, *J* = 8.7 Hz), 2.41 (s, 3H), 1.96 (s, 3H). **^{13}C NMR** (75 MHz, $CDCl_3$) δ 152.42, 145.44, 135.74, 135.36, 132.31, 129.57, 129.19, 128.91, 128.83, 128.65, 126.96, 75.08, 66.09, 24.25, 21.80. **HRMS** (ESI) calculated for $C_{19}H_{19}NO_4$ ($[M+H]^+$): 358.1109, found: 358.1108. **HPLC**: Daicel CHIRALCEL AD-H column, 10% IPA in hexanes, 1.0 mL/min, λ＝254 nm: t_R(major) = 22.3 min, t_R(minor) = 18.8 min.

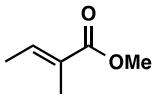

Methyl tiglate: 28% yield (colorless oil). Synthesized according to literature procedure[94] and characterization is consistent with commercially available product. **^{1}H NMR** (500 MHz, $CDCl_3$) δ 6.89 – 6.81 (m, 1H), 3.73 (s, 3H), 1.83 (d, *J* = 1.3 Hz, 3H), 1.78 (d, *J* = 7.1 Hz, 3H). **^{13}C NMR** (126 MHz, $CDCl_3$) δ 168.77, 137.34, 128.63, 51.78, 14.46, 12.18.

CHAPTER 4: APPLICATIONS OF C-H ACTIVATION WITH X-TYPE LIGANDS

Background

Despite their ubiquity in organic compounds, C-H bonds are typically viewed in organic chemistry as unreactive due to their high bond dissociation energies (97-113 kcal/mol).[95] Instead the practice of organic synthesis focuses on the manipulation of more reactive functional groups in order to achieve a desired transformation. This iterative functional group exchange can require numerous steps and necessitate protecting group strategies to prevent undesired functional group reactivity. A transformation that could selectively functionalize a specific C-H bond would not only expedite syntheses, but would provide a new avenue by which to approach the synthesis of complex molecules.

In recent years C-H bond activation has received considerable attention in the literature.[96] Despite numerous breakthroughs in the field two major obstacles in achieving C-H activation remain: 1) cleavage of the C-H bond and 2) selectively reacting a single C-H bond. Conditions to promote C-H insertion are often harsh (strong acids, elevated temperatures) frequently precluding their application in complex systems. Multiple strategies have emerged to rationally functionalize a single C-H bond in a complex molecule including selectively reacting C-H bonds with weaker bond dissociate energies (i.e. allylic, benzylic) or utilizing a directing group on a substrate to coordinate and facilitate C-H insertion for a transition metal catalyst.[97]

Transition metal catalyzed C-H activation occurs through one of two general mechanisms: a) inner-sphere (organometallic) or b) outer-sphere (coordination).[98] While

there are many approaches to achieving C-H activation, one of the most popular is through the use of palladium catalysis. Depending on the ligands and conditions used both Pd^{0}/Pd^{II} and Pd^{II}/Pd^{IV} pathways are operable.[99] Two strategies predominate in Pd-catalyzed C-H insertion: a) direct insertion via an electrophilic aromatic mechanism (electron-rich arenes) or a concerted metalation-deprotonation (electron-deficient arenes); and b) directing group facilitated insertion.

Palladium catalysis with X-type ligands has the potential to address the challenges presented by C-H activation. The electrophilic nature of the catalyst is capable of facilitating C-H insertion under mild conditions that can be tolerant of a variety of functional groups, providing the potential for late-stage functionalization not realized under harsh conditions. Furthermore, the chiral nature of the X-type ligands could be utilized in an enantioselective transformation for C-H activation/C-C or C-heteroatom coupling. Given the electrophilic nature of the catalyst generated, the mode of C-H activation is likely either electrophilic substitution (via a Wheland intermediate) or concerted metalation-deprotonation (CMD) in which the sulfonate ligand abstracts a proton intramolecularly through a six-membered intermediate (Figure 4.1).

Figure 4.1: C-H Insertion via Wheland or Concerted Metallation-Deprotonation Intermediate

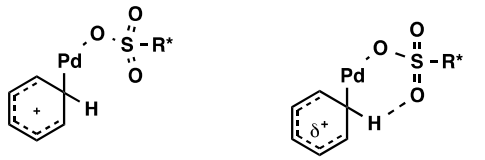

Intramolecular Asymmetric Oxidative Heck

As discussed in Chapter 3, the Oxidative Heck couples an aryl carbon with an alkene. Previously we examined this reaction utilizing boronic acids to facilitate the generation of the aryl-palladium intermediate in the catalytic cycle. However, a more general reaction would not require an activated coupling partner (i.e. boronic acid), but instead generate the aryl-palladium species via direct C-H insertion. The Fujiwara-Moritani (Oxidative Heck) reaction does just that (Figure 4.2).

Figure 4.2: Fujiwara-Moritani (Oxidative Heck) Catalytic Cycle

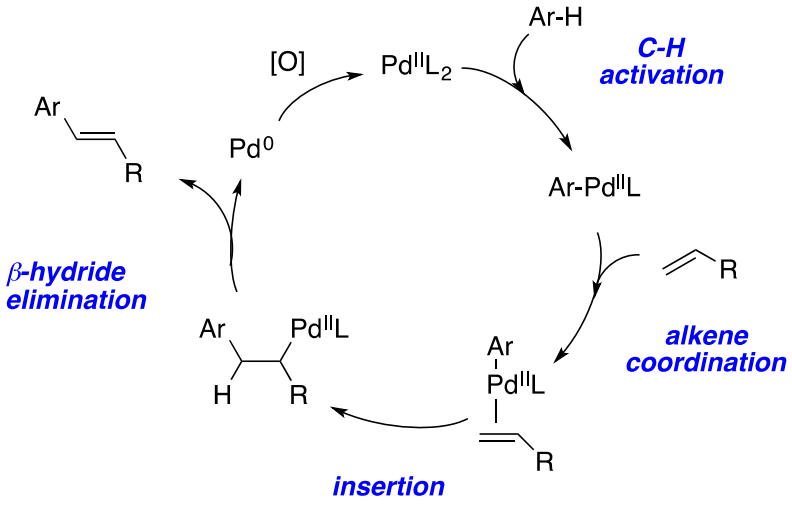

This reaction has found application in natural product total synthesis (in stoichiometric versions) and the syntheses of indoles and dihydrofurans in catalytic transformations.[100] Notable examples by Stoltz include the formation of quaternary carbons in the syntheses of indoles and dihydrobenzofurans (Scheme 4.1).[101]

Scheme 4.1: Catalytic Fujiwara-Moritani Syntheses of Indoles and Dihydrobenzofurans

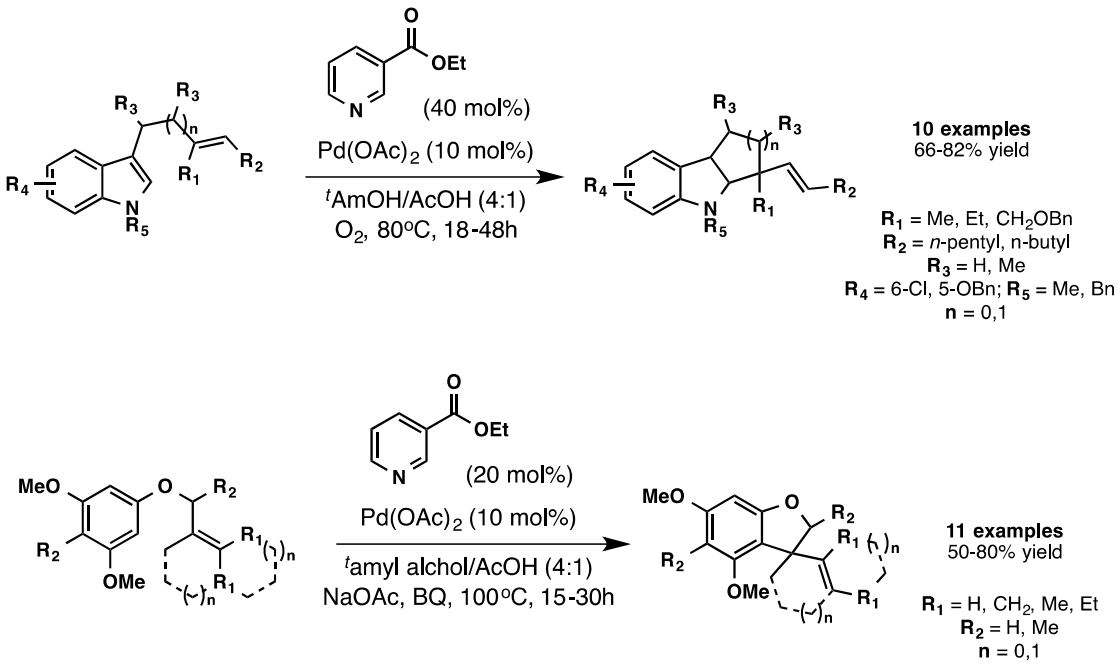

Despite its growing application in synthesis, enantioselective versions of this reaction are rare. The only intramolecular enantioselective Fujiwara-Moritani reaction[102] was discovered by Oestreich in the annulation of indoles and pyrroles with novel PyOx ligands (Scheme 4.2).[103]

Scheme 4.2: Asymmetric Fujiwara-Moritani by Oestreich

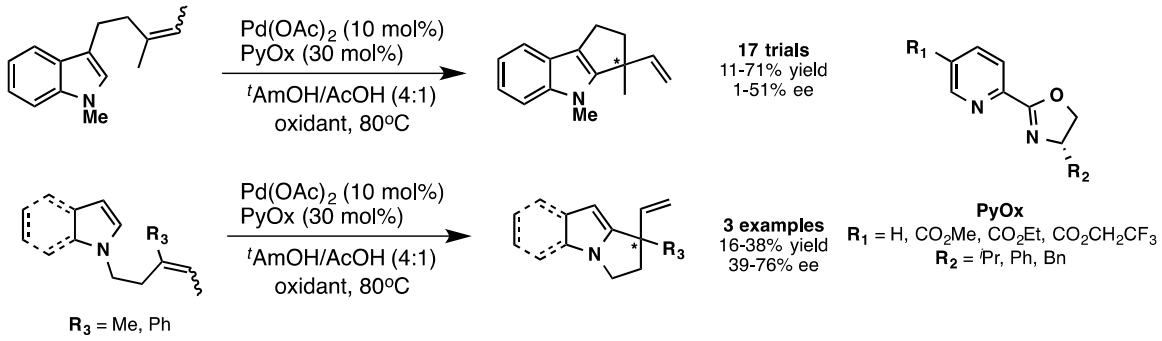

While groundbreaking work, the yields and enantioselectivities for the reactions were modest and highly variable depending on the oxidant. Recognizing the gap in the literature, we decided to apply our chiral X-type ligand system to this transformation. The electrophilic nature of our catalyst should be conducive to C-H insertion, while the chiral ligand can direct the complexation of the alkene giving a stereoselective transformation.

Initial examination of the intramolecular asymmetric oxidative Heck reaction began with electron-rich arene **18** which was synthesized from 3,5-dimethoxylphenol via allylic alkylation (Scheme 4.3). Despite numerous attempts at optimization the conversion for the cyclization was minimal.

Scheme 4.3: Intramolecular Asymmetric Oxidative Heck of 18

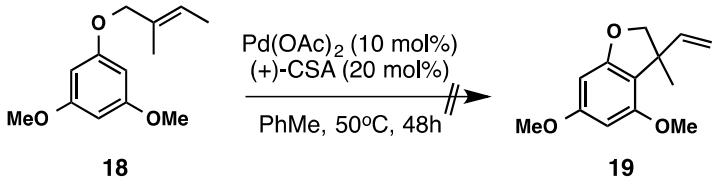

18 **19**

Believing the poor conversion was due to the lack of C-H activation, a directing group was examined in order to facilitate C-H insertion. Dimethylureas have been shown to form palladacycles in situ under mild conditions while directing C-H insertion to a single *ortho*-regioisomer.[104] To test the viability of this directing group, **24a** was reacted with phenylboronic acid (Scheme 4.4). This Suzuki coupling would provide a model system to explore whether directed C-H insertion occurs with the X-type ligand complex as transmetallation and reductive elimination should occur rapidly upon formation of the Ar-Pd^{II} intermediate.[105] The reaction proved effective giving in a good yield.

Scheme 4.4: Directed Oxidative Suzuki Coupling with Phenylboronic Acid

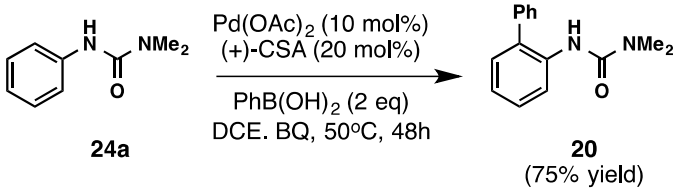

With the success of the directing group strategy shown, a dimethylurea was incorporated into the synthesis of a new substrate **21**. Allylic alkylation of 3-nitrophenol with *trans*-1-bromo-2-methyl-2-butene (synthesized in two step from tiglic acid), followed by reduction of the nitro group and subsequent formation of the urea with dimethylcarbomyl chloride gave **21** in a 44% yield in three steps (Scheme 4.5).

Scheme 4.5: Synthesis of Substrate 21

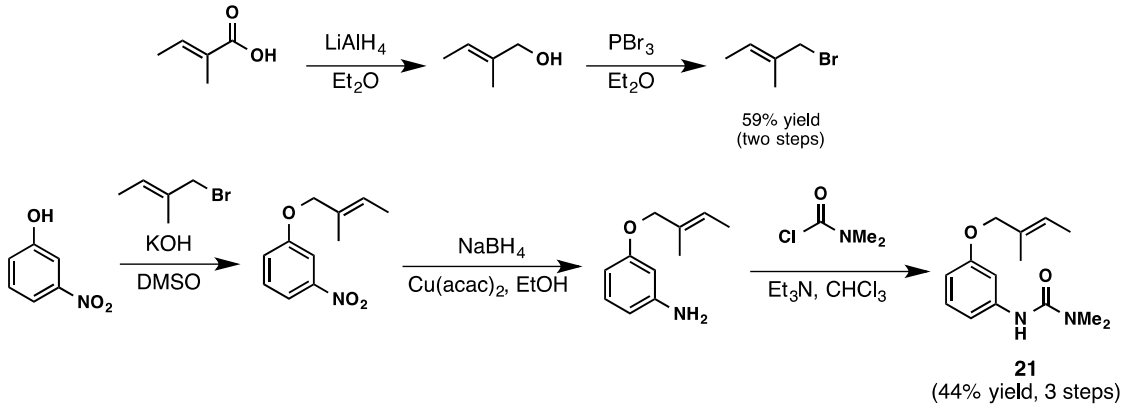

With **21** in hand, the asymmetric oxidative Heck was again examined. Unfortunately, this substrate also did not produce any cyclized product (Scheme 4.6). The lack of reactivity can be rationalized through the formation of intermediate **23**, in which C-H insertion occurs *para* instead of *ortho* to the ether, sequestering the catalyst in a

position that is unable to react intramolecularly with the alkene. Also, no evidence of an intermolecular reaction was present as only starting material was found after workup. While not ideal for this reaction, the *para* regioselectivity is consistent with similar transformations in the literature.[106]

Scheme 4.6: Directed Intramolecular Asymmetric Oxidative Heck

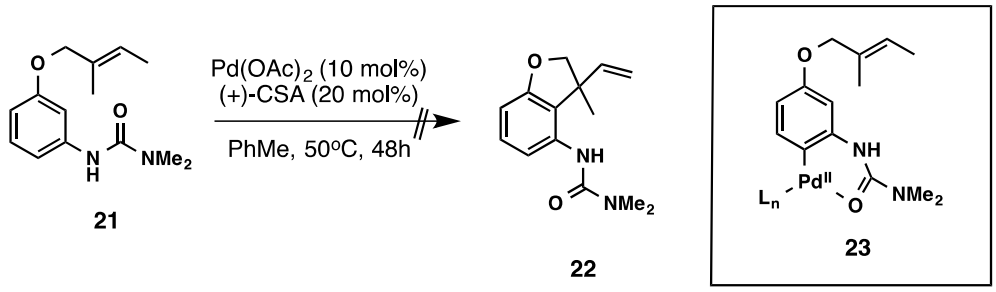

With the lack of reactivity of **18** and **21**, further efforts for an asymmetric oxidative amination were focused on the intermolecular reaction.

Intermolecular Enantioselective Applications with C-H Activation

With C-H activation and subsequent β-hydride elimination most intermolecular oxidative Heck reactions do not have the ability to produce an sp^3-hybridized chiral center. However, if the C-H insertion is coupled with a heteroatom or carbon nucleophile before the formation of the alkene, a new chiral center can be formed. With the success of (+)-CSA in the asymmetric oxidative amination, examination of reactions which utilized sulfonic acid additives were of particular interest.

Intriguingly, the addition of sulfonic acid additives tended to increase the reaction yields. This additive effect was first exploited by de Vries and van Leeuwen in the coupling of *n*-butyl acrylate with a series of anilides (Scheme 4.7).[107] Remarkably, the reaction occurred at room temperature with the addition of TsOH (0.5 eq) substantially increasing yields.

Scheme 4.7: Room Temperature Coupling of Butyl Acrylate and Anilides with TsOH

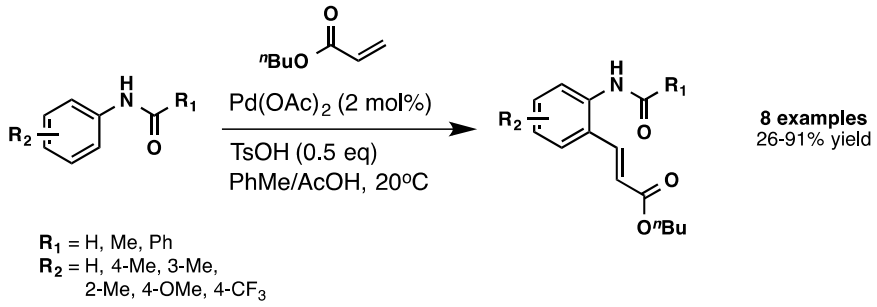

Similar conditions were employed by Lloyd-Jones and Booker-Milburn in the synthesis of indolines via a 1,2-carboamination (Scheme 4.8).[126] Again the addition of TsOH proved essential for reactivity under mild conditions.

Scheme 4.8: 1,2-Carboamination by Lloyd-Jones and Booker-Milburn

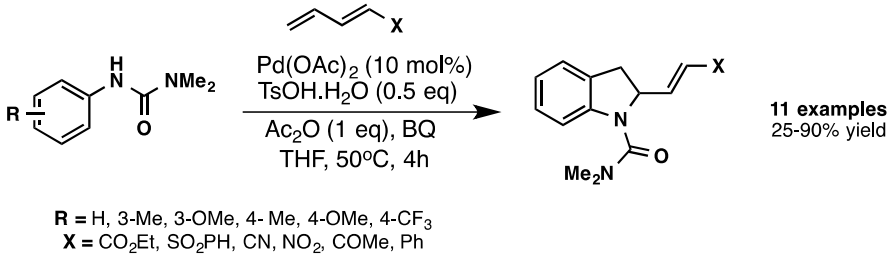

Furthermore, $(MeCN)_2Pd(OTs)_2$ was utilized as a catalyst, implicating the role of the sulfonic acid as a ligand generating an electrophilic Pd^{II} catalyst (Scheme 4.9).

Scheme 4.9: Reactivity of $(MeCN)_2Pd(OTs)_2$ in 1,2-Carboamination

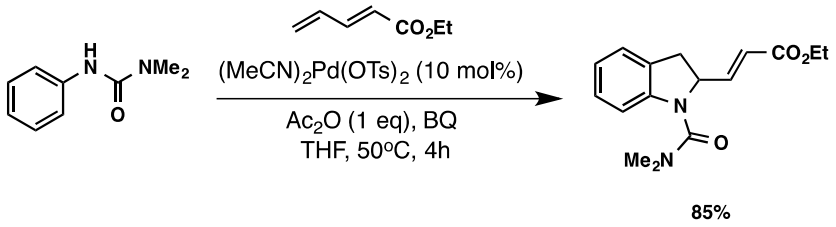

In a subsequent publication Lloyd-Jones and Booker-Milburn synthesized Pd^{II}-aryl complex **25**, showing the η^1-coordination of the tosylate to the palladium catalyst.[108,109] Recognizing the role of this X-type ligand in the both facilitating C-H activation and its presence in the palladacycle, our aim was to introduce a chiral sulfonic acid (namely (+)-CSA) in order to explore asymmetric transformations (Figure 4.3). A reasonable application of this methodology would be the 1,2-carboamination as the nucleophilic attack of the amine is similar to the Wacker-type asymmetric oxidative amination, which we have shown to be successful with (+)-CSA ligands (Chapter 2).

Figure 4.3: Palladacycle 25 and Proposed Chiral Palladacycle 26

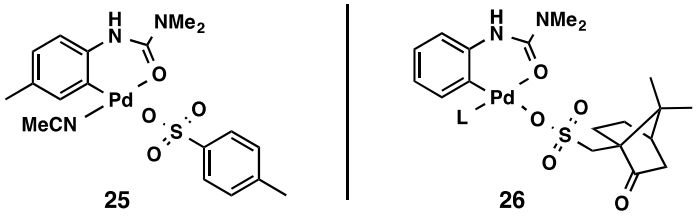

Inspired by the work of Lloyd-Jones and Booker-Milburn, we decided to explore the synthesis of chiral indolines via an asymmetric 1,2-carboamination. The initial experiment reacted substrate **24a** with diene **27a** to give a low yield, but with promising enantioselectivity (Table 4.1). Preliminary optimization showed increased conversion with higher equivalence of (+)-CSA, the incorporation of Ac_2O as a desiccant additive and PhMe as a the solvent .[110] Unfortunately, upon analyzing the stereoselectivity a significant drop in the enantiomeric excess occurred in comparison to the 1,2-dichloroethane (DCE) trial.

Table 4.1: Initial 1,2-Carboamination Trials for 24a

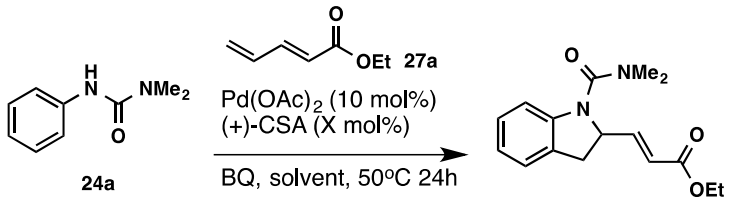

Entry	(+)-CSA (eq)	Conditions	Yield[a] (Conversion[b]) %	ee (%)[c]
1	20 mol%	BQ (2 eq), DCE	30 (40)	36
2	20 mol%	BQ (1 eq), PhMe	36 (68)	n.d.
3	50 mol%	BQ (1 eq), PhMe	37 (93)	n.d.
4[d]	50 mol%	BQ (1 eq), Ac_2O (1 eq), PhMe	52 (75)	11

[a]Isolated yield. [b]Based on crude ^{1}H-NMR. [c]Determined by chiral HPLC. [d]Trial at r.t.

With the stereospecificity of the reaction highly dependent on the solvent, a screen of various organic solvents was conducted. Both 1,2-dichloroethane and chloroform furnished the best results in terms of stereoselectivity and further optimization centered on these solvents (Table 4.2).

Table 4.2: Solvent Screen for 1,2-Carboamination of 24a

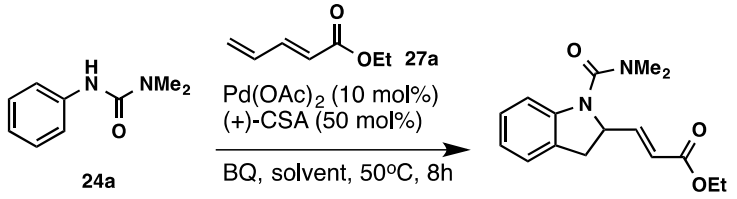

Entry	Solvent	Yield[a] (Conversion[b]) %	ee (%)[c]
1	PhMe	47 (73)	14
2	DCE	51 (67)	35
3	$CHCl_3$	35 (86)	33
4	THF	40 (53)	8
5	dioxane	33 (46)	13
6	MeCN	n.d. (9)	n.d.
7	DME	31 (40)	15

[a]Isolated yield. [b]Based on crude ^{1}H-NMR. [c]Determined by chiral HPLC.

Next the role of additives, the ratio of diene to urea and reaction time were analyzed (Table 4.3). No reaction occurred upon omission of either the palladium catalyst or (+)-CSA, pointing to the formation of the electrophilic palladium source in situ. Examination of chiral phosphoric acid (*S*)-BINOL-PA gave poorer enantioselecivity in comparison to (+)-CSA (entry 3). A diene to urea ratio of 1:1 was optimal, with lower yields occurring with excess diene (entries 8-9). Acetic anhydride provided a better yield in chloroform, but had a negative effect in 1,2-dichloroethane (entries 6-7). Lastly, increasing the reaction time to 24h provided the best overall yield in 1,2-dichloroethane, which provided slightly better enantioselectivity in every trial (entry 12).

Table 4.3: Optimization of 1,2-Carboamination of 24a

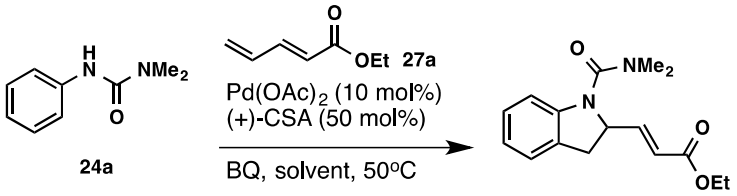

Entry	Conditions	Yield[a] (%)	ee (%)[b]
1[c]	$CHCl_3$, 8h	no rxn	n.d.
2[d]	$CHCl_3$, 8h	no rxn	n.d.
3[e]	$CHCl_3$, 8h	39	8
4	DCE, 8h	51	35
5	$CHCl_3$, 8h	35	33
6	DCE, Ac_2O, 8h	43	36
7	$CHCl_3$, Ac_2O, 8h	57	33
8[f]	DCE, 8h	43	36
9[f]	$CHCl_3$, 8h	51	33
10	DCE, 12h	53	n.d.
11	$CHCl_3$, 12h	48	n.d.
12	DCE, 24h	56	33

[a]Isolated yield. [b]Determined by chiral HPLC. [c]No $Pd(OAc)_2$. [d]No (+)-CSA. [e](*S*)-BINOL-PA (50 mol%). [f]1.5:1 diene/urea ratio

While dimethyl urea has been successfully utilized as directing group in previous C-H activations, other directing groups were analyzed for this reaction. The common aniline protecting group Boc (Table 4.4, entry 2) gave no cyclized product while acetamide (entry 3) did react, but with diminished conversion. Interestingly no reaction occurred with the dimethyl thiourea derivative (entry 4) and the benzanilide substrate similarly gave no carboamination product.

Table 4.4: Examination of Other Directing Groups for 1,2-Carboamination

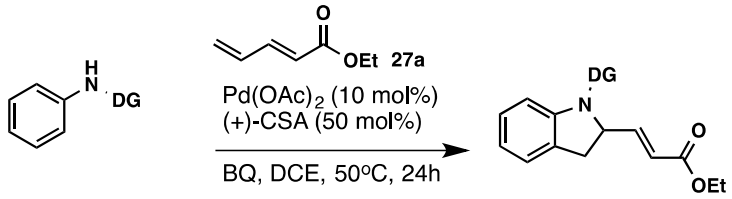

Entry	Directing Group (DG)	Conversion[a] (%)
1		no reaction
2	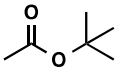	no reaction
3		25
4	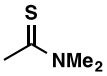	no reaction

[a]Based on crude ^{1}H-NMR.

With the reaction conditions optimized and the directing group chosen attention was turned towards the synthesis of dimethyl urea derivatives to explore the scope of the reaction. A series of substrates were synthesized in one of the following manners: method A) reaction of dimethylamine hydrochloride with phenylisocyanate under basic conditions; or method B) the aniline (either commercially available or reduced in a single step from the nitro group[111]) was acylated with dimethylcarbomyl chloride (Scheme 4.10).[112] Both conditions gave substrates in modest to excellent yields for a variety electron-donating and electron-withdrawing substituents. Additionally, other electron-deficient dienes were synthesized (Scheme 4.11). *Trans*-1-phenyl-1,3-butadiene (**28**) was synthesized via a Wittig reaction from trans-cinnamaldehyde.[113]

Scheme 4.10: Synthesis of Dimethyl Urea Substrates

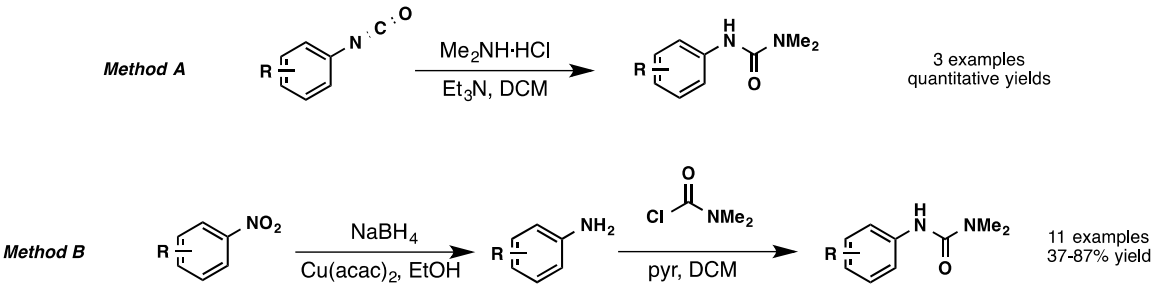

The ester dienes were produced in two steps, beginning with a Knoevenagel condensation of malonic acid and acrolein, then a carbodiimide coupling with EDCI and the corresponding alcohol to give the ester. The Weinreb amide (which provides a synthetic handle to produce ketones and aldehydes) was synthesized analogously under slightly modified conditions.

Scheme 4.11: Synthesis of Electron-Deficient Dienes

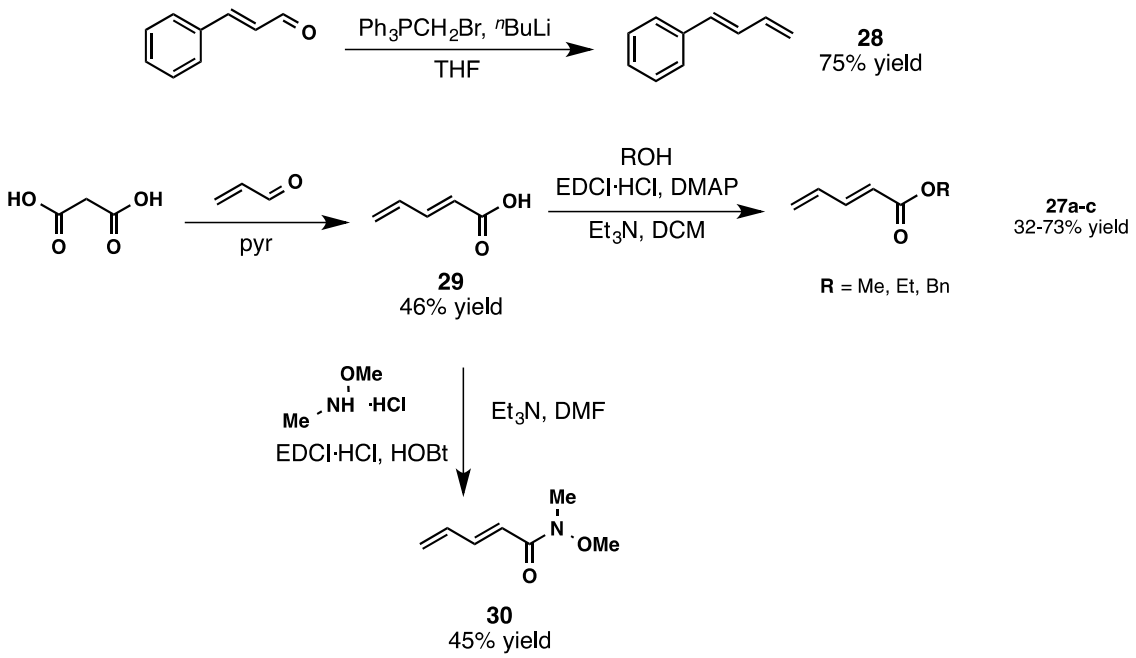

Examination of Substrate Scope
for Asymmetric 1,2-Carboamination

Under the optimized conditions the most successful substrates contained electron-donating groups *para* to the aniline (Table 4.5).

Table 4.5: Substrate Scope for Asymmetric 1,2-Carboamination

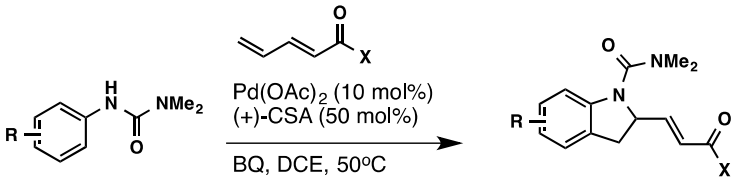

Entry	R	X	Substrate	Product	Yield (%)[a]	ee (%)[b]
1	H	OEt	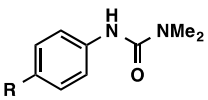	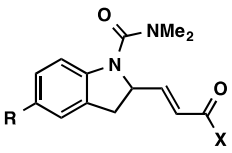	56	33
2	Me	OEt			52	26
3	OMe	OEt			61	34
4	OMe	OMe			59	33
5	OMe	OBn			49	32
6	OMe	NMe(OMe)			37	29
7	OBn	OEt			55	34
8	Br	OEt			27	34
9	Cl	OEt			22	33
10	COMe	OEt			25	38
11	Me	OEt	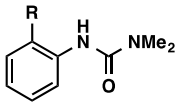	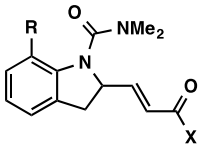	23	46
12	Me	OEt	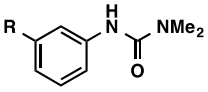	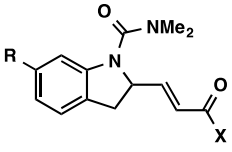	61	4
13		OEt	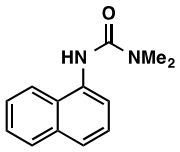	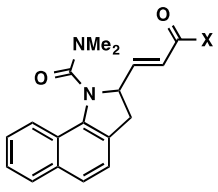	56	29

[a]Isolated yield. [b]Determined by chiral HPLC

The 4-methoxy substrate proved most successful and was used to analyze the other dienes. The methyl and ethyl ester dienes gave similar yields while the benzyl ester gave slightly lower yield. The Weinreb amide gave a significantly lower yield than the ester derivatives. Reactions with and *trans*-1-phenyl-1,3-butadiene **28** and carboxylic acid **29** did not yield any carboamination product. Halogenated substrates were tolerated in the reaction with reduced yields, but no evidence of classic Heck coupling was observed (entries 8 and 9). While the *ortho*-methyl substrate cyclized with a reduced yield, it proved to be the most enantioselective substrate (entry 11). The *meta*-methyl substrate (entry 12) proceeded smoothly to give a single regioisomer, but with almost complete loss of enantioselectivity. Lastly, the reaction of 1-naphtyl substrate (entry 13) gave a similar yield and enantioselectivity as the unsubstituted substrate (entry 1).

A number of synthesized substrates proved unfeasible in the reaction conditions (Figure 4.4).

Figure 4.4: Unsuccessful Substrates

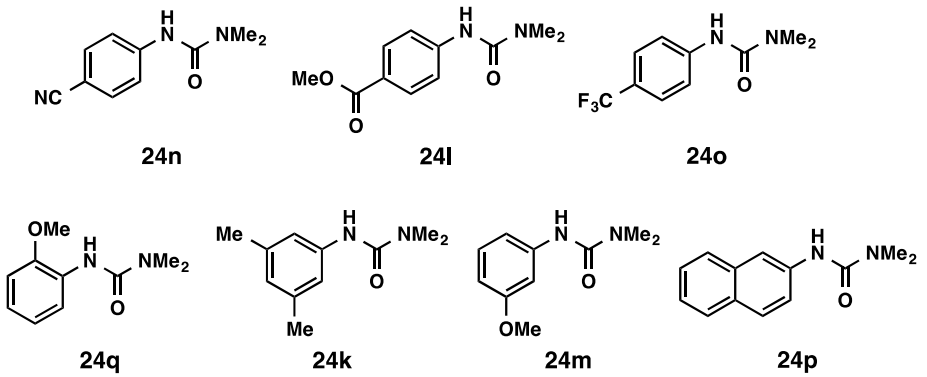

Strongly electron withdrawing groups (**24n**) gave no reaction, while less electron-withdrawing substituents (**24l** and **24o**) gave conversions of less than 10% upon workup.

Similarly, substrate **24q** and **24k** had little reactivity and were difficult to isolate. Lastly, **24m** and **24p** gave a mixture of inseparable regioisomers from non-selective C-H insertion when subjected to the optimized conditions.

Mechanistic Considerations

The proposed mechanism for the asymmetric 1,2-carboamination is shown in Figure 4.5.

Figure 4.5: Catalytic Cycle of Enantioselective 1,2-Carboamination

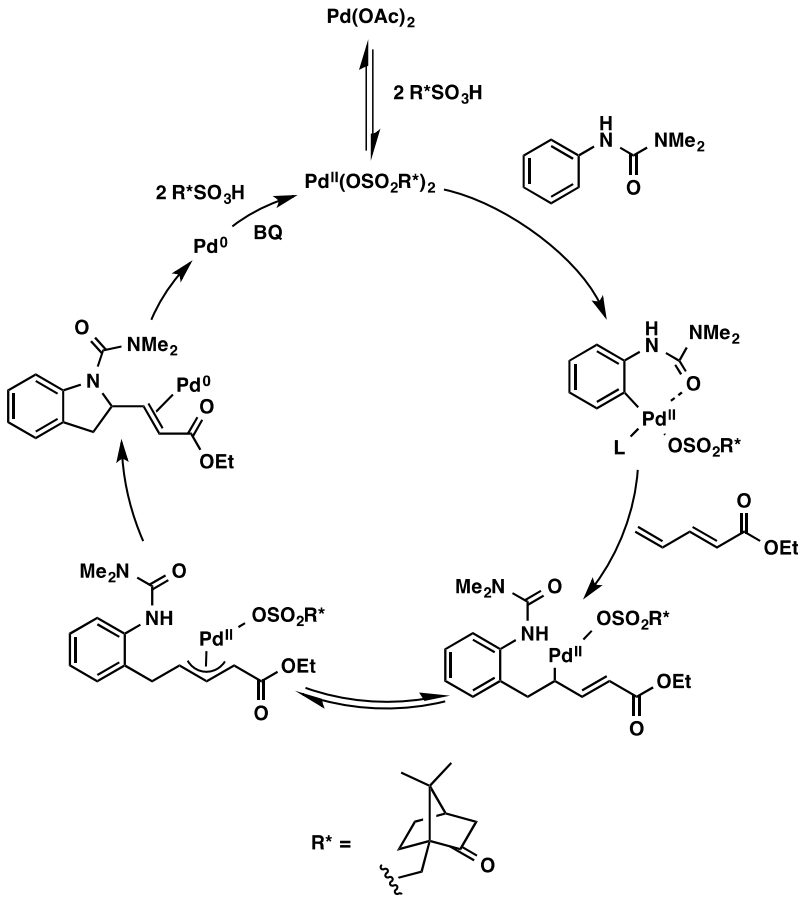

The catalytic cycle begins with two successive acid promoted exchanges with the acetate ligands, generating a more electrophilic Pd[(+)-CSA]$_2$ species. Next dimethyurea directed C-H insertion occurs *ortho* to the aniline. Coordination of the terminal alkene of the diene and subsequent migratory insertion leads to aryl-carbon bond formation. An equilibrium then exists between the η^1 and η^3-Pd-π-allyl intermediate which is attacked by the secondary amine of the urea, creating the chiral indoline. Upon decomplexation with the alkene, Pd^0 is reoxidized by benzoquinone to regenerate the active Pd^{II} catalyst.

Analysis by Brown on a similar palladium X-type catalyst system[114] demonstrated the directed C-H insertion proceeds through an electrophilic Wheland intermediate and is the slow step of the catalytic cycle. The lack of reactivity of strongly electron-withdrawing groups is consistent with this type of intermediate, although another mode of C-H activation, namely concerted metallation-deprotonation, cannot be ruled out.

Conclusion

The use of chiral X-type ligands proved viable for applications in C-H activation. Despite generating an electrophilic catalyst, no conditions were found to successfully facilitate constructive C-H insertion for an asymmetric intramolecular oxidative Heck. Chiral sulfonic acid ligands were successful in the formation of chiral indolines via an asymmetric 1,2-carboamination with yields up to 61% and enantioselectivities as high as 46% ee. To our knowledge this is the first asymmetric oxidative carboamination to utilize chiral X-type ligands.

Experimental

Synthesis of **18** and **21**

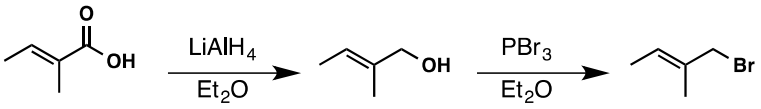

trans-1-bromo-2-methyl-butene: 62% yield over two steps (colorless oil). Synthesized according to literature procedures and characterization is consistent with the literature.[115] **^{1}H NMR** (500 MHz, $CDCl_3$) δ 5.71-5.67 (m, 1H), 3.98 (s, 2H), 1.75 (d, *J* = 1.2 Hz, 3H), 1.63 (d, *J* = 6.9 Hz, 3H). **^{13}C NMR** (75 MHz, $CDCl_3$) δ 132.85, 125.97, 42.00, 14.48, 14.05.

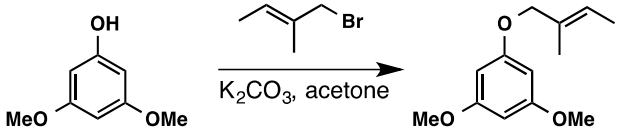

18

To a flame-dried 25mL-round bottom flask was added 3,5-dimethoxyphenol (1.5 mmol) and anhydrous K_2CO_3 (3.0 mmol) in acetone (6 mL) and cooled to 0^{o}C. *trans*-1-bromo-2-methyl-butene (1.65 mmol) was added dropwise to the reaction flask. The reaction was placed under reflux for 12h, diluted with H_2O (10 mL), extracted with Et_2O (3 x 10 mL), dried with $MgSO_4$ and concentrated *in vaccuo*. The crude product was purified by silica column chromatography (2.5% EtOAc/Hex) to give 1,3-dimethoxy-5-(2-methylbut-2-enyloxy)benzene (**18**): 40% yield (colorless oil). Characterization is consistent with the

literature.[116] **^{1}H NMR** (500 MHz, $CDCl_3$) δ 6.11 (d, *J* = 2.2 Hz, 2H), 6.09 – 6.07 (m, 1H), 5.63 (q, *J* = 6.5 Hz, 1H), 4.34 (s, 2H), 3.76 (s, 6H), 1.74 (s, 3H), 1.67 (d, *J* = 6.6 Hz, 3H). **^{13}C NMR** (75 MHz, $CDCl_3$) δ 161.55, 161.04, 131.77, 123.76, 93.76, 93.07, 74.30, 55.45, 13.80, 13.44. **HRMS** (ESI) calculated for $C_{13}H_{18}O_3$ ($[M+H]^+$): 223.1329, found: 223.1366.

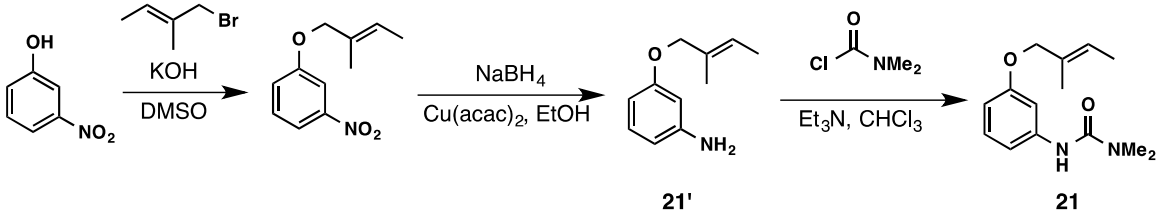

21' was synthesized in two steps according to literature procedures.[69] To a round-bottom flask containing **21'** in $CHCl_3$ (0.5M) was added Et_3N (1.1 eq) and dimethylcarbomyl chloride (1.1 eq). The reaction was stirred at r.t. for 2h, then additional Et_3N (1.1 eq) and dimethylcarbomyl chloride (1.1 eq) was added to the reaction and allowed to stir for 22h at r.t. The crude product was concentrated *in vaccuo*, taken up in a mixture of EtOAc and sat. NH_4Cl. The organic layer was washed with H_2O, brine, dried with $MgSO_4$, and concentrated *in vaccuo*. The product was purified by silica column chromatography (20%-100% EtOAc), to give (*E*)-1,1-dimethyl-3-(3-((2-methylbut-2-en-1-yl)oxy)phenyl)urea (21): 44%, three steps (white solid). **^{1}H NMR** (500 MHz, $CDCl_3$) δ 7.18-7.12 (m, 2H), 6.83 (dd, *J* = 8.0, 2.0 Hz, 1H), 6.60 (dd, *J* = 8.2, 2.5 Hz, 1H), 6.30 (s, 1H), 5.62 (q, *J* = 6.2 Hz, 1H), 4.36 (s, 2H), 3.02 (s, 6H), 1.72 (s, 3H), 1.66 (d, *J* = 6.7 Hz, 3H). **^{13}C NMR** (126 MHz, $CDCl_3$) δ 159.77, 155.70, 140.50, 131.88, 129.50, 123.40, 111.86, 109.92, 106.24, 74.17, 36.61, 13.79, 13.41. **IR** (thin film) 3329, 2921, 2860,

1649, 1605, 1538, 1490, 1434, 1368, 1200, 1156, 1014 cm^{-1}. **TLC**: R_f = 0.21 (50% EtOAc/hexanes, UV & $KMnO_4$ visualization). **HRMS** (ESI) calculated for $C_{14}H_{20}N_2O_2$ ($[M+H]^+$): 249.1598, found: 249.1687.

Directed Oxidative Suzuki Coupling of **24a**

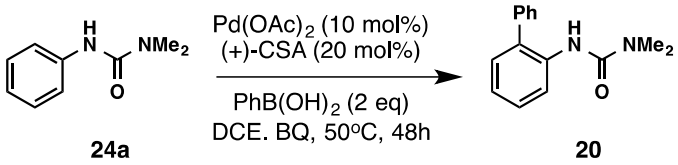

24a **20**

To a flame-dried 2-dram vial was added $Pd(OAc)_2$ (0.01 mmol) and (+)-CSA (0.02 mmol) with DCE (0.4 mmol) and allowed to stir at r.t. for 20 min under Ar. **24a** (0.1 mmol), benzoquinone (0.2 mmol) and $PhB(OH)_2$ (0.15 mmol) were added with DCE (0.6 mL) and the reaction was allowed to stir at r.t. for 24h. The reaction was directly purified by silica column chromatography (40% EtOAc/Hex) to produce 3-(biphenyl-2-yl)-1,1-dimethylurea (20): 75% yield (white solid). Characterization is consistent with the literature.[102] **^{1}H NMR** (500 MHz, $CDCl_3$) δ 8.18 (d, *J* = 8.3 Hz, 1H), 7.49 – 7.32 (m, 6H), 7.20 (d, *J* = 7.4 Hz, 1H), 7.08 (t, *J* = 7.4 Hz, 1H), 6.51 (s, 1H), 2.80 (s, 6H). **^{13}C NMR** (75 MHz, $CDCl_3$) δ 155.58, 138.78, 16.41, 161.44, 129.7, 129.2, 128.59, 127.98, 122.66, 120.44, 36.28.

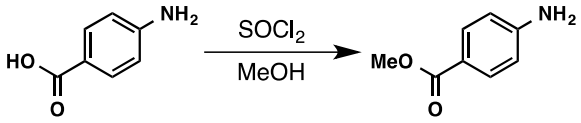

methyl 4-aminobenzoate: 90% yield (white solid). Synthesized according to literature procedure and consistent with literature characterization[117] **^{1}H NMR** (500 MHz, $CDCl_3$) δ 7.85 (d, *J* = 8.3 Hz, 2H), 6.64 (d, *J* = 8.2 Hz, 2H), 4.05 (bs, 2H), 3.85 (s, 3H).

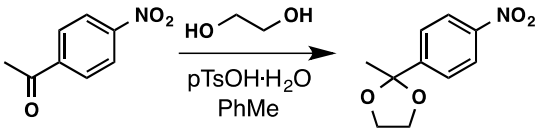

To a flame-dried 25mL-round bottom flask was added *p*-nitroacetophenone (1 eq), pTsOH·H_2O (10 mol%), and ethylene glycol (2.5 eq) dissolved in PhMe. The reaction was refluxed with a Dean-Stark trap for 12h, diluted with DCM, washed with H_2O, dried with $MgSO_4$ and concentrated *in vaccuo* to give 2-methyl-2-(4-nitrophenyl)-1,3-dioxolane (quantitative yield, yellow solid). Characterization consistent with the literature.[118] **^{1}H NMR** (500 MHz, $CDCl_3$) δ 8.20 (d, *J* = 8.8 Hz, 2H), 7.66 (d, *J* = 8.8 Hz, 2H), 4.12 – 4.01 (m, 2H), 3.78 – 3.74 (m, 2H), 1.65 (s, 3H).

<u>Alkylation of Nitrophenols</u>

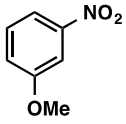

1-methoxy-3-nitrobenzene: 95% yield (red oil). Synthesized according to literature procedure from 3-nitrophenol and iodomethane[119] and consistent with literature characterization.[120] **^{1}H NMR** (500 MHz, $CDCl_3$) δ 7.83 (d, *J* = 8.1 Hz, 1H), 7.73 (app t, *J* = 2.3 Hz, 1H), 7.43 (app. t, *J* = 8.2 Hz, 1H), 7.23 (dd, *J* = 8.2, 2.6 Hz, 1H), 3.89 (s, 3H).

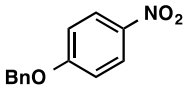

1-(benzyloxy)-4-nitrobenzene: 97% yield (white solid). Synthesized according to literature procedure from 4-nitrophenol and benzyl chloride[121] and consistent with literature characterization.[122] **^{1}H NMR** (500 MHz, $CDCl_3$) δ 8.21 (d, *J* = 9.2 Hz, 2H), 7.50 – 7.32 (m, 5H), 7.03 (d, *J* = 9.2 Hz, 2H), 5.17 (s, 2H).

Reduction of Arylnitro Substrates[123]

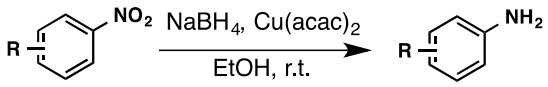

A flame dried 50mL-round bottom flask was charged with $NaBH_4$ (1 eq) and $Cu(acac)_2$ (20 mol%) and stirred at room temperature for 10 min with EtOH (0.27 M) under Ar. The corresponding arylnitro substrate was added (1 eq), then additional $NaBH_4$ (2 eq) and EtOH (2.5 M). The reaction was stirred at r.t. until no arylnitro substrate was present by TLC (1.5-18h), quenched with H_2O and concentrated *in vaccuo*. The crude product was further diluted with H_2O, extracted with EtOAc (3 x 20mL), dried with $MgSO_4$, filtered and concentrated *in vaccuo*. The product was either used without further purification or purified by silica column chromatography (10-30% EtOAc/Hex).

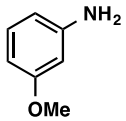

3-methoxylaniline: 99% yield (colorless oil). Characterization consistent with the literature.[124] **^{1}H NMR** (500 MHz, $CDCl_3$) δ 7.06 (t, *J* = 8.0 Hz, 1H), 6.33 (dd, *J* = 8.2, 2.3 Hz), 6.30 (dd, *J* = 7.9, 2.1 Hz), 6.25 (t, *J* = 2.4 Hz, 1H), 3.77 (s, 3H), 3.65 (bs, 2H).

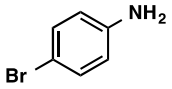

4-bromoaniline: 60% yield (white solid). Characterization consistent with the literature.[122] **^{1}H NMR** (300 MHz, $CDCl_3$) δ 7.23 (d, *J* = 8.7 Hz, 2H), 6.57 (d, *J* = 8.7 Hz, 2H), 3.69 (bs, 2H).

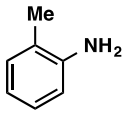

2-methylaniline: quantitative yield (colorless oil). Characterization consistent with the literature.[122] **^{1}H NMR** (500 MHz, $CDCl_3$) δ 7.10 – 7.01 (m, 2H), 6.76 – 6.66 (m, 2H), 2.18 (bs, 3H).

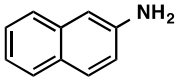

2-aminonaphthalene: 92% yield (brown solid). Characterization consistent with the literature.[122] **^{1}H NMR** (500 MHz, $CDCl_3$) δ 7.74 – 7.64 (m, 2H), 7.59 (d, *J* = 8.3 Hz, 1H), 7.37 (t, *J* = 7.5 Hz, 1H), 7.21 (t, *J* = 7.4 Hz, 1H), 7.04 – 6.87 (m, 2H), 3.73 (bs, 2H).

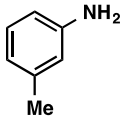

3-methylaniline: quantitative yield (colorless oil). Characterization consistent with the literature.[122] **^{1}H NMR** (500 MHz, $CDCl_3$) δ 7.05 (t, *J* = 7.6 Hz, 1H), 6.59 (d, *J* = 7.5 Hz, 1H), 6.55 – 6.48 (m, 2H), 3.60 (bs, 2H), 2.27 (s, 3H).

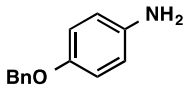

1-(benzyloxy)-4-nitrobenzene: 98% yield (yellow oil). Characterization consistent with the literature.[125] **^{1}H NMR** (500 MHz, $CDCl_3$) δ 7.42 (d, *J* = 7.0 Hz, 2H), 7.37 (t, *J* = 7.5 Hz, 2H), 7.31 (t, *J* = 7.2 Hz, 1H), 6.82 (d, *J* = 8.7 Hz, 2H), 6.64 (d, *J* = 8.6 Hz, 2H), 4.99 (s, 2H), 3.43 (bs, 2H).

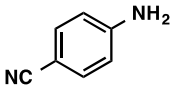

4-aminobenzonitrile: 33% yield (white solid). Characterization consistent with the literature.[122] **^{1}H NMR** (500 MHz, $CDCl_3$) δ 7.42 (d, *J* = 8.6 Hz, 2H), 6.65 (d, *J* = 8.6 Hz, 2H), 4.14 (bs, 2H).

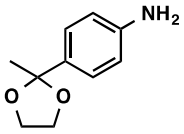

4-(2-methyl-1,3-dioxolan-2-yl)aniline: 91% yield (white solid). Characterization consistent with the literature.[126] **^{1}H NMR** (500 MHz, $CDCl_3$) δ 7.27 (d, *J* = 8.5 Hz, 2H), 6.66 (d, *J* = 8.5 Hz, 2H), 4.04 – 4.00 (m, 2H), 3.81 – 3.77 (m, 2H), 3.68 (bs, 2H), 1.64 (s, 3H).

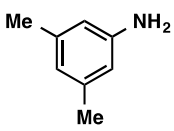

3,5-dimethylaniline: 85% yield (light red oil). Characterization consistent with the literature.[127] **^{1}H NMR** (500 MHz, CDCl3) δ 6.43 (s, 1H), 6.34 (s, 2H), 3.55 (s, 2H), 2.23 (s, 6H).

Synthesis of Dimethylureas

Method A: The substrates were synthesized from the corresponding arylisocyante according to existing literature procedure. [128]

Method B: To a flame-dried round bottom flask was added an aniline and dichloromethane (1M). Pyridine (1.05 eq) was added to the solution and after stirring for 5 minutes at r.t. dimethylcarbomyl chloride (1.75 eq) was added dropwise. The reaction was stirred at reflux for 24h and the crude product was poured through a silica plug with EtOAc and concentrated. Based off of the crude ^{1}H-NMR the product was either recrystallized in PhMe (minor impurities) or purified by silica column chromatography (25%-100% EtOAc/Hex).

Method C: The substrates were synthesized from the corresponding aniline according to existing literature procedure.[129]

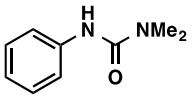

Method A, 1,1-dimethyl-3-phenylurea (**24a**): quantitative yield (white solid), mp 125-126°C. **^{1}H NMR** (500 MHz, $CDCl_3$) ^{1}H δ 7.40 – 7.36 (m, 2H), 7.30 – 7.26 (m, 2H), 7.02 (m, 1H), 6.31 (bs, 1H), 3.03 (s, 6H). **^{13}C NMR** (75 MHz, $CDCl_3$ δ 155.83, 139.32, 128.94, 123.02, 119.95, 36.57. **IR** (thin film) 3344, 3303, 1641, 1592, 1525, 1437, 1373, 1306, 1248, 1187 cm^{-1}. **TLC**: R_f = 0.21 (50% EtOAc/hexanes, UV & $KMnO_4$ visualization). **HRMS** (ESI) calculated for $C_9H_{12}N_2O$ ($[M+H]^+$): 165.1022, found: 165.1095.

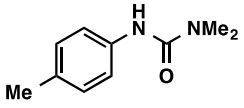

Method C, 1,1-dimethyl-3-(*p*-tolyl)urea (**24b**): 85% yield (white solid), mp 146-147°C. **^{1}H NMR** (500 MHz, $CDCl_3$) ^{1}H δ 7.24 (d, *J* = 7.1 Hz, 2H), 7.07 (d, *J* = 7.4 Hz, 2H), 6.22 (bs, 1H), 3.00 (s, 6H), 2.27 (s, 3H). **^{13}C NMR** (75 MHz, $CDCl_3$) δ 156.01, 136.69, 132.55, 129.43, 120.19, 36.55, 20.85. . **IR** (thin film) 3341, 3307, 2918, 1655, 1598, 1523, 1403, 1372, 1244, 1187 cm^{-1}. **TLC**: R_f = 0.21 (50% EtOAc/hexanes, UV & $KMnO_4$ visualization). **HRMS** (ESI) calculated for $C_{10}H_{14}N_2O$ ($[M+H]^+$): 179.1179, found: 179.1241.

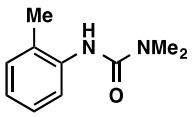

Method B, 1,1-dimethyl-3-(*o*-tolyl)urea (**24h**): 48% yield (white solid), mp 131-132°C. **^{1}H NMR** (500 MHz, $CDCl_3$) ^{1}H NMR δ 7.72 (d, *J* = 8.1 Hz, 1H), 7.21 – 7.13 (m, 2H), 7.00 (app t, *J* = 7.4, 1H), 6.11 (bs, 1H), 3.04 (s, 6H), 2.25

(s, 3H). **^{13}C NMR** (75 MHz, $CDCl_3$) δ 156.01, 137.29, 130.32, 128.41, 126.81, 123.83, 122.59, 36.56, 17.88. **IR** (thin film) 3272, 2925, 1639, 1521, 1488, 1378, 1251 cm^{-1}. **TLC**: R_f = 0.17 (50% EtOAc/hexanes, UV & $KMnO_4$ visualization). **HRMS** (ESI) calculated for $C_{10}H_{14}N_2O$ ($[M+H]^+$): 179.1179, found: 179.1281.

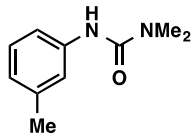

Method B, 1,1-dimethyl-3-(*m*-tolyl)urea (**24i**): 77% yield (white solid), mp 120-121°C. **^{1}H NMR** (300 MHz, $CDCl_3$) δ 7.21 – 7.09 (m, 2H), 6.84 (d, *J* = 6.3 Hz, 1H), 6.26 (s, 1H), 3.02 (s, 6H), 2.32 (s, 3H). **^{13}C NMR** (75 MHz, $CDCl_3$) δ 155.86, 139.20, 138.80, 128.74, 123.84, 120.65, 116.94, 36.56, 21.62. **IR** (thin film) 3310, 2921, 1645, 1593, 1535, 1486, 1372, 1261, 1202 cm^{-1}. **TLC**: R_f = 0.24 (50% EtOAc/hexanes, UV & $KMnO_4$ visualization).

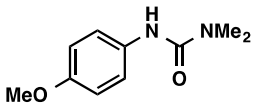

Method B, 3-(4-methoxyphenyl)-1,1-dimethylurea (**24c**): 47% yield (white solid), mp 123-124°C. **^{1}H NMR** (500 MHz, $CDCl_3$) δ 7.28 – 7.25 (m, 2H), 6.88 – 6.80 (m, 2H), 6.20 (bs, 1H), 3.77 (s, 3H), 3.01 (s, 6H). **^{13}C NMR** (75 MHz, $CDCl_3$) δ 156.32, 155.83, 132.34, 122.38, 114.14, 55.61, 36.53. **IR** (thin film) 3301, 2936, 2908, 2837, 1644, 1600, 1531, 1375, 1294, 1237 cm^{-1}. **TLC**: R_f = 0.11 (50% EtOAc/hexanes, UV & $KMnO_4$ visualization). **HRMS** (ESI) calculated for $C_{10}H_{14}N_2O_2$ ($[M+H]^+$): 195.1128, found: 195.1253.

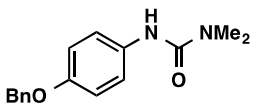

Method B, 3-(4-(benzyloxy)phenyl)-1,1-dimethylurea (**24d**): 54% yield (white solid), mp 152-153°C. **^{1}H NMR** (500 MHz, $CDCl_3$) δ

7.42 (d, *J* = 7.5 Hz, 2H), 7.38 (t, *J* = 7.5 Hz, 2H), 7.33 – 7.27 (m, 3H), 6.91 (d, *J* = 8.8 Hz, 2H), 6.16 (bs, 1H), 5.03 (s, 2H), 3.02 (s, 6H). **^{13}C NMR** (75 MHz, $CDCl_3$) δ 156.25, 155.06, 137.27, 132.59, 128.66, 128.01, 127.60, 122.26, 115.29, 70.47, 36.57. **IR** (thin film) 3301, 3048, 2907, 2864, 1633, 1595, 1570, 1372, 1288, 1234 cm^{-1}. **TLC**: R_f = 0.17 (50% EtOAc/hexanes, UV & $KMnO_4$ visualization). **HRMS** (ESI) calculated for $C_{16}H_{18}N_2O_2$ ($[M+H]^+$): 271.1441, found: 271.1453.

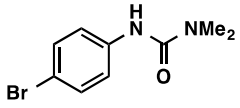

Method B, 3-(4-bromophenyl)-1,1-dimethylurea (**24e**): 87% yield (white solid), mp 161-162°C. **^{1}H NMR** (500 MHz, $CDCl_3$) δ 7.38 (d, *J* = 8.4 Hz, 2H), 7.29 (d, *J* = 8.5 Hz, 2H), 6.29 (bs, 1H), 3.03 (s, 6H). **^{13}C NMR** (75 MHz, $CDCl_3$) δ 155.51, 138.46, 131.83, 121.48, 115.45, 36.59. **IR** (thin film) 3301, 2925, 1643, 1587, 1513, 1491, 1397, 1347, 1245, 1187cm^{-1}. **TLC**: R_f = 0.26 (50% EtOAc/hexanes, UV & $KMnO_4$ visualization). **HRMS** (ESI) calculated for $C_9H_{11}BrN_2O$ ($[M+H]^+$): 243.0128, found: 243.0235.

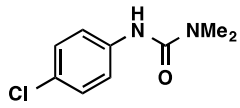

Method B, 3-(4-chlorophenyl)-1,1-dimethylurea (**24f**): 77% yield (white solid), mp 161-162°C. **^{1}H NMR** (500 MHz, $CDCl_3$) δ 7.37 – 7.30 (m, 2H), 7.25 – 7.21 (m, 2H), 6.31 (bs, 1H), 3.02 (s, 6H). **^{13}C NMR** (75 MHz, $CDCl_3$) δ 155.59, 137.92, 128.90, 127.97, 121.18, 36.58. **IR** (thin film) 3297, 2928, 1644, 1591, 1508, 1496, 1375, 1246, 1188, 832 cm^{-1}. **TLC**: R_f = 0.24 (50% EtOAc/hexanes, UV & $KMnO_4$ visualization). **HRMS** (ESI) calculated for $C_9H_{10}ClN_2O$ ($[M+H]^+$): 199.0633, found: 199.0752.

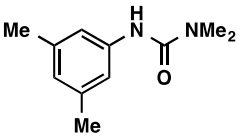

Method B, 3-(3,5-dimethylphenyl)-1,1-dimethylurea (**24k**): 75% yield (white solid), mp 148-150°C. **^{1}H NMR** (500 MHz, $CDCl_3$) δ 7.02 (s, 2H), 6.67 (s, 1H), 6.20 (bs, 1H), 3.02 (s, 6H), 2.28 (s, 6H). **^{13}C NMR** (75 MHz, $CDCl_3$) δ 155.87, 139.10, 138.63, 124.83, 117.65, 36.57, 21.52. **IR** (thin film) 3306, 2919, 1645, 1612, 1550, 1491, 1450, 1370, 1324, 1205, 840 cm^{-1}. **TLC**: R_f = 0.31 (50% EtOAc/hexanes, UV & $KMnO_4$ visualization). **HRMS** (ESI) calculated for $C_{11}H_{16}N_2O$ ($[M+H]^+$): 215.1179, found: 215.1240.

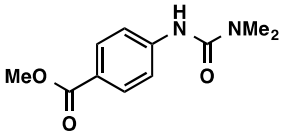

Method B, methyl 4-(3,3-dimethylureido)benzoate (**24l**) 64% yield (white solid), mp 161-162°C. **^{1}H NMR** (500 MHz, $CDCl_3$) δ 7.96 (d, *J* = 8.5 Hz, 2H), 7.47 (d, *J* = 8.4 Hz, 2H), 6.53 (s, 1H), 3.88 (s, 3H), 3.05 (s, 6H). **^{13}C NMR** (75 MHz, $CDCl_3$) δ 166.97, 155.14, 143.81, 130.84, 124.15, 118.45, 52.01, 36.63. **IR** (thin film) 3363, 2951, 1715, 1654, 1593, 1523, 1411, 1318, 1281, 1250, 1173, 1109 cm^{-1}. **TLC**: R_f = 0.19 (50% EtOAc/hexanes, UV & $KMnO_4$ visualization). **HRMS** (ESI) calculated for $C_{10}H_{14}N_2O_2$ ($[M+H]^+$): 223.1077, found: 223.1193.

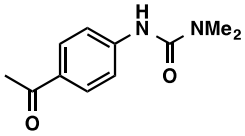

Method B, 3-(4-acetylphenyl)-1,1-dimethylurea (**24g**): 65% yield (white solid), mp 133-134°C. **^{1}H NMR** (500 MHz, $CDCl_3$) δ 7.90 (d, *J* = 8.8 Hz, 2H), 7.50 (d, *J* = 8.7 Hz, 2H), 6.55 (s, 1H), 3.06 (s, 6H), 2.56 (s, 3H).**^{13}C NMR** (75 MHz, $CDCl_3$) δ 197.20, 155.12, 144.10, 131.62, 129.81, 118.49, 36.65, 26.50. **IR** (thin film) 3330, 2929, 1659, 1589, 1523, 1410, 1362, 1275, 1525, 1177, 838 cm^{-1}.

TLC: R_f = 0.14 (50% EtOAc/hexanes, UV & $KMnO_4$ visualization). **HRMS** (ESI) calculated for $C_{11}H_{14}N_2O_2$ ($[M+H]^+$): 207.1128, found: 207.1237.

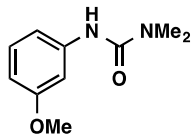

Method C, 3-(3-methoxyphenyl)-1,1-dimethylurea (**24m**): 60% yield (white solid), mp 132-133°C. **^{1}H NMR** (500 MHz, $CDCl_3$) δ 7.20 – 7.12 (m, 2H), 6.81 (dd, *J* = 8.0, 2.1 Hz, 1H), 6.57 (dd, *J* = 8.3, 2.4 Hz, 1H), 6.29 (s, 1H), 3.78 (s, 3H), 3.01 (s, 6H). **^{13}C NMR** (75 MHz, $CDCl_3$) δ 160.28, 155.71, 140.64, 129.53, 111.85, 109.11, 105.26, 55.37, 36.58. **IR** (thin film) 3329, 2935, 1649, 1606, 1536, 1462, 1450, 1426, 1375, 1293, 1214, 1160, 1038, 846 cm^{-1}. **TLC**: R_f = 0.22 (50% EtOAc/hexanes, UV & $KMnO_4$ visualization). **HRMS** (ESI) calculated for $C_{10}H_{14}N_2O_2$ ($[M+H]^+$): 195.1128, found: 195.1108.

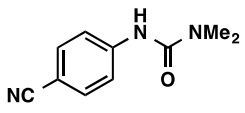

Method B, 3-(4-cyanophenyl)-1,1-dimethylurea (**24n**): 39% yield (white solid), mp 143-145°C. **^{1}H NMR** (500 MHz, $CDCl_3$) δ 7.61 – 7.49 (m, 4H), 6.52 (s, 1H), 3.06 (s, 6H). **^{13}C NMR** (75 MHz, $CDCl_3$) δ 154.84, 143.74, 133.21, 119.39, 119.21, 105.34, 36.67.**IR** (thin film) 3319, 2931, 2222, 1660, 1590, 1517, 1413, 1377, 1314, 1252, 1177, 836 cm^{-1}. **TLC**: R_f = 0.17 (50% EtOAc/hexanes, UV & $KMnO_4$ visualization). **HRMS** (ESI) calculated for $C_{10}H_{11}N_3O$ ($[M+H]^+$): 190.0975, found: 190.1059.

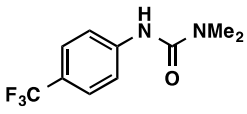

Method B, 1,1-dimethyl-3-(4-(trifluoromethyl)phenyl)urea (**24o**): 78% yield (white solid), mp 179-181°C. **^{1}H NMR** (500 MHz,

$CDCl_3$) δ 7.57 – 7.47 (m, 4H), 6.47 (s, 1H), 3.06 (s, 6H). **^{13}C NMR** (75 MHz, $CDCl_3$) δ 155.25, 142.52, 126.21 (q, *J* = 3.8 Hz), 126.14, 119.10, 36.63. **IR** (thin film) 3321, 2936, 1657, 1600, 1532, 1489, 1415, 1320, 1252, 1153, 1110, 1066, 836 cm^{-1}. **TLC**: R_f = 0.15 (50% EtOAc/hexanes, UV & $KMnO_4$ visualization). **HRMS** (ESI) calculated for $C_{10}H_{11}F_3N_2O$ ($[M+H]^+$): 233.0896, found: 233.0991.

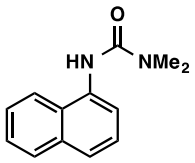

Method A, 1,1-dimethyl-3-(naphthalen-1-yl)urea (**24j**): quantitative yield (white solid), mp 160-161°C. **^{1}H NMR** (500 MHz, $CDCl_3$) δ 7.86 (d, *J* = 8.0 Hz, 2H), 7.77 (d, *J* = 7.5 Hz, 1H), 7.65 (d, *J* = 8.2 Hz, 1H), 7.54 – 7.43 (m, 3H), 6.63 (s, 1H), 3.12 (s, 6H). **^{13}C NMR** (75 MHz, $CDCl_3$) δ 156.58, 134.30, 134.10, 128.79, 127.96, 126.08, 125.97, 125.87, 124.88, 121.07, 120.71, 36.74. **IR** (thin film) 3274, 2922, 1638, 1601, 1540, 1500, 1386, 1373, 1286, 1230, 1191, 858, 818 cm^{-1}. **TLC**: R_f = 0.22 (50% EtOAc/hexanes, UV & $KMnO_4$ visualization). **HRMS** (ESI) calculated for $C_{13}H_{14}N_2O$ ($[M+H]^+$): 215.1179, found: 215.1217.

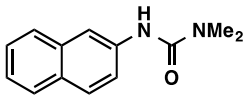

Method B, 1,1-dimethyl-3-(naphthalen-2-yl)urea (**24p**): 37% yield (brown solid), mp 199-200°C. **^{1}H NMR** (500 MHz, $CDCl_3$) δ 7.98 (d, *J* = 2.2 Hz, 1H), 7.79 – 7.71 (m, 3H), 7.45 – 7.40 (m, 2H), 7.37-7.33 (m, 1H), 6.47 (s, 1H), 3.08 (s, 6H). **^{13}C NMR** (75 MHz, $CDCl_3$) δ 155.86, 136.81, 134.19, 130.17, 128.66, 127.62, 127.49, 126.41, 124.50, 120.58, 115.84, 36.66. **IR** (thin film) 3274, 3048, 2925, 1641, 1596, 1528, 1499, 1375, 1271, 1196, 793, 769 cm^{-1}. **TLC**: R_f = 0.29 (50%

EtOAc/hexanes, UV & $KMnO_4$ visualization). **HRMS** (ESI) calculated for $C_{13}H_{14}N_2O$ ($[M+H]^+$): 215.1179, found: 215.1240.

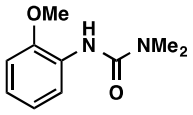

Method C, 3-(2-methoxyphenyl)-1,1-dimethylurea (**24q**): 51% yield (purple oil). **^{1}H NMR** (500 MHz, $CDCl_3$) δ 8.25 – 8.13 (m, 1H), 7.08 (s, 1H), 6.98 – 6.90 (m, 2H), 6.87-6.82 (m, 1H), 3.88 (s, 3H), 3.04 (s, 6H). **^{13}C NMR** (75 MHz, $CDCl_3$) δ 155.56, 147.59, 129.10, 121.85, 121.18, 118.86, 109.70, 55.78, 36.35. **IR** (thin film) 3446, 2936, 1674, 1601, 1530, 1459, 1363, 1249, 1173, 1116, 1027, 752 cm^{-1}. **TLC**: R_f = 0.39 (??% EtOAc/hexanes, UV & $KMnO_4$ visualization). **HRMS** (ESI) calculated for $C_{10}H_{14}N_2O_2$ ($[M+H]^+$): 195.1128, found: 195.1258.

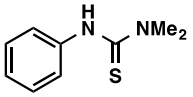

Method A (with phenylisothiocyanate), 1,1-dimethyl-3-phenylthiourea (**24r**): quantitative yield (white solid), mp 121-123^{o}C. **^{1}H NMR** (500 MHz, $CDCl_3$) δ 7.35 (t, *J* = 7.8 Hz, 2H), 7.25 (d, *J* = 7.8 Hz, 2H), 7.19 (t, *J* = 7.4 Hz, 1H), 7.05 (s, 1H), 3.34 (s, 6H). **^{13}C NMR** (75 MHz, $CDCl_3$) δ 182.44, 139.91, 128.86, 125.65, 125.01, 41.59. **IR** (thin film) 3246, 2924, 1596, 1536, 1496, 1372, 1337, 1307, 1258, 1138 cm^{-1}. **TLC**: R_f = 0.49 (50% EtOAc/hexanes, UV & $KMnO_4$ visualization). **HRMS** (ESI) calculated for $C_9H_{12}N_2S$ ($[M+H]^+$): 181.0794, found: 181.0883.

<u>Synthesis of Substrates with Other Directing Groups</u>

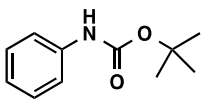

tert-butyl phenylcarbamate: quantitative yield (white solid). Synthesized according to literature procedure[130] and consistent with

literature spectra.[131] **^{1}H NMR** (500 MHz, $CDCl_3$) δ 7.35 (d, *J* = 8.0 Hz, 2H), 7.29 (t, *J* = 7.8 Hz, 2H), 7.03 (t, *J* = 7.2 Hz, 1H), 6.45 (bs, 1H), 1.52 (s, 9H). **^{13}C NMR** (75 MHz, $CDCl_3$) δ 152.88, 138.45, 129.10, 123.15, 118.65, 80.63, 28.49.

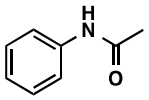

N-phenylacetamide: quantitative yield (tan solid). Synthesized according to literature procedure and consistent with literature characterization.[132] **^{1}H NMR** (500 MHz, $CDCl_3$) δ 7.50 (d, *J* = 7.9 Hz, 2H), 7.32 (t, *J* = 7.8 Hz, 2H), 7.11 (t, *J* = 7.3 Hz, 1H), 2.18 (s, 3H).

Synthesis of Dienes

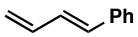

Synthesized according to literature procedure via Wittig reaction from *trans*-cinnamaldehyde (**28**): 75% yield (yellow oil).[133] **^{1}H NMR** (500 MHz, $CDCl_3$) δ 7.41 (d, *J* = 7.5 Hz, 2H), 7.35 – 7.28 (m, 2H), 7.26 – 7.21 (m, 1H), 6.80 (dd, *J* = 15.6, 10.5 Hz, 1H), 6.62 – 6.47 (m, 2H), 5.34 (d, *J* = 16.9 Hz, 1H), 5.18 (d, *J* = 10.1 Hz, 1H). **^{13}C NMR** (75 MHz, $CDCl_3$) δ 137.31, 132.98, 129.75, 128.74, 127.76, 126.57, 117.77.

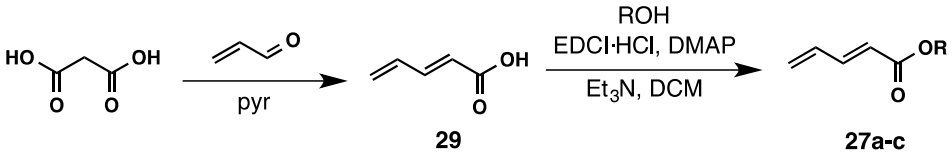

29 **27a-c**

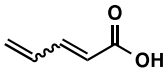

penta-2,4-dienoic acid (**29**): 46% yield (white solid, 94:6 *E*/*Z* isomer). Synthesized according to literature procedure via Knoevenagel condensation of malonic acid and acrolein[134] and is consistent with the literature.[135] **^{1}H NMR** (500 MHz, $CDCl_3$) *E* isomer δ 7.36 (dd, *J* = 15.4, 11.1 Hz, 1H), 6.49 (dt, *J* = 16.8,

10.5 Hz, 1H), 5.92 (d, *J* = 15.4 Hz, 1H), 5.67 (d, *J* = 16.9 Hz, 1H), 5.56 (d, *J* = 10.0 Hz, 1H); *Z*-isomer identical (or unseen) as *E*-isomer except for δ 7.64 – 7.55 (m, 1H), 6.68 (t, *J* = 11.4 Hz, 1H). **^{13}C NMR** (75 MHz, $CDCl_3$) δ 172.71, 147.21, 134.66, 126.98, 121.48.

Synthesis of Diene Esters

To a flame-dried 25mL round-bottom flask was added EDCI·HCl (1 eq) with DCM (0.5 M) and cooled to 0^{o}C. To the reaction flask was added the Et_3N with DCM (1.0M) and allowed to come to r.t. over 5 min before adding DMAP (0.25 eq), **29** (1 eq), and corresponding alcohol (1.25 eq). The reaction was stirred at r.t. under Ar for 24h, concentrated *in vaccuo*. The crude product was purified by silica column chromatography (2.5% EtOAc/Hex or 5% Et_2O/pentane).

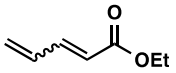

ethyl penta-2,4-dienoate (**27a**): 73% yield (light yellow oil, 97:3 *E*/*Z* isomer). ^{1}H NMR (500 MHz, $CDCl_3$) *E* isomer δ 7.30 – 7.26 (m, 1H), 6.45 (dt, *J* = 16.9, 10.8 Hz, 1H), 5.91 (d, *J* = 15.4 Hz, 1H), 5.61 (d, *J* = 16.9 Hz, 1H), 5.49 (d, *J* = 10.0 Hz, 1H), 4.21 (q, *J* = 7.1 Hz, 2H), 1.30 (t, *J* = 7.1 Hz, 3H); *Z*-isomer identical (or unseen) as *E*-isomer except for δ 7.59 (dt, *J* = 16.9, 10.5 Hz, 1H), 6.54 (t, *J* = 11.3 Hz, 1H). **^{13}C NMR** (75 MHz, $CDCl_3$) δ 167.00, 144.77, 134.91, 125.61, 122.39, 60.54, 14.43. **IR** (thin film) 2928, 1716, 1644, 1600, 1305, 1267, 1203, 1145, 1038, 1010 cm^{-1}. **HRMS** (ESI) calculated for $C_7H_{10}O_2$ ($[M+H]^+$): 127.0754, found: 127.0788.

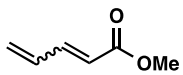

methyl penta-2,4-dienoate (**27b**): 49% yield (light yellow oil, 97:3 *E*/*Z*

isomer). **^{1}H NMR** (500 MHz, $CDCl_3$) *E* isomer δ 7.27 (dd, *J* = 15.4, 11.0 Hz, 1H), 6.45 (dt, *J* = 16.9, 10.5 Hz, 1H), 5.91 (d, *J* = 15.5 Hz, 1H), 5.61 (d, *J* = 16.9 Hz, 1H), 5.49 (d, *J* = 10.0 Hz, 1H), 3.75 (s, 3H); *Z*-isomer identical (or unseen) as *E*-isomer except for δ 7.58 (dt, *J* = 16.9, 10.6 Hz, 1H), 6.56 (t, *J* = 11.6, 10.8 Hz, 1H). **^{13}C NMR** (75 MHz, $CDCl_3$) δ 167.43, 145.06, 134.85, 125.82, 121.88, 51.75. **IR** (thin film) 3006, 2952, 1722, 1645, 1601, 1437, 1311, 1270, 1207, 1147, 1101 cm^{-1}.

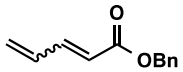

benzyl penta-2,4-dienoate (**27c**): 59% yield (light yellow oil, 94:6 *E*/*Z* isomer). **^{1}H NMR** (500 MHz, $CDCl_3$) *E* isomer δ 7.40 – 7.32 (m, 5H), 6.46 (dt, *J* = 17.0, 10.5 Hz, 1H), 5.96 (d, *J* = 15.4 Hz, 1H), 5.62 (d, *J* = 16.9 Hz, 1H), 5.50 (d, *J* = 10.0 Hz, 1H), 5.20 (s, 2H); *Z*-isomer identical (or unseen) as *E*-isomer except for 6.62 – 6.54 (m, 1H), 5.74 (d, *J* = 11.8 Hz, 2H). **^{13}C NMR** (75 MHz, $CDCl_3$) δ 166.77, 145.33, 136.15, 134.83, 128.70, 128.36, 127.78, 127.12, 125.98, 121.97, 66.38. **IR** (thin film) 3090, 3065, 3032, 2949, 1715, 1641, 1600, 1305, 1266, 1200, 1141, 1009 cm^{-1}. **TLC**: R_f = 0.30 (5% EtOAc/hexanes, UV & $KMnO_4$ visualization).

<u>Synthesis of Diene Weinreb Amide[136]</u>

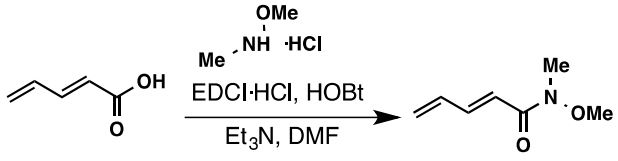

30

To a flame-dried 25mL-round bottom flask was added EDCI·HCl (1.1 eq), HOBt (1.1 eq) with DMF (1 M) and stirred under Ar for 10 min at r.t, then **29** (1.0 eq) was added and allowed to stir at r.t. for 1h. N,O-dimethylhydroxylamine·HCl (1.0 eq) and Et_3N were then added with additional DMF (1 M) and allowed to stir for 16h at r.t. The reaction was diluted with H_2O, extracted with DCM, washed with H_2O, dried with $MgSO_4$, and concentrated *in vaccuo.* The product was purified by silica column chromatography (25% EtOAc/Hex).

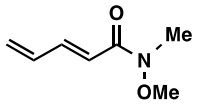

(*E*)-*N*-methoxy-*N*-methylpenta-2,4-dienamide (**30**): 45% yield (yellow oil). **^{1}H NMR** (500 MHz, $CDCl_3$) δ 7.31 (dd, *J* = 15.3, 11.0 Hz, 1H), 6.60 – 6.43 (m, 2H), 5.60 (d, *J* = 17.0 Hz, 1H), 5.46 (d, *J* = 9.9 Hz, 1H), 3.71 (s, 3H), 3.26 (s, 3H). **^{13}C NMR** (75 MHz, $CDCl_3$) δ 167.06, 143.64, 135.35, 124.97, 119.96, 61.93, 32.55. **IR** (thin film) 3003, 2968, 2938, 1658, 1621, 1598, 1463, 1428, 1379, 1182, 1007cm^{-1}. **TLC**: R_f = 0.27 (25% EtOAc/hexanes, UV & $KMnO_4$ visualization). **HRMS** (ESI) calculated for $C_7H_{11}NO_2$ ($[M+H]^+$): 142.0863, found: 142.0983.

<u>Asymmetric 1,2-Carboamination</u>

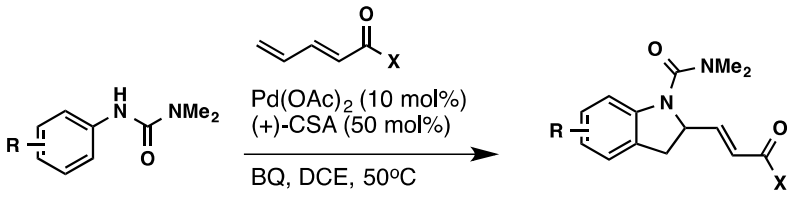

To a flame-dried 2-dram vial was added $Pd(OAc)_2$ (2.2 mg, 0.01 mmol) and (+)-CSA (4.6 mg, 0.02 mmol) and stirred under Ar for 5 min at r.t. with DCE (0.4 mL). To the

reaction flask was added the dimethylurea (0.1 mmol) and benzoquinone (10.9 mg, 0.1 mmol) with additional DCE (0.3 mL) and stirred under Ar for an additional 5 min at r.t.. The diene (0.101 mmol) was added with DCE (0.3 mL) capped and stirred at 50^{o}C for 24h. The crude product was diluted with EtOAc (3 mL) and washed with sat. K_2CO_3 (3 x 5 mL), water (5 mL), and brine (5 mL) dried with $MgSO_4$ and concentrated *in vacuo*. The crude product was purified by silica column chromatography (20-100% EtOAc/Hex or 100% Et_2O).

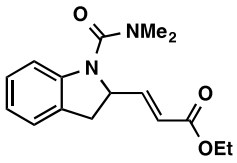

ethyl (*E*)-3-(1-(dimethylcarbamoyl)indolin-2-yl)acrylate (**30a**): 56% yield (purple oil). **^{1}H NMR** (500 MHz, $CDCl_3$) δ 7.17 – 7.10 (m, 2H), 6.97 (dd, *J* = 15.6, 7.2 Hz, 1H), 6.88 (app t, *J* = 7.4 Hz, 1H), 6.74 (d, *J* = 8.2 Hz, 1H), 6.01 (dd, *J* = 15.6, 1.1 Hz, 1H), 5.06 – 4.97 (m, 1H), 4.18 (t, *J* = 7.1, 2H), 3.26 (dd, *J* = 15.5, 9.0 Hz, 1H), 2.98 (s, 6H), 2.88 (dd, *J* = 15.5, 9.1 Hz, 1H), 1.27 (t, *J* = 7.1 Hz, 3H). **^{13}C NMR** (75 MHz, $CDCl_3$) δ 166.42, 159.24, 146.98, 144.54, 129.15, 127.58, 125.07, 122.61, 121.66, 111.98, 62.58, 60.61, 37.97, 35.10, 14.36. **IR** (thin film) 2979, 2926, 2853, 1718, 1662, 1479, 1385, 1268, 1176, 1031 cm^{-1}. **TLC**: R_f = 0.28 (30% EtOAc/hexanes, UV & $KMnO_4$ visualization). **HRMS** (ESI) calculated for $C_{16}H_{20}N_2O_3$ ($[M+H]^+$): 289.1547, found: 289.1610. **HPLC**: Daicel CHIRALCEL AS-H column, 10% IPA in hexanes, 1.0 mL/min, λ＝254 nm: t_R(major) = 21.8 min, t_R(minor) = 26.3 min.

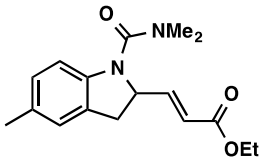

ethyl (*E*)-3-(1-(dimethylcarbamoyl)-5-methylindolin-2-yl)acrylate (**30b**): 52% yield (colorless oil). **^{1}H NMR** (500 MHz, $CDCl_3$) δ 6.99 – 6.91 (m, 3H), 6.64 (d, *J* = 8.1 Hz, 1H), 5.99 (d, *J* = 15.6 Hz, 1H), 5.01 – 4.96 (m, 1H), 4.17 (q, *J* = 7.1 Hz, 2H), 3.22 (dd, *J* = 15.5, 9.0 Hz, 1H), 2.95 (s, 6H), 2.84 (dd, *J* = 15.4, 8.7 Hz, 1H), 2.27 (s, 3H), 1.27 (t, *J* = 7.1 Hz, 3H).**^{13}C NMR** (75 MHz, $CDCl_3$) δ 166.45, 159.43, 147.15, 142.14, 131.20, 129.30, 127.84, 125.83, 122.41, 111.86, 62.61, 60.57, 38.02, 35.07, 20.87, 14.36. **IR** (thin film) 2921, 1718, 1661, 1487, 1444, 1385, 1268, 1180, 1040 cm^{-1}. **TLC**: R_f = 0.29 (30% EtOAc/hexanes, UV & $KMnO_4$ visualization). **HRMS** (ESI) calculated for $C_{17}H_{22}N_2O_3$ ($[M+H]^+$): 303.1703, found: 303.1767. **HPLC**: Daicel CHIRALCEL OJ-H column, 10% IPA in hexanes, 1.0 mL/min, λ＝254 nm: t_R(major) = 9.4 min, t_R(minor) = 16.0 min.

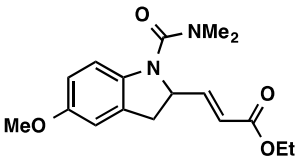

ethyl (*E*)-3-(1-(dimethylcarbamoyl)-5-methoxyindolin-2-yl)acrylate (**30ca**): 61% yield (brown oil). **^{1}H NMR** (300 MHz, $CDCl_3$) δ 6.95 (dd, *J* = 15.6, 7.1 Hz, 1H), 6.77 – 6.62 (m, 3H), 5.99 (dd, *J* = 15.7, 1.2 Hz, 1H), 5.02 – 4.94 (m, 1H), 4.17 (q, *J* = 7.1 Hz, 2H), 3.75 (s, 3H), 3.24 (dd, *J* = 15.6, 9.0 Hz, 1H), 2.94 (s, 6H), 2.84 (dd, *J* = 15.8, 8.6 Hz, 1H), 1.27 (t, *J* = 7.1 Hz, 3H). **^{13}C NMR** (75 MHz, $CDCl_3$) δ 166.42, 159.63, 155.15, 147.04, 138.08, 130.61, 122.38, 112.77, 112.19, 111.62, 62.65, 60.59, 55.88, 38.08, 35.30, 14.36. **IR** (thin film) 2935, 1717, 1659, 1487, 1384, 1298, 1263, 1231, 1179, 1035 cm^{-1}. **TLC**: R_f = 0.31 (30% EtOAc/hexanes, UV & $KMnO_4$ visualization). **HRMS** (ESI) calculated for $C_{17}H_{22}N_2O_3$ ($[M+H]^+$): 319.1652, found: 319.1715. **HPLC**: Daicel CHIRALCEL OJ-H

column, 10% IPA in hexanes, 1.0 mL/min, λ＝254 nm: t_R(major) = 19.5 min, t_R(minor) = 29.1 min.

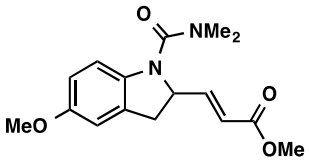

methyl (*E*)-3-(1-(dimethylcarbamoyl)-5-methoxyindolin-2-yl)acrylate (**30cb**): 59% yield (colorless oil). **^{1}H NMR** (500 MHz, $CDCl_3$) δ 6.97 (dd, *J* = 15.7, 7.1 Hz, 1H), 6.74 (s, 1H), 6.71 – 6.65 (m, 2H), 6.00 (d, *J* = 15.7 Hz, 1H), 5.00 – 4.95 (m, 1H), 3.76 (s, 3H), 3.71 (s, 3H), 3.24 (dd, *J* = 15.6, 9.0 Hz, 1H), 2.94 (s, 6H), 2.83 (dd, *J* = 15.6, 8.4 Hz, 1H). **^{13}C NMR** (75 MHz, $CDCl_3$) δ 166.83, 159.60, 155.17, 147.41, 138.05, 130.59, 121.95, 112.76, 112.21, 111.64, 62.64, 55.89, 51.73, 38.09, 35.28. **IR** (thin film) 2950, 2850, 1723, 1659, 1487, 1383, 1263, 1193, 1176, 1034 cm^{-1}. **TLC**: R_f = 0.18 (40% EtOAc/hexanes, UV & $KMnO_4$ visualization). **HRMS** (ESI) calculated for $C_{16}H_{20}N_2O_4$ ($[M+H]^+$): 305.1496, found: 304.1556. **HPLC**: Daicel CHIRALCEL OJ-H column, 10% IPA in hexanes, 1.0 mL/min, λ＝254 nm: t_R(major) = 26.6 min, t_R(minor) = 49.0 min.

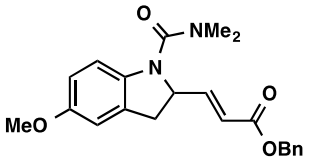

benzyl (*E*)-3-(1-(dimethylcarbamoyl)-5-methoxyindolin-2-yl)acrylate (**30cc**): 49% yield (yellow oil). **^{1}H NMR** (500 MHz, $CDCl_3$) δ 7.40 – 7.30 (m, 5H), 7.01 (dd, *J* = 15.6, 7.0 Hz, 1H), 6.75 – 6.66 (m, 3H), 6.05 (dd, *J* = 15.7, 1.1 Hz, 1H), 5.16 (s, 2H), 5.06 – 4.97 (m, 1H), 3.76 (s, 3H), 3.24 (dd, *J* = 15.6, 9.0 Hz, 1H), 2.94 (s, 6H), 2.84 (dd, *J* = 15.5, 8.4 Hz, 1H). **^{13}C NMR** (126 MHz, $CDCl_3$) δ 166.22, 159.62, 155.19, 147.77, 138.08, 135.99, 130.58, 128.66, 128.51, 128.36, 121.99, 112.78, 112.24, 111.65, 66.48, 62.65, 55.90,

38.10, 35.28. **IR** (thin film) 2950, 1717, 1657, 1486, 1455, 1382, 1263, 1232, 1173, 1155, 1032 cm^{-1}. **TLC**: R_f = 0.28 (40% EtOAc/hexanes, UV & $KMnO_4$ visualization). **HRMS** (ESI) calculated for $C_{22}H_{24}N_2O_4$ ($[M+H]^+$): 381.1809, found: 381.1841. **HPLC**: Daicel CHIRALCEL AD-H column, 20% IPA in hexanes, 1.0 mL/min, λ＝254 nm: t_R(major) = 33.7 min, t_R(minor) = 26.6 min.

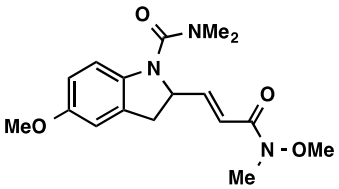

(*E*)-5-methoxy-2-(3-(methoxy(methyl)amino)-3-oxoprop-1-en-1-yl)-*N*,*N*-dimethylindoline-1-carboxamide (**30cd**): 37% yield (brown oil). **^{1}H NMR** (500 MHz, $CDCl_3$) δ 6.93 (dd, *J* = 15.4, 7.4 Hz, 1H), 6.74 (s, 1H), 6.71 – 6.64 (m, 2H), 6.60 (d, *J* = 15.4 Hz, 1H), 5.05 – 5.00 (m, 1H), 3.75 (s, 3H), 3.67 (s, 3H), 3.27 – 3.19 (m, 4H), 2.94 (s, 6H), 2.87 (dd, *J* = 15.8, 9.0 Hz, 1H). **^{13}C NMR** (75 MHz, $CDCl_3$) δ 166.44, 159.68, 155.08, 145.38, 138.41, 130.78, 120.25, 112.51, 112.17, 111.63, 63.09, 61.95, 55.92, 38.03, 35.47, 32.53. . **IR** (thin film) 2930, 1662, 1639, 1486, 1466, 1432, 1384, 1261, 1231, 1034 cm^{-1}. **TLC**: R_f = 0.18 (100% EtOAc, UV & $KMnO_4$ visualization). **HRMS** (ESI) calculated for $C_{17}H_{23}N_3O_4$ ($[M+H]^+$): 334.1761, found: 334.1820. **HPLC**: Daicel CHIRALCEL AD-H column, 25% IPA in hexanes, 1.0 mL/min, λ＝254 nm: t_R(major) = 20.1 min, t_R(minor) = 24.5 min.

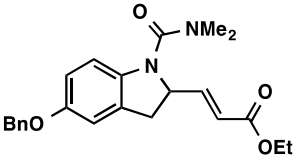

ethyl (*E*)-3-(5-(benzyloxy)-1-(dimethylcarbamoyl)indolin-2-yl)acrylate (**30d**): 55% yield (yellow oil). **^{1}H NMR** (500 MHz, $CDCl_3$) δ 7.44 – 7.36 (m, 4H), 7.32 (t, *J* = 7.1 Hz, 1H), 6.96

(dd, *J* = 15.6, 7.1 Hz, 1H), 6.82 (d, *J* = 2.6 Hz, 1H), 6.75 (dd, *J* = 8.7, 2.6 Hz, 1H), 6.69 (d, *J* = 8.7 Hz, 1H), 6.00 (dd, *J* = 15.7, 1.0 Hz, 1H), 5.04 – 4.95 (m, 3H), 4.17 (q, *J* = 7.1 Hz, 2H), 3.24 (dd, *J* = 15.6, 9.0 Hz, 1H), 2.95 (s, 6H), 2.84 (dd, *J* = 15.6, 8.5 Hz, 1H), 1.27 (t, *J* = 7.1 Hz, 3H). **^{13}C NMR** (75 MHz, $CDCl_3$) δ 166.42, 159.61, 154.34, 147.02, 138.36, 137.28, 130.60, 128.70, 128.05, 127.56, 122.42, 113.41, 112.73, 112.69, 70.83, 62.66, 60.60, 38.08, 35.30, 14.36. **IR** (thin film) 2926, 1716, 1659, 1485, 1383, 1264, 1227, 1179, 1155, 1027 cm^{-1}. **TLC**: R_f = 0.35 (40% EtOAc/hexanes, UV & $KMnO_4$ visualization). **HRMS** (ESI) calculated for $C_{23}H_{26}N_2O_4$ ($[M+H]^+$): 395.1965, found: 395.2002. **HPLC**: Daicel CHIRALCEL AD-H column, 25% IPA in hexanes, 1.0 mL/min, λ = 254 nm: t_R(major) = 34.6 min, t_R(minor) = 27.2 min.

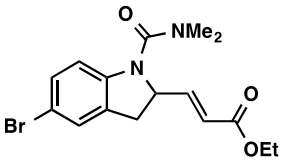

ethyl (*E*)-3-(5-bromo-1-(dimethylcarbamoyl)indolin-2-yl)acrylate (**30e**): 27% yield (brown oil). **^{1}H NMR** (500 MHz, $CDCl_3$) δ 7.26 – 7.21 (m, 2H), 6.93 (dd, *J* = 15.6, 7.2 Hz, 1H), 6.61 (d, *J* = 8.2 Hz, 1H), 6.00 (dd, *J* = 15.7, 1.1 Hz, 1H), 5.04 – 4.87 (m, 1H), 4.18 (q, *J* = 7.1 Hz, 2H), 3.25 (dd, *J* = 15.8, 9.0 Hz, 1H), 2.96 (d, *J* = 1.0 Hz, 6H), 2.87 (dd, *J* = 15.7, 8.9 Hz, 1H), 1.27 (t, *J* = 7.1 Hz, 3H). **^{13}C NMR** (75 MHz, $CDCl_3$) δ 166.27, 158.88, 146.19, 143.74, 131.46, 130.38, 128.14, 122.99, 113.81, 113.40, 62.74, 60.72, 37.97, 34.80, 14.36. **IR** (thin film) 2923, 1717, 1662, 1473, 1385, 1268, 1173, 1064, 1039 cm^{-1}. **TLC**: R_f = 0.44 (40% EtOAc/hexanes, UV & $KMnO_4$ visualization). **HRMS** (ESI) calculated for $C_{16}H_{19}BrN_2O_3$ ($[M+H]^+$): 367.0652, found: 367.0685. **HPLC**: Daicel

CHIRALCEL OD-H column, 10% IPA in hexanes, 1.0 mL/min, λ＝254 nm: t_R(major) = 12.0 min, t_R(minor) = 14.4 min.

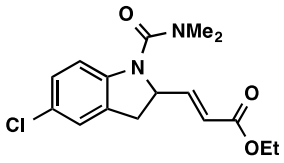

ethyl (*E*)-3-(5-chloro-1-(dimethylcarbamoyl)indolin-2-yl)acrylate (**30f**): 22% yield (yellow oil). **^{1}H NMR** (500 MHz, $CDCl_3$) δ 7.14 – 7.08 (m, 2H), 6.93 (dd, *J* = 15.7, 7.2 Hz, 1H), 6.66 (d, *J* = 8.2 Hz, 1H), 6.00 (dd, *J* = 15.7, 1.0 Hz, 1H), 5.05 – 4.99 (m, 1H), 4.21 – 4.15 (m, 2H), 3.25 (dd, *J* = 15.7, 9.0 Hz, 1H), 2.96 (s, 6H), 2.86 (dd, *J* = 15.7, 8.9 Hz, 1H), 1.28 (t, *J* = 7.1 Hz, 3H). **^{13}C NMR** (75 MHz, $CDCl_3$) δ 166.28, 158.97, 146.26, 143.24, 131.03, 127.47, 126.59, 125.32, 122.96, 112.89, 62.79, 60.72, 37.98, 34.87, 14.37. **IR** (thin film) 2925, 1718, 1663, 1475, 1385, 1266, 1200, 1175, 1038 cm^{-1}. **TLC**: R_f = 0.42 (40% EtOAc/hexanes, UV & $KMnO_4$ visualization). **HRMS** (ESI) calculated for $C_{16}H_{19}ClN_2O_3$ ($[M+H]^+$): 323.1157, found: 323.1116. **HPLC**: Daicel CHIRALCEL OD-H column, 10% IPA in hexanes, 1.0 mL/min, λ＝254 nm: t_R(major) = 11.1 min, t_R(minor) = 13.6 min.

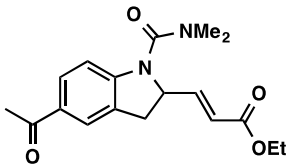

ethyl (*E*)-3-(5-acetyl-1-(dimethylcarbamoyl)indolin-2-yl)acrylate (**30g**): 25% yield (brown solid) **^{1}H NMR** (500 MHz, $CDCl_3$) δ 7.80 (d, *J* = 8.4 Hz, 1H), 7.77 (s, 1H), 6.94 (dd, *J* = 15.6, 7.4 Hz, 1H), 6.73 (d, *J* = 8.4 Hz, 1H), 6.02 (d, *J* = 15.6 Hz, 1H), 5.14 – 5.05 (m, 1H), 4.18 (q, *J* = 7.1 Hz, 2H), 3.32 (dd, *J* = 15.7, 9.1 Hz, 1H), 3.00 (s, 6H), 2.92 (dd, *J* = 15.6, 9.2 Hz, 1H), 2.54 (s, 3H), 1.28 (t, *J* = 7.1 Hz, 3H). **^{13}C NMR** (75 MHz, $CDCl_3$) δ

196.70, 166.19, 158.21, 148.87, 145.88, 131.32, 129.78, 129.51, 125.34, 123.30, 110.94, 63.04, 60.76, 37.91, 34.54, 26.53, 14.35. **IR** (thin film) 2925, 1717, 1670, 1606, 1580, 1488, 1442, 1388, 1364, 1296, 1267, 1195, 1061, 1041 cm^{-1}. **TLC**: R_f = 0.23 (50% EtOAc/hexanes, UV & $KMnO_4$ visualization). **HRMS** (ESI) calculated for $C_{18}H_{22}N_2O_4$ ($[M+H]^+$): 331.1652, found: 331.1731. **HPLC**: Daicel CHIRALCEL OD-H column, 10% IPA in hexanes, 1.0 mL/min, λ=254 nm: t_R(major) = 29.5 min, t_R(minor) = 26.4 min.

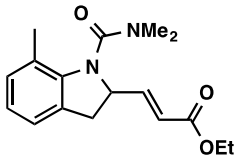

ethyl (*E*)-3-(1-(dimethylcarbamoyl)-7-methylindolin-2-yl)acrylate (**30h**): 23% yield (colorless oil). **^{1}H NMR** (500 MHz, $CDCl_3$) δ 7.01 (t, *J* = 6.8 Hz, 2H), 6.98 – 6.90 (m, 2H), 5.92 (dd, *J* = 15.5, 1.4 Hz, 1H), 4.75 – 4.67 (m, 1H), 4.19 – 4.10 (m, 2H), 3.54 (dd, *J* = 15.3, 8.9 Hz, 1H), 2.94 (s, 6H), 2.73 (dd, *J* = 15.3, 1.9 Hz, 1H), 2.17 (s, 3H), 1.26 (t, *J* = 7.1 Hz, 3H). **^{13}C NMR** (75 MHz, $CDCl_3$) δ 166.35, 161.05, 147.32, 143.66, 131.30, 129.51, 128.17, 124.43, 122.30, 121.24, 64.19, 60.74, 38.25, 36.96, 18.51, 14.33. **IR** (thin film) 2918, 2852, 1717, 1657, 1466, 1385, 1292, 1275, 1174, 1042 cm^{-1}. **TLC**: R_f = 0.35 (100% Et_2O, UV & $KMnO_4$ visualization). **HRMS** (ESI) calculated for $C_{17}H_{22}N_2O_3$ ($[M+H]^+$): 303.1703, found: 303.1772. **HPLC**: Daicel CHIRALCEL AD-H column, 10% IPA in hexanes, 1.0 mL/min, λ=254 nm: t_R(major) = 18.1 min, t_R(minor) = 16.3 min.

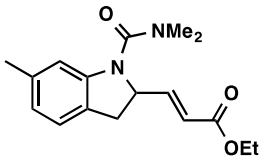

ethyl (*E*)-3-(1-(dimethylcarbamoyl)-6-methylindolin-2-yl)acrylate (**30i**): 61% yield (colorless oil). **^{1}H NMR** (500 MHz, $CDCl_3$) δ 7.01 (d, *J* = 7.4 Hz, 1H), 6.96 (dd, *J* = 15.6, 7.2 Hz, 1H), 6.70 (d, *J*

= 7.4 Hz, 1H), 6.55 (s, 1H), 5.99 (d, *J* = 15.7 Hz, 1H), 5.04 – 4.94 (m, 1H), 4.17 (q, *J* = 7.1 Hz , 2H), 3.21 (dd, *J* = 15.3, 9.0 Hz, 1H), 2.97 (s, 6H), 2.82 (dd, *J* = 15.4, 8.8 Hz, 1H), 2.31 (s, 3H), 1.27 (t, *J* = 7.1 Hz, 3H). **^{13}C NMR** (75 MHz, $CDCl_3$) δ 166.44, 159.29, 147.10, 144.62, 137.46, 126.21, 124.68, 122.44, 122.29, 116.14, 112.91, 62.85, 60.59, 38.00, 34.77, 21.88, 14.34. **IR** (thin film) 2978, 2923, 1718, 1662, 1497, 1446, 1383, 1268, 1189, 1036 cm^{-1}. **TLC**: R_f = 0.30 (30% EtOAc/hexanes, UV & $KMnO_4$ visualization). **HRMS** (ESI) calculated for $C_{17}H_{22}N_2O_3$ ($[M+H]^+$): 303.1703, found: 303.1779. **HPLC**: Daicel CHIRALCEL AD-H column, 10% IPA in hexanes, 1.0 mL/min, λ＝254 nm: t_R(major) = 11.4 min, t_R(minor) = 15.2 min.

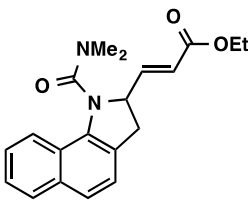

ethyl (*E*)-3-(1-(dimethylcarbamoyl)-2,3-dihydro-1*H*-benzo[*g*]indol-2-yl)acrylate (**30j**): 56% yield (colorless oil). **^{1}H NMR** (500 MHz, $CDCl_3$) δ 7.83 (d, *J* = 8.1 Hz, 1H), 7.65 (d, *J* = 8.3 Hz, 1H), 7.60 (d, *J* = 8.2 Hz, 1H), 7.47 (t, *J* = 7.5 Hz, 1H), 7.42 (t, *J* = 7.4 Hz, 1H), 7.32 (d, *J* = 8.2 Hz, 1H), 7.01 (dd, *J* = 15.5, 5.5 Hz, 1H), 5.99 (d, *J* = 15.5 Hz, 1H), 4.93 – 4.84 (m, 1H), 4.16 – 4.07 (m, 2H), 3.75 (dd, *J* = 15.4, 8.8 Hz, 1H), 3.01 (s, 6H), 2.88 (dd, *J* = 15.4, 1.7 Hz, 1H), 1.21 (t, *J* = 7.1 Hz, 3H). **^{13}C NMR** (75 MHz, $CDCl_3$) δ 166.34, 161.82, 147.16, 140.58, 133.79, 128.56, 127.57, 126.11, 125.45, 125.35, 125.25, 123.45, 122.75, 121.25, 64.97, 60.71, 38.31, 37.43, 14.27. **IR** (thin film) 2936, 1716, 1660, 1488, 1384, 1372, 1299, 1275, 1187, 1163, 1042 cm^{-1}. **TLC**: R_f = 0.27 (100% Et_2O, UV & $KMnO_4$ visualization). **HRMS** (ESI) calculated for $C_{20}H_{22}N_2O_3$ ($[M+H]^+$): 339.1703,

found: 339.1739. **HPLC**: Daicel CHIRALCEL AD-H column, 10% IPA in hexanes, 1.0 mL/min, λ＝254 nm: t_R(major) = 30.8 min, t_R(minor) = 28.8 min.

CHAPTER 5: SUMMARY OF RESEARCH

The successful applications of (+)-CSA in both the asymmetric oxidative amination and 1,2-carboamination have proven the viability of chiral sulfonic acid ligands in enantioselective, oxidative catalysis. To our knowledge, these examples mark the first palladium-catalyzed enantioselective reactions to utilize chiral sulfonic acids as ligands. The formation of the electrophilic $Pd[(+)\text{-}CSA]_2$ complex in situ is conducive for the reactivity of underfunctionalized substrates. Specifically, the coordination of unactivated alkenes and subsequent formation of a reactive Pd^{II}-π-alkene complex promotes mild, efficient nucleophilic attack. Further exploration of other intramolecular nucleophiles, such as oxygen, is warranted. Also, the Pd^{II}-bis-sulfonate complex has shown applicability in mild, substrate directed C-H activation. Presumably through electrophilic C-H activation, the highly electron-deficient catalyst forms a chiral palladacycle with the urea directing group under mild conditions that can be utilized for a variety of transformations, including asymmetric 1,2-carboamination. Other tandem C-H activation/nucleophilic attack reactions could be explored for the formation of chiral heterocycles besides indolines. Also, utilization of a more labile directing group should be an emphasis in reaction development going forward. Lastly, although previous attempts to use chiral sulfonic acids in an asymmetric Fujiwara-Moritani reaction were unsuccessful, a more exhaustive exploration of the substrate scope, including indoles and pyrroles, may lead to a breakthrough in this underexplored transformation.

While encouraged by the success of (+)-CSA it appears this model ligand has achieved its ceiling when it comes to enantioselectivity. More rational approaches need to

be taken in order to further improve the stereoselectivity for both the oxidative amination and the 1,2-carboamination reactions. In order to arrive at the appropriate ligand for proper stereoinduction a more modular ligand scaffold should be utilized. Camphor, while inexpensive and available in both enantiomers, possesses only a few functional handles that would allow for the easy derivitization needed for efficient screening. In contrast, BINOL provides a modular scaffold in which groups varying in both steric and electronic properties can be introduced at the 3 and 3'-positions. Furthermore, literature precedent for this type of ligand exists. While only a few derivatives are known at present, in concurrent work Ishihara[137] and List[138] have synthesized BINOL-derived 1,1'-binaphthyl-2,2-disulfonic acid (BINSA) (Scheme 5.1).

Scheme 5.1: Synthesis of BINSA by Ishihara

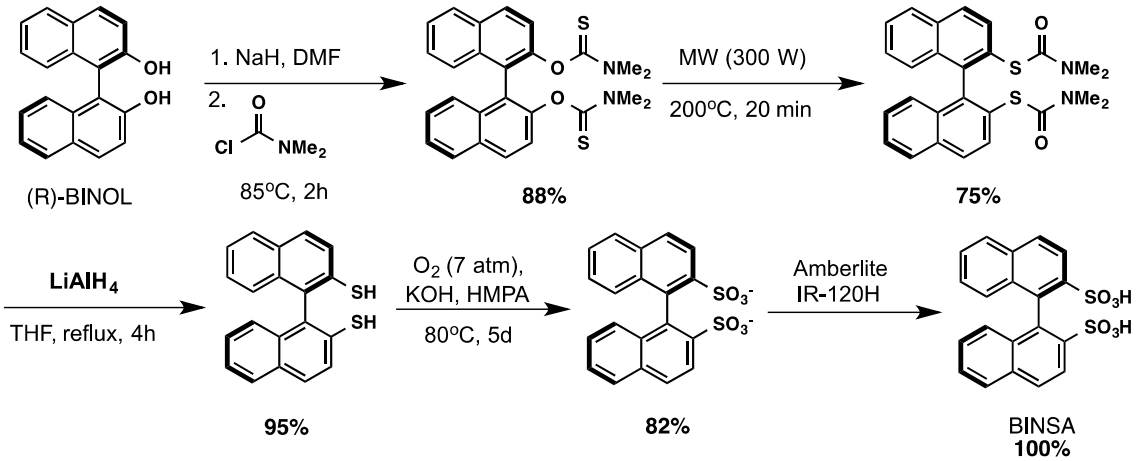

The chelating coordination of BINSA would provide a bidentate ligand in contrast to the monodentate (+)-CSA. Also, novel monosulfonic acids could be developed utilizing oxygen at the 2-position of the BINOL scaffold. Varying the ether protecting group of the oxygen provides an opportunity to tune the steric environment. Also, modifying the

electronics of the ether can modulate the extent of the L-type coordination through the oxygen, potentially stabilizing the bis-sulfonate complex.

In summation, this dissertation discusses the development of enantioselective Pd^{II}-catalyzed oxidative reactions utilizing chiral X-type ligands. Chiral sulfonic acids, specifically (+)-CSA, were more successful in terms of stereoinduction compared to BINOL-derived chiral phosphoric acids. The in situ generated $Pd[(+)\text{-CSA}]_2$ complex was employed in the synthesis of chiral indolines via an asymmetric oxidative amination and a 1,2-carboamination with enantioselectivies up to 45% and 46% ee, respectively. Challenges in the oxidative amination reaction include loss of stereoselectivity with *ortho*-substituted substrates and in the cyclization of six-membered heterocycles. Limitations to the 1,2-carboamination include lack of reactivity for electron-deficient substrates as well as inconsistent reactivity for *ortho*- and *meta*-substituted ureas. Future studies will focus on addressing the modest levels of enantioselectivity for both reactions. One remedy, where additional chiral sulfonic acid ligands are synthesized, is proposed.

REFERENCES CITED

[1] Nicolaou, K. C.; Bulger, P. G.; Sarlah, D. Palladium-Catalyzed Cross-Coupling Reactions in Total Synthesis *Angew. Chem. Int. Ed.* **2005**, *44*, 4442-4489.

[2] Other oxidation states of palladium have been explored in catalysis although to a lesser extent: for Pd(IV) see a) Xu, L.-M.; Li, B.-J.; Yang, Z.; Shi, Z.-J. Organopalladium(IV) Chemistry *Chem. Soc. Rev.* **2010**, *39*, 712-733 and references therein; for Pd(III) applications: Powers, D. C.; Ritter, T. *Top Organomet. Chem.* **2011**, *35*, 129-156 and references therein.

[3] Seechurn, C. C. C.; Kitching, M. O.; Colacot, T. J.; Snieckus, V. Palladium-Catalyzed Cross-Coupling: A Historical Contextual Perspective to the 2010 Nobel Prize *Angew. Chem. Int. Ed.* **2012**, *51*, 5062-5085.

[4] Trost, B. M. Asymmetric Allylic Alkylation, an Enabling Methodology *J. Org. Chem.* **2004**, *69*, 5813-5837.

[5] Popp, B. V.; Stahl, S. S. Palladium-Catalyzed Oxidation Reactions: Comparison of Benzoquinone and Molecular Oxygen as Stiochiometric Oxidants *Top Organomet. Chem.* **2007**, *22*, 149-189.

[6] Beccalli, E. M.; Broggini, G.; Martinelli, M.; Sottocornola, S. C-C, C-O, C-N Bond Formation on sp^2 Carbon by Pd(II)-Catalyzed Reactions Involving Oxidant Agents *Chem. Rev.* **2007**, *107*, 5318-5365.

[7] A third classification of ligand is also described: Z-type, in which both electrons of the bond are provided by the metal; Green, M. L. H. A New Approach to the Formal Classification of Covalent Compounds of the Elements *J. Organomet. Chem.* **1995**, *500*, 127-148.

[8] Tietz, L. F.; Ila, H.; Bell, H. P. Enantioselective Palladium-Catalyzed Transformations *Chem. Rev.* **2004**, *104*, 3453-3516.

[9] Parra, A.; Reboredo, S.; Martin Castro, A. M.; Aleman, J. Metallic Organophosphates as Catalysts in Asymmetric Synthesis: A Return Journey *Org. Biomol. Chem.* **2012**, *10*, 5001-5020.

[10] Parmar, D.; Sugiono, E.; Raja, S.; Rueping, M. A Complete Field Guide to Asymmetric BINOL-Phosphate Derive Bronsted Acid and Metal Catalysis: History and Classification by Mode of Activation; Bronsted Acidity, Hydrogen Bonding, Ion Pairing, and Metal Phosphates *Chem. Rev.* **2014**, *114*, 9047-9153.

[11] Ambiguity about the exact role the chiral species plays in mechanism of these reactions along with conflicting terminology in the literature makes the delineation of these categories difficult. The following provides four categories of catalytic modes combining metals and chiral phosphoric acids: Lv, J.; Luo, S. Asymmetric Binary Acid Catalysis: Chiral Phosphoric Acid as Dual Ligand and Acid *Chem. Commun.* **2013**, *49*, 847-858.

[12] Patil, N. T.; Shinde, V. S.; Gajula, B. A One-Pot Catalysis: The Strategic Classification with Some Recent Examples *Org. Biomol. Chem.* **2012**, *10*, 211-224, and references therein.

[13] a) Ohmatsu, K.; Ito, M. Kunieda, T.; Ooi, T. Ion-paired Chiral Ligands for Asymmetric Palladium Catalysis *Nature Chem.* **2012**, *4*, 473-477. b) Ohmatsu, K.; Ito, M. Kunieda, T.; Ooi, T. Exploiting the Modularity of Ion-Paired Chiral Ligands for Palladium-Catalyzed Enantioselective Allylation of Benzofuran-2(3*H*)-ones *J. Am. Chem. Soc.* **2013,** *135*, 590-593.

[14] Examples in which Pd-catalyzed enantioselective reactions utilizing chiral phosphoric acids do not proceed through a π-allyl intermediate include, C-H activation: a) Yan, S.-B.; Zhang, S.; Duan, W.-L. Palladium-Catalyzed Asymmetric Arylation of C(sp^3)-H Bonds of Aliphatic Amides: Controlling Enantioselectivity Using Chiral Phosphoric Amides/Acids *Org. Lett.* **2015**, *17*, 2458-2461. b) Nelson, H. N.; Williams, B. D.; Miro, J.; Toste, F. D. Enantioselective 1,1-Arylborylation of Alkenes: Merging Chiral Anion Phase Transfer with Pd Catalysis *J. Am. Chem. Soc.* **2015**, *137*, 3213-3216. Oxa-Diels Alder Reaction: c) Yu, S.-Y.; Zhang, H.; Gao, Y.; Mo, L.; Wang, S.; Yao, Z.-J. Asymmetric Cascade Annulation Based on Enantioselective Oxa-Diels-Alder Cycloaddition of in Situ Generated Isochromenyliums by Cooperative Binary Catalysis of $Pd(OAc)_2$ and (*S*)-Trip *J. Am. Chem. Soc.* **2013**, *135*, 11402-11407. Synthesis of substituted chiral pyrroles: d) Zhang, D.; Qiu, H.; Jiang, L.; Lv, F.; Ma. C.; Hu, W. Enantioselective Palladium(II) Phosphate Catalyzed Three-Component Reactions of Pyrrole, Diazoesters and Imines *Angew. Chem. Int. Ed.* **2013**, *53*, 13356-13360.

[15] Tao, Z.-L.; Zhang, W.-Q.; Chen, D.-F.; Adele, A.; Gong, L.-Z. Pd-Catalyzed Asymmetric Allylic Alkylation of Pyrazol-5-ones with Allylic Alcohols: The Role of Chiral Phosphoric Acid in C-O Bond Cleavage and Stereocontrol *J. Am. Chem. Soc.* **2013**, 8255-9258.

[16] Banerjee, D.; Junge, K.; Beller, M. Cooperative Catalysis by Palladium and a Chiral Phosphoric Acid: Enantioselective Amination of Racemic Allylic Alcohols *Angew. Chem. Int. Ed.* **2014**, *53*, 13049-13953.

[17] a) Mukherjee, S.; List, B. Chiral Counteranions in Asymmetric Transition-Metal Catalysis: Highly Enantioselective Pd/Bronsted Acid-Catalyzed Direct α–Allylation of Aldehydes *J. Am. Chem. Soc.* **2007**, *129*, 11336-11337. b) Jiang, G.; List, B. Direct

Asymmetric α-Allylation of Aldehydes with Simple Allylic Alcohols Enabled by the Converted Action of Three Different Catalysts *Angew. Chem. Int. Ed.* **2011**, *50*, 9471-9474.

[18] Chai, Z.; Rainey, T. J. Pd(II)/Bronsted Acid Catalyzed Enantioselective Allylic C-H Activation for the Synthesis of Spirocyclic Rings *J. Am. Chem. Soc.* **2012**, *134*, 3615-3618.

[19] Retrospective: Jira, Reinhard; Acetaldehyde from Ethylene—A Retrospective on the Discovery of the Wacker Process. *Agnew. Chem. Int. Ed.* **2009**, *48*, 9034-9037.

[20] Seminal Publications: a) Smidt, J.; Hafner, W.; Jira, R.; Sedlmeier, J.; Sieber, R.; Ruttinger, R.; Kojer, H. Catalytic Reactions of Olefins on Compounds of the Platinum Group. *Angew. Chem* **1959**, *71*, 176-182. b) Smidt, J.; Oxidation of Olefins with Palladium Chloride Catalysts. *Chem. Ind.* **1962**, 54-61. c) Smidt, J.; Hafner, W.; Jira, R.; Sieber, R.; Sabel, A.; Palladium Chloride-Catalyzed Oxidation of Olefins. *Angew. Chem.* **1962**, *74*, 93-102.

[21] Seminal publication: a) Hosokawa, T.; Uno, T.; Inui, S.; Murahashi, S.-I. Palladium(II)-Catalyzed Asymmetric Oxidative Cyclization of 2-Allylphenols in the Presence of Copper(II) Acetate and Molecular Oxygen. Study of the Catalysis of the Wacker-Type Oxidation *J. Am. Chem. Soc.* **1981**, *103*, 2318-2323. Other representative examples: b) Trend, R. M.; Ramtohul, Y. K.; Stoltz, B. M. Oxidative Cyclizations in a Nonpolar Solvent Using Molecular Oxygen and Studies on the Stereochemistry of Oxypalladation *J.Am. Chem. Soc.* **2005**, *127*, 17778-17788. c) Zhang, Y. J.; Wang, F.; Zhang, W. Chelation-Induced Axially Chiral Palladium Complex System with Tetraoxazoline Ligands for Highly Enantioselective Wacker-Type Cyclization *J. Org. Chem.* **2007**, *72*, 9208-9213.

[22] Hegedus, L. S.; Soderberg, B. C. G. *Transition Metals in the Synthsis of Organic Molecules*, 3rd Ed; University Science Books: Sausalito, CA, 2010.

[23] Hartwig, J. F. *Organotransition Metal Chemistry: From Bonding to Catalysis*, 1st Ed; University Science Books: Sausalito, CA, 2010.

[24] Hegedus, L. S.; Allen, G. F.; Bozell, J. J.; Waterman, E. L. Palladium-Assisted Intramolecular Amination of Olefins. Synthesis of Nitrogen Heterocycles *J. Am. Chem. Soc.* **1978**, *100*, 5800-5807.

[25] Hegedus, L. S.; McKearin, J. M. Palladium-Catalyzed Cyclization of ω–Olefinic Tosamides. Synthesis of Nonaromatic Nitrogen Heterocycles *J. Am. Chem. Soc.* **1982**, *104*, 2444-2451.

[26] Larock, R. C.; Hightower, T. R.; Hasvold, L. A.; Peterson, K. P. Palladium(II)-Catalyzed Cyclization of Olefinic Tosylamides *J. Org. Chem.* **1996**, *61*, 3584-3585.

[27] Ronn, M, Backvall, J. E.; Andersson Palladium(II)-Catalyzed Cyclization Using Molecular Oxygen as Reoxidant *Tetrahedron Lett.* **1995**, *36*, 7749-7752.

[28] van Benthem, R. A. T. M.; Hiemstra, H.; Michels, J. J.; Speckamp, W. N. Formamide as a Superior Nitrogen Nucleophile in Palladium(II) Mediated Synthesis of Imidazolidines *Tetrahedron Lett.* **1994**, *35*, 9281-9284.

[29] Uemura originally used $Pd(OAc)_2$/pyridine system with 3Å molecular sieves for oxidation of alcohols to ketones and aldehydes: a) Nishimura, T.; Onoue, T.; Ohe, K.; Uemura, S. $Pd(OAc)_2$-Catalyzed Oxidation of Alcohols to Aldehydes and Ketones by Molecular Oxygen *Tetrahedron Lett.* **1998**, *39*, 6011-6014. b) Nishimura, T.; Onoue, T.; Ohe, K.; Uemura, S. Palladium(II)-Catalyzed Oxidation of Alcohols to Aldehydes and Ketones by Molecular Oxygen *J. Org. Chem.* **1999**, *64*, 6750-6755.

[30] Fix, S. R.; Brice, J. L.; Stahl, S. S. Efficient Intramolecular Oxidative Amination of Olefins through Direct Dioxygen Coupled Palladium Catalysis *Angew. Chem. Int. Ed.* **2002**, *41*, 164-167.

[31] Stahl, S. S. Palladium Oxidase Catalysis: Selective Oxidation of Organic Chemicals by Direct Dioxygen-Coupled Turnover *Angew. Chem. Int. Ed.* **2004**, *43*, 3400-3420.

[32] Yip, K.-T.; Yang, M.; Law, K.-L.; Zhu, N.-Y.; Yang, D. Pd(II)-Catalyzed Enantioselective Oxidative Tandem Cyclization Reactions. Synthesis of Indolines through C-N and C-C Bond Formation *J. Am. Soc.* **2006**, *128*, 3130-3131.

[33]Ye, X.; Liu, G.; Popp, B. V.; Stahl, S. S. Mechanistic Studies of Wacker-Type Intramolecular Aerobic Oxidative Amination of Alkenes Catalyzed by $Pd(OAc)_2$/Pyridine *J. Org. Chem.* **2011**, *76*, 1031-1044

[34] Liu, G.; Stahl, S. S. Two-Faced Reactivity of Alkenes: *cis*- versus *trans*-Aminopalladation in Aerobic Pd-Catalyzed Intramolecular Aza-Wacker Reactions *J. Am. Chem. Soc.* **2007**¸ *129*, 6328-6335.

[35] Trend, R. M.; Ramtohul, Y. K.; Ferreira, E. M.; Stoltz, B. M. Palladium-Catalyzed Oxidative Wacker Cyclizations in Nonpolar Organic Solvents with Molecular Oxygen: A Stepping Stone to Asymmetric Aerobic Cyclizations *Angew. Chem. Int. Ed.* **2003**, *42*, 2892-2895.

[36] a) Smith, B. T.; Wendt, J. A.; Aube, J. First Asymmetric Total Synthesis of (+)-Sparteine *Org. Lett.* **2002**, *4*, 2577-2579. b) O'Brien, P. Basic Instinct: Design, Synthesis

and Evaluation of (+)-Sparteine Surrogates for Asymmetric Synthesis *Chem. Commun.* **2008**, 655-667.

[37] Rogers, M. M.; Wendlandt, J. E.; Guzei, I. A.; Stahl, S. S. Aerobic Intramolecular Oxidative Amination of Alkenes Catalyzed by NHC-Coordinated Palladium Complexes *Org. Lett.* **2006**, *8*¸ 2257-2260.

[38] Scarborough, C. C.; Bergant, A.; Sazama, G. T.; Guzei, I. A.; Spencer, L. C.; Stahl, S. S. Synthesis of Pd^{II} Complexes Bearing an Enantiomerically Resolved 7-Membered *N*-Heterocyclic Carbene Ligand and Initial Studies of their Asymmetric Wacker-type Oxidative Cyclization Reactions *Tetrahedron* **2009**, *65*, 5084-5092.

[39] a) Jia, Y.-X.; Hilgren, J. M.; Watson, E. J.; Marsden, S. P.; Kundig, E. P. Chiral *N*-Heterocyclic Carbene Ligands for Asymmetric Catalytic Oxindole Synthesis *Chem. Comm.* **2008**, 4040-4042. b) Kundig, E. P. Seidel, T. M.; Jia, Y.-X.; Bernardinelli, G. Chiral Carbene Ligands and their Application in the Palladium-Catalyzed Asymmetric Intramolecular α–Arylation of Amides *Angew. Chem. Int. Ed.* **2007**, *46*, 8484-8487.

[40] Yip, K.-T.; Zhu, N.-Y.; Yang, D. Palladium-Catalyzed Highly Diastereoselective Oxidative Cascade Cyclization Reactions *Org. Lett.* **2009**, *11*, 1911-1914.

[41] He, W.; Yip, K.-T.; Zhu, N.-Y.; Yang, D. Pd(II)/^{t}Bu-quinolineoxazoline: An Air-Stable and Modular Chiral Catalyst System for Enantioselective Oxidative Cascade Cyclization *Org. Lett.* **2009**, *11*, 5626-5628.

[42] Jiang, F.; Wu, Z.; Zhang, W. Pd-catalyzed Asymetric aza-Wacker-type Cyclization Reaction of Olefinic Tosylamides *Tetrahedron Lett.* **2010**, *51*, 5124-5126.

[43] McDonald, R. I.; White, P. B.; Weinstein, A. B.; Tam, C. P.; Stahl, S. S. Enantioselective Pd(II)-Catalyzed Aerobic Oxidative Amidation of Alkenes and Insights into the Role of Electronic Asymmetry in Pyridine-Oxazoline Ligands *Org. Lett.* **2011**, *13*, 2830-2833.

[44] Yang, G.; Shen, C.; Zhang, W. An Asymmetric Aerobic Aza-Wacker-Type Cyclization: Synthesis of Isoindolinones Bearing Tetrasubstituted Carbon Stereocenters *Angew. Chem. Int. Ed.* **2012**, *51*, 9141-9145.

[45] Chai, Z.; Rainey, T. J. Pd(II)/Bronsted Acid Catalyzed Enantioselective Allylic C-H Activation for the Synthesis of Spirocyclic Rings *J. Am. Chem. Soc.* **2012**, *134*, 3615-3618.

[46] See ref 10.

[47] A more exhaustive solvent screen was conducted during an earlier iteration of reaction optimization that also concluded that PhH was the optimal solvent for the reaction.

[48] Fonseca, M. H.; Eibler, E.; Zabel, M.; Konig, B. Synthesis of Novel Nitrogen-Containing Ligands for the Enantioselective Addition of Diethylzinc to Aldehydes *Tetrahedron: Asym.* **2003**, *14*, 1989-1994

[49] Yang, Q.-Q.; Xiao, C.; Lu, L.-Q.; An, J.; Tan, F.; Li, B.-J., Xiao, W.-J. Synthesis of Indoles through Highly Efficent Cascade Reactions of Sulfur Ylides and *N*-(*ortho*-Chloromethyl)aryl Amides *Angew. Chem. Int. Ed.* **2012**, *51*, 9137-9140.

[50] Larock, R. C.; Pace, P.; Yang, H.; Russell, C. E.; Cacchi, S.; Fabrizi, G. Synthesis of Nitrogen Heterocycles via Pd-Catalyzed Cross-Coupling of *o*-Alkenyl Anilides with Vinylic Halides and Triflates *Tetrahedron* **1998**, *54*, 9961-9980.

[51] Boeckman, R. K. Jr.; Pero, J. E.; Boehmler, D. J. Toward the Development of a General Chiral Auxiliary. Enantioselective Alkylation and a New Catalytic Asymmetric Addition of Silyloxyfurans: Application to a Total Synthesis of (-)-Rasfonin. *J. Am. Chem. Soc.* **2006**, *128*, 11032-11033.

[52] Fletcher, R. J.; Lampard, C.; Murphy, J. A.; Lewis, N. Tetrathiafulvalene: a Catalyst for Sequential Radical-Polar Reactions *J. Chem. Soc., Perkin Trans. 1* **1995**, 623-633.

[53] Lu, Z.; Stahl, S. S. Intramolecular Pd(II)-Catalyzed Aerobic Oxidative Amination of Alkenes: Synthesis of Six-Membered N-Heterocycles *Org. Lett.* **2012**, *14*, 1234-1237.

[54] Weinstein, A. B.; Stahl, S. S.; Reconciling the Stereochemical Course of Nucleopalladation with the Development of Enatioselective Wacker-Type Cyclizations *Angew. Chem. Int. Ed.* **2012**, *51*, 11505-11509.

[55] Mai, N. D.; Wolfe, J. P. Asymmetric Palladium-Catalyzed Carboamination Reactions for the Synthesis of Enantiomerically Enriched 2-(Arylmethyl-)- and 2-(Alkenylmethyl)pyrrolidines *J. Am. Chem. Soc.* **2010**, *132*, 12157-12159.

[56] Timohkin, V. I.; Stahl, S. S. Bronsted Base-Modulated Regioselectivity in the Aerobic Oxidative Amination of Styrene Catalyzed by Palladium *J. Am. Chem. Soc.* **2005**, *127*, 17888-17893.

[57] Elliott, L. D.; Wrigglesworth, J. W.; Cox, B.; Lloyd-Jones, G.; Booker-Millburn, K. 2,2-Difunctionalization of Alkenes via Pd(II)-Catalyzed Aza-Wacker Reactions *Org. Lett.* **2011**, *13*, 728-731.

[58] Perrin, D. D.; Armarego, W. L. F. *Purification of Laboratory Chemicals*, 3rd Ed; Pergamon Press: Oxford, 1988.

[59] Still, W. C.; Kahn, M.; Mitra, A. Rapid Chromatographic Technique for the Preparative Seperations with Moderate Resolution *J. Org. Chem.* **1978**, *43*, 2923-2925.

[60] Cronk, W. C.; Mukhina, O. A., Kutateladze, A. G. Intramolecular Photoassisted Cycloadditions of Azaxylylenes and Postphotochemical Capstone Modifications via Suzuki Coupling Provide Access to Complex Polyheterocyclic Biaryls *J. Org. Chem.* **2014**, *79*, 1235-1246.

[61] Ida, Y.; Matsubara, A.; Nemoto, T.; Saito, M.; Hirayama, S.; Fujii, H.; Nagase, H. Synthesis of Quinolinomporphinan Derivatives as Highly Selective d Opioid Receptor Ligands *Bioorg. Med. Chem.* **2012**, *20*, 5810-581.

[62] Fonseca, M. H.; Eibler, E.; Zabel, M.; Konig, B. Synthesis of Novel Nitrogen-Containing Ligands for the Enantioselective Addition of Diethylzinc to Aldehydes *Tetrahedron: Asym.* **2003**, *14*, 1989-1994

[63] Sriramurthy, V.; Kwon, O. Diphosphine-Catalyzed Mixed Double-Michael Reaction: A Unified Synthesis of Indolines, Dihydropyrrolopyridines, Benzimidaolines, Tetrahydroquinolines, Tetrahydroisoquinolines, Dihydrobenzo-1,4-Oxazines and Dihydrobenzo-3,1-oxazines *Org. Lett.* **2010**, *12*, 1084-1087.

[64] Jiang, F.; Wu, Z.; Zhang, W. Pd(II)-Catalyzed Oxidative Cyclization Reaction for the Preparation of 2-substituted 1,2,3,4-tetrahydroquninolines with Halide Functionality *Tetrahedron* **2011**, *67*, 1501-1505.

[65] Yang, Q.-Q.; Xiao, C.; Lu, L.-Q.; An, J.; Tan, F.; Li, B.-J., Xiao, W.-J. Synthesis of Indoles through Highly Efficient Cascade Reactions of Sulfur Ylides and *N*-(*ortho*-Chloromoethyl)aryl Amides *Angew. Chem. Int. Ed.* **2012**, *51*, 9137-9140.

[66] Yang, Q.-Q.; Wang, Q.; An, J.; Chen, J.-R.; Lu, L.-Q., Xiao, W.-J. Construction of Optically Active Indolines by Formal [4+1] Annulation of Sulfur Ylides and *N*-(*ortho*-Chloromoethyl)aryl Amides *Chem. Eur. J.* **2013**, *19*, 8401-8404.

[67] Larock, R. C.; Pace, P.; Yang, H.; Russell, C. E.; Cacchi, S.; Fabrizi, G. Synthesis of Nitrogen Heterocyles via Pd-Catlyzed Cross-Coupling of *o*-Alkenyl Anilides with Vinylic Halides and Triflates *Tetrahedron* **1998**, *54*, 9961-9980.

[68] Boeckman, R. K. Jr.; Pero, J. E.; Boehmler, D. J. Toward the Development of a General Chiral Auxiliary. Enantioselective Alkylation and a New Catalytic Asymmetic

Addiotnof Silyloxyfurans: Application to a Total Synthesis of (-)-Rasfonin *J. Am. Chem. Soc.* **2006**, *128*, 11032-11033.

[69] a) Fletcher, R. J.; Lampard, C.; Murphy, J. A.; Lewis, N. Tetrathiafulvalene: A Catlyst for Sequential Radical-Polar Reactions *J. Chem. Soc., Perkin Trans. 1* **1995**, 623-633. b) Lu, Z.; Stahl, S. S. Intramolecular Pd(II)-Catalyzed Aerobic Oxidative Amination of Alkenes: Synthesis of Six-Membered *N*-Heterocycles *Org. Lett.* **2012**, *14*, 1234-1237

[70] Timokhin, V. I.; Anastasi, N. R.; Stahl, S. S. Dioxygen-Coupled Oxidative Amination of Styrene *J. Am. Chem Soc.* **2003**, *125*, 12996.

[71]a) Benanson, M.; Pottel, J.; Bilbeisi, R.; Tomieux, S.; Cueto, M.; Moitessier, N. Stereo- and Regioselective Synthesis of Polysubstituted Chiral 1,4-Oxazepanes *J. Org. Chem.* **2013**, *78*, 872-885.

[72] Miura, T.; Biyajiama, T.; Fujii, T.; Murakami, M. Synthesis of a-Amino Ketones from Terminal Alkynes via Rhodium-Catalyzed Denitrogenative Hydration of N-Sulfonyl-1,2,3-Triazoles *J. Am. Chem. Soc.* **2012**, *134*, 194-196.

[73] Beletskaya, I. P.; Cheprakov, A. V. Heck Reaction as a Sharpening Stone of Palladium Catalysis *Chem. Rev.* **2000**, *100*, 3009-3066.

[74] Oestreich, M. *The Mizoroki-Heck Reaction;* John Wiley & Sons, Ltd. Chicester, UK, **2009**.

[75] Heck, R. F. Arylation, Methylation, and Carboxyalkylation of Olefins by Group VIII Metal Derivatives *J. Am. Chem. Soc.* **1968**, *90*, 5518-5526.

[76] Odell, L. R.; Savmarker, J.; Lindh, J.; Nilsson P.; Lahred, M. 7.18 Addition Reactions with Formation of Carbon-Carbon Bonds: (V) The Oxidative Heck Reaction, 492-537 in *Comprehensive Organic Synthesis, Second Edition;* Elsiver, **2014**

[77] Karimi, B.; Behzadnia, H.; Elmaifar, D.; Akhavan, P. F.; Esfahani, F. K.; Zamani, A. Transition-Metal-Catalyzed Oxidative Heck Reactions *Synthesis*, **2010**, 1399-1427.

[78] A successful oxidative Heck reaction by Sigman highlighted the importance of an electrophilic palladium catalyst for the reactivity of unbiased alkenes: Sigman, M. S.; Werner, E. E. Imparting Catalyst Control upon Classical Palladium-Catalyzed Alkenyl C-H Bond Functionalization Reactions *Acc. Chem. Res.* **2012**, *45*, 874-884.

[79] Werner, E. W.; Sigman, M. S. A Highly and General Palladium Catalyst for the Oxidative Heck Reaction of Electronically Nonbiased Olefins *J. Am. Chem. Soc.* **2010**, *132*, 13981-13983.

[80] Du, X.; Suguro, M.; Hirabayashi, K.; Mori, A. Mizoroki-Heck Type Reaction of Organoboron Reagents with Alkenes and Alkynes. A Pd(II) Catalyzed Pathway with $Cu(OAc)_2$ as an Oxidant *Org. Lett.* **2001**, *3*, 3313-3316.

[81] Catalyst loadings as low as 2 mol% Pd^{II} for identical reactions are in the following: Lindh, J.; Enquist, P.-A.; Pilotti, A.; Nilsson, P.; Larhed, M. Efficient Palladium (II) Catalysis under Air. Base-Free Oxidative Heck Reactions at Room Temperature or with Microwave Heating *J. Org. Chem.* **2007**, *72*, 7957.

[82] Shibasaki, M.; Vogl, E. M. The Palladium-Catalysed Arylation and Vinylation of Alkenes—Enantioselective Fashion *J. Organomet. Chem.* **1999**, *576*, 1-15, and references therein

[83] Penn, L.; Shpruhman, A.; Gelman, D. Enantio- and Regioselective Heck-Type Reaction of Arylboronic Acids with 2,3-Dihydrofuran *J. Org. Chem.* **2007**, *72*, 3875-3879.

[84] Akiyama, K.; Wakabayashi, K.; Mikami Enantioselective Heck-Type Reaction Catalyzed by *tropos*-Pd(II) Complex with Chiraphos Ligand *Adv. Synth. Catal.* **2005**, *347*, 1569-1575.

[85] Akiyama, K.; Mikami, K. Pd(II)-Catlayzed Enantioselective Intramolecular Heck-Type Reaction to Construct Chiral Sulfonamide Rings *Heterocycles*, **2007**, *74*, 827-834.

[86] Yoo, K. S.; Park, C. P.; Yoon, C. H.; Sakaguchi, S.; O'Neill, J.; Jung, K. W. Asymmetric Intermolecular Heck-Type Reaction of Acyclic Alkenes via Oxidative Palladium(II) Catalysis *Org. Lett.* **2007**, *9*, 3933-3955.

[87] Mei, T.-M.; Werner, E. W.; Burckle, A. J.; Sigman, M. S Enantioselective Redox-Relay Oxidative Heck Arylations of Acyclic Alkenyl Alcohols using Boronic Acids *J. Am. Chem. Soc.* **2013**, *135*, 6830-6833.

[88] Yoo, K. S.; O'Neil, J.; Sakaguchi, S.; Giles, R.; Lee, J. H.; Jung, K. W. Asymmetric Intermolecular Boron Heck-Type Reactions via Oxidative Palladium(II) Catalysis with Chiral Tridentate NHC-Amidate-Alkoxide Ligands *J. Org. Chem.***2010**, *75*, 95-101.

[89] Sakaguchi, S.; Yoo, K. S.; O'Neill, J.; Lee, J. H.; Stewart, T.; Jung, K. W. Chiral Palladium(II) Complexes Possessing a Tridentate N-Heterocyclic Carbene Amidate Alkoxide Ligand: Access to Oxygen Bridging Dimer Structures *Angew. Chem. Int. Ed.* **2008**, *47*, 9326-9329.

[90] Zhou, X.; Luo, J.; Liu, J.; Peng, S.; Deng, G.-J. Pd-Catalyzed Desulfitative Heck Coupling with Dioxygen as the Terminal Oxidant *Org. Lett.* **2011**, *13*, 1432-1435.

[91] Sun, P.; Zhu, Y.; Yang, H.; Yan, H.; Lu, L. Zhang, X.; Mao, J.; The Ligand and Base-Free Pd-Catalyzed Oxidative Heck Reaction Arylboronic Acids and Olefins *Org. Biomol. Chem.* **2012**, *10*, 4512-4515.

[92] Penafiel, I.; Pastor, I. M.; Yus, M. Heck-Matsuda Reaction Catalyzed by a Hydroxyalkyl-Functionalized NHC and Palladium Acetate *Eur. J. Org Chem.* **2012**, 3151-3156.

[93] Belger, C.; Plietker, B. Aryl-Aryl Interactions as Directing Motifs in the Stereodivergent Iron-Catalyzed Hydrosilylation of Internal Alkynes *Chem. Commun.* **2012**, *48*, 5419-5421.

[94] Archibald, S. C.; Barden, D. J.; Bazin, J. F. Y.; Fleming, I.; Foster, C. F.; Mandal, Aj. K.; Mandal, Am. K.; Parker, D.; Takaki, K.; Ware, A. C.; Williams, A. R. B.; Zwicky, A. B. Stereocontrol in Organic Synthesis using Silicon-Containing Compounds. Studies Directed Towards the Synthesis of Ebelactone A *Org. Biomol. Chem.* **2004**, *2*, 1051-1064.

[95] Blansky, S. J.; Ellison, G. B. Bond Dissociation Energies of Organic Molecules *Acc. Chem. Res.* **2003**, *36*, 255-263.

[96] a) Li, J. J. ed., C-H Bond Activation in Organic Synthesis, CRC Press, Boca Raton, FL, 2015. b) Yu, J.-Q.; Shi, Z. ed., C-H Activation, *Topics in Current Chemistry*, Springer, 2010. c) Yueng, C. S.; Dong, V. M. Catalytic Dehydrogenative Cross-Coupling: Forming Carbon-Carbon Bonds by Oxidizing Two Carbon-Hydrogen Bonds *Chem. Rev.* **2011**, *111*, 1215-1292.

[97] Neufeldt, S. R.; Sanford, M. S. Controlling Site Selectivity in Palladium-Catalyzed C-H Bond Functionalization *Acc. Chem. Res.* **2012**, *45*, 936-946.

[98] Dick, A. R.; Sanford, M. S.; Transition Metal Catalyzed Oxidative Functionalization of Carbon-Hydrogen Bonds *Tetrahedron* **2006**, *62*, 2439-2463

[99] a) Chen, K.; Engle, K. M.; Wang, D.-H., Yu, J.-Q. Palladium(II)-Catalyzed C-H Activation/C-C Cross Coupling Reactions: Versatility and Practicality *Angew. Chem. Int. Ed.* **2009**, *48*, 5094-5115. b) Lyons, T. W.; Sanford, M. S. Palladium-Catalyzed Ligand-Directed C-H Functionalization Reactions *Chem. Rev.* **2010**, *110*, 1147-1169.

[100] Ferreira, E. M.; Zhang, H.; Stoltz, B. M. Chapter 9: Oxidative Heck-Type Reactions (Fujiwara-Moritani Reactions), 345-382, *The Mizoroki-Heck Reaction;* John Wiley & Sons, Ltd. Chicester, UK, **2009**.

[101] a) Ferreira, E. M.; Stoltz, B. M. Catalytic C-H Bond Functionalization with Palladium(II): Aerobic Oxidative Annulations of Indoles *J. Am. Chem. Soc.* **2003**, *125*, 9578-9579. b) Zhang, H.; Ferreira, E. M.; Stoltz, B. M. Direct Oxidative Heck Cyclizations: Intramolecular Fujiwara-Moritani Arylations for the Synthesis of Functionalized Benzofurans and Dihydrobenzofurans *Angew. Chem. Int. Ed.* **2004**, *43*, 6144-6148.

[102] A single example of an enantioselective intermolecular Fujiwara-Moritani reaction exists: Mikami, K.; Hatano, M.; Terada, M. Catalytic C-H Bond Activation-Asymmetric Olefin Coupling Reaction: The First Example of Asymmetric Fujiwara-Moritani Reaction Catalyzed by Chiral Palladium(II) Complexes *Chem. Lett.* **1999**, *28*, 55-56.

[103] Schiffner, J. A.; Woste, T. H.; Oestreich, M. Enantioselective Fujiwara-Moritani Indole and Pyrrole Annulations Catalyzed by Chiral Palladium(II)-NicOx Complex *Eur. J. Org. Chem.* **2010**, 174-182.

[104] Nishikata, T.; Abela, A. R.; Huang, S.; Lipshutz, B. H. Cationic Palladium(II) Catalysis: C-H Activation/Suzuki-Miyaura Coupling at Room Temperature *J. Am. Chem. Soc.* **2010**, *132*, 4978-4979.

[105] Examples of this reaction exist in the literature: ref 8; Stille coupling with (+)-CSA: Xue, D.; Li, J.; Liu, Y.-X.; Hang, W.-Y.; Zhang, Z.-T.; Wang, C.; Xiao, J. Room-Temperature Stille Coupling of Tetraarylstannanes via Palladium-Catalyzed C-H Activation *Synthesis*, **2012**, *23*, 1941-1946.

[106] See ref. 103 and 127.

[107] Boele, M. D. K.; van Strijdonck, G. P. F.; de Vries, A. H. M.; Kamer, P. C. J. de Vries, J. G.; van Leeuwen, P. W. N. M. Selective Pd-Catalyzed Oxidative Coupling of Anilides with Olefins through C-H Bond Activation at Room Temperature *J. Am. Chem. Soc.* **2002**, *124*, 1586-1587.

[108] Houlden, C. E.; Hutchby, M.; Bailey, C. D.; Ford, J. G.; Tyler, S. N. G.; Gagnew, M. R.; Lloyd-Jones, G. C.; Booker- Milburn, K. I. Room-Temperature Palladium-Catalyzed C-H Activation: *ortho*-Carbonylation of Aniline Derivatives *Angew. Chem. Int. Ed.* **2009**, *48*, 1830-1833.

[109] X-ray crystal structures of palladacycles with an actamide directing group unambiguously show the η^1-coordination of the tosylate: a) Rauf, W.; Thompson, A. L.; Brown, J. M Anilide Activation of Adjacent C-H Bonds in the Palladium-Catalysed

Fujiwara-Moritani Reaction *Dalton Trans.* **2010**, *39*, 10414-10421. b) Giri, R.; Lam, J. K.; Yu, J.-Q. Synthetic Applications of Pd(II)-Catalyzed C-H Carboxylation and Mechanistic Insights: Expedient Routes to Anthranilic Acids, Oxazolinones, Quinazolinones *J. Am. Chem. Soc.* **2010**, *132*, 686-693.

[110] Shown to have better conversion, ref. 127; Previous application of Ac_2O as a drying agent in Pd-catalyzed reaction: Jia, C.; Lu, W.; Kitamura, T.; Fujiwara, Y. Highly Efficent Pd-Catlyzed Coupling of Arenes with Olefins in the Presence of tert-Butyl Hydroperoxide as Oxidant *Org. Lett.* **1999**, *1*, 2097-2100.

[111] See ref 51.

[112] Two substrates were made according to a different procedure before Method B was developed: a) Degani, I.; Fochi, R.; Magistris, C.; Migliaccio. Preparation of N,N-Dimethyl-N'-ArylureasUsing S,S-Dimethyl Dithiocarbonate as a Carbonylating Reagent *Synthesis*, **2009**, 801-808. b) Maggi, R.; Schlosser, M. Optional Site Selectivity in the Metalation of o- and p-Anisidine through Matching of Reagents with Neighboring Groups *J. Org. Chem.* **1996**, *61*, 5430-5434.

[113] Wei, X.-J.; Yang, D.-T.; Wang, L.; Song, T.; Wu, L.-Z.; Liu, Q. A Novel Intermolecular Synthesis of –Lactones via Visible-Light Photoredox Catalysis *Org. Lett.* **2013**, *15*, 6054-6057.

[114] Ref 9a; the reaction of phenyl acetamide with n-butyl acrylate with catalyzed by an in situ generated $Pd(OTs)_2$ catalyst.

[115] a) Boeckman Jr., R. K.; Pero, J. E.; Boehmler, D. J. Toward the Development of General Chiral Auxilary. Enantionselective Alkylation and a New Catalytic Asymmetric Addition of Silyloxyfurans: Application to a Total Synthesis of (-)-Rasfonin *J. Am. Chem. Soc.* **2006**, *128*, 11032-11033. b) Bonazzi, S.; Guttinger, S.; Kemp, I.; Kutay, U.; Gademann, K. Total Synthesis, Configuration, and Biological Evaluation of Anguinomycin C *Angew. Chem. Int. Ed.***2007**, *46*, 8707-8710.

[116] Zhang, H.; Ferreira, E. M.; Stoltz, B. M. Direct Oxidative Heck Cyclizations: Intramolecular Fujiwara-Moritani Arylations for the Synthesis of Functionalized Benzofurans and Dihydrobenzofurans *Angew. Chem. Int. Ed.* **2004**, *43*, 6144-*6148.*

[117] Hinsberger, S.; de Jong, J. C.; Groh, M.; Haupenthal, J.; Hartmann, R. W. Benzamidobenzoic acids as Potent PqsD Inhibitors for the Treatment of *Pseudomonas aeruginosa* Infections *Eur. J. Med Chem.* **2014**, *76*, 343-351.

[118] Aterburn, J. B.; Perry, M. C. Selective Rhednium-Catalyzed Oxidation of Secondary Alcohols with Methyl Sulfoxide in the Presence of Ethylene Glycol, a Convenient One-Pot Synthesis of Ketals *Org. Lett.* **1999**, *1*, 769-771.

[119] Zhang, J.; Wang, J.; Wu, H.; He, Y.; Zhu, G.; Cui, X.; Tang, L. Design, Synthesis and Insulin-Sensitizing of Indomethacin and Diclofenac Derivatives *Bioorg. Med. Chem. Lett.* **2009**, *19*, 3324-3327.

[120] Nadiu, A. B.; Jaseer, E. A.; Sekar, G. General, Mild, and Intermolecular Ullmann-Type Synthesis of Diaryl and Alkyl Aryl Ethers Catalyzed by Diol-Copper(I) Complex *J. Org. Chem.* **2009**, *74*, 3675-3679.

[121] Zhao, Y.; Liu, Y.; Chen, D.; Wei, Z.; Liu, W.; Gong, P. Synthesis and Biological Evaluation of 1H-benzimidazol-5-ols as Potent HBV Inhibitors *Bioorg. Med. Chem. Lett.* **2010**, *20*, 7230-7233.

[122] Kuninobu, Y.; Sueki, S. Copper-Catalyzed N- and O-Alkylation of Amines and Phenols Using Alkylborane Reagents *Org. Lett.* **2013**, *15*, 1544-1547.

[123] Fletcher, R. J.; Lampard, C.; Murphy, J. A.; Lewis, N. Tetrathiafulvalene: A Catalyst for Sequential Radical-Polar Reactions *J. Chem. Soc., Perkin Trans. 1* **1995**, 623-625.

[124] Yu, J.; Zhang, P.; Wu, J.; Shang, Z. Metal-Free C-N Bond-Forming Reaction: Straightforward Synthesis of Anilines, through Cleavage of Aryl C-O Bond and Amide C-N Bond *Tetrahedron Lett.* **2013**, *54*, 3167-3170.

[125] Cheung, C. W.; Surry, D. S.; Buchwald, S. L. Mild and Highly Selective Palladium-Catalyzed Monoarylation of Ammonia Enabled by the Used of Bulky Biaryl Phosphine Ligands and Palladacycle Precatalysts *Org. Lett.* **2013**, *15*, 3734-3737.

[126] Green, R. A.; Hartwig, J. F. Palladium-Catalyzed Amination of Aryl Chloride and Bromides with Ammonium Salts *Org. Lett.* **2014**, *16*, 4388-4391.

[127] Zeng, X.; Huang, W.; Qiu, Y.; Jiang, S. An Efficient Copper-Catalyzed Synthesis of Anilines by Employing Aqueous Ammonia *Org. Biomol. Chem.* **2011**, *9*, 8224-8227.

[128] Houlden, C. E.; Bailey, C. D.; Ford, J. G.; Gagne, M. R.; Lloyd-Jones, G. C.; Booker-Millburn, K. I. Distinct Reactivity of $Pd(OTs)_2$: The Intermolecular Pd(II)-Catalyzed 1,2-Carboamination of Dienes

[129] a) Degani, I.; Fochi, R.; Magistris, C.; Migliaccio. Preparation of N,N-Dimethyl-N'-ArylureasUsing S,S-Dimethyl Dithiocarbonate as a Carbonylating Reagent *Synthesis* **2009**, 801-808. b) Maggi, R.; Schlosser, M. Optional Site Selectivity in the Metalation of

o- and p-Anisidine through Matching of Reagents with Neighboring Groups *J. Org. Chem.* **1996**, *61*, 5430-5434.

[130] Tayama, E.; Sugai, S.; A Facile Method for the Stereoselective Preparation of (1E, 3E)-4-Substituted-1-Amino-1,3-Dienes via 1,4-Elimination *Tetrahedron Lett.* **2007**, *48*, 6163-6166.

[131] Davis, M. C.; Groshens, T. J. Nitration of tert-butyloxycarbonylated Aniline and 1,3,5-Triaminobenze by Acetyl Nitrate *Tetrahedron Lett.* **2012**, *53*, 4154-4155.

[132] Stuart, D. R.; Bertrand-Laperle, M.; Burgess, K. M. N.; Fagnou, K. Indole Synthesis via Rhodium Catalyzed Oxidative Coupling of Acetanilides and Internal Alkynes *J. Am. Chem. Soc.* **2008**, *130*, 16474-16475.

[133] Wei, X.-J.; Yang, D.-T.; Wang, L.; Song. T.; Wu, L.-Z. Liu, Q. A Novel Intermolecular Synthesis of g-Lactones via Visible-Light Photredox Catalysis *Org. Lett.* **2013**, *15*, 6054-6056.

[134] Sparrow, K.; Barker, D.; Brimble, M. A. The Enantioselective Synthesis of Tetracyclic Methyllycaconitine Analogues *Tetrahedron* **2011**, *67*, 7989-7999.

[135] Wimmer, L.; Schonbauer, D.; Pakeifer, P.; Schoffmann, A.; Khom, S.; Hering, S.; Mihovilovic, M. D. Developing Piperine Towards TRPV1 and $GABA_A$ Receptor Ligands—Synthesis of Piperine Analogs via Heck-Coupling of Conjuated Dienes *Org. Biomol. Chem.* **2015**, 990-994.

[136] www.commonorganicchemistry.com

[137] Hatano, M.; Ishihara, K. Chiral 1,1'-Binaphthyl-2,2'-Disulfonic Acid (BINSA) and Its Derivatives for Asymmetric Catalysis *Asian J. Org. Chem.* **2014**, *3*, 325-365, and references therein

[138] Kampen, D.; Ladepeche, A.; Claben, G.; List, B. Bronsted Acid-Catalyzed Three-Component Hosomi-Sakurai Reactions *Adv. Synth. Catal.* **2008**, *350*, 962-966.

APPENDIX A

SPECTRAL DATA

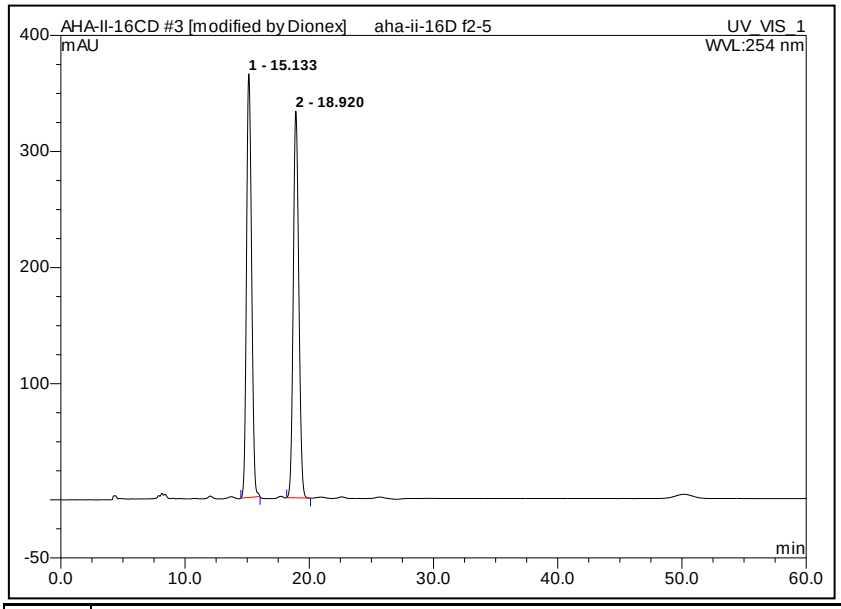

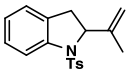

***rac*-11a**

No.	Ret.Time min	Peak Name	Height mAU	Area mAU*min	Rel.Area %	Amount	Type
1	15.13	n.a.	364.866	173.601	50.20	n.a.	BMB*
2	18.92	n.a.	332.979	172.235	49.80	n.a.	BMB*
Total:			697.845	345.836	100.00	0.000	

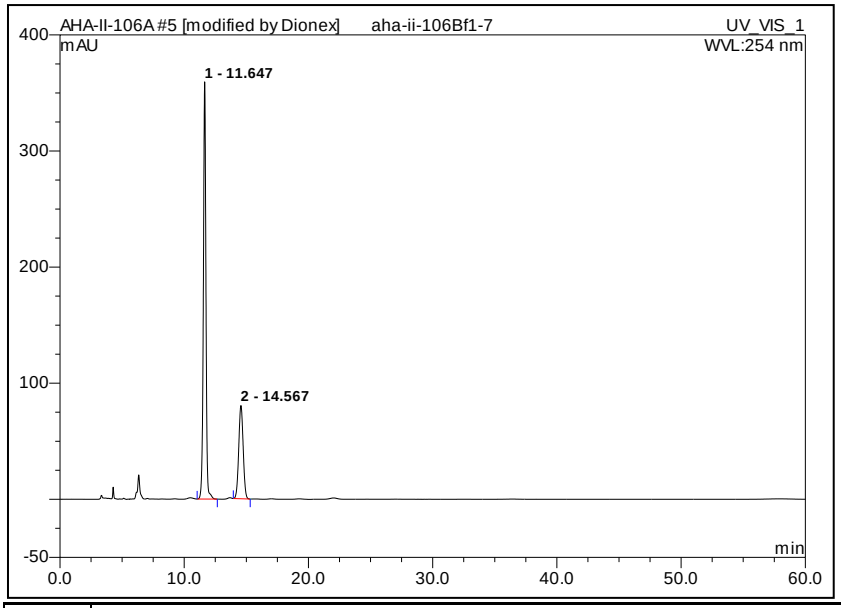

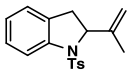

***chiral*-11a**

No.	Ret.Time min	Peak Name	Height mAU	Area mAU*min	Rel.Area %	Amount	Type
1	11.65	n.a.	359.314	86.389	72.24	n.a.	BMB
2	14.57	n.a.	80.289	33.202	27.76	n.a.	BMB
Total:			439.603	119.591	100.00	0.000	

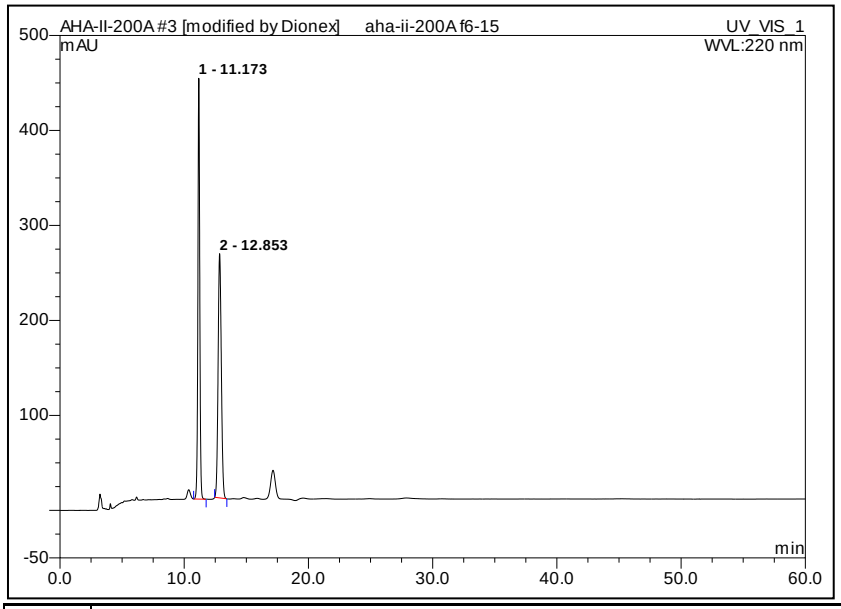

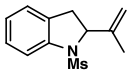

***rac*-11aa**

No.	Ret.Time min	Peak Name	Height mAU	Area mAU*min	Rel.Area %	Amount	Type
1	11.17	n.a.	443.035	77.426	49.98	n.a.	BMB*
2	12.85	n.a.	257.098	77.492	50.02	n.a.	BMB*
Total:			700.132	154.918	100.00	0.000	

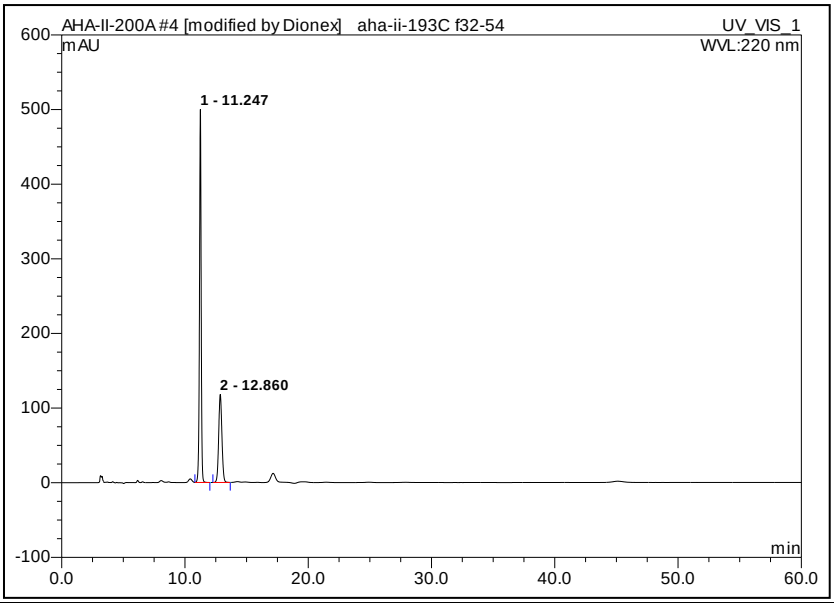

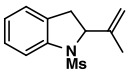

***chiral*-11aa**

No.	Ret.Time min	Peak Name	Height mAU	Area mAU*min	Rel.Area %	Amount	Type
1	11.25	n.a.	499.775	78.924	68.83	n.a.	BMB*
2	12.86	n.a.	117.941	35.749	31.17	n.a.	BMB
Total:			617.716	114.673	100.00	0.000	

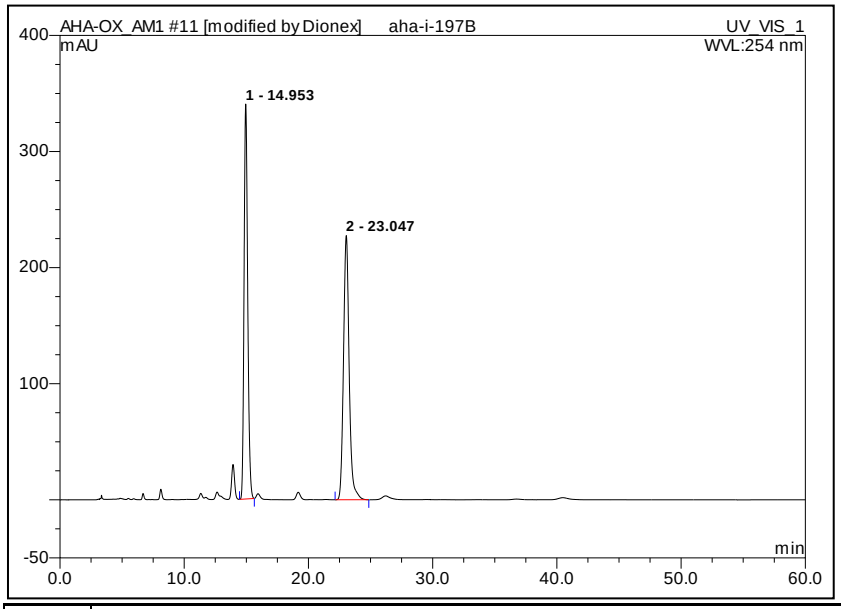

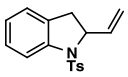

***rac*-12a**

No.	Ret.Time min	Peak Name	Height mAU	Area mAU*min	Rel.Area %	Amount	Type
1	14.95	n.a.	340.203	115.662	49.03	n.a.	BMB*
2	23.05	n.a.	227.559	120.261	50.97	n.a.	BMB
Total:			567.761	235.924	100.00	0.000	

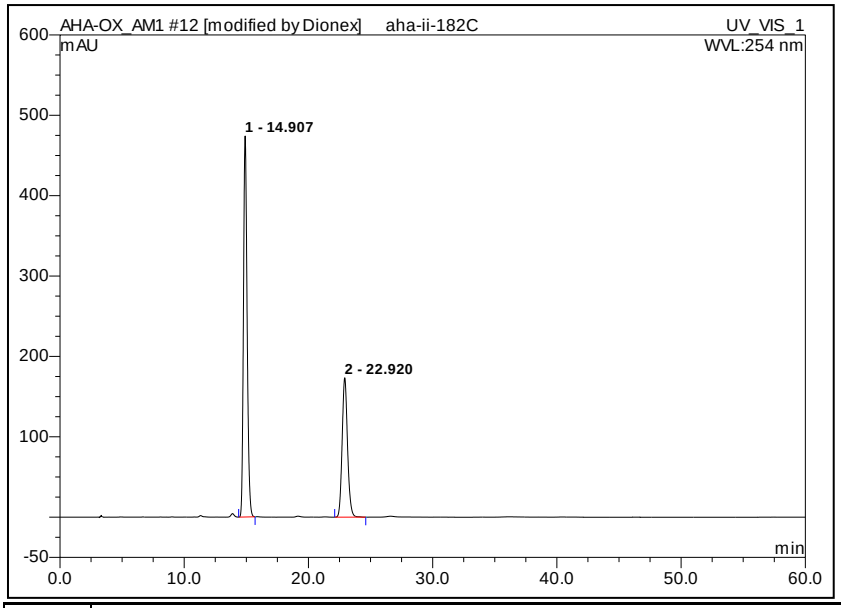

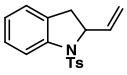

***chiral*-12a**

No.	Ret.Time min	Peak Name	Height mAU	Area mAU*min	Rel.Area %	Amount	Type
1	14.91	n.a.	473.993	161.978	65.02	n.a.	BMB
2	22.92	n.a.	173.424	87.157	34.98	n.a.	BMB
Total:			647.417	249.136	100.00	0.000	

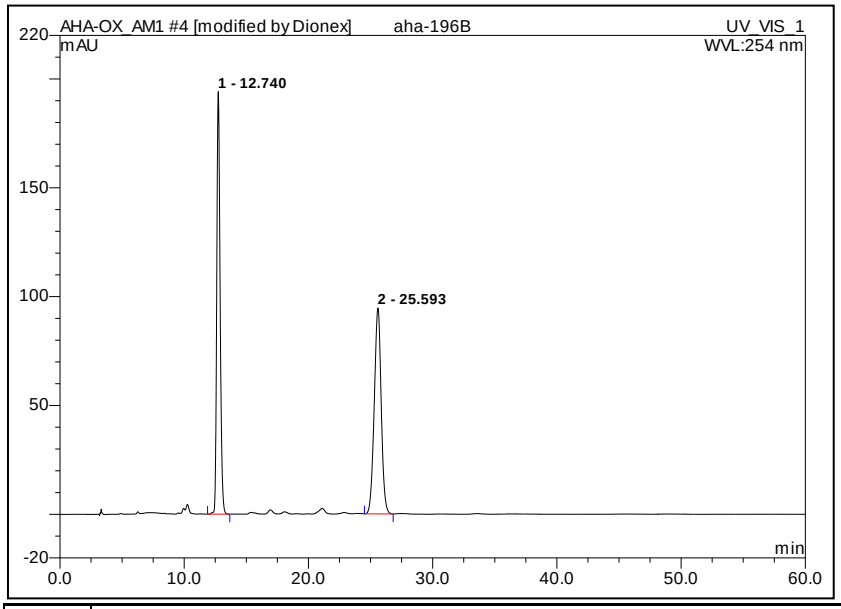

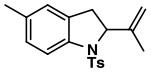

***rac*-11b**

No.	Ret.Time min	Peak Name	Height mAU	Area mAU*min	Rel.Area %	Amount	Type
1	12.74	n.a.	194.086	60.982	49.93	n.a.	BMB
2	25.59	n.a.	94.590	61.141	50.07	n.a.	BMB
Total:			288.676	122.124	100.00	0.000	

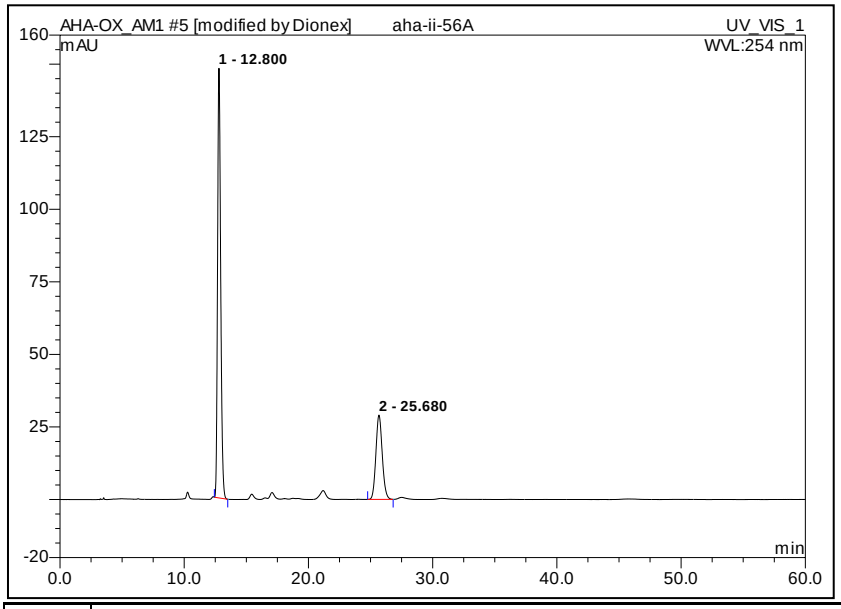

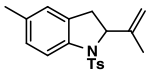

***chiral*-11b**

No.	Ret.Time min	Peak Name	Height mAU	Area mAU*min	Rel.Area %	Amount	Type
1	12.80	n.a.	148.034	43.141	71.50	n.a.	BMB
2	25.68	n.a.	29.040	17.197	28.50	n.a.	BMB
Total:			177.074	60.338	100.00	0.000	

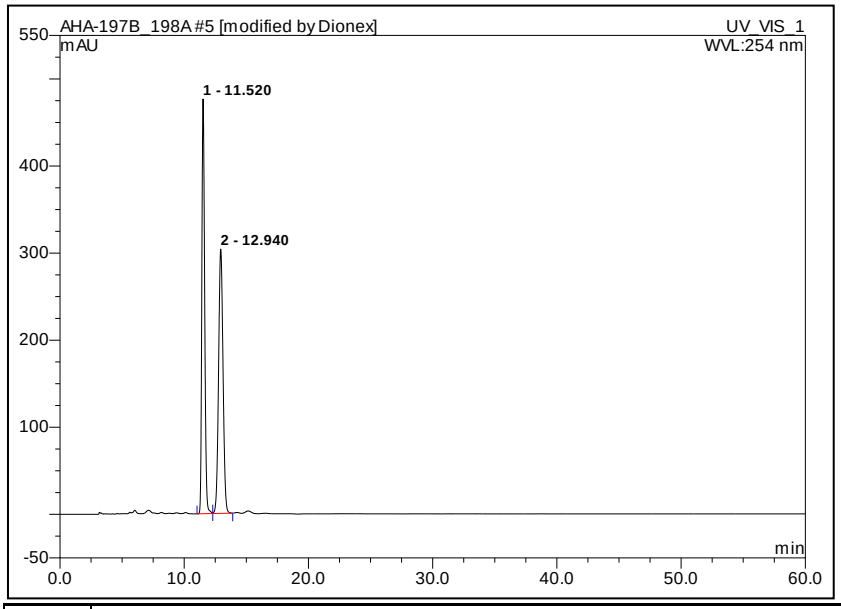

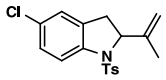

***rac*-11c**

No.	Ret.Time min	Peak Name	Height mAU	Area mAU*min	Rel.Area %	Amount	Type
1	11.52	n.a.	476.245	126.515	50.09	n.a.	BM
2	12.94	n.a.	303.531	126.073	49.91	n.a.	MB
Total:			779.776	252.588	100.00	0.000	

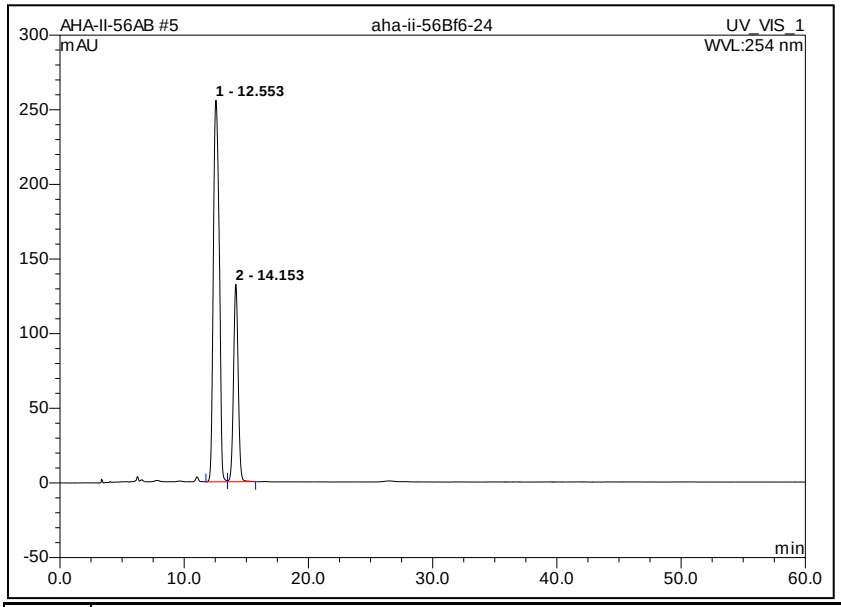

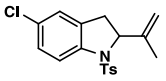

***chiral*-11c**

No.	Ret.Time min	Peak Name	Height mAU	Area mAU*min	Rel.Area %	Amount	Type
1	12.55	n.a.	255.589	140.411	71.03	n.a.	BM
2	14.15	n.a.	132.167	57.258	28.97	n.a.	MB
Total:			387.755	197.669	100.00	0.000	

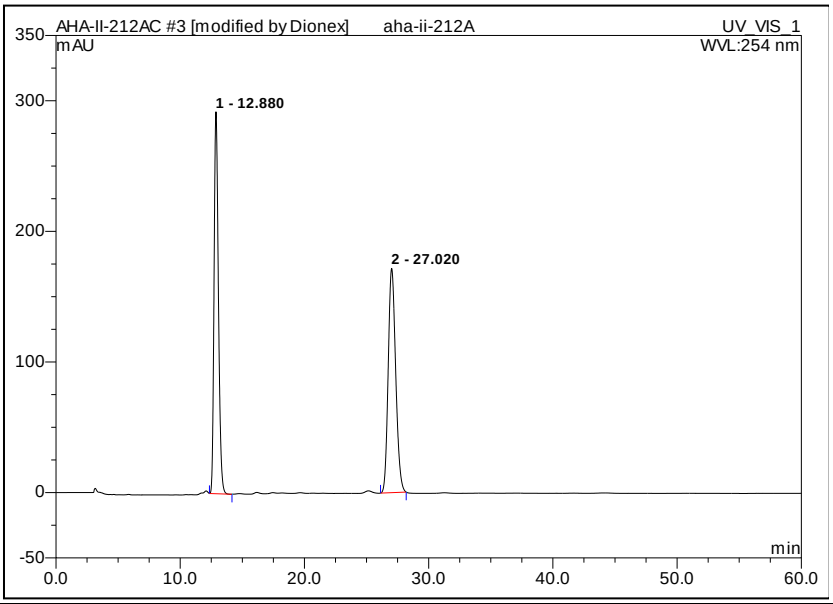

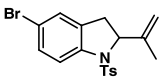

***rac*-11d**

No.	Ret.Time min	Peak Name	Height mAU	Area mAU*min	Rel.Area %	Amount	Type
1	12.88	n.a.	292.428	118.879	49.80	n.a.	BMB*
2	27.02	n.a.	171.709	119.818	50.20	n.a.	BMB*
Total:			464.136	238.697	100.00	0.000	

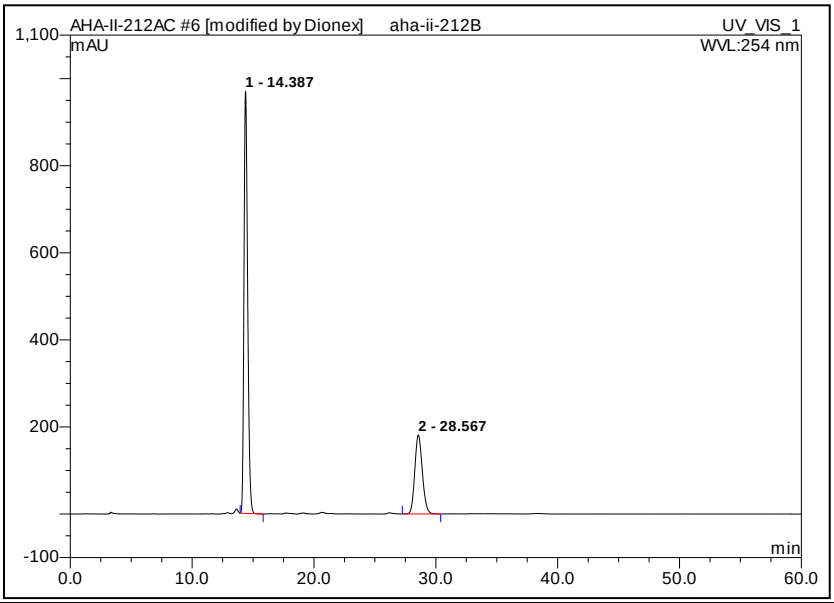

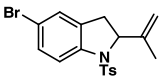

***chiral*-11d**

No.	Ret.Time min	Peak Name	Height mAU	Area mAU*min	Rel.Area %	Amount	Type
1	14.39	n.a.	969.555	339.639	72.30	n.a.	BMB*
2	28.57	n.a.	181.343	130.107	27.70	n.a.	BMB*
Total:			1150.898	469.746	100.00	0.000	

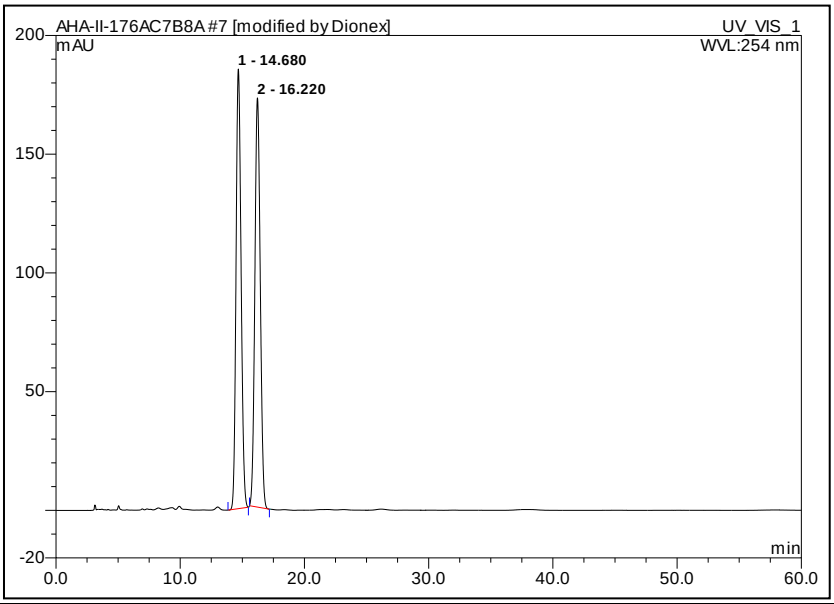

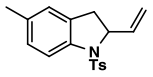

***rac*-12b**

No.	Ret.Time min	Peak Name	Height mAU	Area mAU*min	Rel.Area %	Amount	Type
1	14.68	n.a.	185.118	87.046	49.97	n.a.	BMB*
2	16.22	n.a.	172.291	87.136	50.03	n.a.	BMB*
Total:			357.409	174.183	100.00	0.000	

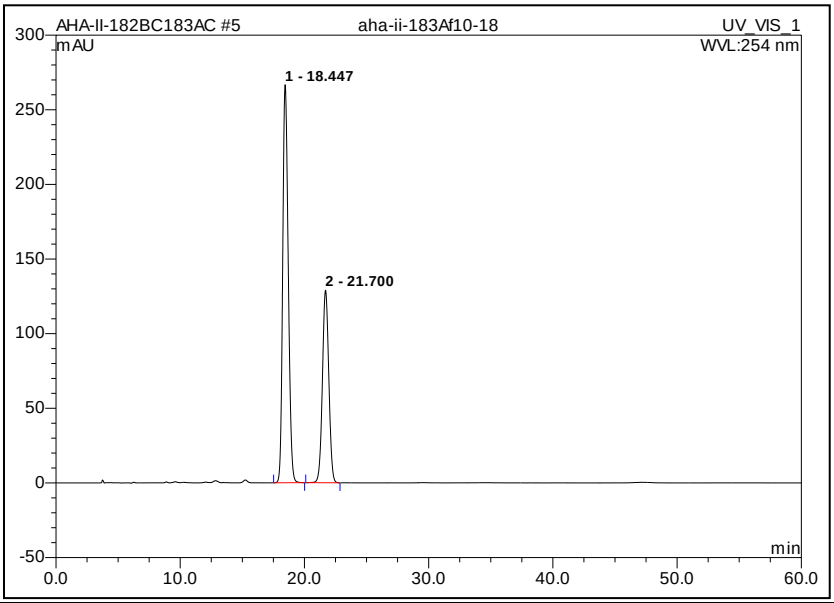

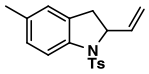

***chiral*-12b**

No.	Ret.Time min	Peak Name	Height mAU	Area mAU*min	Rel.Area %	Amount	Type
1	18.45	n.a.	266.681	137.785	64.29	n.a.	BMB
2	21.70	n.a.	128.964	76.530	35.71	n.a.	BMB
Total:			395.645	214.315	100.00	0.000	

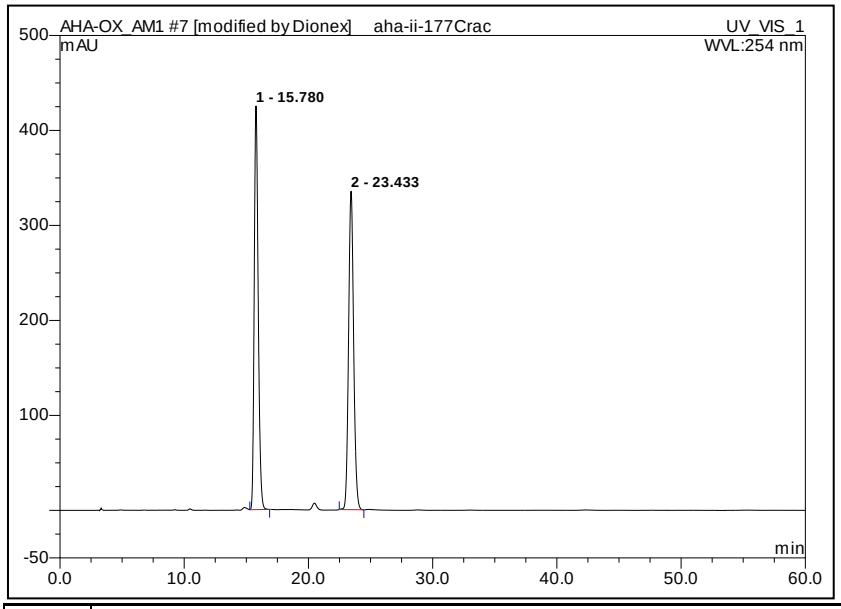

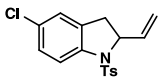

***rac*-12c**

No.	Ret.Time min	Peak Name	Height mAU	Area mAU*min	Rel.Area %	Amount	Type
1	15.78	n.a.	424.927	157.823	49.90	n.a.	BMB*
2	23.43	n.a.	335.261	158.460	50.10	n.a.	BMB*
Total:			760.188	316.283	100.00	0.000	

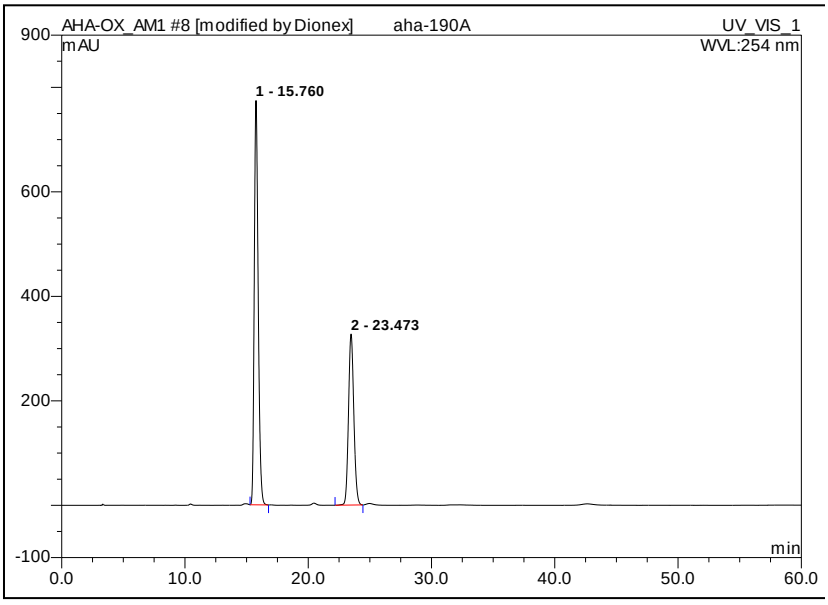

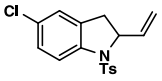

***chiral*-12c**

No.	Ret.Time min	Peak Name	Height mAU	Area mAU*min	Rel.Area %	Amount	Type
1	15.76	n.a.	773.904	286.436	63.63	n.a.	BMB
2	23.47	n.a.	327.241	163.735	36.37	n.a.	BMB*
Total:			1101.145	450.170	100.00	0.000	

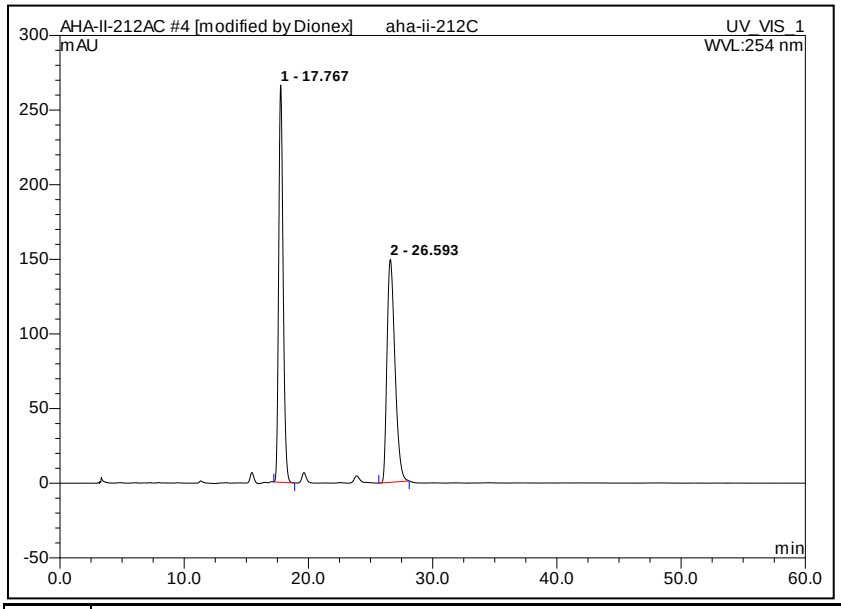

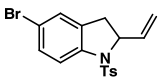

***rac*-12d**

No.	Ret.Time min	Peak Name	Height mAU	Area mAU*min	Rel.Area %	Amount	Type
1	17.77	n.a.	266.070	110.865	49.99	n.a.	BMB
2	26.59	n.a.	149.282	110.929	50.01	n.a.	BMB*
Total:			415.352	221.793	100.00	0.000	

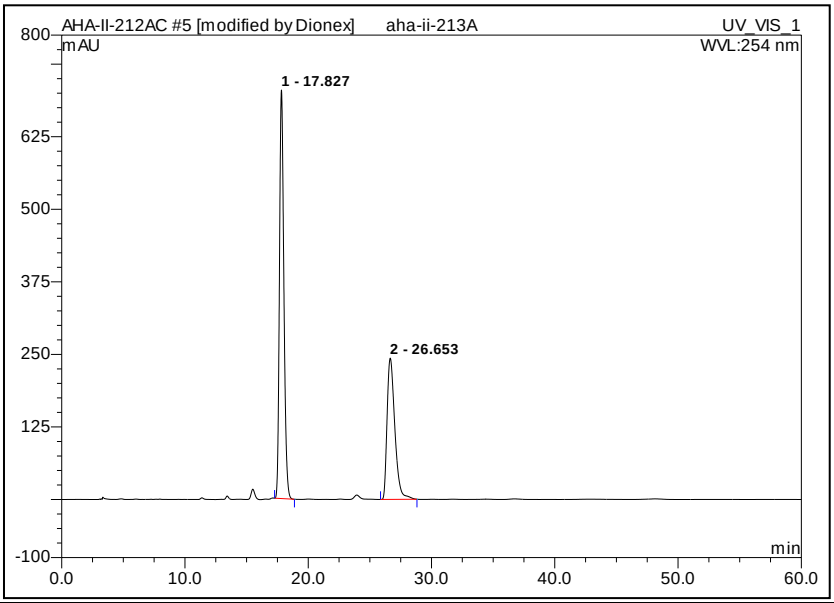

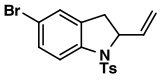

***chiral*-12d**

No.	Ret.Time min	Peak Name	Height mAU	Area mAU*min	Rel.Area %	Amount	Type
1	17.83	n.a.	703.821	291.677	62.21	n.a.	BMB
2	26.65	n.a.	243.339	177.210	37.79	n.a.	BMB*
Total:			947.160	468.886	100.00	0.000	

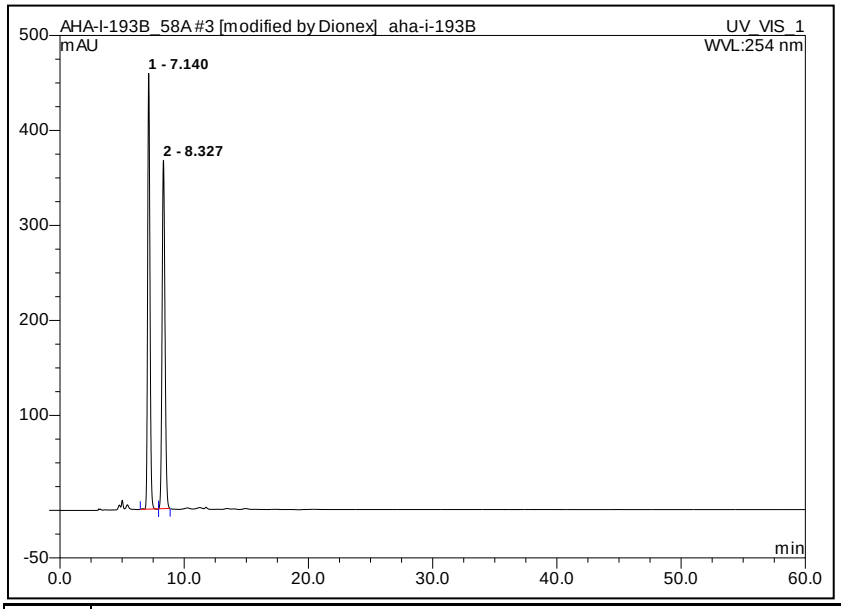

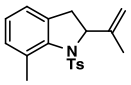

***rac*-11e**

No.	Ret.Time min	Peak Name	Height mAU	Area mAU*min	Rel.Area %	Amount	Type
1	7.14	n.a.	458.702	99.110	49.86	n.a.	BMb*
2	8.33	n.a.	366.772	99.664	50.14	n.a.	bMB*
Total:			825.474	198.774	100.00	0.000	

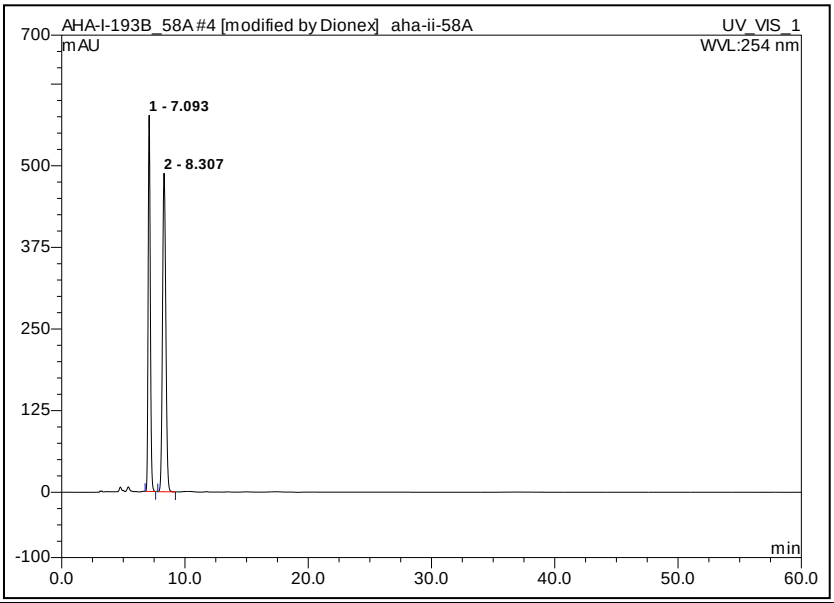

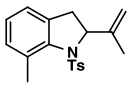

***chiral*-11e**

No.	Ret.Time min	Peak Name	Height mAU	Area mAU*min	Rel.Area %	Amount	Type
1	7.09	n.a.	575.894	117.534	43.62	n.a.	BMB
2	8.31	n.a.	487.690	151.945	56.38	n.a.	BMB
Total:			1063.585	269.479	100.00	0.000	

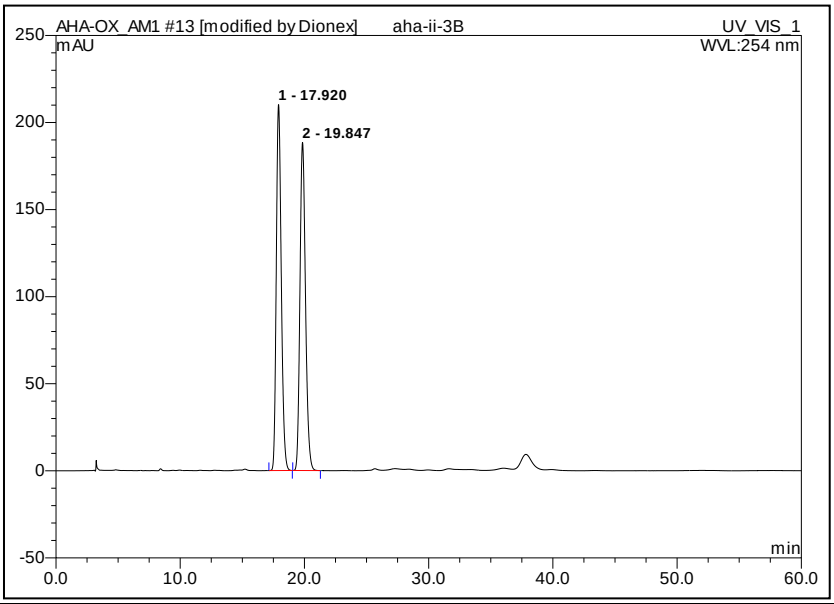

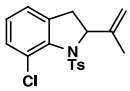

***rac*-11f**

No.	Ret.Time min	Peak Name	Height mAU	Area mAU*min	Rel.Area %	Amount	Type
1	17.92	n.a.	210.150	97.862	50.00	n.a.	BMB
2	19.85	n.a.	188.393	97.845	50.00	n.a.	BMB
Total:			398.544	195.707	100.00	0.000	

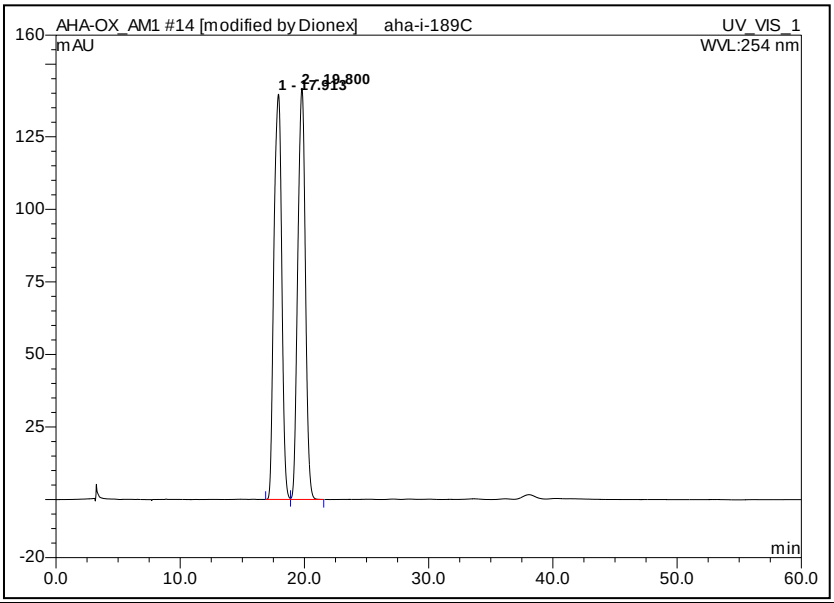

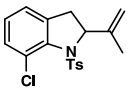

***chiral*-11f**

No.	Ret.Time min	Peak Name	Height mAU	Area mAU*min	Rel.Area %	Amount	Type
1	17.91	n.a.	139.612	101.921	50.26	n.a.	BM *
2	19.80	n.a.	141.668	100.852	49.74	n.a.	MB*
Total:			281.280	202.773	100.00	0.000	

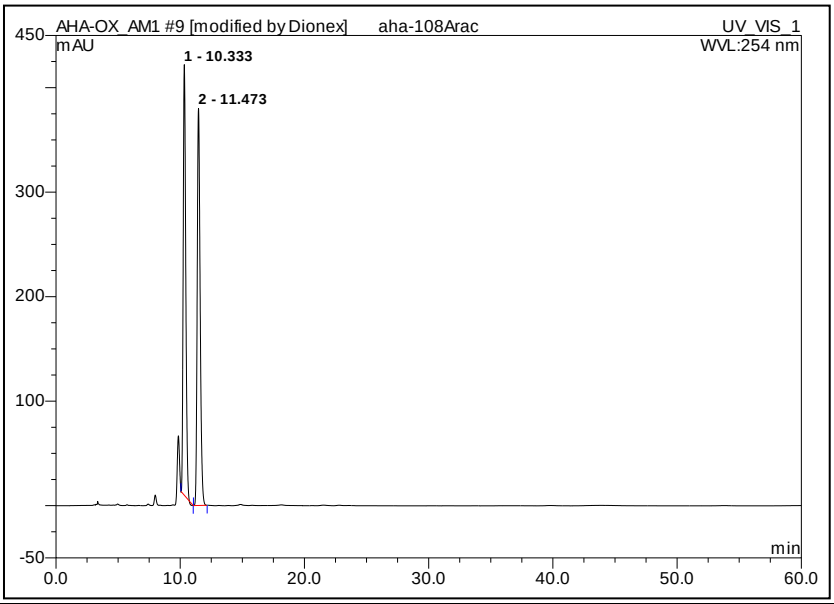

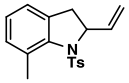

***rac*-12e**

No.	Ret.Time min	Peak Name	Height mAU	Area mAU*min	Rel.Area %	Amount	Type
1	10.33	n.a.	412.117	98.604	48.56	n.a.	BMB*
2	11.47	n.a.	380.009	104.460	51.44	n.a.	BMB
Total:			792.126	203.064	100.00	0.000	

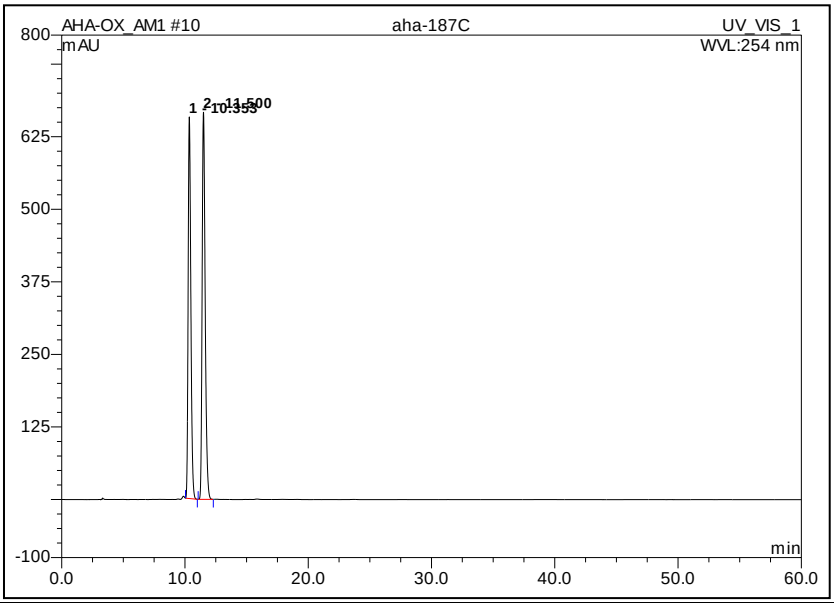

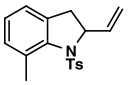

***chiral*-12e**

No.	Ret.Time min	Peak Name	Height mAU	Area mAU*min	Rel.Area %	Amount	Type
1	10.35	n.a.	657.408	167.543	46.72	n.a.	BMB
2	11.50	n.a.	666.898	191.041	53.28	n.a.	BMB
Total:			1324.306	358.584	100.00	0.000	

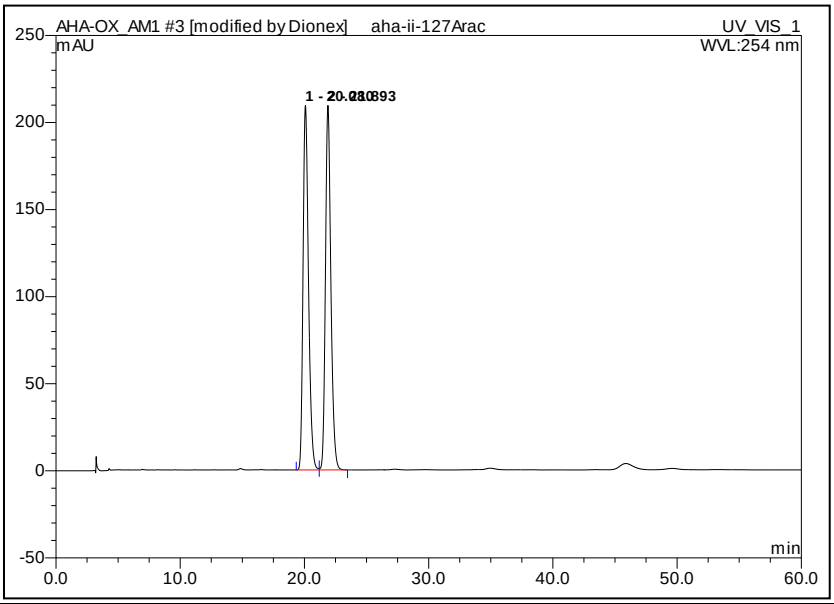

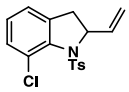

***rac*-12e**

No.	Ret.Time min	Peak Name	Height mAU	Area mAU*min	Rel.Area %	Amount	Type
1	20.08	n.a.	209.353	106.116	49.98	n.a.	BM
2	21.89	n.a.	209.291	106.208	50.02	n.a.	MB
Total:			418.644	212.325	100.00	0.000	

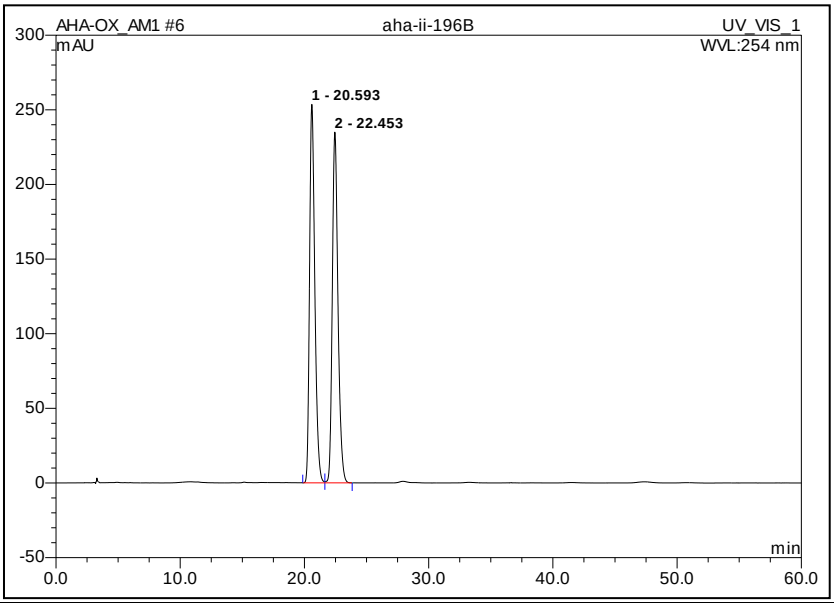

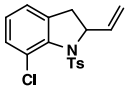

***chiral*-12e**

No.	Ret.Time min	Peak Name	Height mAU	Area mAU*min	Rel.Area %	Amount	Type
1	20.59	n.a.	253.536	125.009	50.10	n.a.	BM
2	22.45	n.a.	234.897	124.532	49.90	n.a.	MB
Total:			488.432	249.541	100.00	0.000	

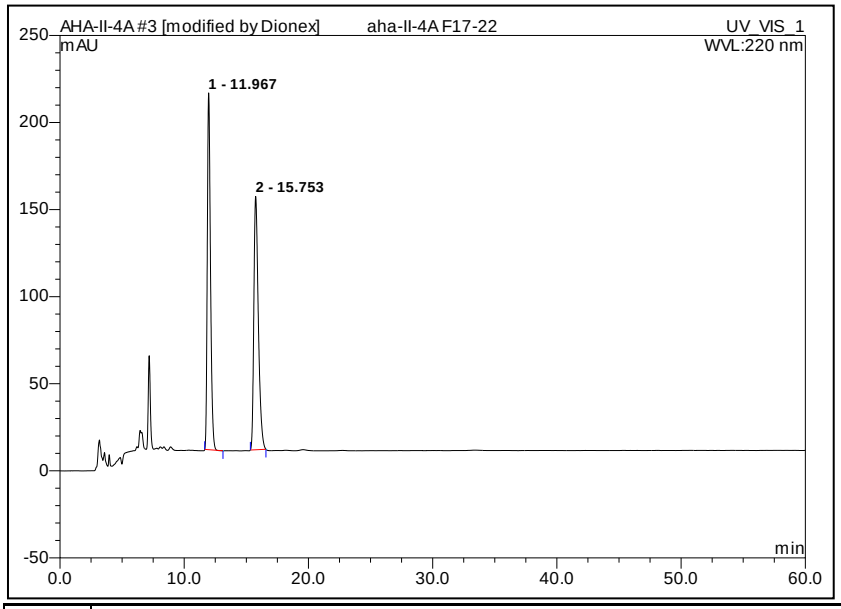

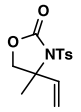

***rac*-13**

No.	Ret.Time min	Peak Name	Height mAU	Area mAU*min	Rel.Area %	Amount	Type
1	11.97	n.a.	204.891	61.042	49.98	n.a.	BMB*
2	15.75	n.a.	145.527	61.096	50.02	n.a.	BMB*
Total:			350.418	122.138	100.00	0.000	

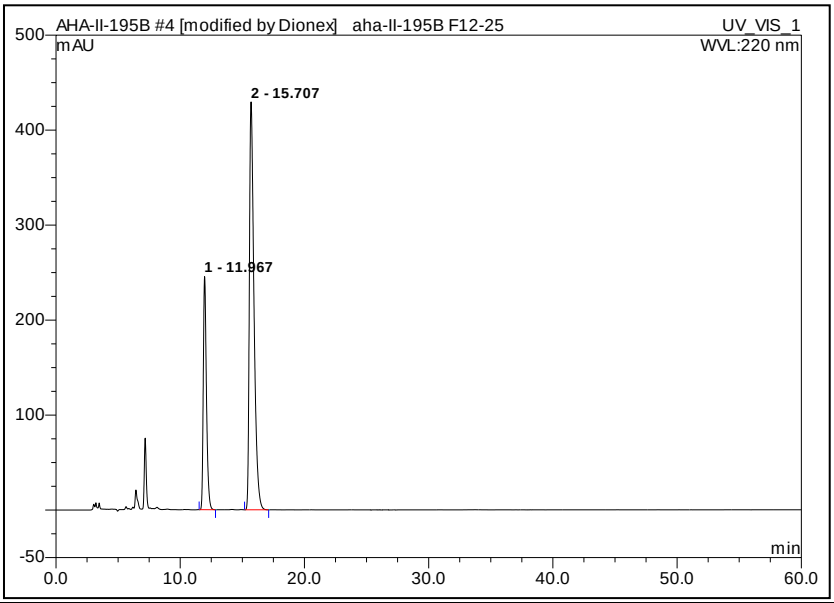

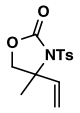

***chiral*-13**

No.	Ret.Time min	Peak Name	Height mAU	Area mAU*min	Rel.Area %	Amount	Type
1	11.97	n.a.	245.422	72.446	28.12	n.a.	BMB
2	15.71	n.a.	429.450	185.176	71.88	n.a.	BMB
Total:			674.872	257.622	100.00	0.000	

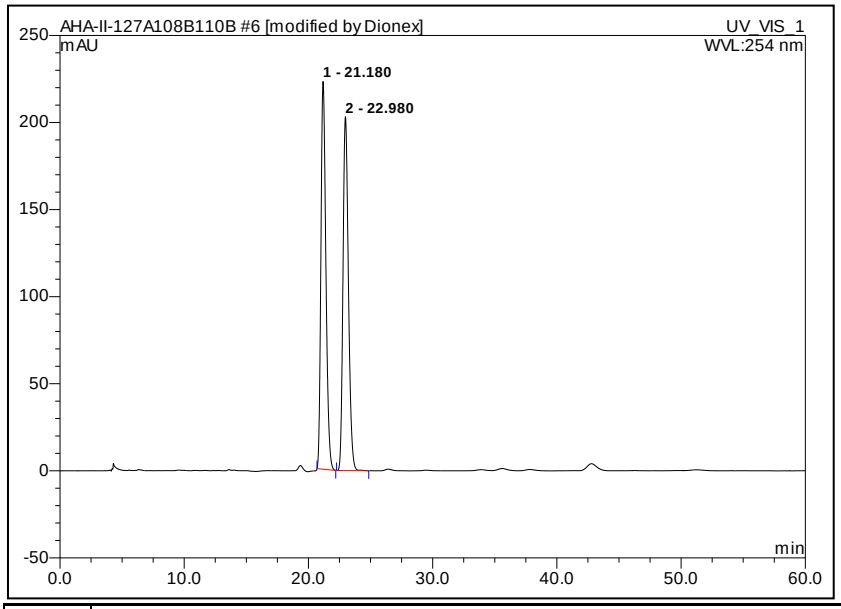

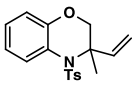

***rac*-14**

No.	Ret.Time min	Peak Name	Height mAU	Area mAU*min	Rel.Area %	Amount	Type
1	21.18	n.a.	222.632	103.217	50.05	n.a.	BMB*
2	22.98	n.a.	203.165	103.026	49.95	n.a.	BMB*
Total:			425.797	206.242	100.00	0.000	

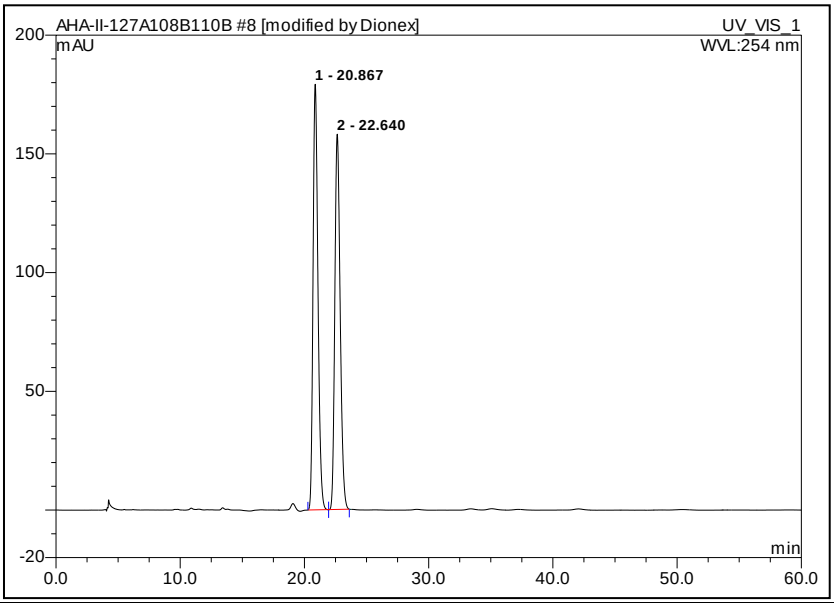

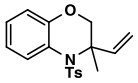

***chiral*-14**

No.	Ret.Time min	Peak Name	Height mAU	Area mAU*min	Rel.Area %	Amount	Type
1	20.87	n.a.	179.217	81.989	50.88	n.a.	BM *
2	22.64	n.a.	158.005	79.148	49.12	n.a.	MB*
Total:			337.222	161.136	100.00	0.000	

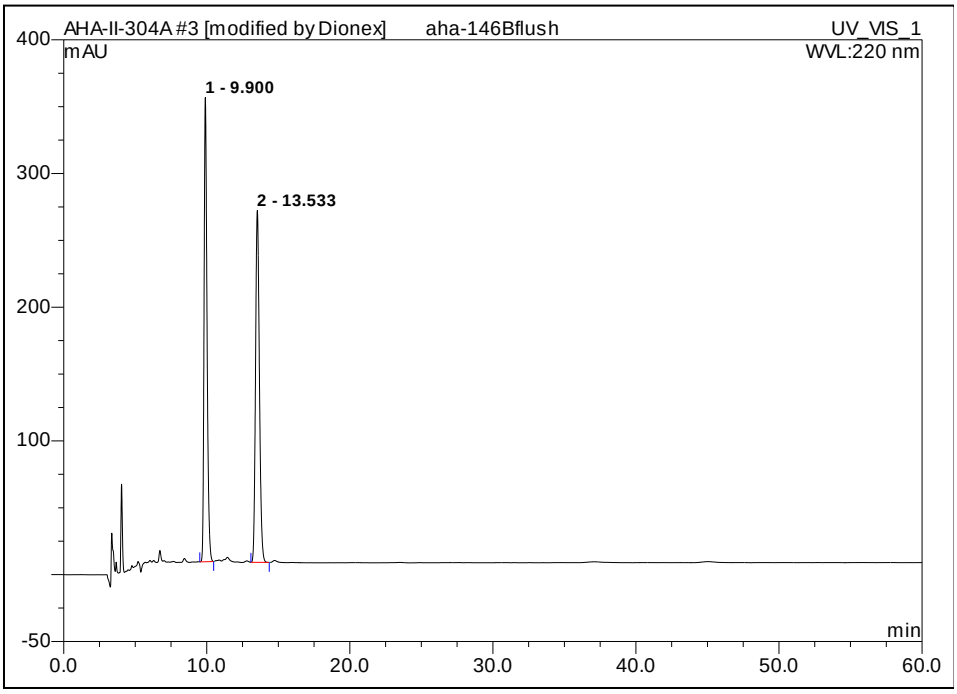

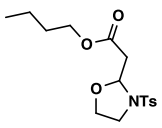

16

No.	Ret.Time min	Peak Name	Height mAU	Area mAU*min	Rel.Area %	Amount	Type
1	9.90	n.a.	347.192	83.616	50.27	n.a.	BMB
2	13.53	n.a.	263.161	82.728	49.73	n.a.	BMB
Total:			610.353	166.345	100.00	0.000	

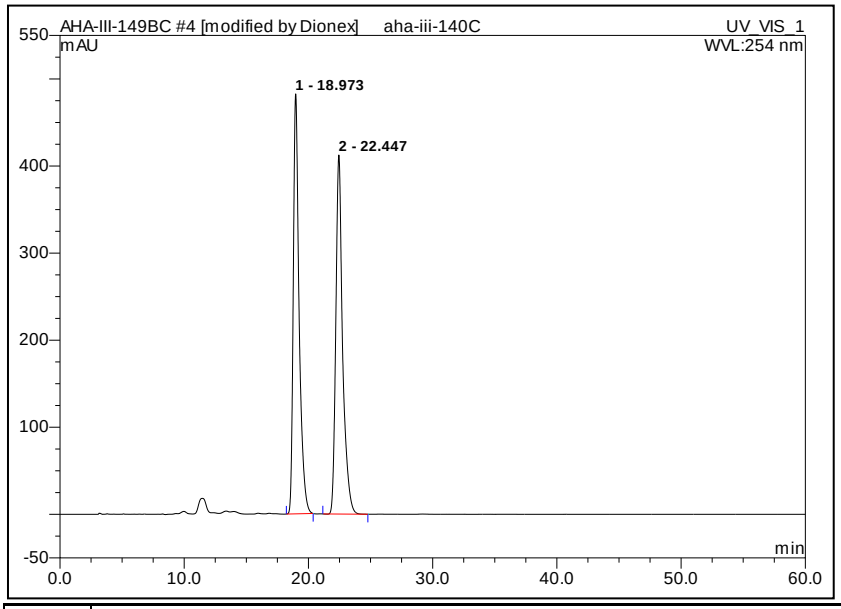

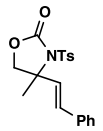

***rac*-17**

No.	Ret.Time min	Peak Name	Height mAU	Area mAU*min	Rel.Area %	Amount	Type
1	18.97	n.a.	482.305	262.592	50.08	n.a.	BMB*
2	22.45	n.a.	412.279	261.748	49.92	n.a.	BMB*
Total:			894.585	524.340	100.00	0.000	

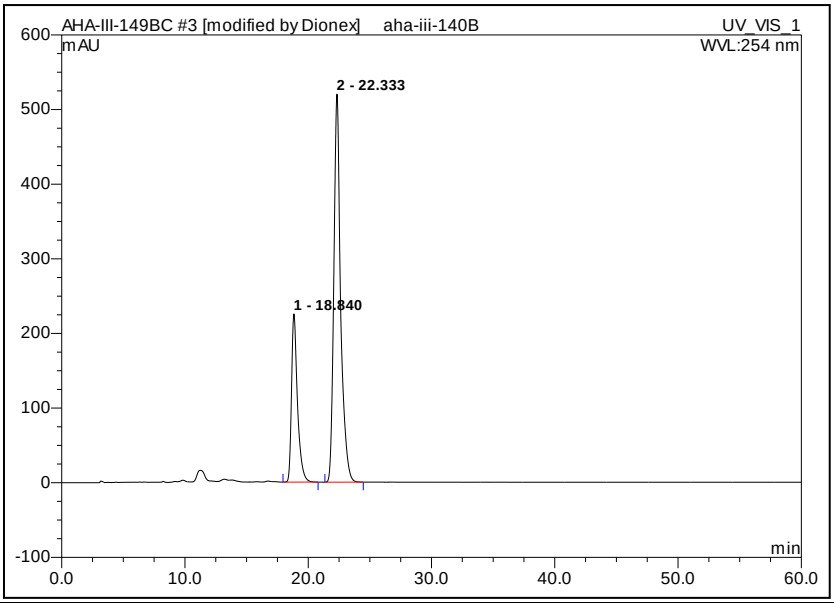

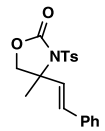

***chiral*-17**

No.	Ret.Time min	Peak Name	Height mAU	Area mAU*min	Rel.Area %	Amount	Type
1	18.84	n.a.	225.339	125.704	27.42	n.a.	BMB
2	22.33	n.a.	519.862	332.695	72.58	n.a.	BMB
Total:			745.202	458.399	100.00	0.000	

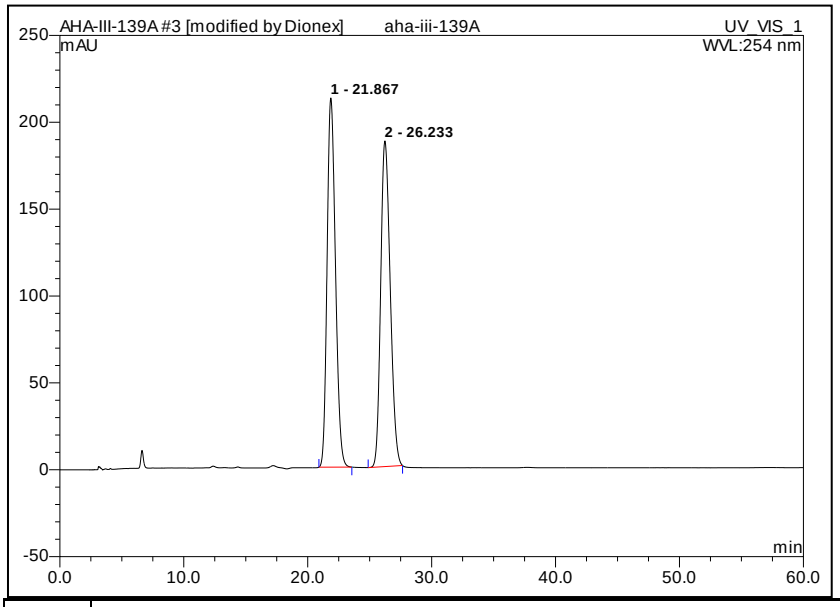

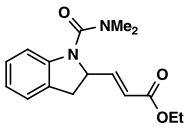

***rac*-30a**

No.	Ret.Time min	Peak Name	Height mAU	Area mAU*min	Rel.Area %	Amount	Type
1	21.87	n.a.	212.456	166.514	49.93	n.a.	BMB*
2	26.23	n.a.	187.402	166.954	50.07	n.a.	BMB*
Total:			399.858	333.468	100.00	0.000	

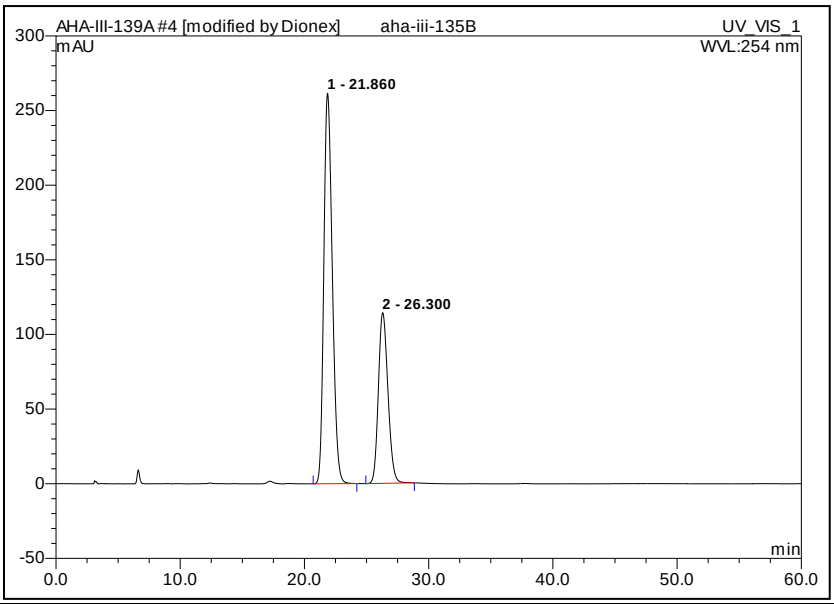

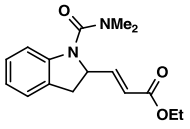

***chiral*-30a**

No.	Ret.Time min	Peak Name	Height mAU	Area mAU*min	Rel.Area %	Amount	Type
1	21.86	n.a.	261.529	207.240	67.04	n.a.	BMB
2	26.30	n.a.	114.335	101.895	32.96	n.a.	BMB*
Total:			375.864	309.135	100.00	0.000	

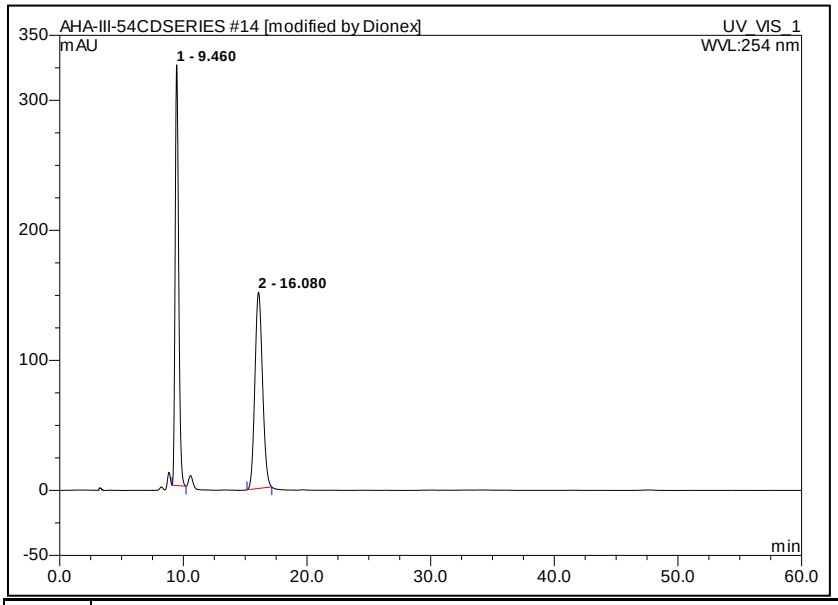

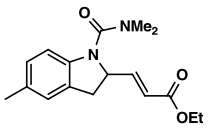

***rac*-30b**

No.	Ret.Time min	Peak Name	Height mAU	Area mAU*min	Rel.Area %	Amount	Type
1	9.46	n.a.	323.538	106.947	49.81	n.a.	BMB*
2	16.08	n.a.	150.976	107.761	50.19	n.a.	BMB*
Total:			474.514	214.708	100.00	0.000	

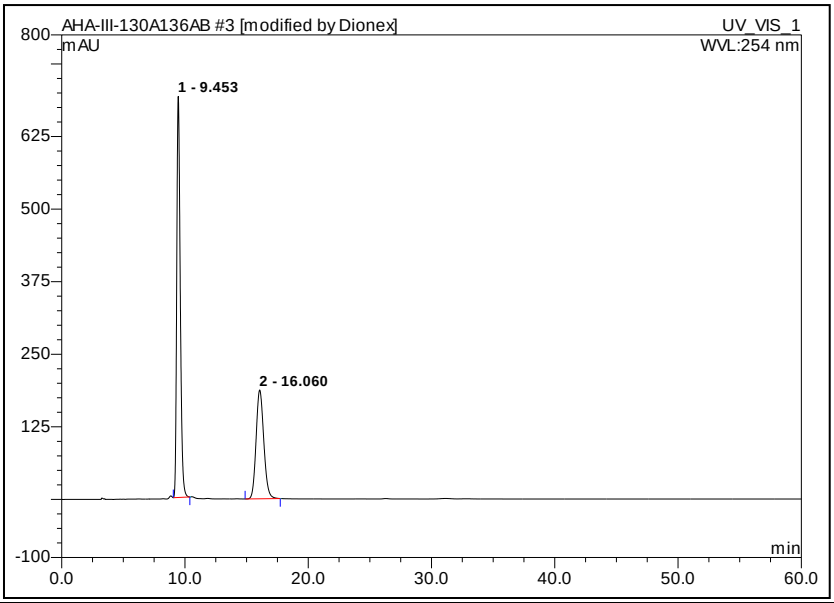

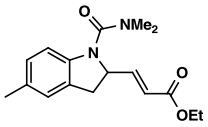

***chiral*-30b**

No.	Ret.Time min	Peak Name	Height mAU	Area mAU*min	Rel.Area %	Amount	Type
1	9.45	n.a.	690.836	229.026	62.87	n.a.	BMB*
2	16.06	n.a.	187.391	135.235	37.13	n.a.	BMB*
Total:			878.226	364.262	100.00	0.000	

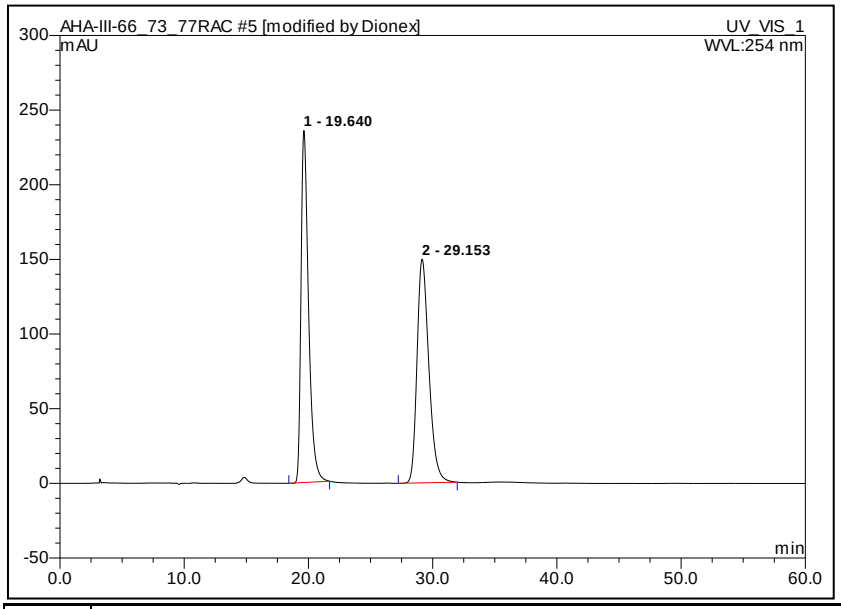

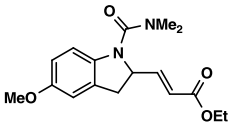

***rac*-30ca**

No.	Ret.Time min	Peak Name	Height mAU	Area mAU*min	Rel.Area %	Amount	Type
1	19.64	n.a.	235.771	165.726	50.01	n.a.	BMB*
2	29.15	n.a.	149.885	165.648	49.99	n.a.	BMB*
Total:			385.656	331.374	100.00	0.000	

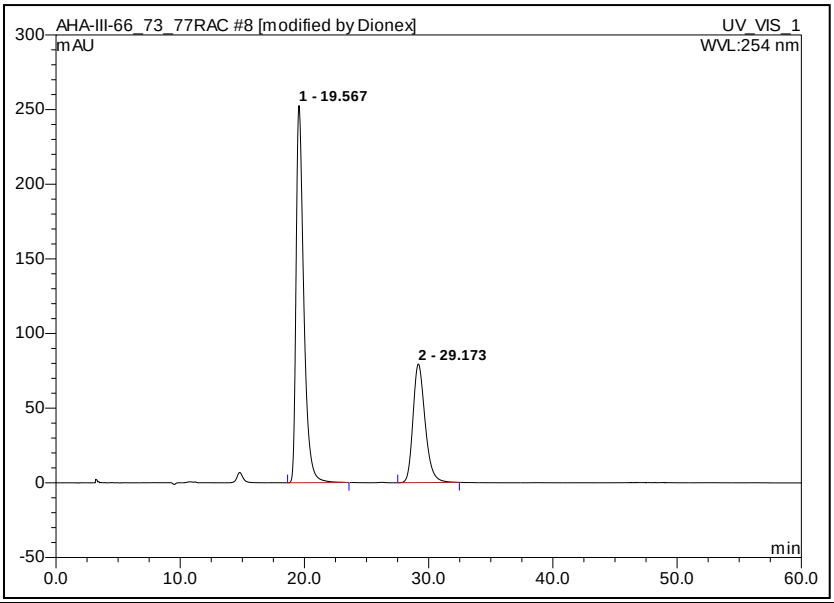

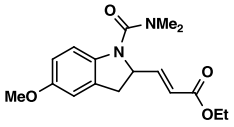

***chiral*-30ca**

No.	Ret.Time min	Peak Name	Height mAU	Area mAU*min	Rel.Area %	Amount	Type
1	19.57	n.a.	252.636	181.602	66.94	n.a.	BMB
2	29.17	n.a.	79.432	89.700	33.06	n.a.	BMB
Total:			332.068	271.302	100.00	0.000	

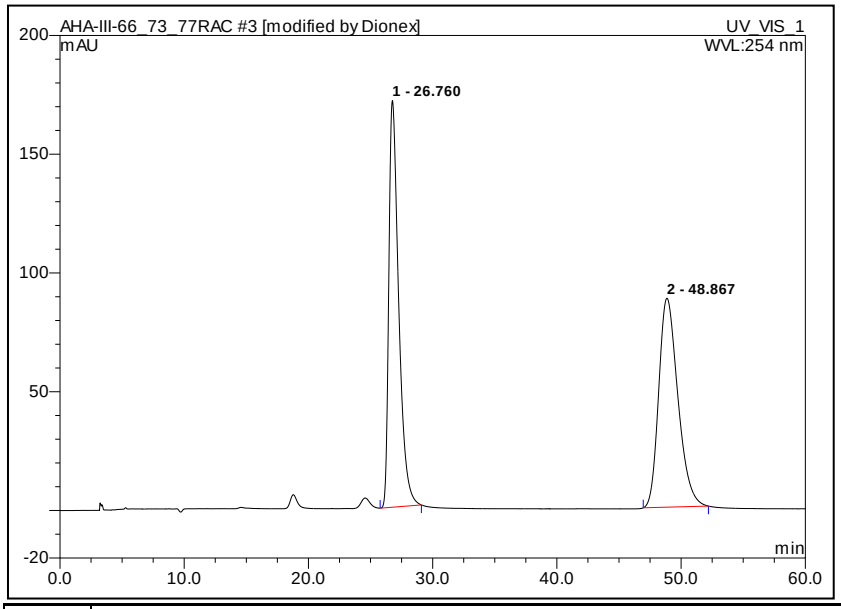

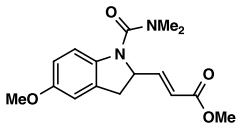

***rac*-30cb**

No.	Ret.Time min	Peak Name	Height mAU	Area mAU*min	Rel.Area %	Amount	Type
1	26.76	n.a.	171.187	157.003	49.99	n.a.	BMB*
2	48.87	n.a.	87.961	157.054	50.01	n.a.	BMB*
Total:			259.147	314.056	100.00	0.000	

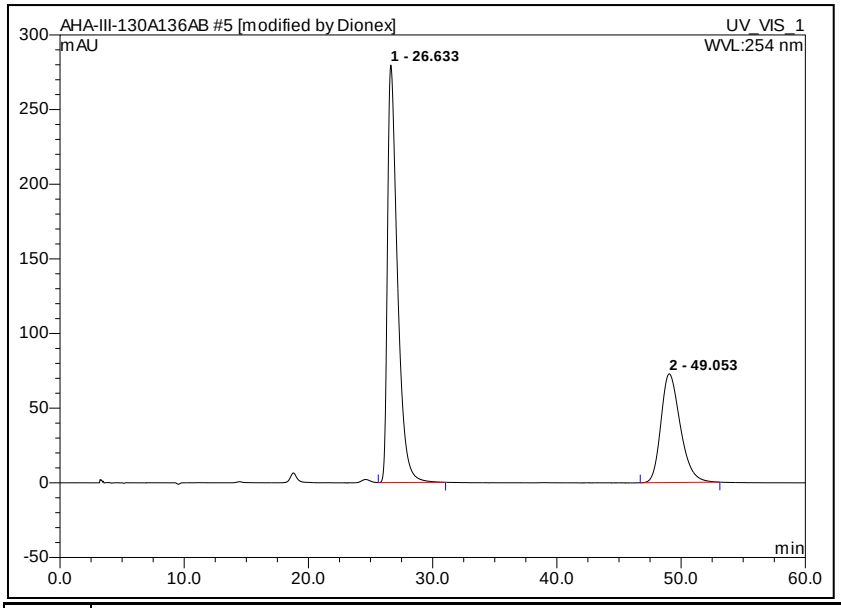

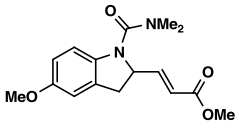

***chiral*-30cb**

No.	Ret.Time min	Peak Name	Height mAU	Area mAU*min	Rel.Area %	Amount	Type
1	26.63	n.a.	279.649	260.999	66.46	n.a.	BMB*
2	49.05	n.a.	72.810	131.722	33.54	n.a.	BMB*
Total:			352.459	392.721	100.00	0.000	

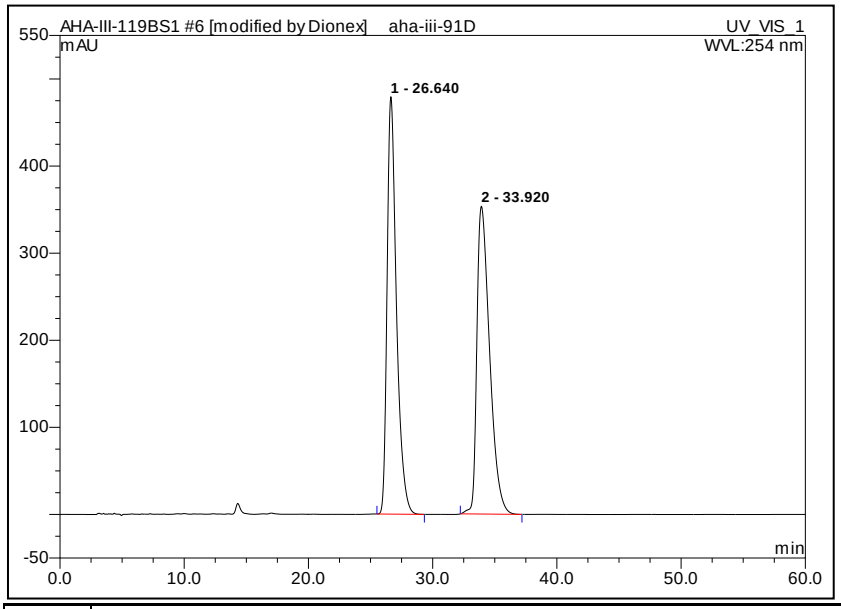

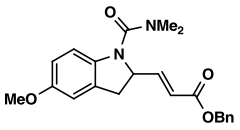

***rac*-30cc**

No.	Ret.Time min	Peak Name	Height mAU	Area mAU*min	Rel.Area %	Amount	Type
1	26.64	n.a.	479.263	419.235	49.95	n.a.	BMB*
2	33.92	n.a.	353.335	420.155	50.05	n.a.	BMB*
Total:			832.598	839.390	100.00	0.000	

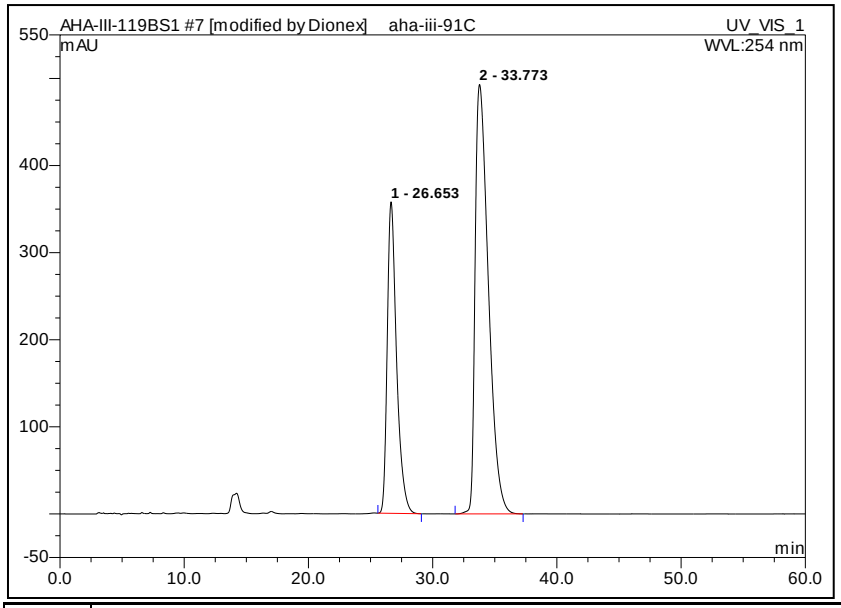

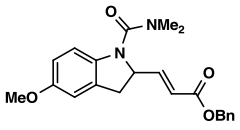

***chiral*-30cc**

No.	Ret.Time min	Peak Name	Height mAU	Area mAU*min	Rel.Area %	Amount	Type
1	26.65	n.a.	357.617	311.026	33.78	n.a.	BMB
2	33.77	n.a.	493.001	609.838	66.22	n.a.	BMB
Total:			850.617	920.864	100.00	0.000	

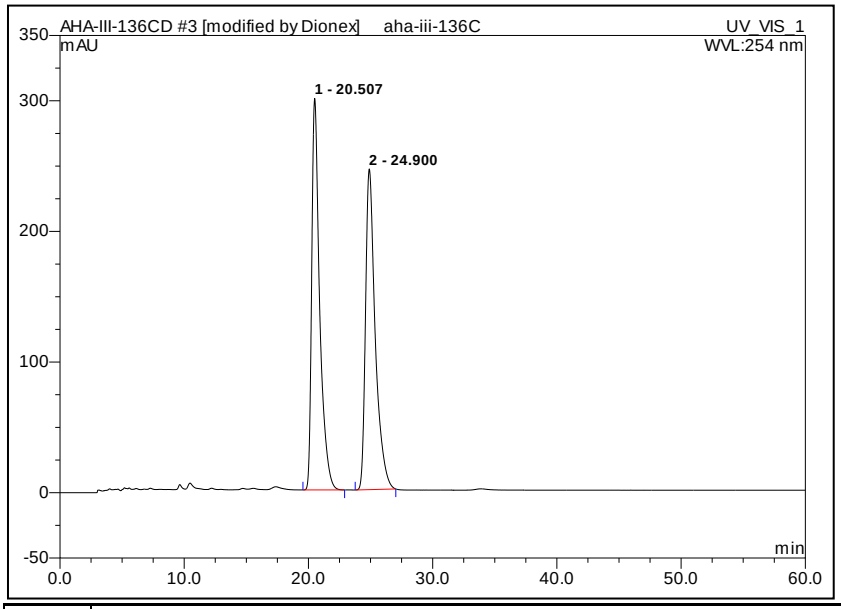

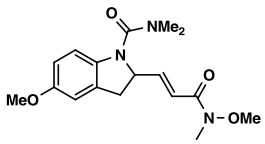

***rac*-30cd**

No.	Ret.Time min	Peak Name	Height mAU	Area mAU*min	Rel.Area %	Amount	Type
1	20.51	n.a.	299.644	222.434	49.98	n.a.	BMB
2	24.90	n.a.	245.461	222.634	50.02	n.a.	BMB*
Total:			545.105	445.067	100.00	0.000	

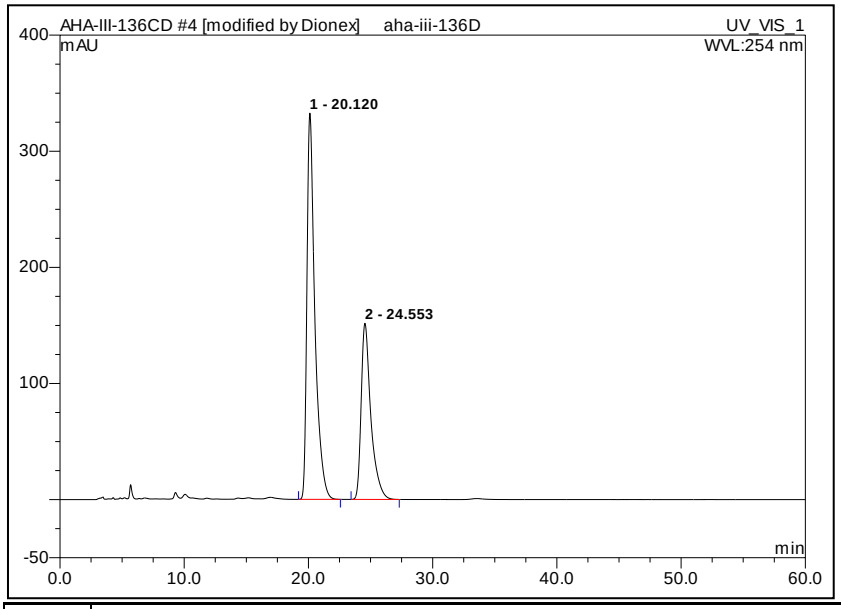

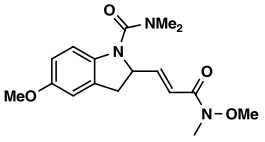

***chiral*-30cd**

No.	Ret.Time min	Peak Name	Height mAU	Area mAU*min	Rel.Area %	Amount	Type
1	20.12	n.a.	332.592	246.989	64.28	n.a.	BMB
2	24.55	n.a.	151.675	137.254	35.72	n.a.	BMB
Total:			484.267	384.243	100.00	0.000	

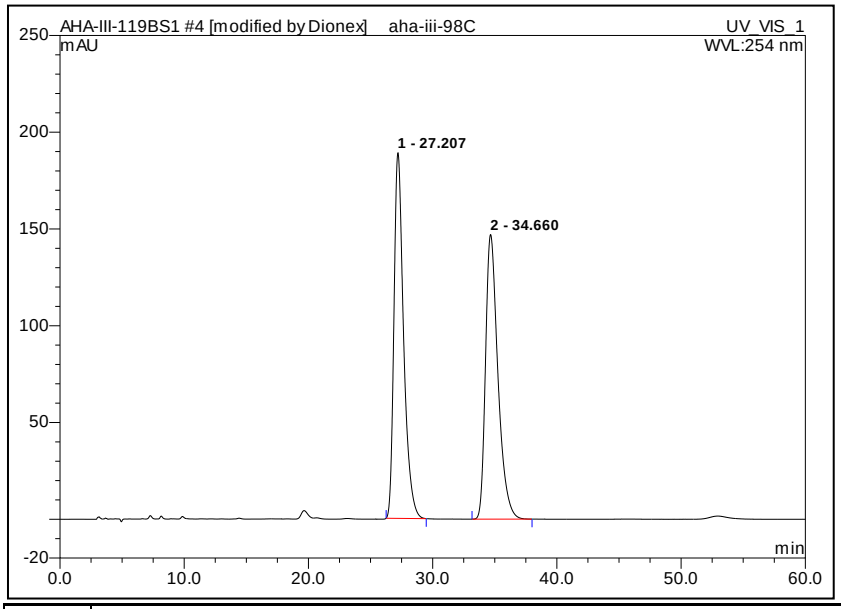

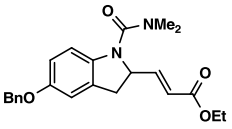

***rac*-30d**

No.	Ret.Time min	Peak Name	Height mAU	Area mAU*min	Rel.Area %	Amount	Type
1	27.21	n.a.	188.976	170.396	50.09	n.a.	BMB*
2	34.66	n.a.	147.060	169.814	49.91	n.a.	BMB*
Total:			336.036	340.210	100.00	0.000	

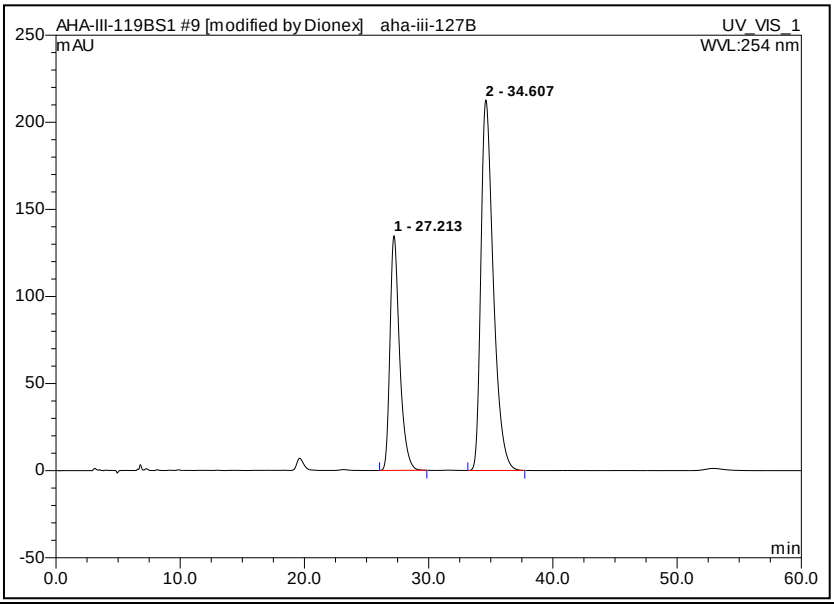

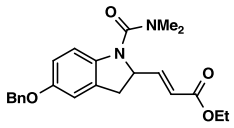

***chiral*-30d**

No.	Ret.Time min	Peak Name	Height mAU	Area mAU*min	Rel.Area %	Amount	Type
1	27.21	n.a.	134.823	121.190	32.92	n.a.	BMB
2	34.61	n.a.	212.765	246.994	67.08	n.a.	BMB
Total:			347.589	368.184	100.00	0.000	

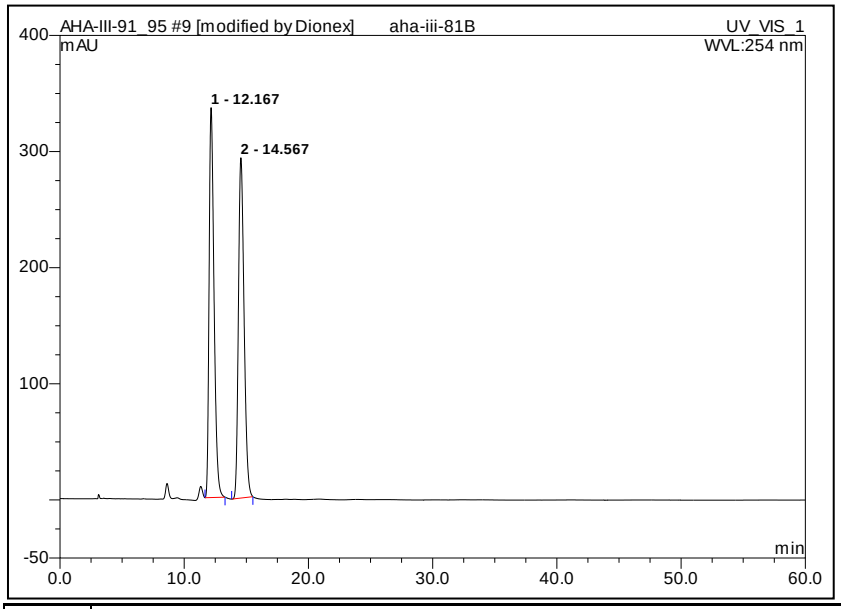

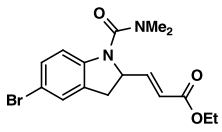

***rac*-30e**

No.	Ret.Time min	Peak Name	Height mAU	Area mAU*min	Rel.Area %	Amount	Type
1	12.17	n.a.	335.714	154.402	49.97	n.a.	BMB*
2	14.57	n.a.	293.055	154.557	50.03	n.a.	BMB*
Total:			628.769	308.959	100.00	0.000	

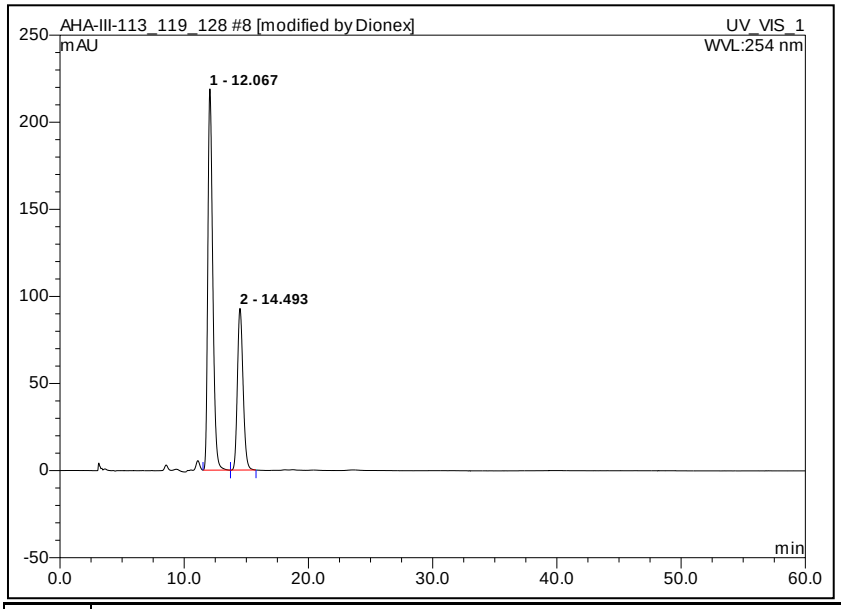

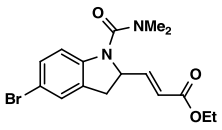

***chiral*-30e**

No.	Ret.Time min	Peak Name	Height mAU	Area mAU*min	Rel.Area %	Amount	Type
1	12.07	n.a.	218.871	100.715	67.25	n.a.	BM *
2	14.49	n.a.	92.828	49.036	32.75	n.a.	MB*
Total:			311.699	149.751	100.00	0.000	

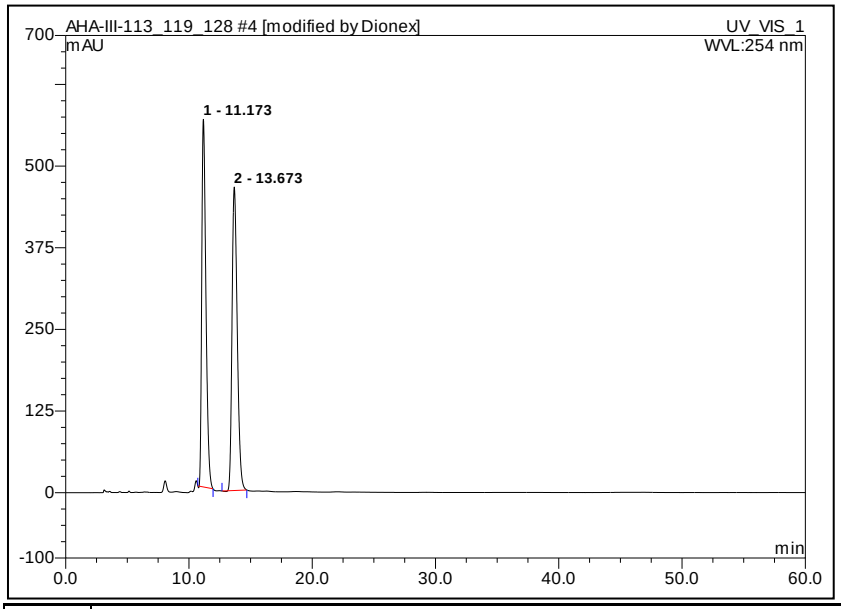

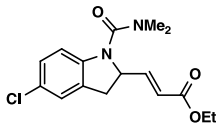

***rac*-30f**

No.	Ret.Time min	Peak Name	Height mAU	Area mAU*min	Rel.Area %	Amount	Type
1	11.17	n.a.	562.808	220.550	49.31	n.a.	BMB*
2	13.67	n.a.	464.523	226.758	50.69	n.a.	BMB*
Total:			1027.331	447.308	100.00	0.000	

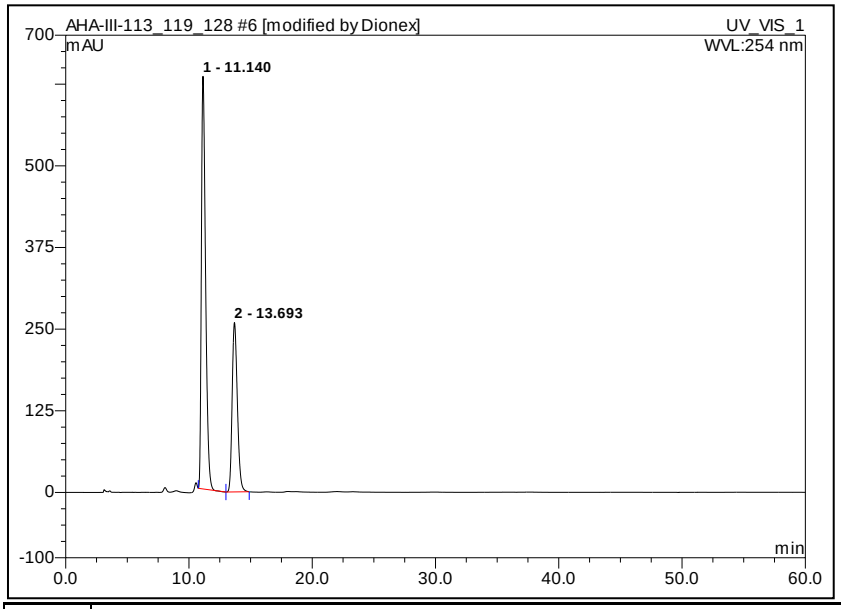

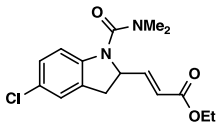

***chiral*-30f**

No.	Ret.Time min	Peak Name	Height mAU	Area mAU*min	Rel.Area %	Amount	Type
1	11.14	n.a.	631.766	249.069	66.23	n.a.	BMb*
2	13.69	n.a.	259.355	127.020	33.77	n.a.	bMB*
Total:			891.121	376.089	100.00	0.000	

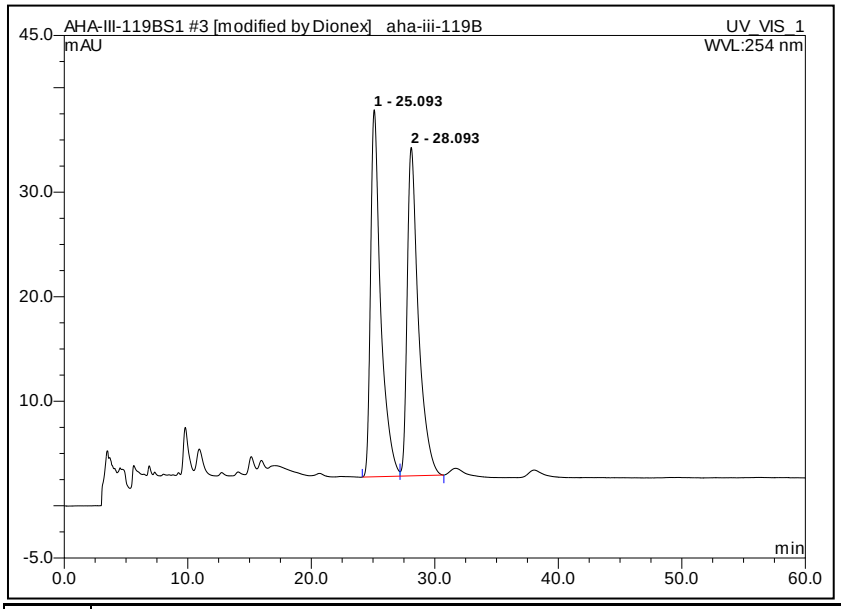

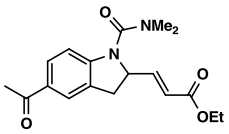

***rac*-30g**

No.	Ret.Time min	Peak Name	Height mAU	Area mAU*min	Rel.Area %	Amount	Type
1	25.09	n.a.	35.116	33.460	50.22	n.a.	BM *
2	28.09	n.a.	31.423	33.162	49.78	n.a.	MB*
Total:			66.539	66.621	100.00	0.000	

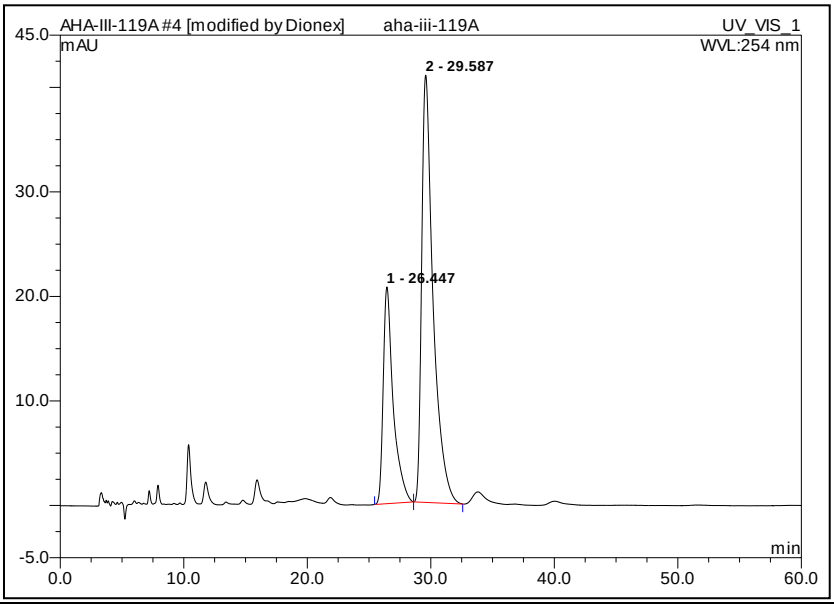

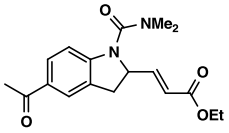

***chiral*-30g**

No.	Ret.Time min	Peak Name	Height mAU	Area mAU*min	Rel.Area %	Amount	Type
1	26.45	n.a.	20.737	19.499	30.71	n.a.	BMb
2	29.59	n.a.	40.876	44.000	69.29	n.a.	bMB
Total:			61.613	63.498	100.00	0.000	

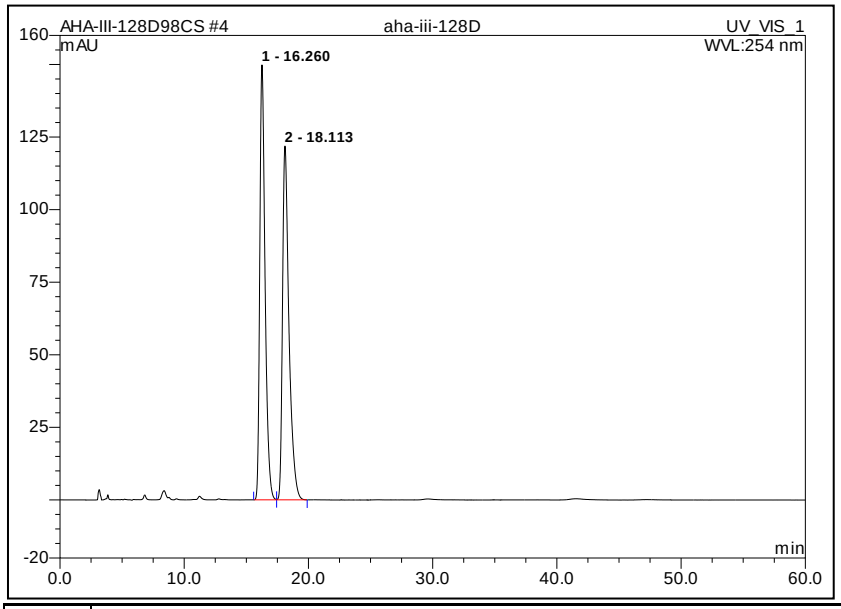

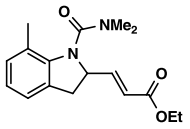

***rac*-30h**

No.	Ret.Time min	Peak Name	Height mAU	Area mAU*min	Rel.Area %	Amount	Type
1	16.26	n.a.	149.804	74.209	50.23	n.a.	BM
2	18.11	n.a.	121.859	73.522	49.77	n.a.	MB
Total:			271.663	147.731	100.00	0.000	

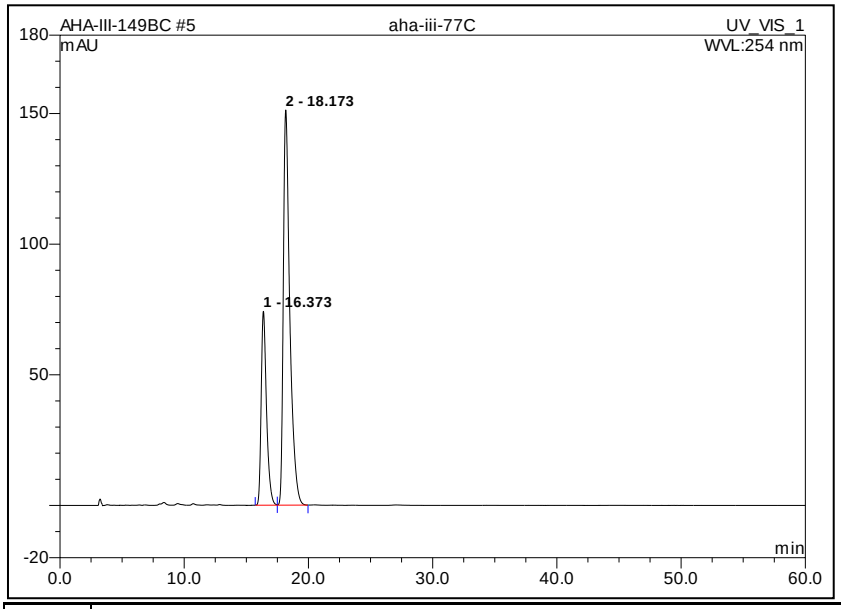

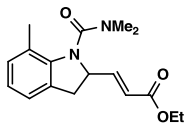

***chiral*-30h**

No.	Ret.Time min	Peak Name	Height mAU	Area mAU*min	Rel.Area %	Amount	Type
1	16.37	n.a.	74.193	36.849	28.59	n.a.	BM
2	18.17	n.a.	151.236	92.043	71.41	n.a.	MB
Total:			225.429	128.892	100.00	0.000	

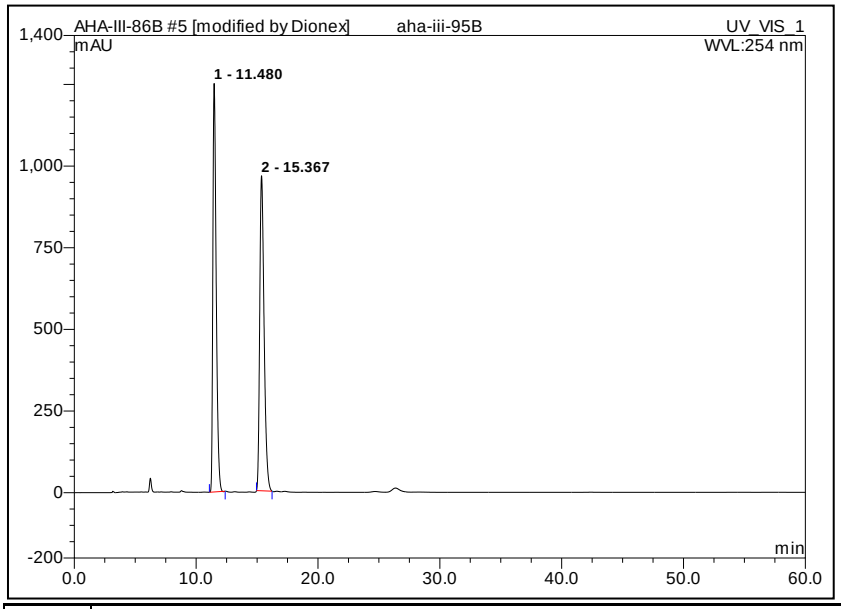

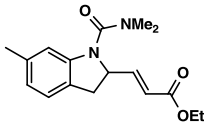

***rac*-30i**

No.	Ret.Time min	Peak Name	Height mAU	Area mAU*min	Rel.Area %	Amount	Type
1	11.48	n.a.	1250.715	398.246	49.82	n.a.	BMB*
2	15.37	n.a.	964.544	401.172	50.18	n.a.	BMB*
Total:			2215.259	799.418	100.00	0.000	

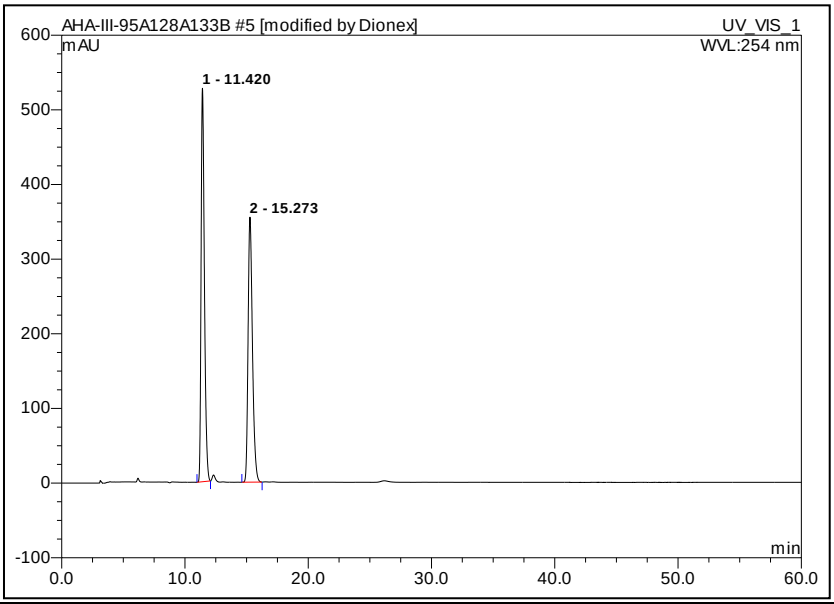

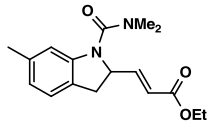

***chiral*-30i**

No.	Ret.Time min	Peak Name	Height mAU	Area mAU*min	Rel.Area %	Amount	Type
1	11.42	n.a.	527.048	164.261	52.97	n.a.	BMB*
2	15.27	n.a.	355.006	145.845	47.03	n.a.	BMB
Total:			882.054	310.106	100.00	0.000	

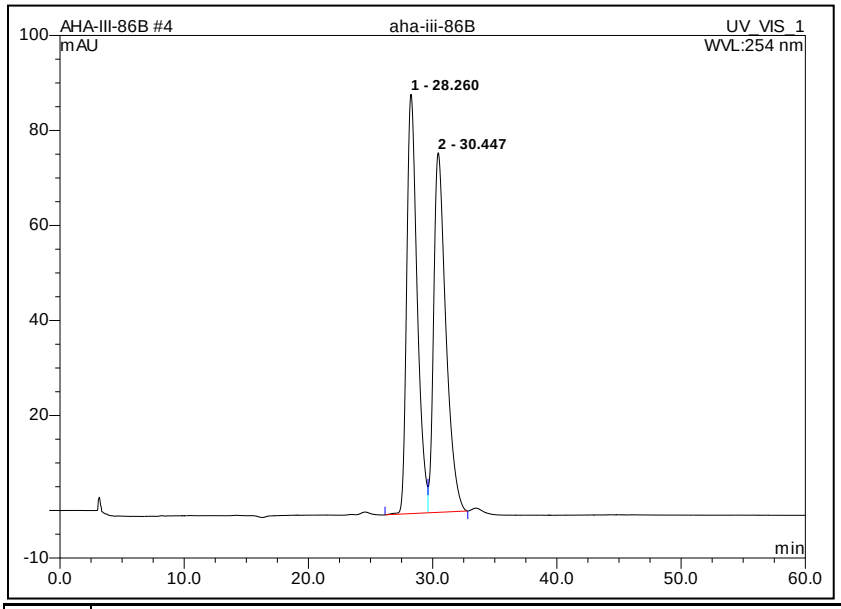

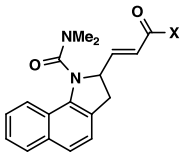

rac-30j

No.	Ret.Time min	Peak Name	Height mAU	Area mAU*min	Rel.Area %	Amount	Type
1	28.26	n.a.	88.288	86.563	49.99	n.a.	BM
2	30.45	n.a.	75.694	86.596	50.01	n.a.	MB
Total:			163.982	173.160	100.00	0.000	

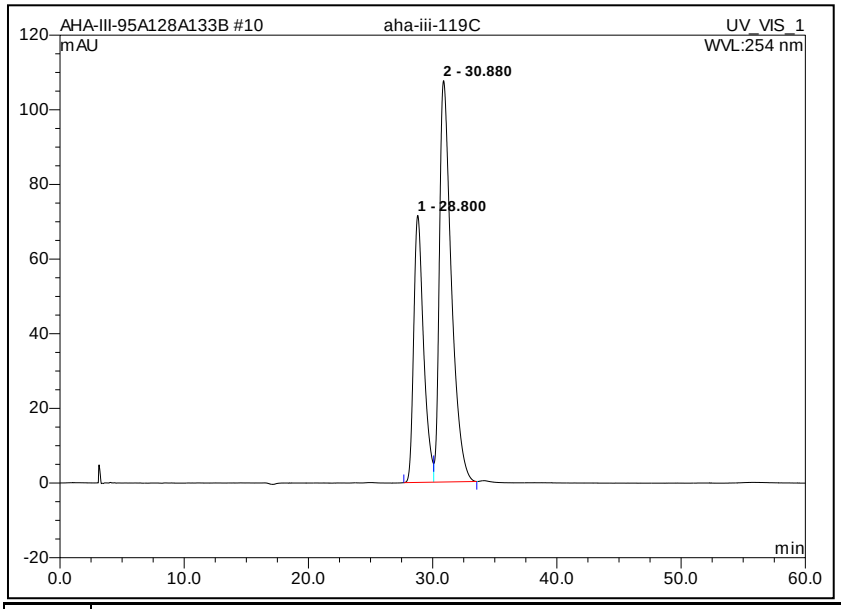

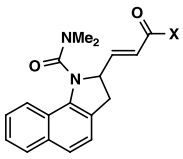

chiral-30j

No.	Ret.Time min	Peak Name	Height mAU	Area mAU*min	Rel.Area %	Amount	Type
1	28.80	n.a.	71.543	66.001	35.53	n.a.	BM
2	30.88	n.a.	107.532	119.767	64.47	n.a.	MB
Total:			179.076	185.768	100.00	0.000	

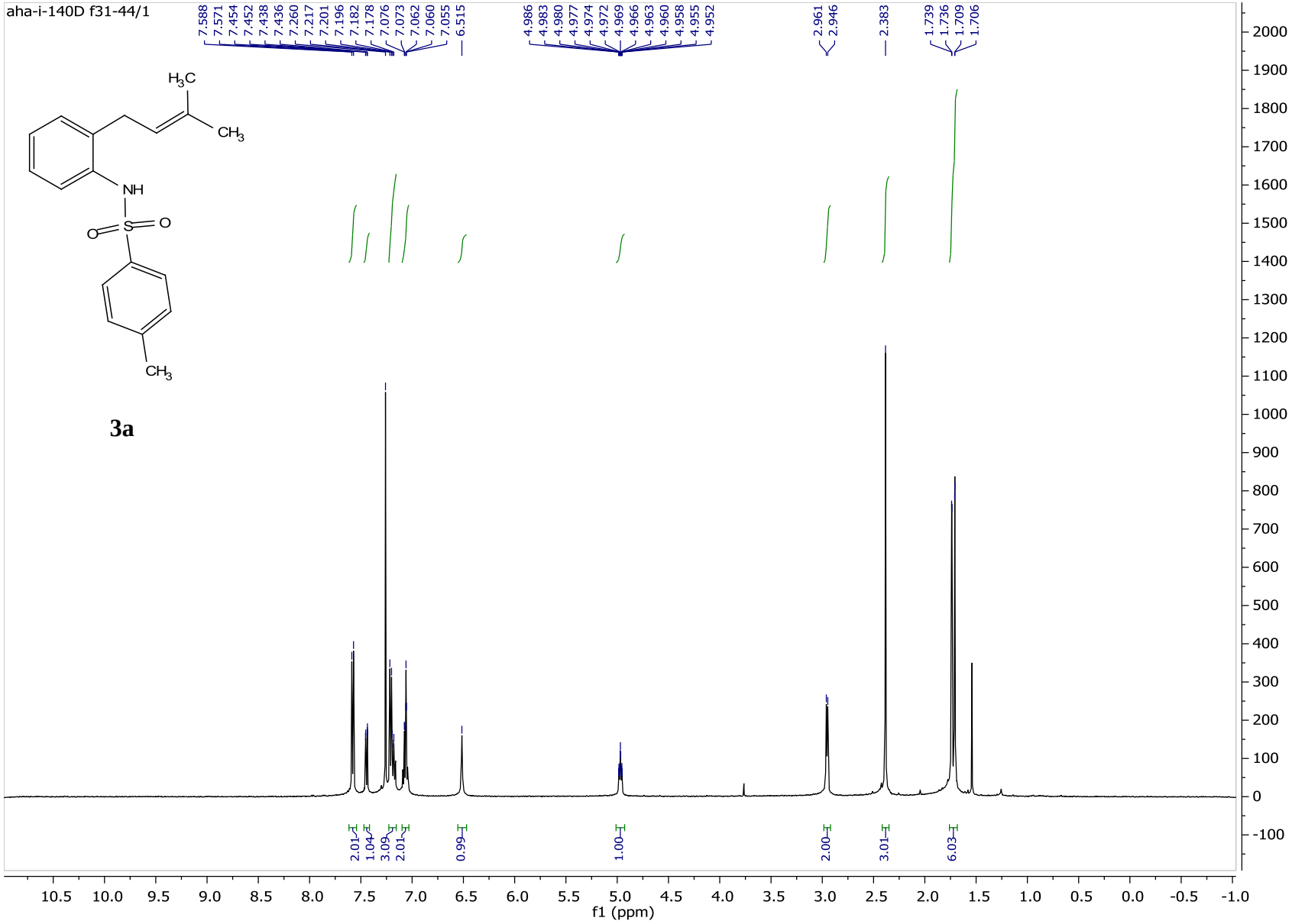
aha-i-140D f31-44/1
7.588
7.571
7.454
7.452
7.438
7.436
7.260
7.217
7.201
7.196
7.182
7.178
7.076
7.073
7.062
7.060
7.055
6.515
4.986
4.983
4.980
4.977
4.974
4.972
4.969
4.966
4.963
4.960
4.958
4.955
4.952
2.961
2.946
2.383
1.739
1.736
1.709
1.706
H3C
CH3
NH
O
S
O
CH3
3a
2.01
1.04
3.09
2.01
0.99
1.00
2.00
3.01
6.03
f1 (ppm)

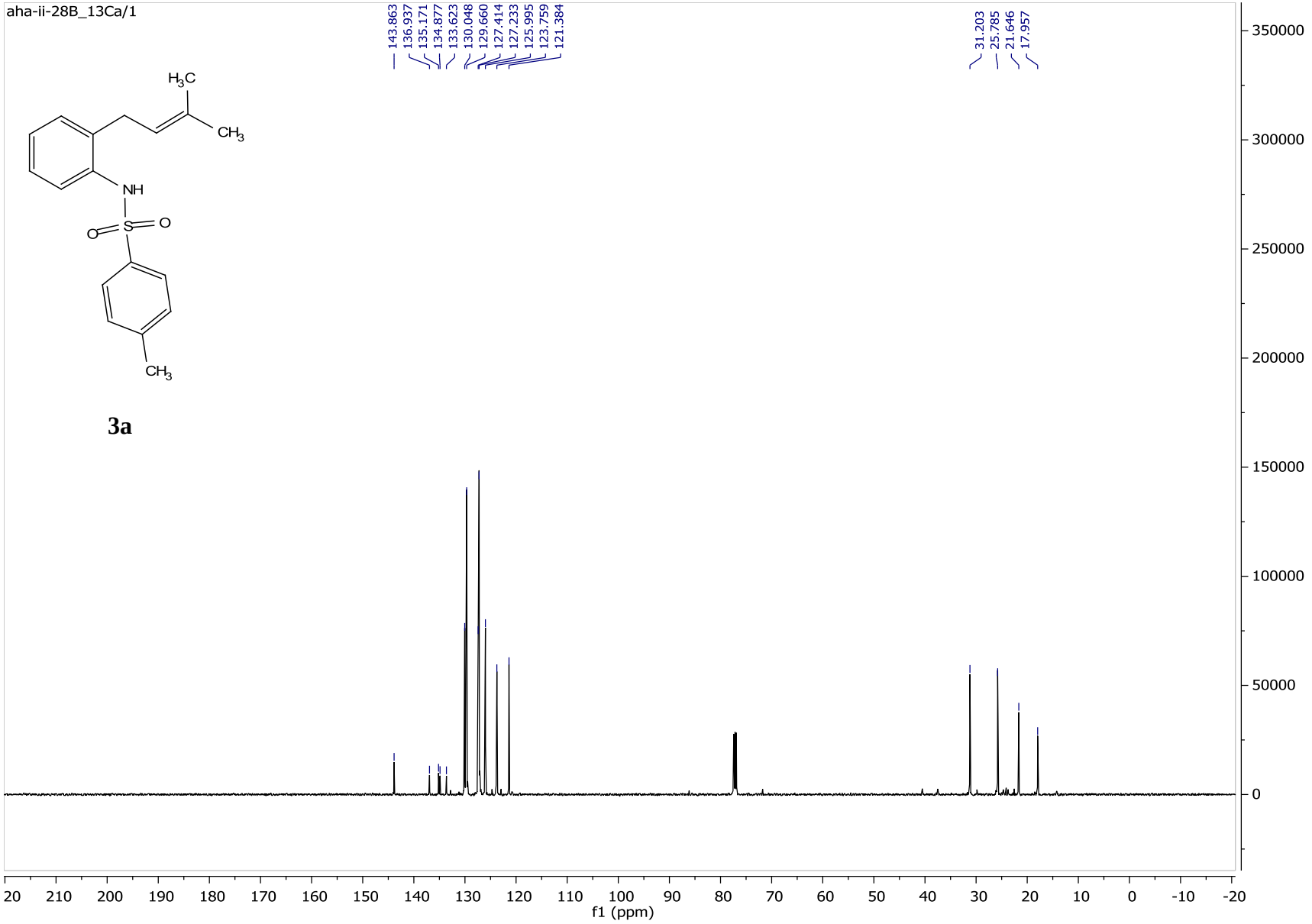
aha-ii-28B_13Ca/1
143.863
136.937
135.171
134.877
133.623
130.048
129.660
127.414
127.233
125.995
123.759
121.384
31.203
25.785
21.646
17.957
H3C
CH3
NH
S
O
O
CH3
3a
350000
300000
250000
200000
150000
100000
50000
0
20
210
200
190
180
170
160
150
140
130
120
110
100
90
80
70
60
50
40
30
20
10
0
-10
-20
f1 (ppm)

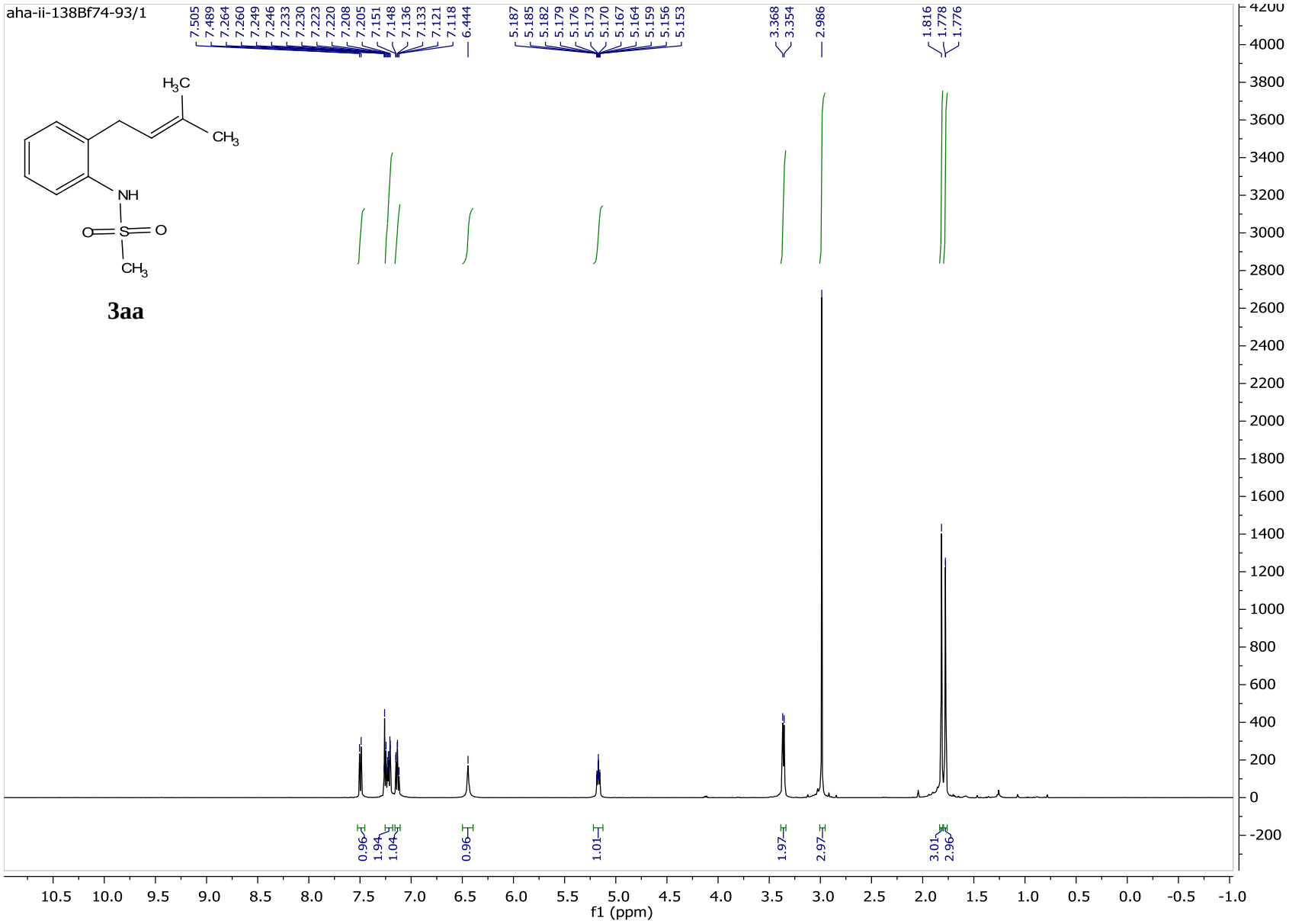
aha-ii-138Bf74-93/1
7.505
7.489
7.264
7.260
7.249
7.246
7.233
7.230
7.223
7.220
7.208
7.205
7.151
7.148
7.136
7.133
7.121
7.118
6.444
5.187
5.185
5.182
5.179
5.176
5.173
5.170
5.167
5.164
5.159
5.156
5.153
3.368
3.354
2.986
1.816
1.778
1.776
H3C
CH3
NH
O
S
O
CH3
0.96
1.94
1.04
0.96
1.01
1.97
2.97
3.01
2.96
f1 (ppm)

3aa

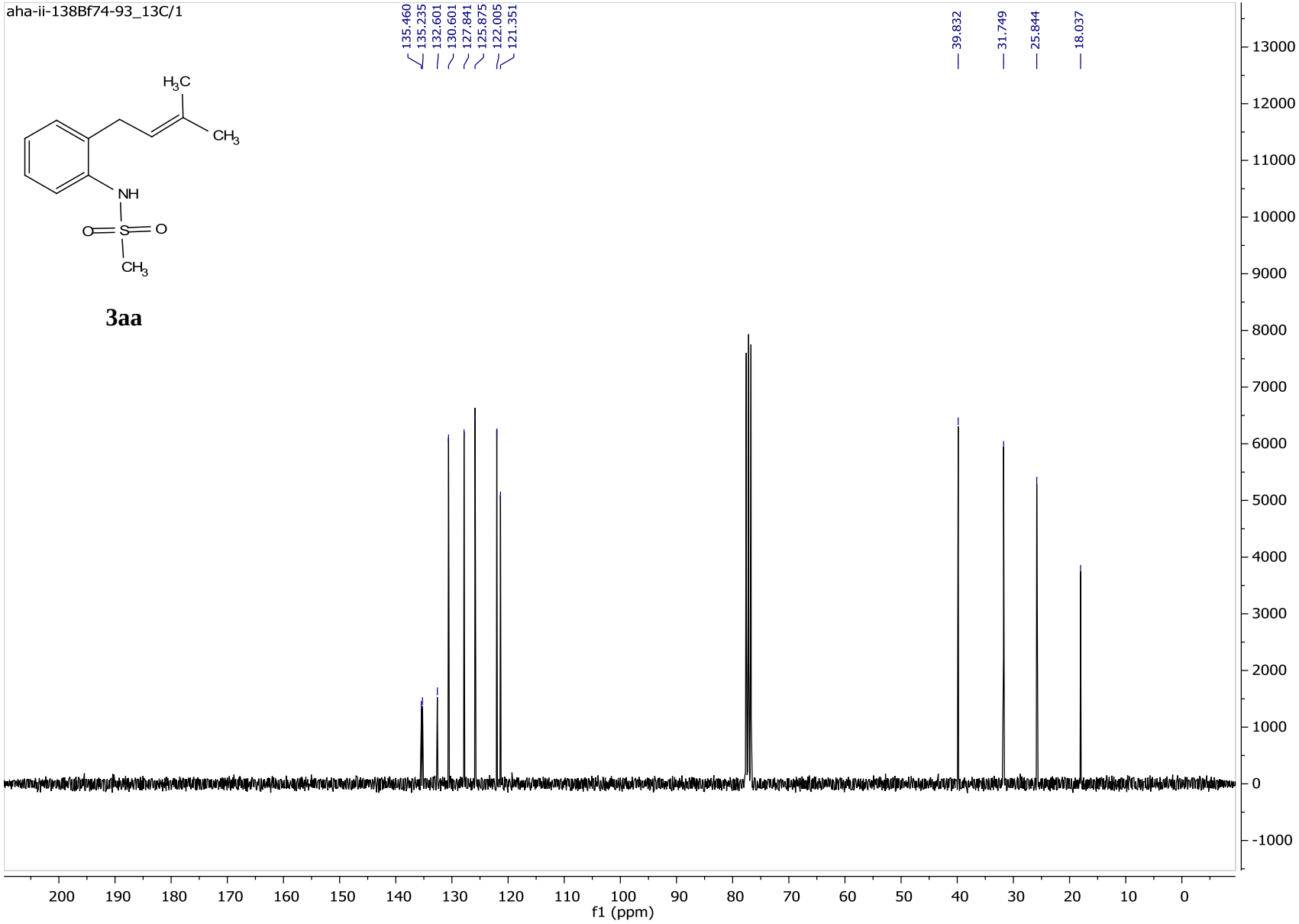
aha-ii-138Bf74-93_13C/1
135.460
135.235
132.601
130.601
127.841
125.875
122.005
121.351
39.832
31.749
25.844
18.037
H3C
CH3
NH
O
S
O
CH3
3aa
f1 (ppm)

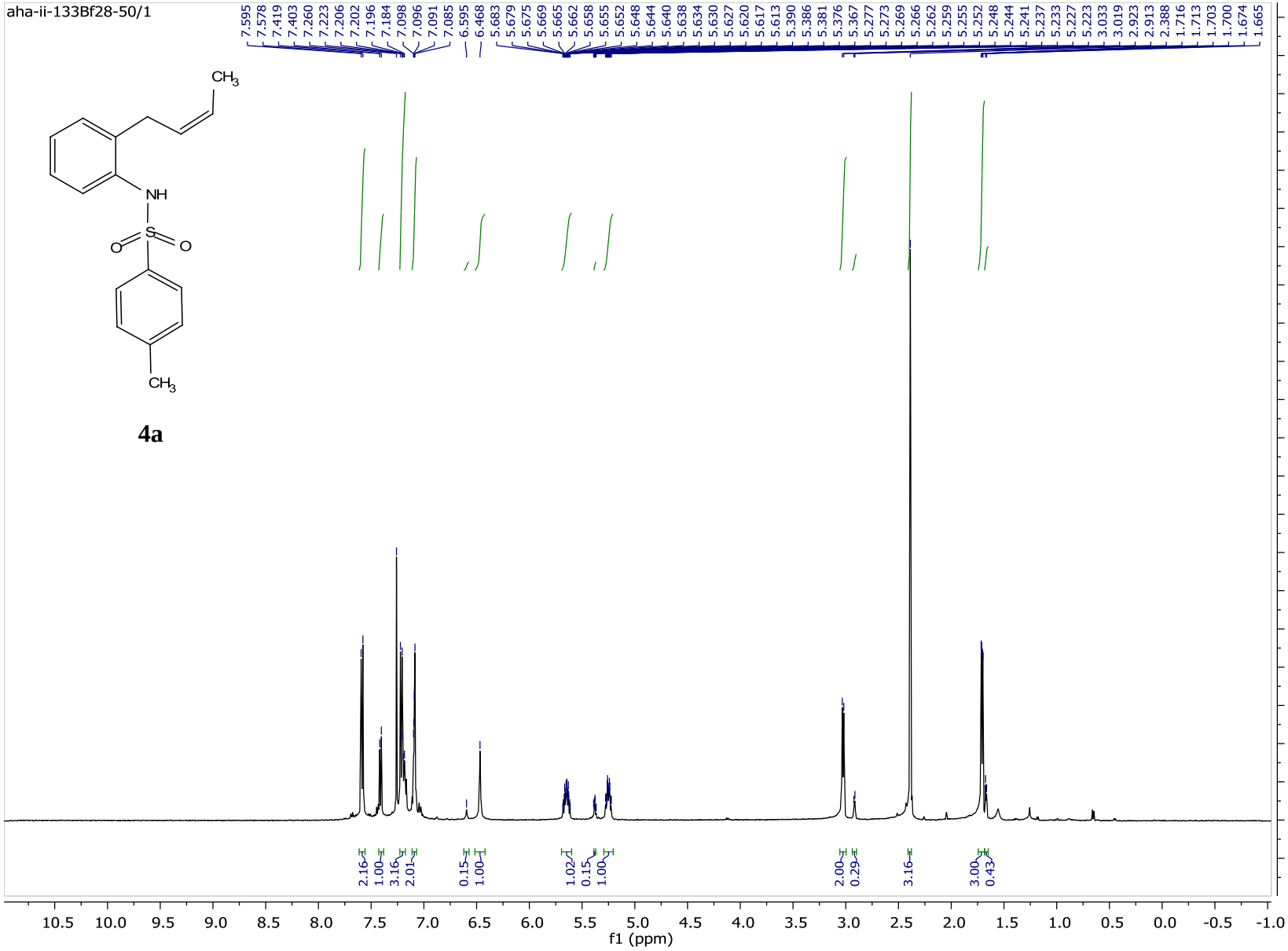
aha-ii-133Bf28-50/1
7.595 7.578 7.419 7.403 7.260 7.223 7.206 7.202 7.196 7.184 7.098 7.096 7.091 7.085 6.595 6.468 5.683 5.679 5.675 5.669 5.665 5.662 5.658 5.655 5.652 5.648 5.644 5.640 5.638 5.634 5.630 5.627 5.620 5.617 5.613 5.390 5.386 5.381 5.376 5.367 5.277 5.273 5.269 5.266 5.262 5.259 5.255 5.252 5.248 5.244 5.241 5.237 5.233 5.227 5.223 3.033 3.019 2.923 2.913 2.388 1.716 1.713 1.703 1.700 1.674 1.665
CH3
NH
S
O
O
CH3
2.16 1.00 3.16 2.01 0.15 1.00 1.02 0.15 1.00 2.00 0.29 3.16 3.00 0.43
f1 (ppm)

4a

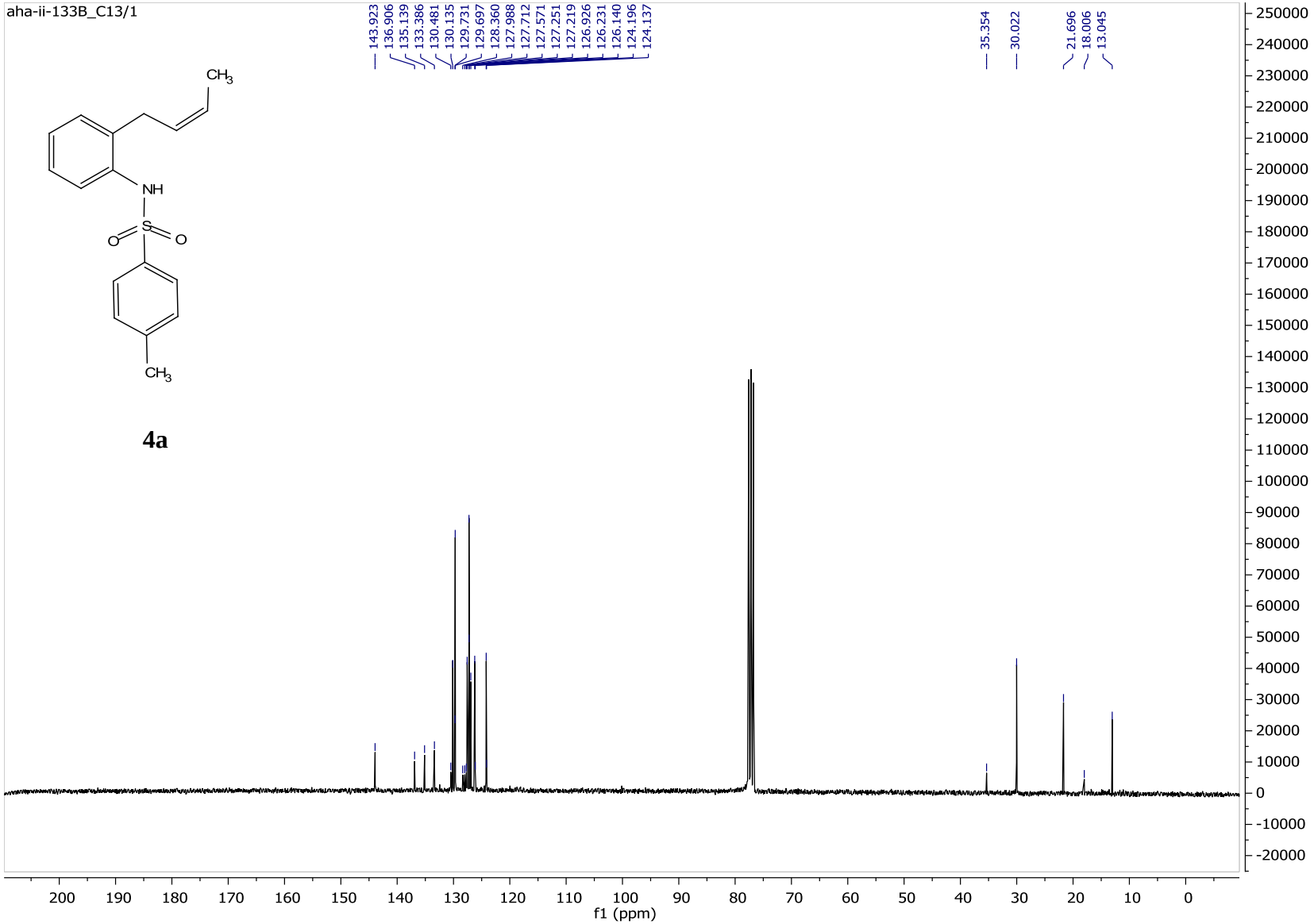
aha-ii-133B_C13/1
143.923
136.906
135.139
133.386
130.481
130.135
129.731
129.697
128.360
127.988
127.712
127.571
127.251
127.219
126.926
126.231
126.140
124.196
124.137
35.354
30.022
21.696
18.006
13.045
CH3
NH
S
O
O
CH3
f1 (ppm)

4a

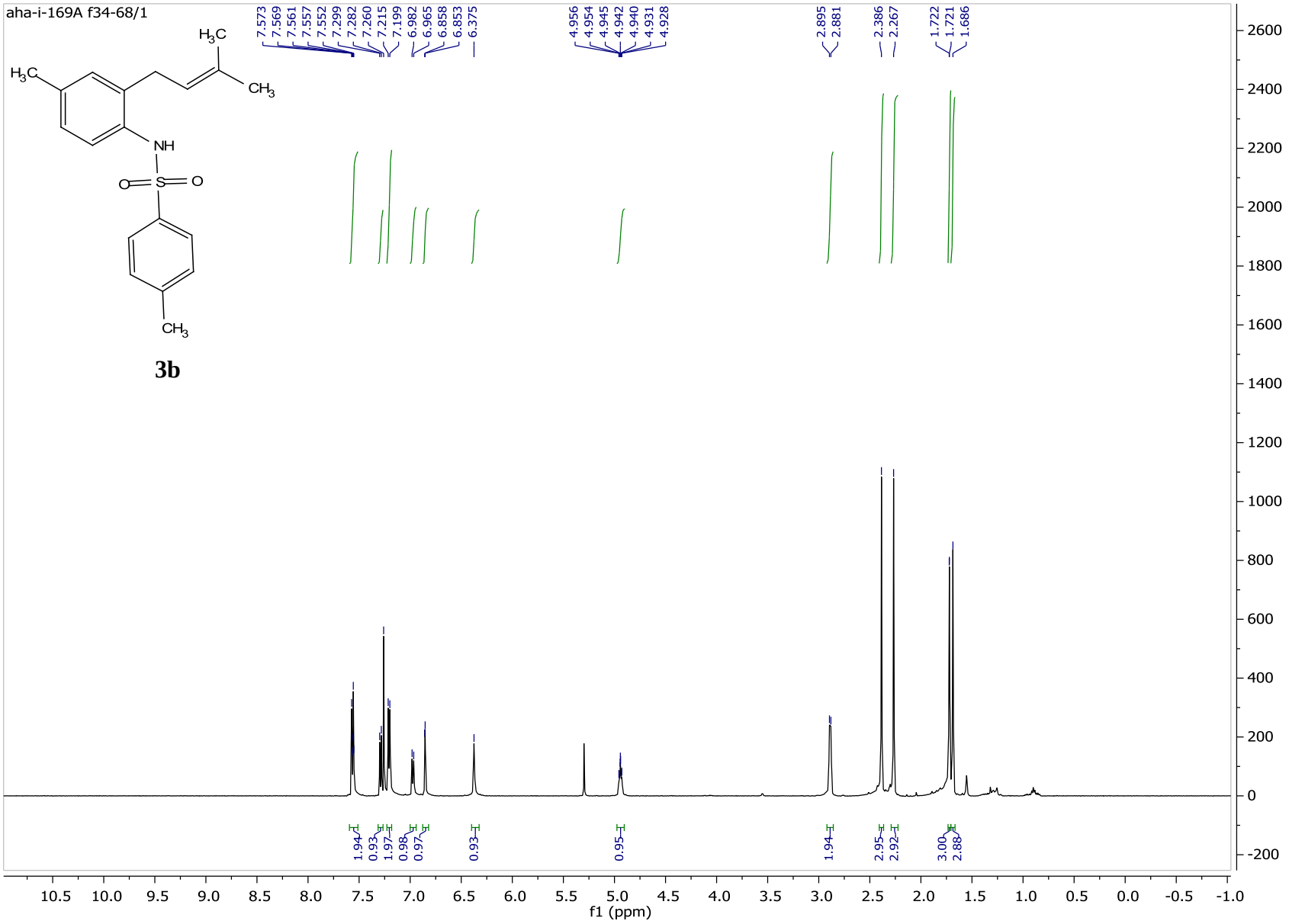
aha-i-169A f34-68/1
7.573
7.569
7.561
7.557
7.552
7.299
7.282
7.260
7.215
7.199
6.982
6.965
6.858
6.853
6.375
4.956
4.954
4.945
4.942
4.940
4.931
4.928
2.895
2.881
2.386
2.267
1.722
1.721
1.686
H3C
CH3
H3C
NH
O
S
O
CH3
3b
1.94
0.93
1.97
0.98
0.97
0.93
0.95
1.94
2.95
2.92
3.00
2.88
f1 (ppm)

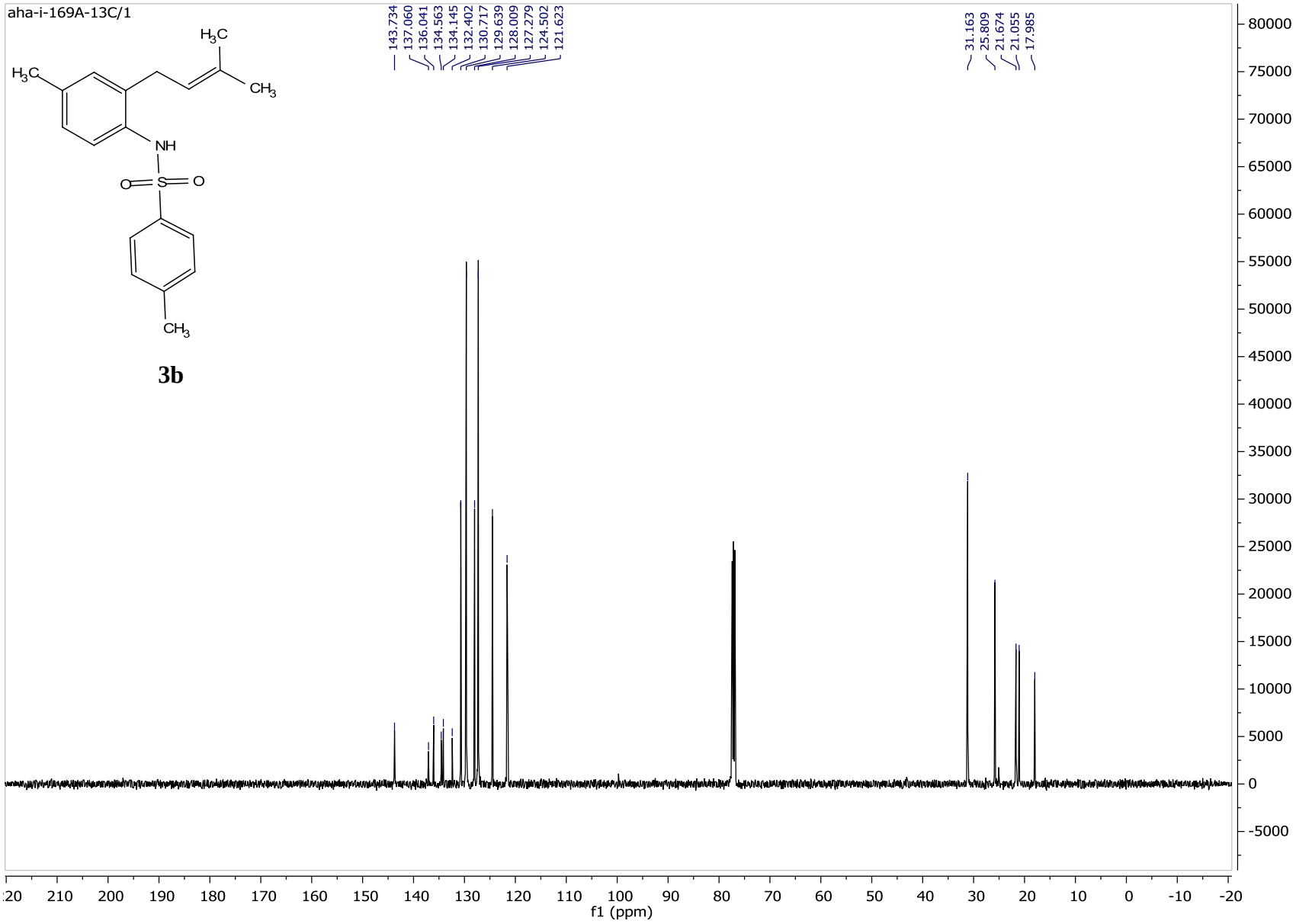
aha-i-169A-13C/1
143.734
137.060
136.041
134.563
134.145
132.402
130.717
129.639
128.009
127.279
124.502
121.623
31.163
25.809
21.674
21.055
17.985
f1 (ppm)

3b

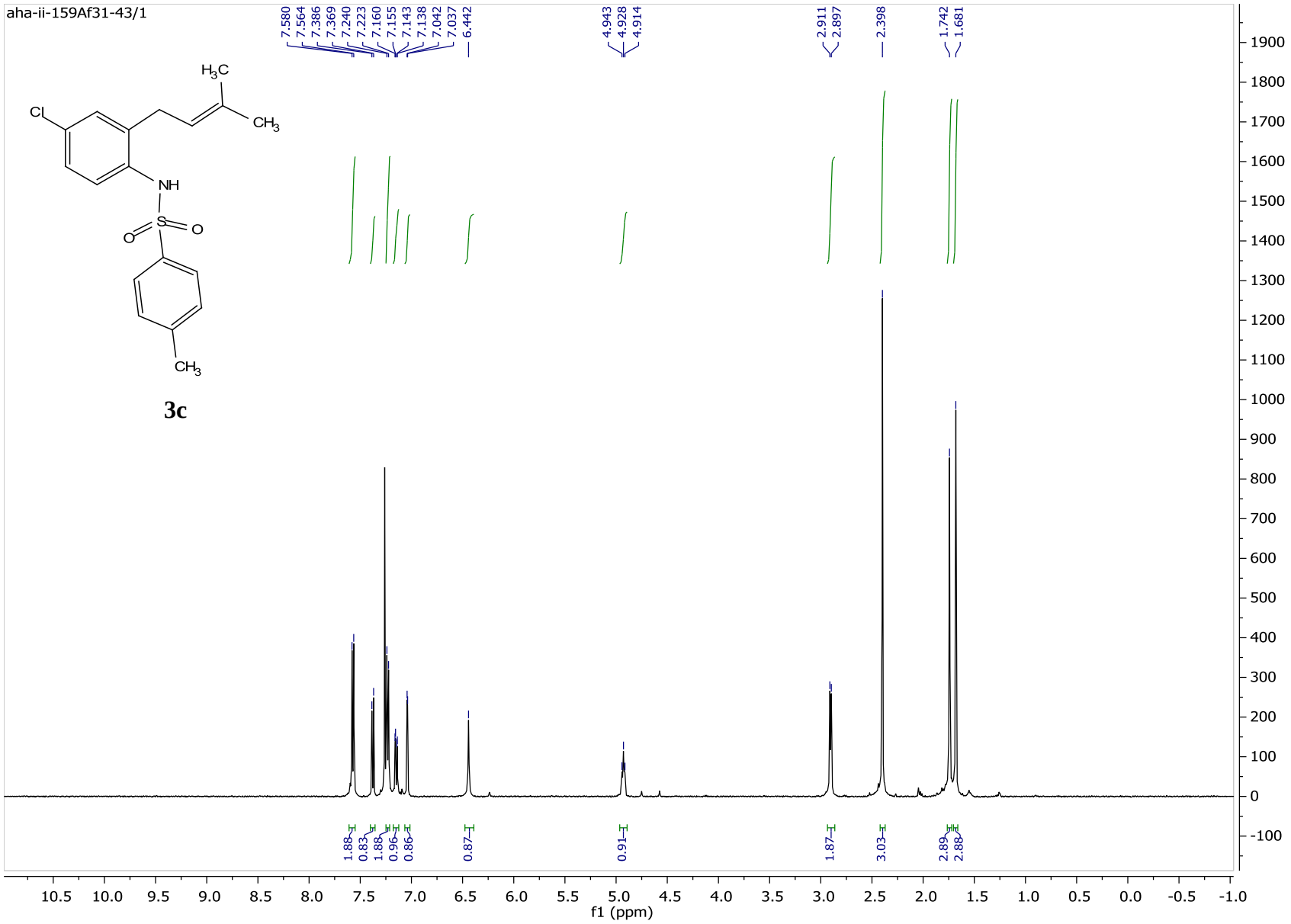
aha-ii-159Af31-43/1
7.580
7.564
7.386
7.369
7.240
7.223
7.160
7.155
7.143
7.138
7.042
7.037
6.442
4.943
4.928
4.914
2.911
2.897
2.398
1.742
1.681
Cl
H3C
CH3
NH
S
O
O
CH3
3c
1.88
0.83
1.88
0.96
0.86
0.87
0.91
1.87
3.03
2.89
2.88
f1 (ppm)

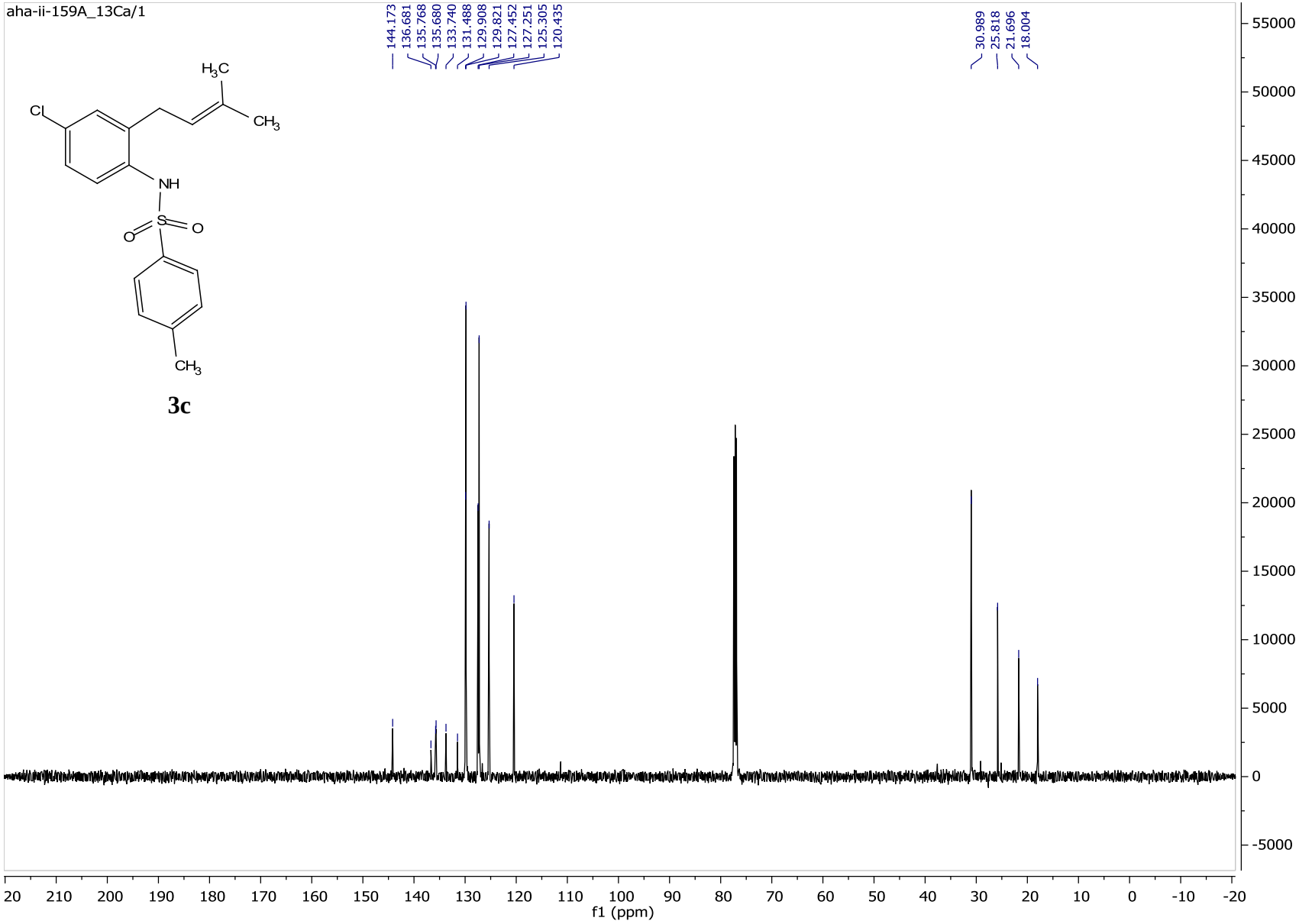
aha-ii-159A_13Ca/1
144.173
136.681
135.768
135.680
133.740
131.488
129.908
129.821
127.452
127.251
125.305
120.435
30.989
25.818
21.696
18.004
Cl
H3C
CH3
NH
S
O
O
CH3
3c
55000
50000
45000
40000
35000
30000
25000
20000
15000
10000
5000
0
-5000
20
210
200
190
180
170
160
150
140
130
120
110
100
90
80
70
60
50
40
30
20
10
0
-10
-20
f1 (ppm)

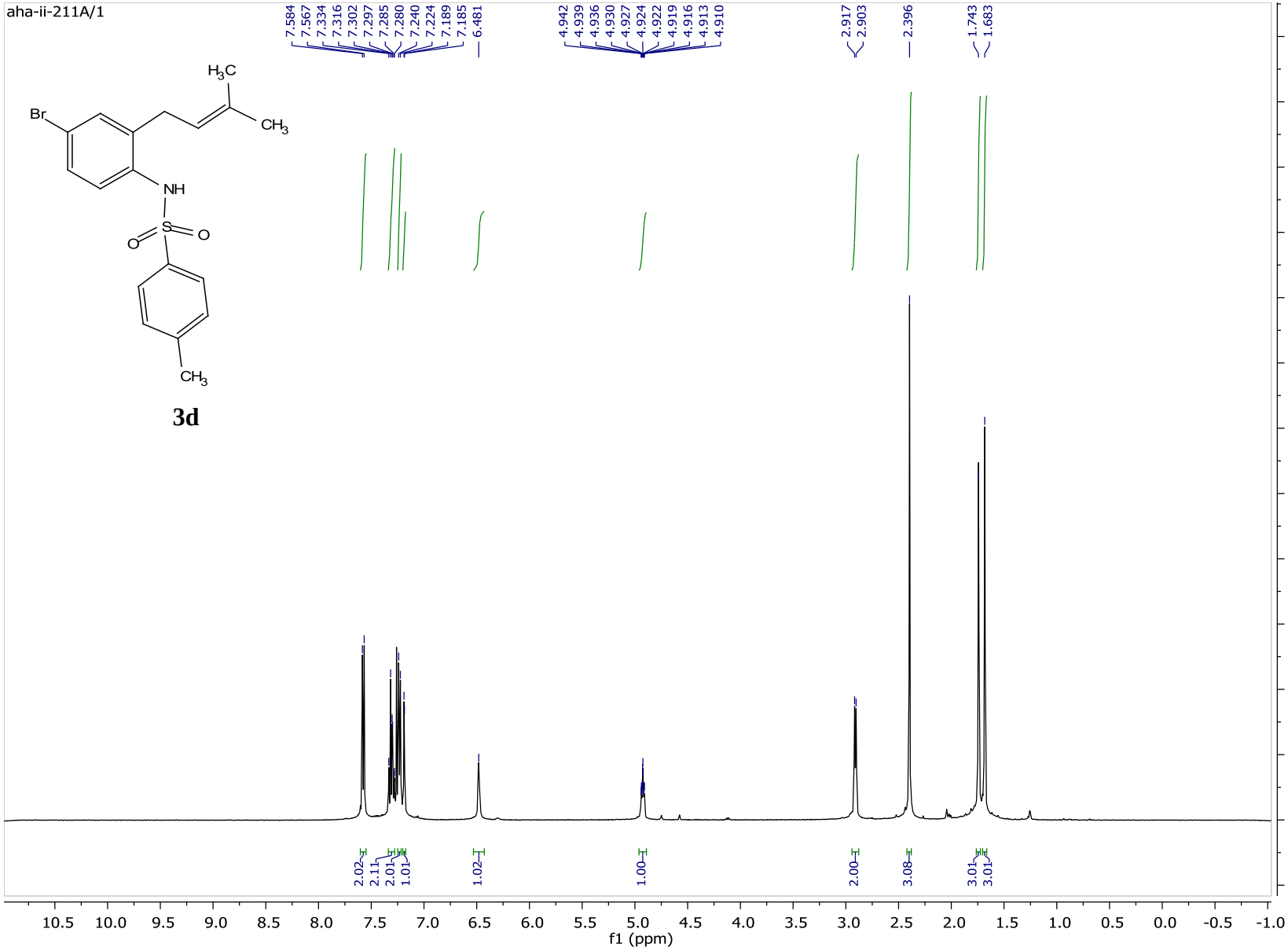
aha-ii-211A/1
7.584
7.567
7.334
7.316
7.302
7.297
7.285
7.280
7.240
7.224
7.189
7.185
6.481
4.942
4.939
4.936
4.930
4.927
4.924
4.922
4.919
4.916
4.913
4.910
2.917
2.903
2.396
1.743
1.683
Br
H3C
CH3
NH
S
O
O
CH3
2.02
2.11
2.01
1.01
1.02
1.00
2.00
3.08
3.01
3.01
f1 (ppm)

3d

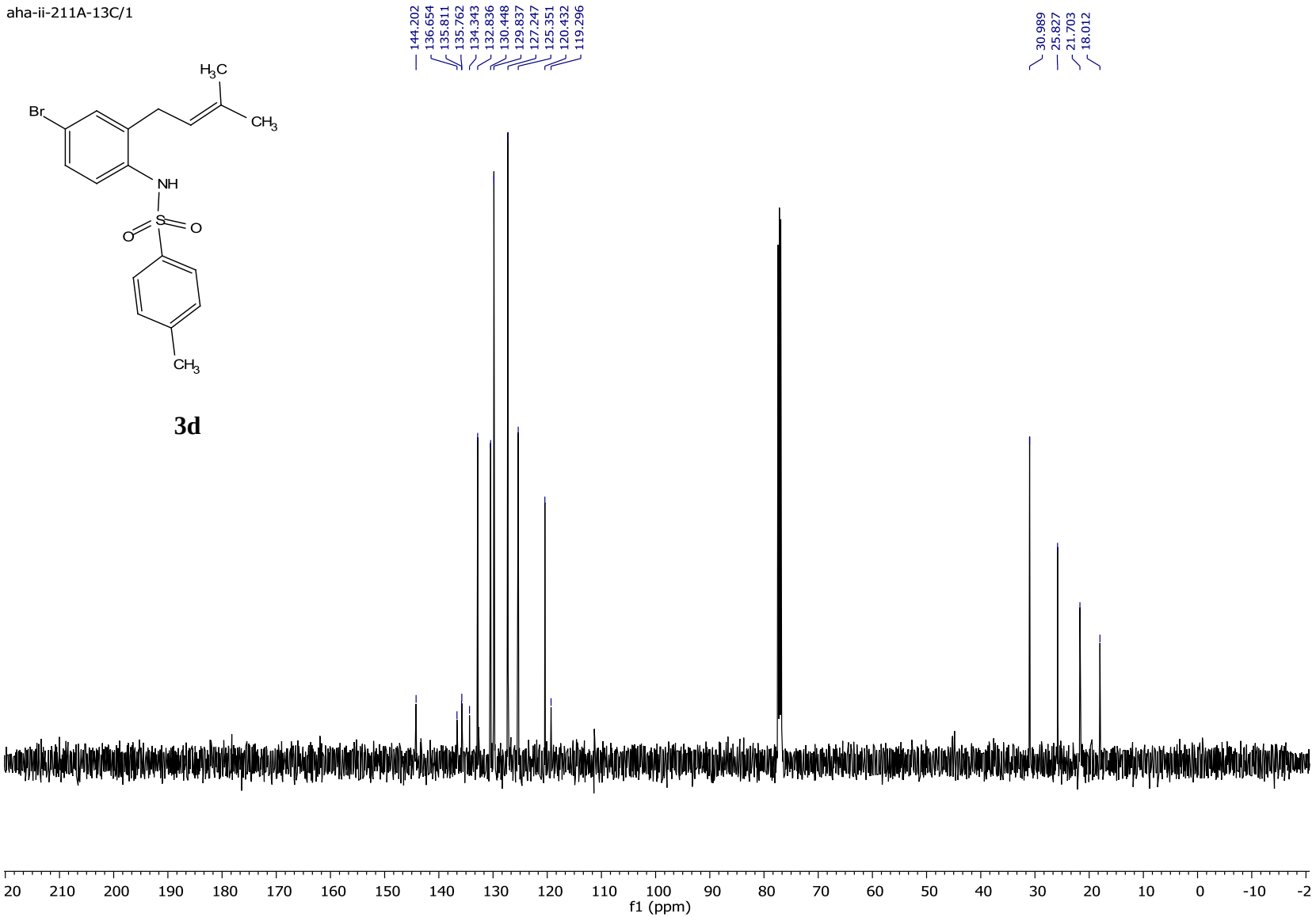
aha-ii-211A-13C/1
144.202
136.654
135.811
135.762
134.343
132.836
130.448
129.837
127.247
125.351
120.432
119.296
30.989
25.827
21.703
18.012
Br
H3C
CH3
NH
S
O
O
CH3
20
210
200
190
180
170
160
150
140
130
120
110
100
90
80
70
60
50
40
30
20
10
0
-10
-2
f1 (ppm)

3d

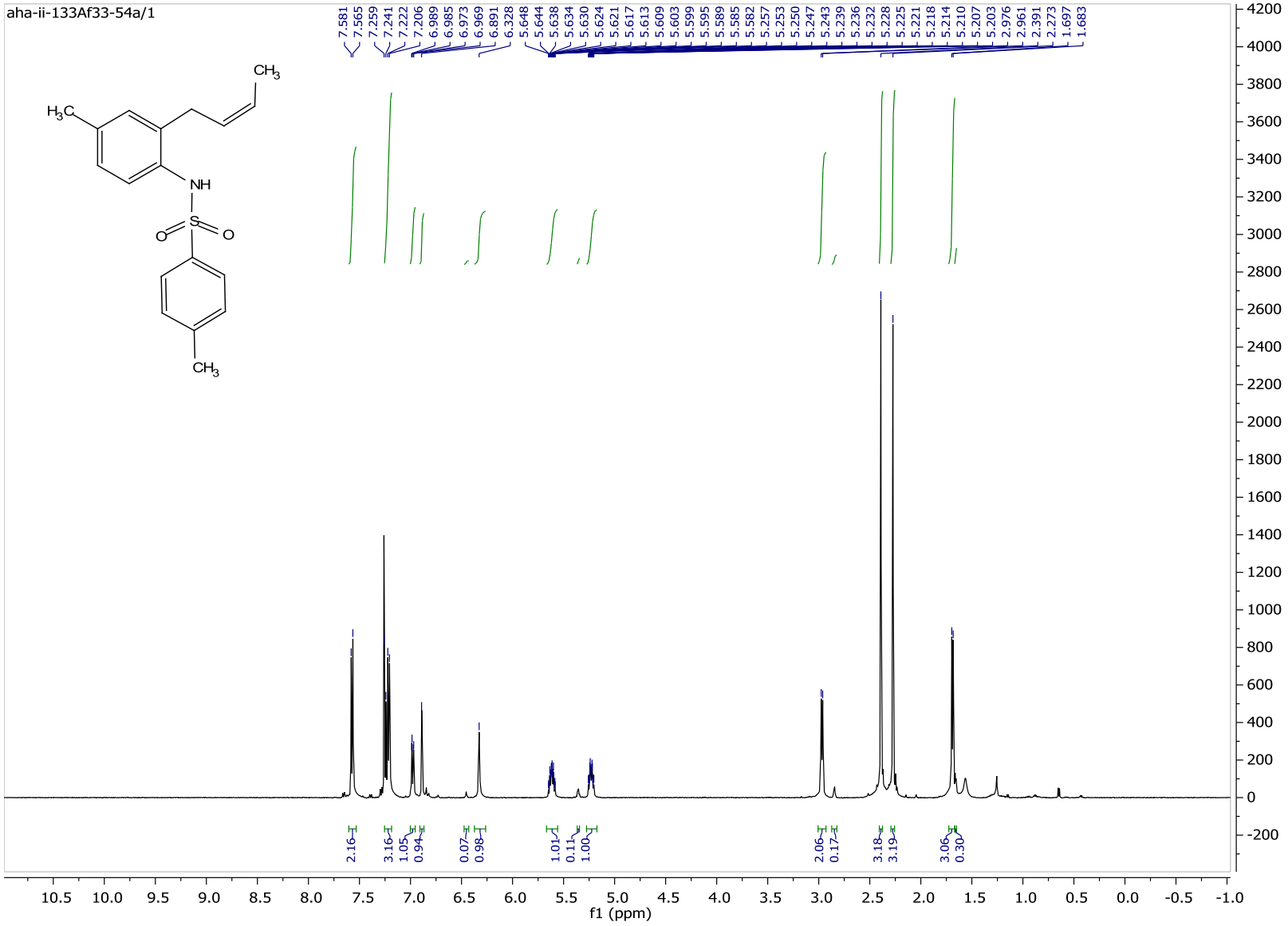
aha-ii-133Af33-54a/1
7.581
7.565
7.259
7.241
7.222
7.206
6.989
6.985
6.973
6.969
6.891
6.328
5.648
5.644
5.638
5.634
5.630
5.624
5.621
5.617
5.613
5.609
5.603
5.599
5.595
5.589
5.585
5.582
5.257
5.253
5.250
5.247
5.243
5.239
5.236
5.232
5.228
5.225
5.221
5.218
5.214
5.210
5.207
5.203
2.976
2.961
2.391
2.273
1.697
1.683
CH3
H3C
NH
S
O
O
CH3
2.16
3.16
1.05
0.94
0.07
0.98
1.01
0.11
1.00
2.06
0.17
3.18
3.19
3.06
0.30
f1 (ppm)

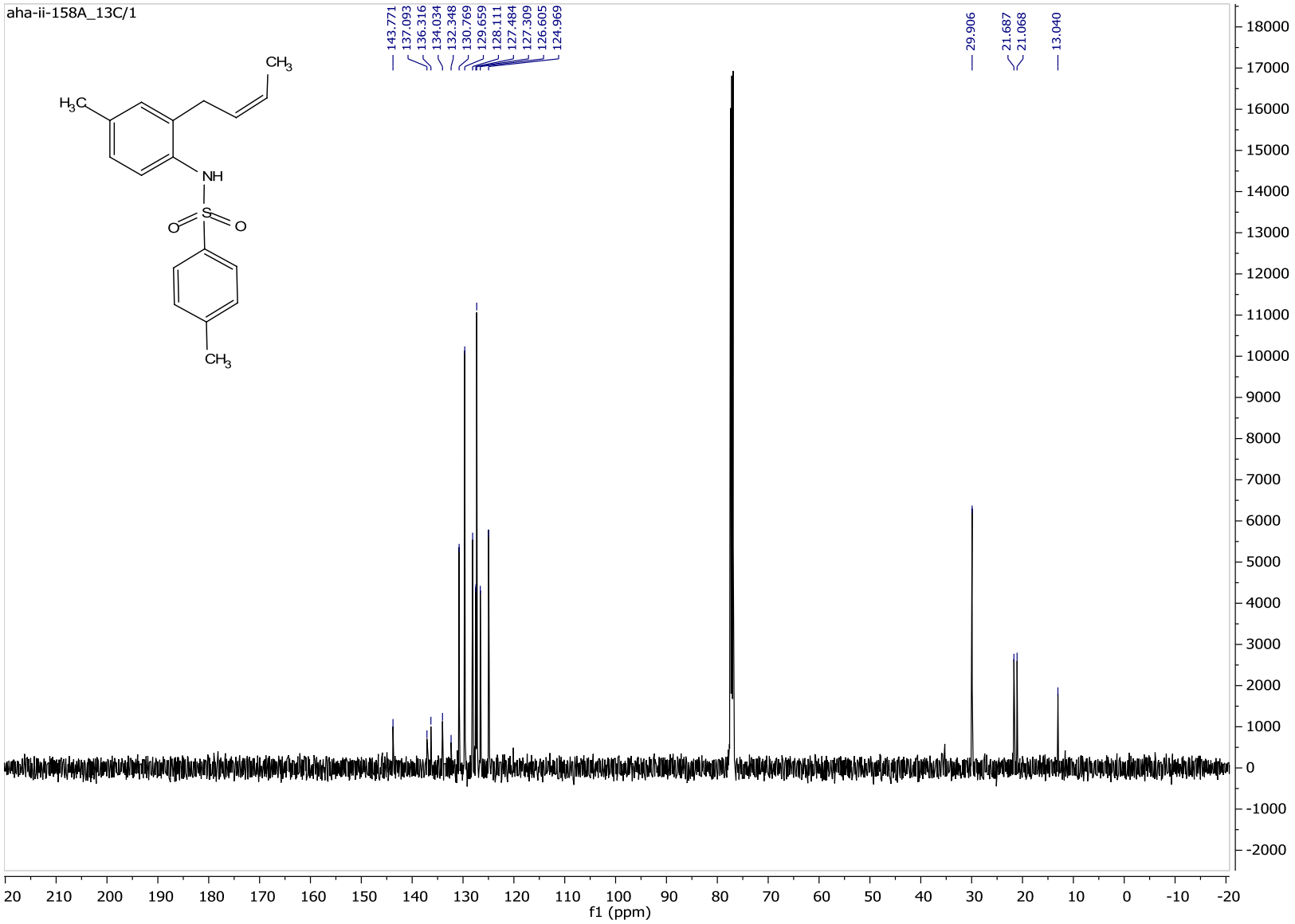
aha-ii-158A_13C/1
143.771
137.093
136.316
134.034
132.348
130.769
129.659
128.111
127.484
127.309
126.605
124.969
29.906
21.687
21.068
13.040
CH3
H3C
NH
S
O
O
CH3
f1 (ppm)

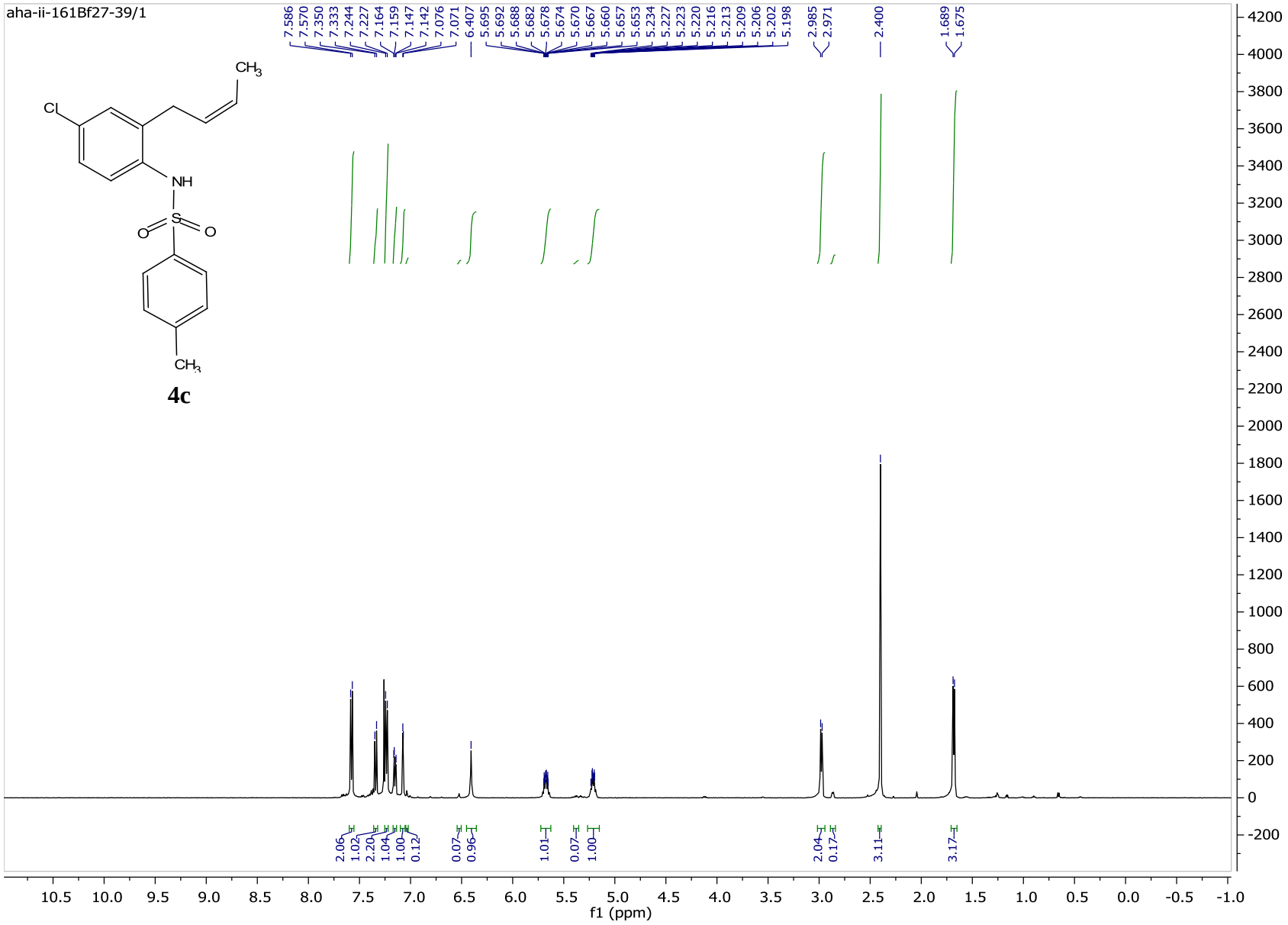
aha-ii-161Bf27-39/1
7.586
7.570
7.350
7.333
7.244
7.227
7.164
7.159
7.147
7.142
7.076
7.071
6.407
5.695
5.692
5.688
5.682
5.678
5.674
5.670
5.667
5.660
5.657
5.653
5.234
5.227
5.223
5.220
5.216
5.213
5.209
5.206
5.202
5.198
2.985
2.971
2.400
1.689
1.675
Cl
NH
S
O
O
CH3
CH3
4c
2.06
1.02
2.20
1.04
1.00
0.12
0.07
0.96
1.01
0.07
1.00
2.04
0.17
3.11
3.17
f1 (ppm)

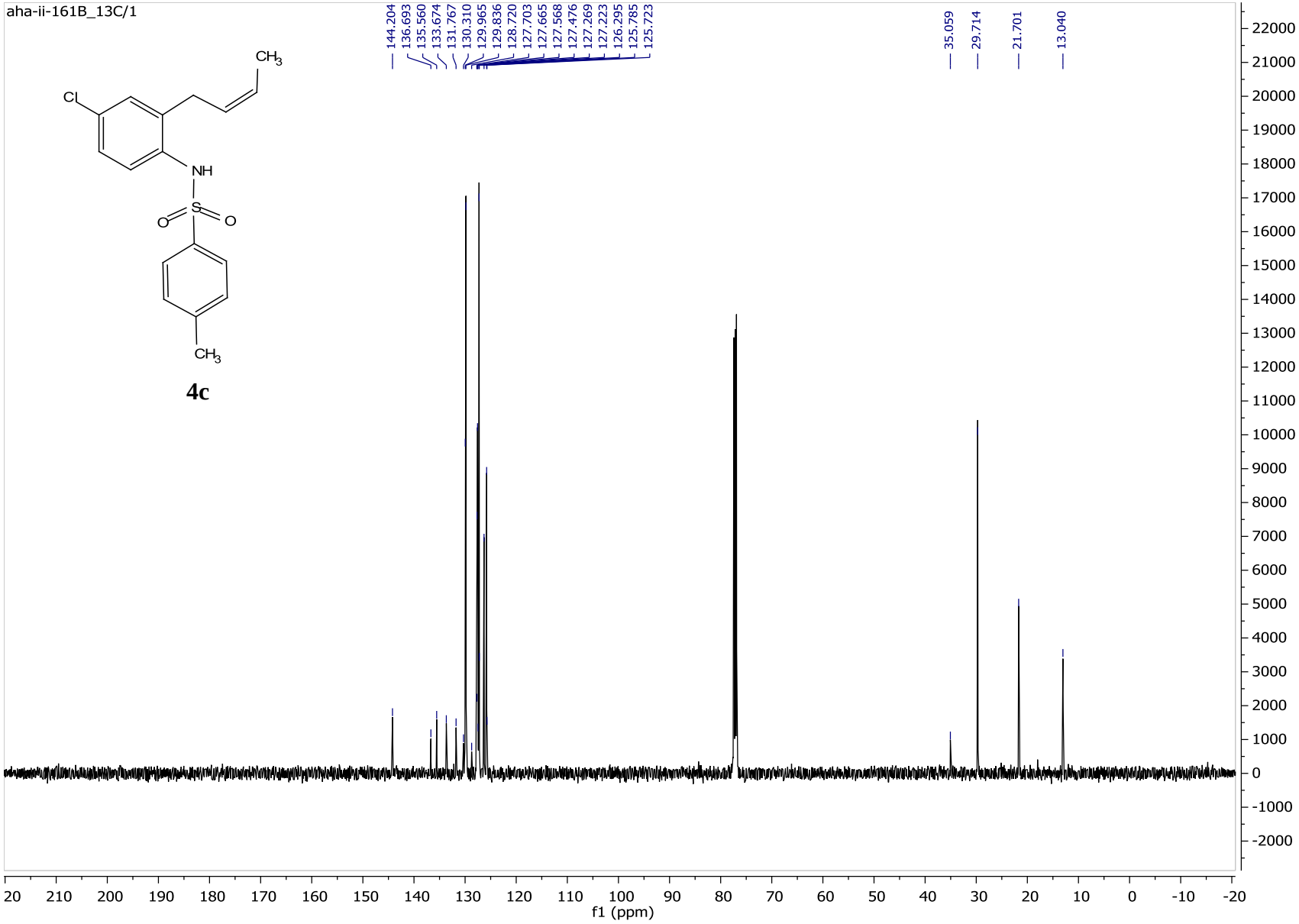
aha-ii-161B_13C/1
144.204
136.693
135.560
133.674
131.767
130.310
129.965
129.836
128.720
127.703
127.665
127.568
127.476
127.269
127.223
126.295
125.785
125.723
35.059
29.714
21.701
13.040
Cl
CH3
NH
S
O
O
CH3
4c
f1 (ppm)

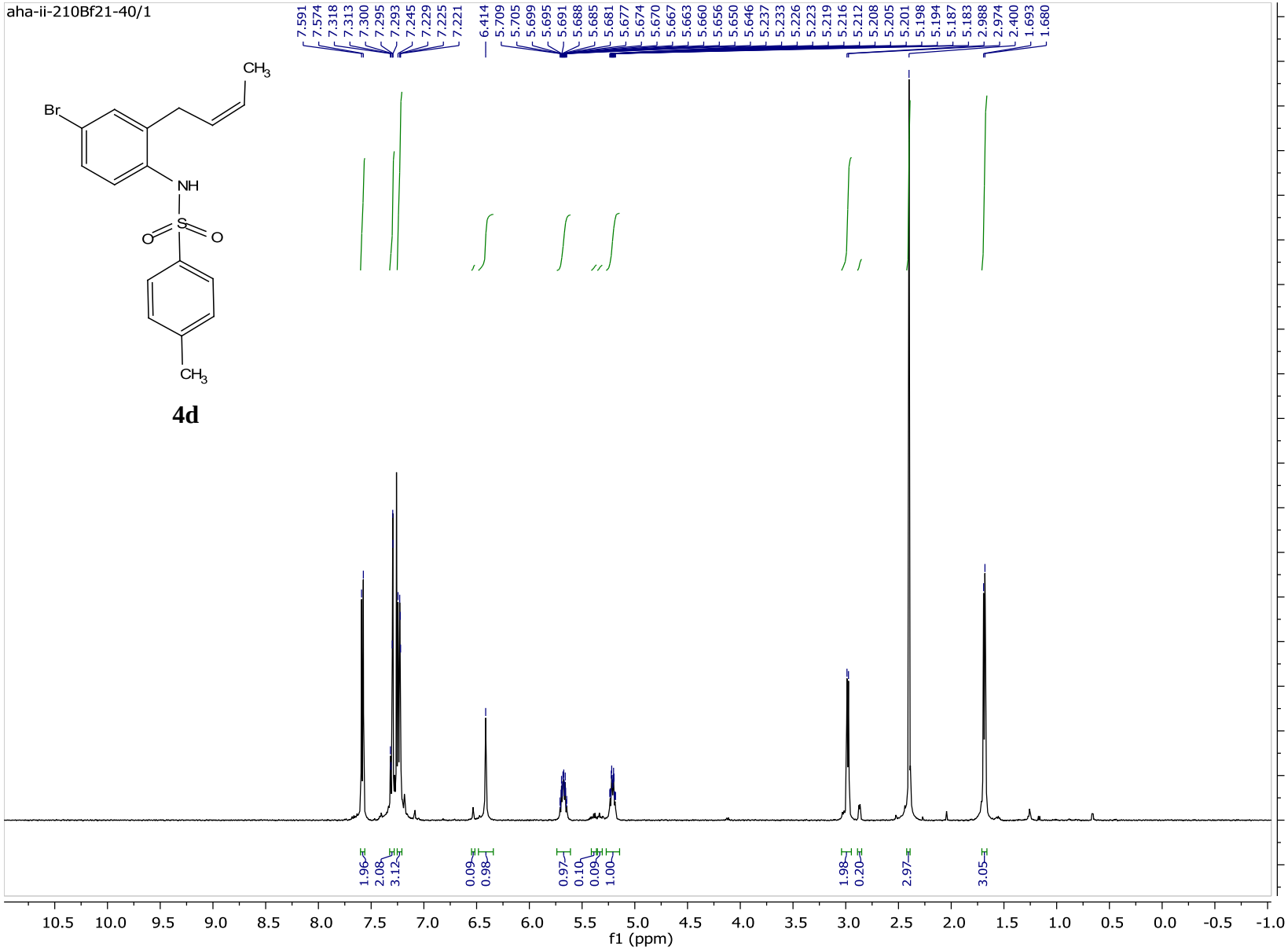
aha-ii-210Bf21-40/1
7.591
7.574
7.318
7.313
7.300
7.295
7.293
7.245
7.229
7.225
7.221
6.414
5.709
5.705
5.699
5.695
5.691
5.688
5.685
5.681
5.677
5.674
5.670
5.667
5.663
5.660
5.656
5.650
5.646
5.237
5.233
5.226
5.223
5.219
5.216
5.212
5.208
5.205
5.201
5.198
5.194
5.187
5.183
2.988
2.974
2.400
1.693
1.680
Br
NH
S
O
O
CH3
CH3
4d
1.96
2.08
3.12
0.09
0.98
0.97
0.10
0.09
1.00
1.98
0.20
2.97
3.05
f1 (ppm)

aha-ii-210B-13C/1

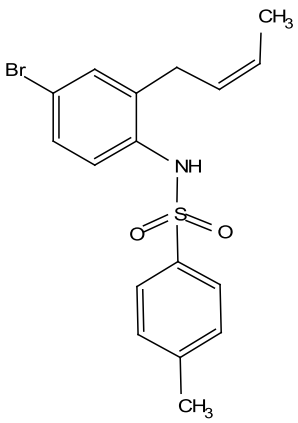

4d

144.217
136.647
135.720
134.233
133.207
132.860
130.655
130.528
129.840
127.673
127.455
127.251
127.205
126.275
125.875
125.794
119.595

34.979
29.631
21.692
13.030

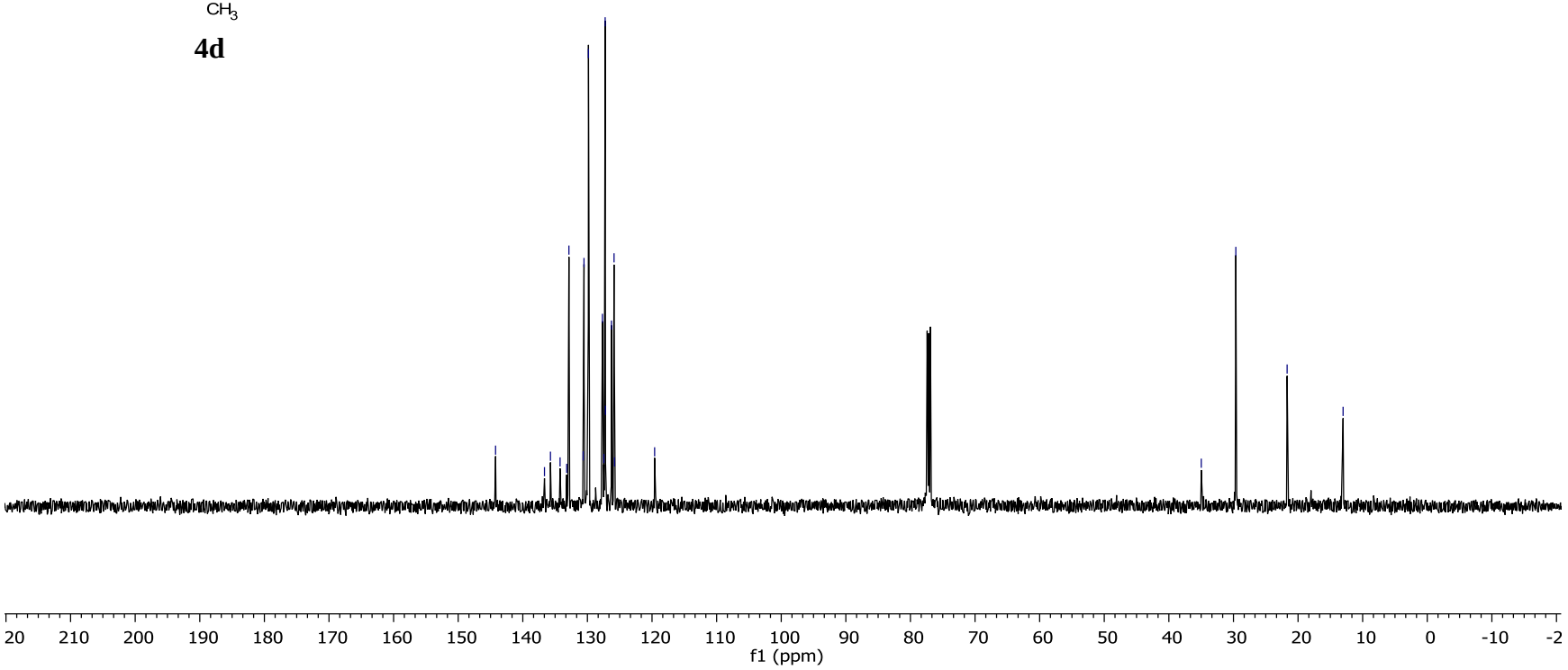

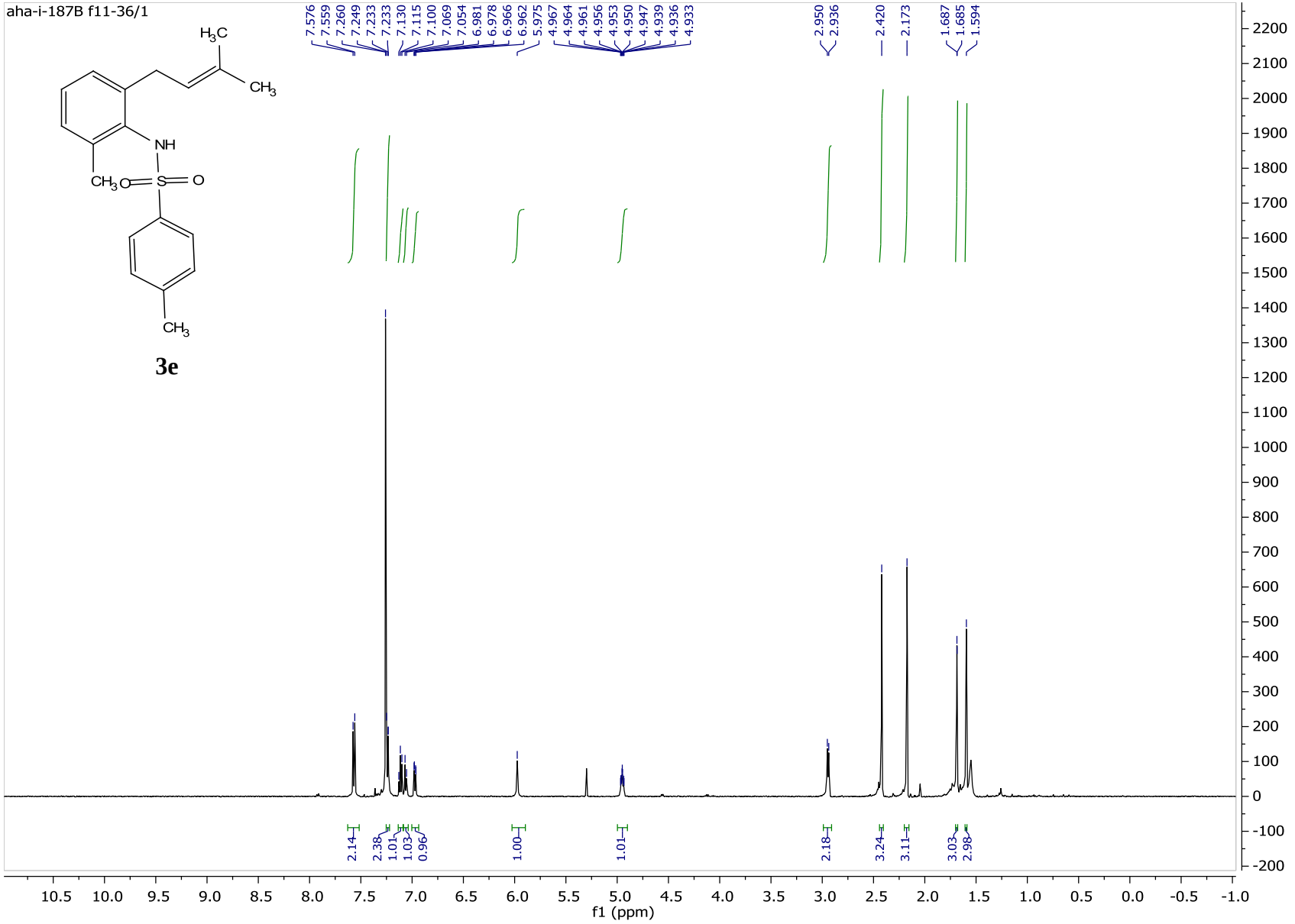
aha-i-187B f11-36/1
7.576
7.559
7.260
7.249
7.233
7.233
7.130
7.115
7.100
7.069
7.054
6.981
6.978
6.966
6.962
5.975
4.967
4.964
4.961
4.956
4.953
4.950
4.947
4.939
4.936
4.933
2.950
2.936
2.420
2.173
1.687
1.685
1.594
2.14
2.38
1.01
1.03
0.96
1.00
1.01
2.18
3.24
3.11
3.03
2.98
f1 (ppm)

3e

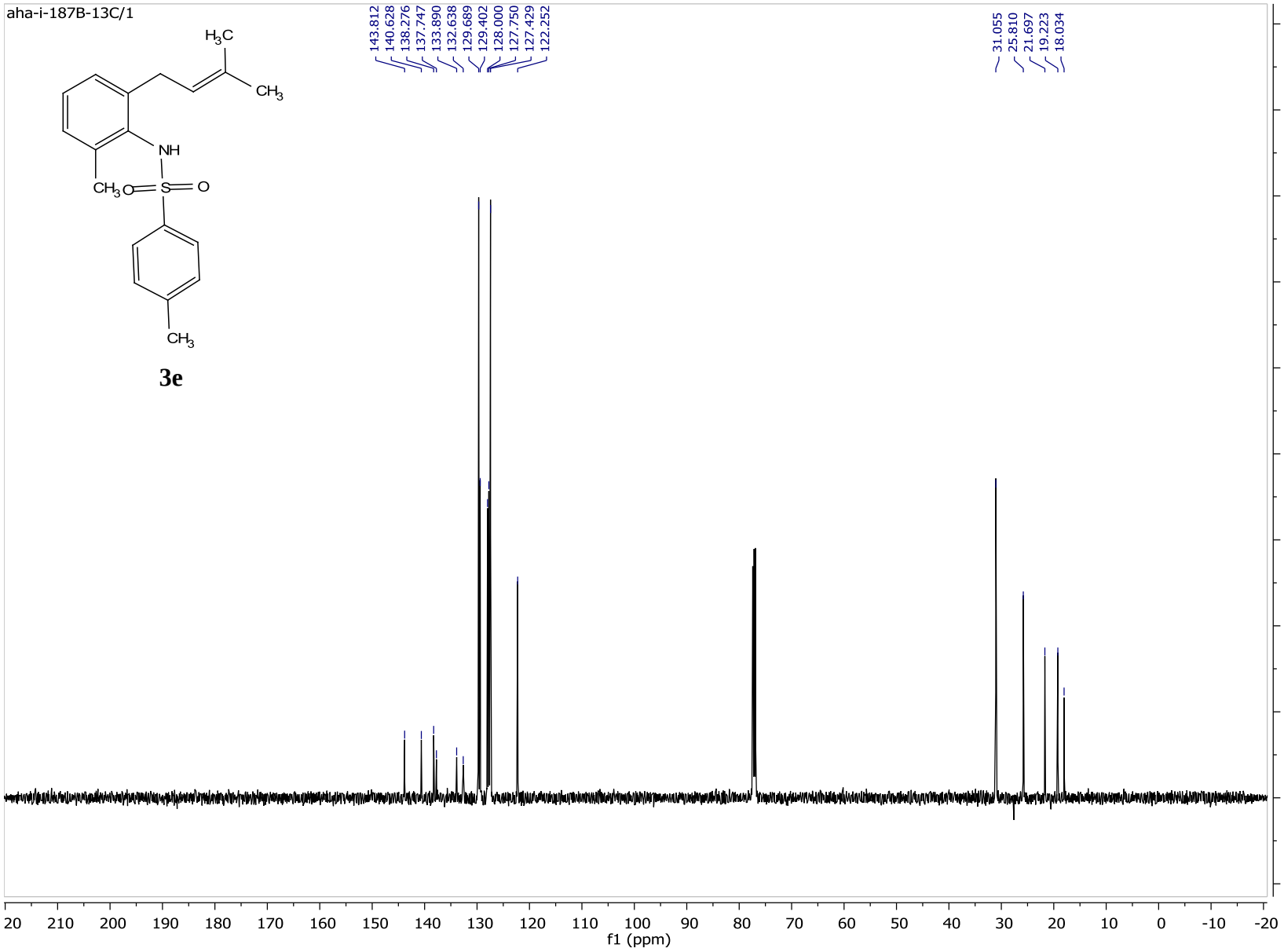
aha-i-187B-13C/1
143.812
140.628
138.276
137.747
133.890
132.638
129.689
129.402
128.000
127.750
127.429
122.252
31.055
25.810
21.697
19.223
18.034
45000
40000
35000
30000
25000
20000
15000
10000
5000
0
-5000
20
210
200
190
180
170
160
150
140
130
120
110
100
90
80
70
60
50
40
30
20
10
0
-10
-20
f1 (ppm)

3e

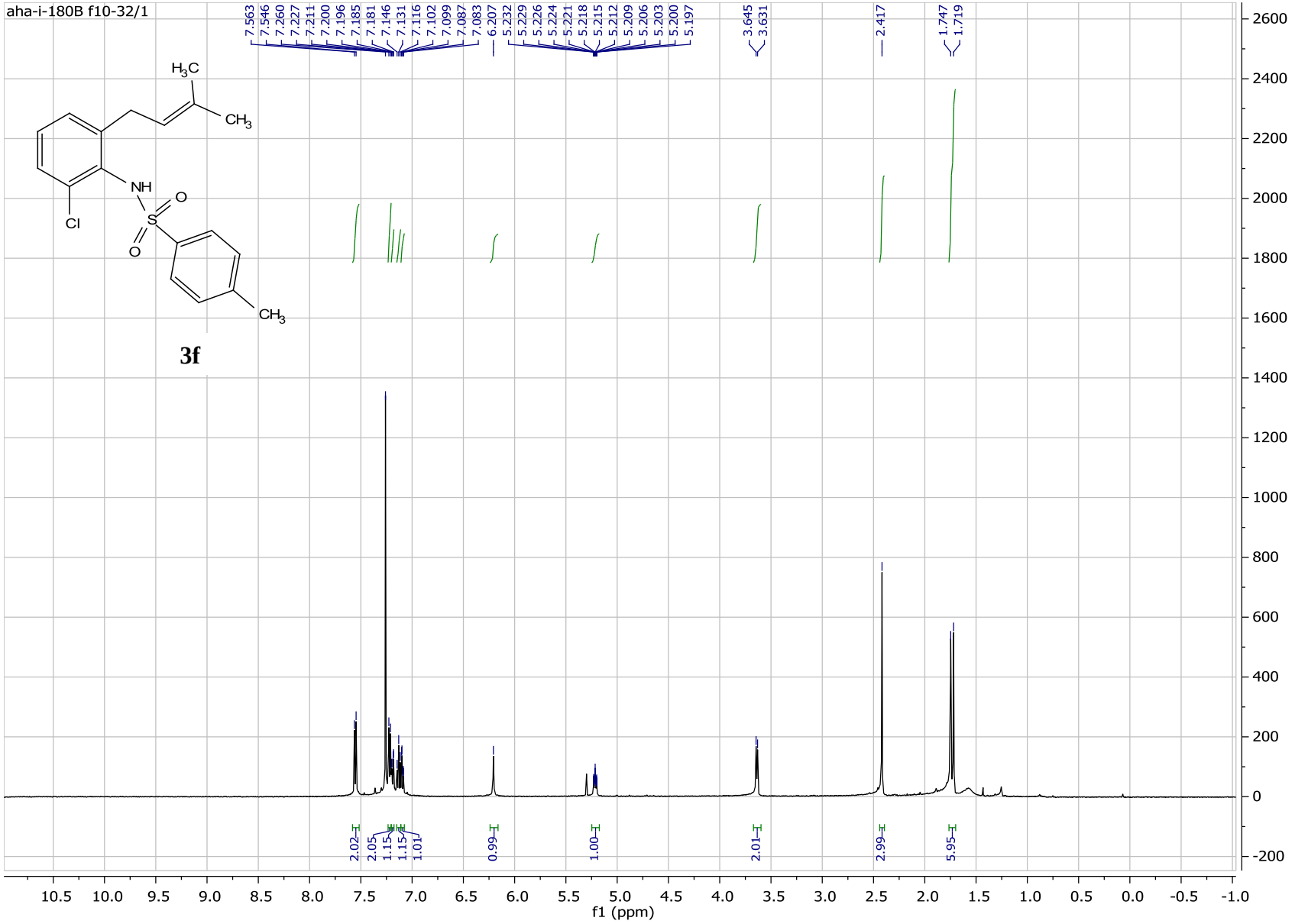
aha-i-180B f10-32/1
7.563
7.546
7.260
7.227
7.211
7.200
7.196
7.185
7.181
7.146
7.131
7.116
7.102
7.099
7.087
7.083
6.207
5.232
5.229
5.226
5.224
5.221
5.218
5.215
5.212
5.209
5.206
5.203
5.200
5.197
3.645
3.631
2.417
1.747
1.719
H3C
CH3
NH
O
S
O
Cl
CH3
3f
2.02
2.05
1.15
1.15
1.01
0.99
1.00
2.01
2.99
5.95
f1 (ppm)

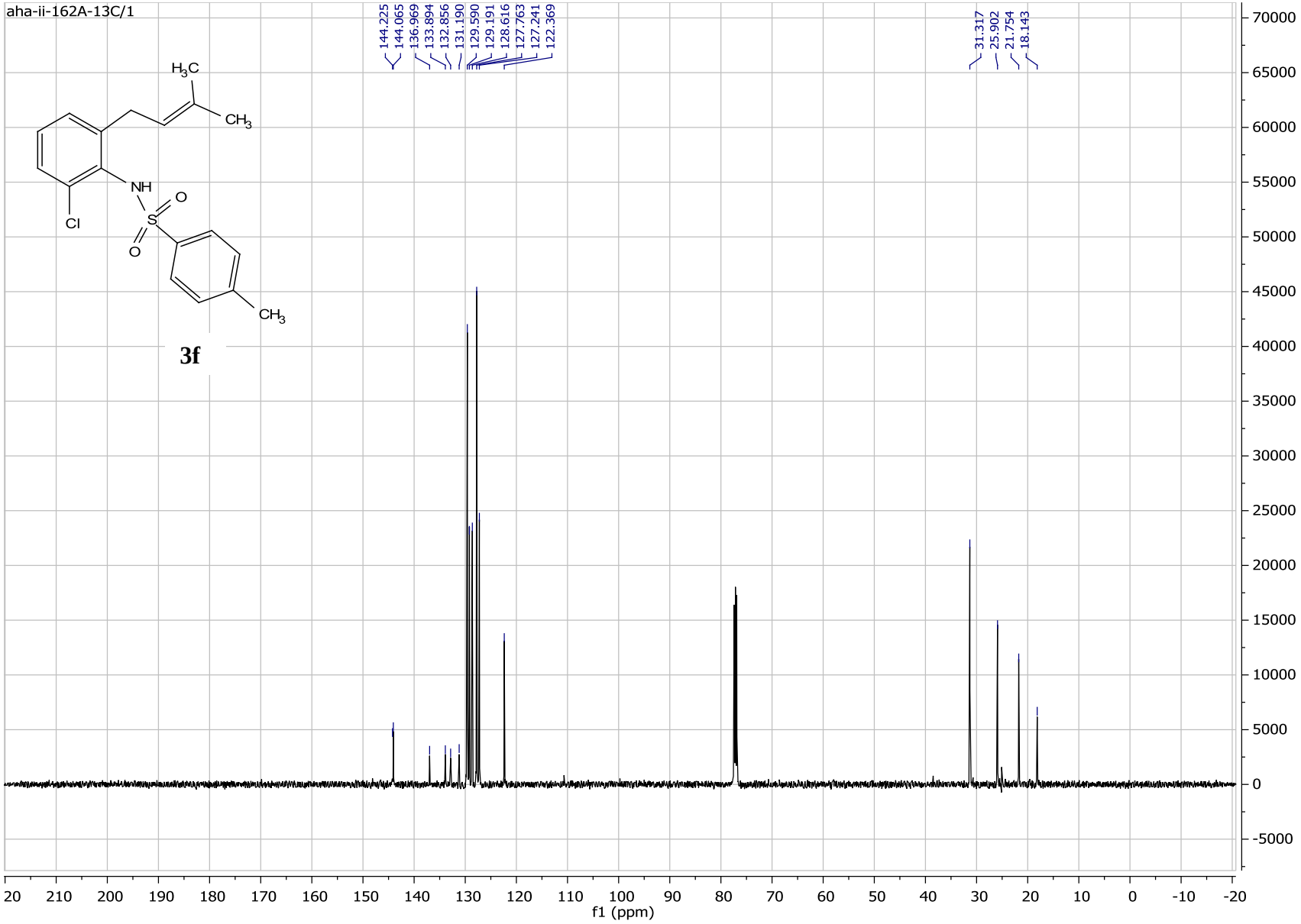
aha-ii-162A-13C/1
144.225
144.065
136.969
133.894
132.856
131.190
129.590
129.191
128.616
127.763
127.241
122.369
31.317
25.902
21.754
18.143
H3C
CH3
NH
O
S
O
Cl
CH3
3f
f1 (ppm)

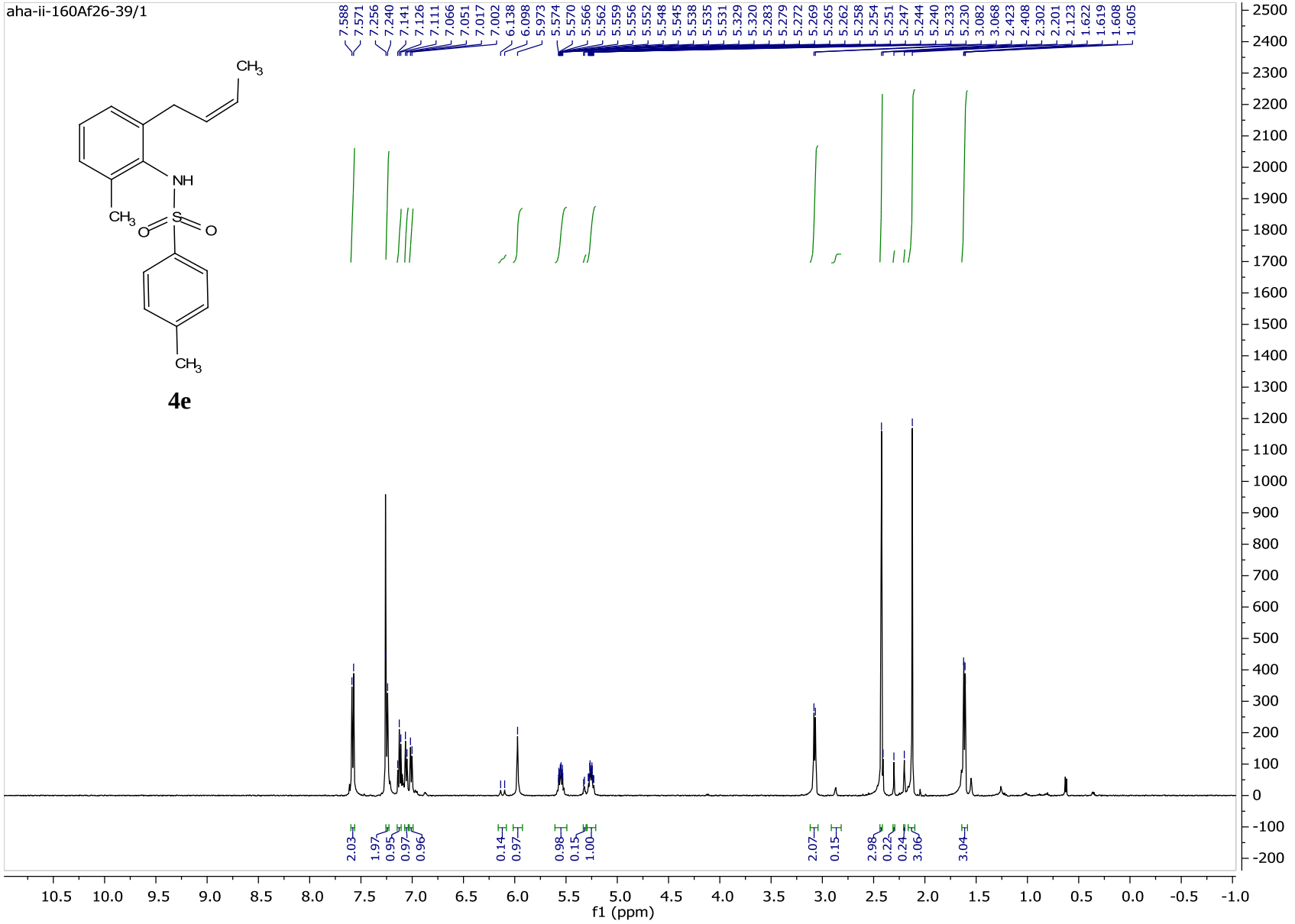
aha-ii-160Af26-39/1
7.588
7.571
7.256
7.240
7.141
7.126
7.111
7.066
7.051
7.017
7.002
6.138
6.098
5.973
5.574
5.570
5.566
5.562
5.559
5.556
5.552
5.548
5.545
5.538
5.535
5.531
5.329
5.320
5.283
5.279
5.272
5.269
5.265
5.262
5.258
5.254
5.251
5.247
5.244
5.240
5.233
5.230
3.082
3.068
2.423
2.408
2.302
2.201
2.123
1.622
1.619
1.608
1.605
CH3
NH
CH3
S
O
O
CH3
4e
2.03
1.97
0.95
0.97
0.96
0.14
0.97
0.98
0.15
1.00
2.07
0.15
2.98
0.22
0.24
3.06
3.04
f1 (ppm)

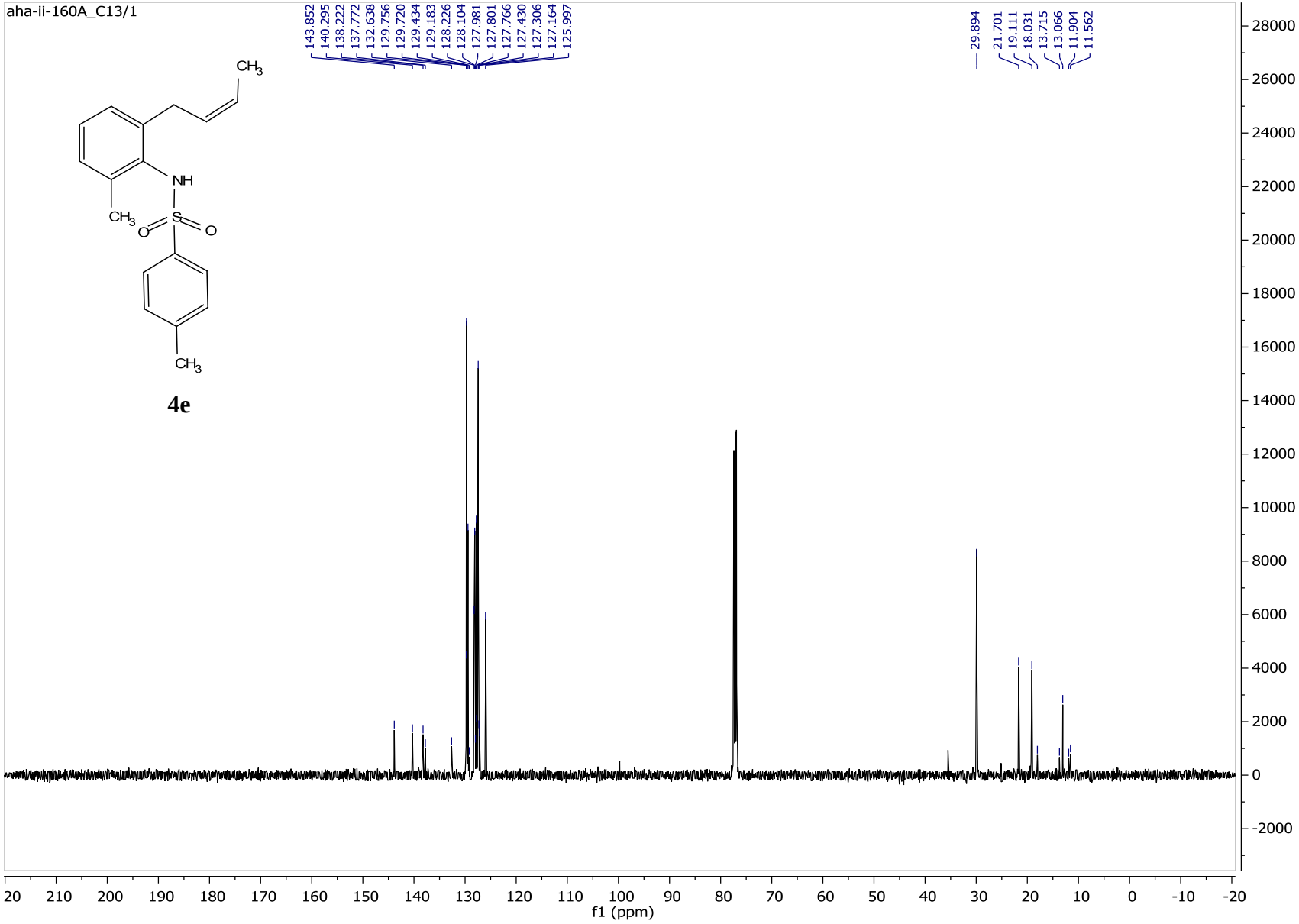
aha-ii-160A_C13/1
143.852
140.295
138.222
137.772
132.638
129.756
129.720
129.434
129.183
128.226
128.104
127.981
127.801
127.766
127.430
127.306
127.164
125.997
29.894
21.701
19.111
18.031
13.715
13.066
11.904
11.562
CH3
NH
CH3
S
O
O
CH3
4e
f1 (ppm)

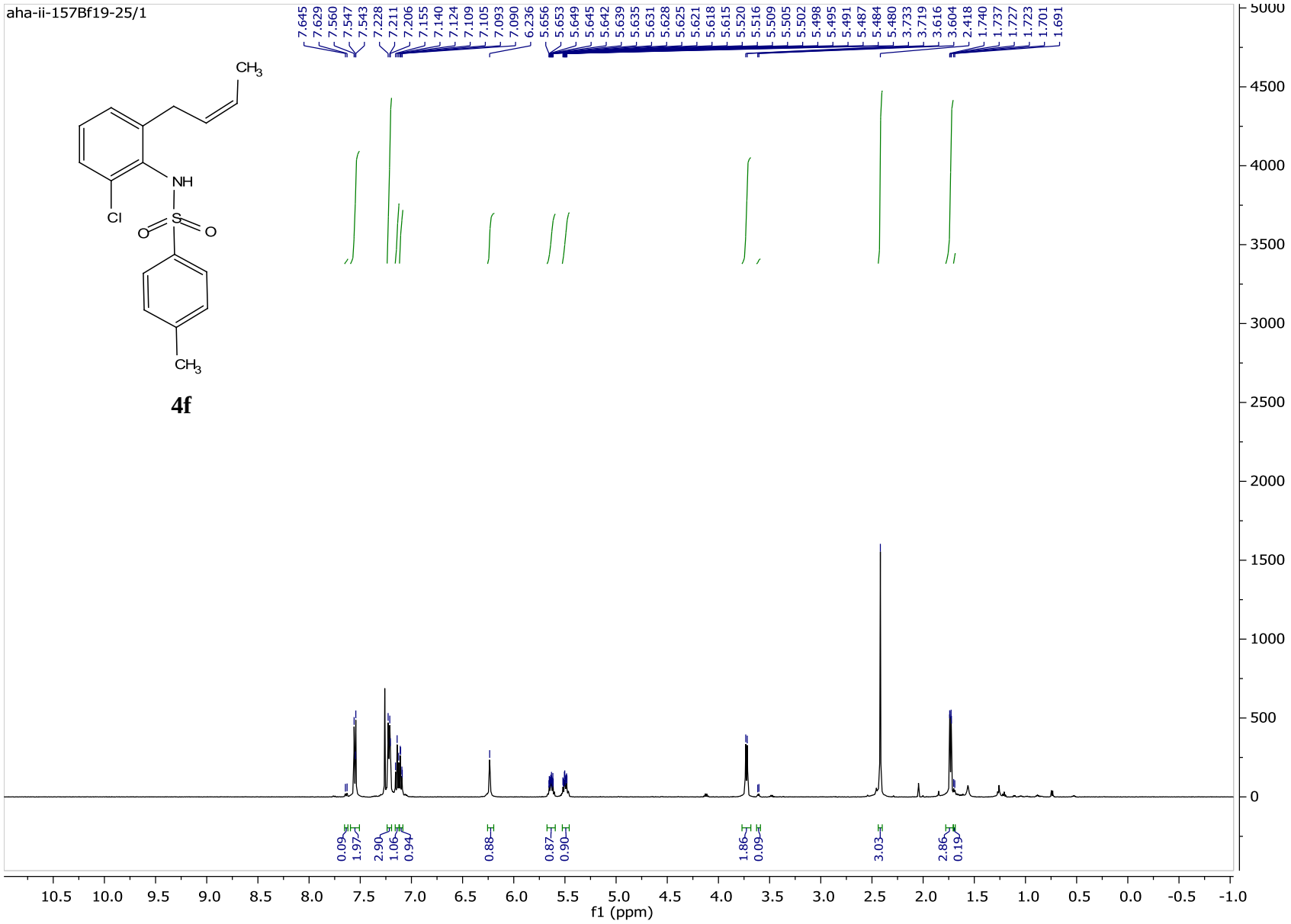
aha-ii-157Bf19-25/1
7.645
7.629
7.560
7.547
7.543
7.228
7.211
7.206
7.155
7.140
7.124
7.109
7.105
7.093
7.090
6.236
5.656
5.653
5.649
5.645
5.642
5.639
5.635
5.631
5.628
5.625
5.621
5.618
5.615
5.520
5.516
5.509
5.505
5.502
5.498
5.495
5.491
5.487
5.484
5.480
3.733
3.719
3.616
3.604
2.418
1.740
1.737
1.727
1.723
1.701
1.691
CH3
NH
Cl
S
O
O
CH3
4f
0.09
1.97
2.90
1.06
0.94
0.88
0.87
0.90
1.86
0.09
3.03
2.86
0.19
f1 (ppm)

aha-ii-121A_13Cx.1.fid

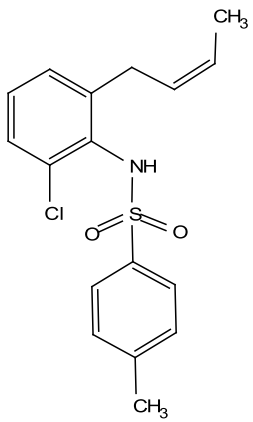

4f

144.116
143.641
136.794
132.824
131.217
129.604
129.182
128.667
128.265
127.737
127.329
126.097
30.113
21.766
13.151

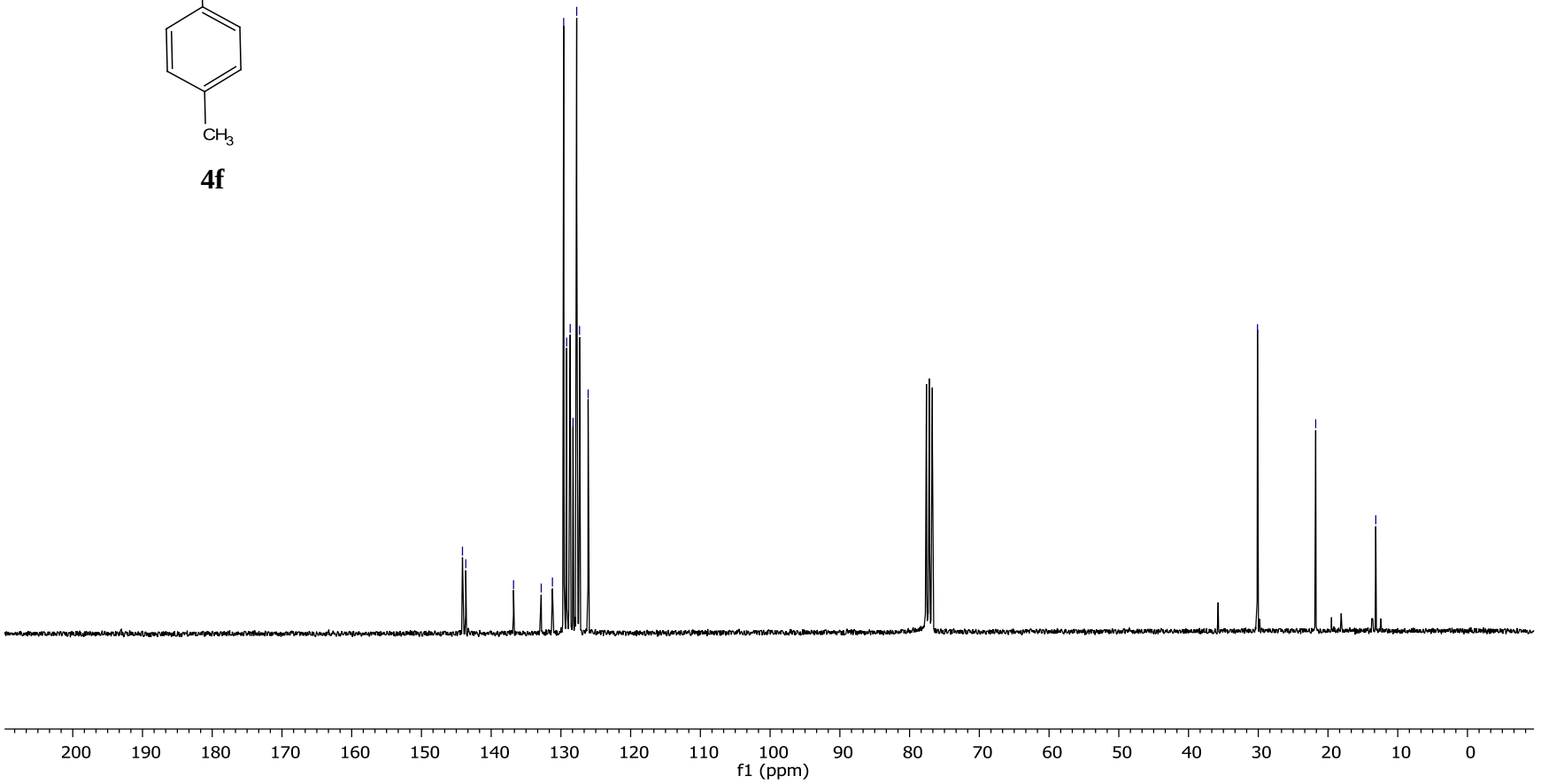

aha-iii-140Af12-36a.1.fid

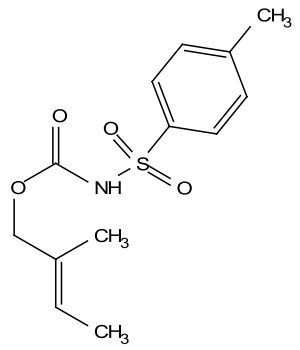

9

aha-iii-140A_13Cx.1.fid

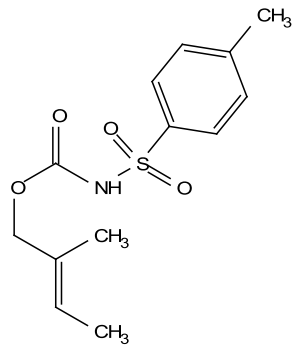

9

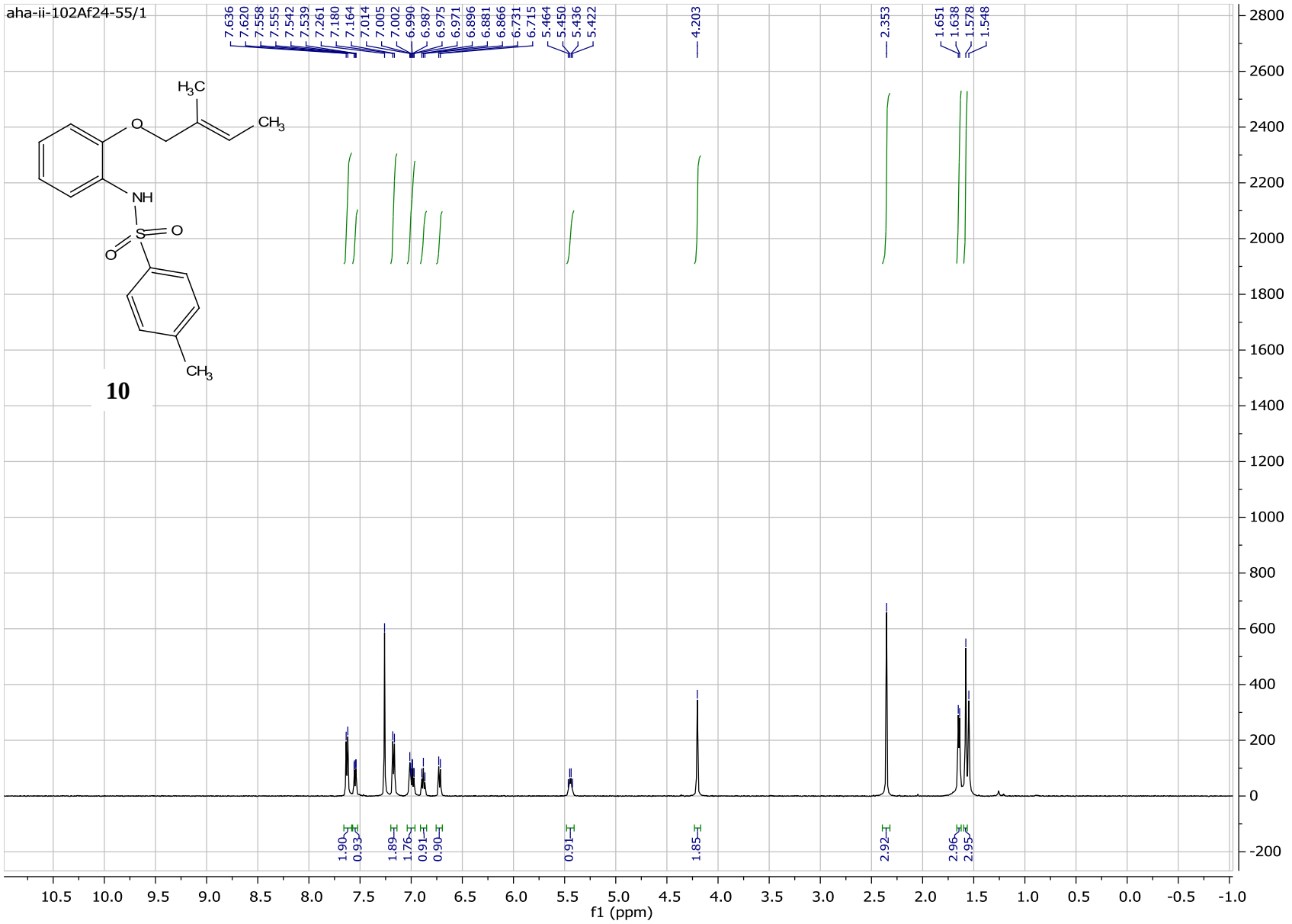
aha-ii-102Af24-55/1
7.636
7.620
7.558
7.555
7.542
7.539
7.261
7.180
7.164
7.014
7.005
7.002
6.990
6.987
6.975
6.971
6.896
6.881
6.866
6.731
6.715
5.464
5.450
5.436
5.422
4.203
2.353
1.651
1.638
1.578
1.548
H3C
CH3
O
NH
S
O
O
CH3
10
1.90
0.93
1.89
1.76
0.91
0.90
0.91
1.85
2.92
2.96
2.95
f1 (ppm)

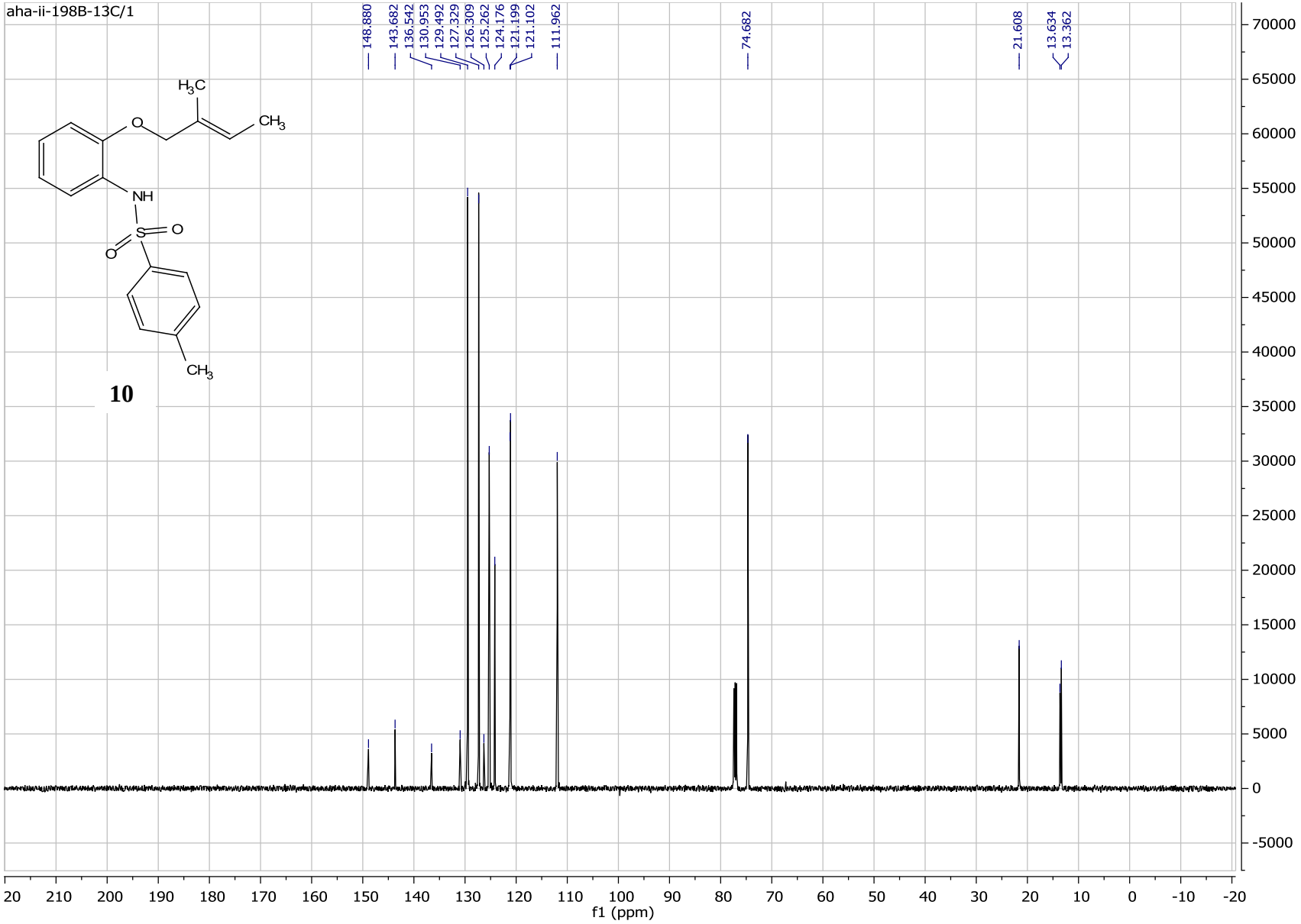
aha-ii-198B-13C/1
148.880
143.682
136.542
130.953
129.492
127.329
126.309
125.262
124.176
121.199
121.102
111.962
74.682
21.608
13.634
13.362
H3C
O
CH3
NH
S
O
O
CH3
10
f1 (ppm)

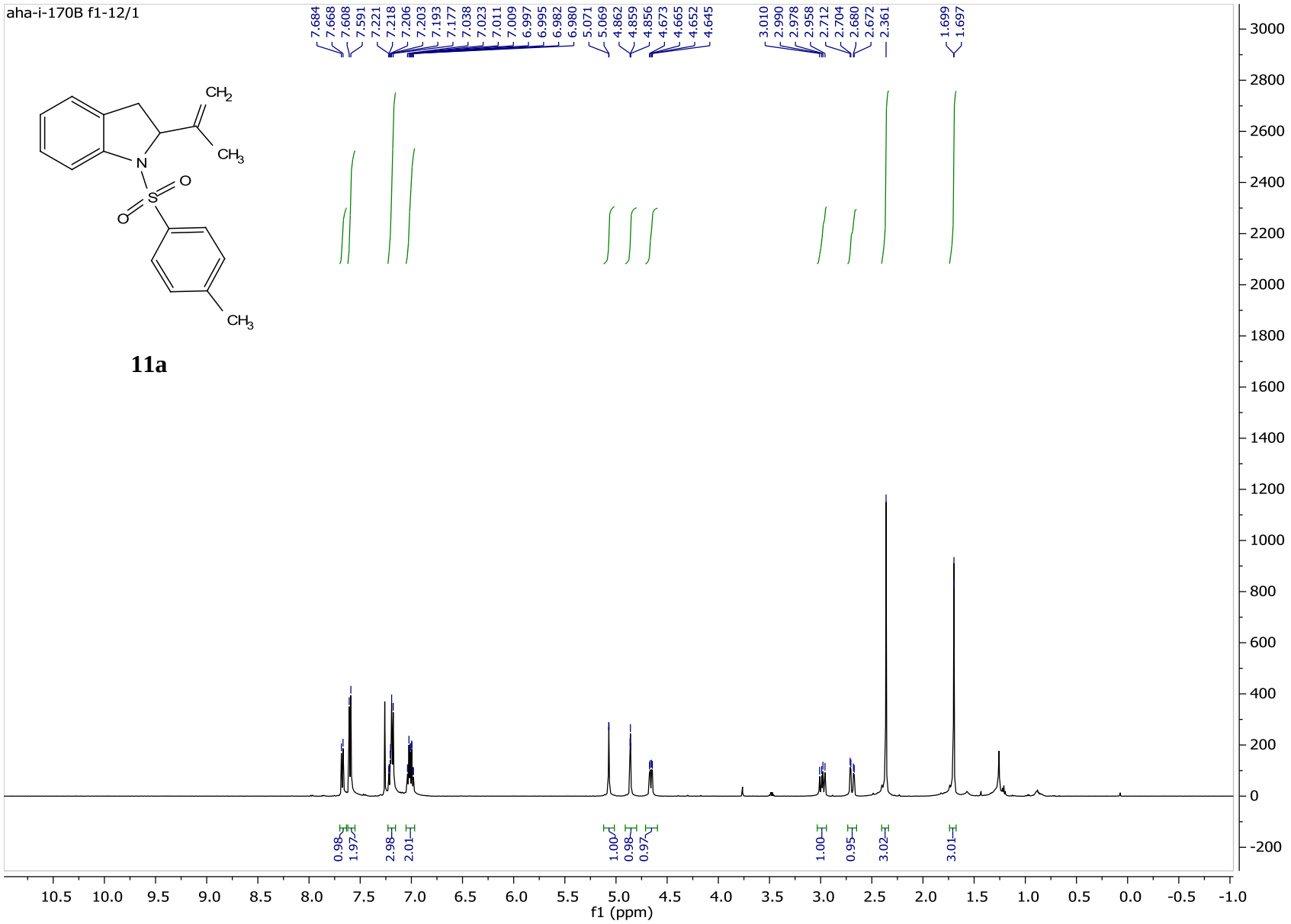
aha-i-170B f1-12/1
7.684
7.668
7.608
7.591
7.221
7.218
7.206
7.203
7.193
7.177
7.038
7.023
7.011
7.009
6.997
6.995
6.982
6.980
5.071
5.069
4.862
4.859
4.856
4.673
4.665
4.652
4.645
3.010
2.990
2.978
2.958
2.712
2.704
2.680
2.672
2.361
1.699
1.697
CH2
CH3
N
S
O
O
CH3
0.98
1.97
2.98
2.01
1.00
0.98
0.97
1.00
0.95
3.02
3.01
f1 (ppm)

11a

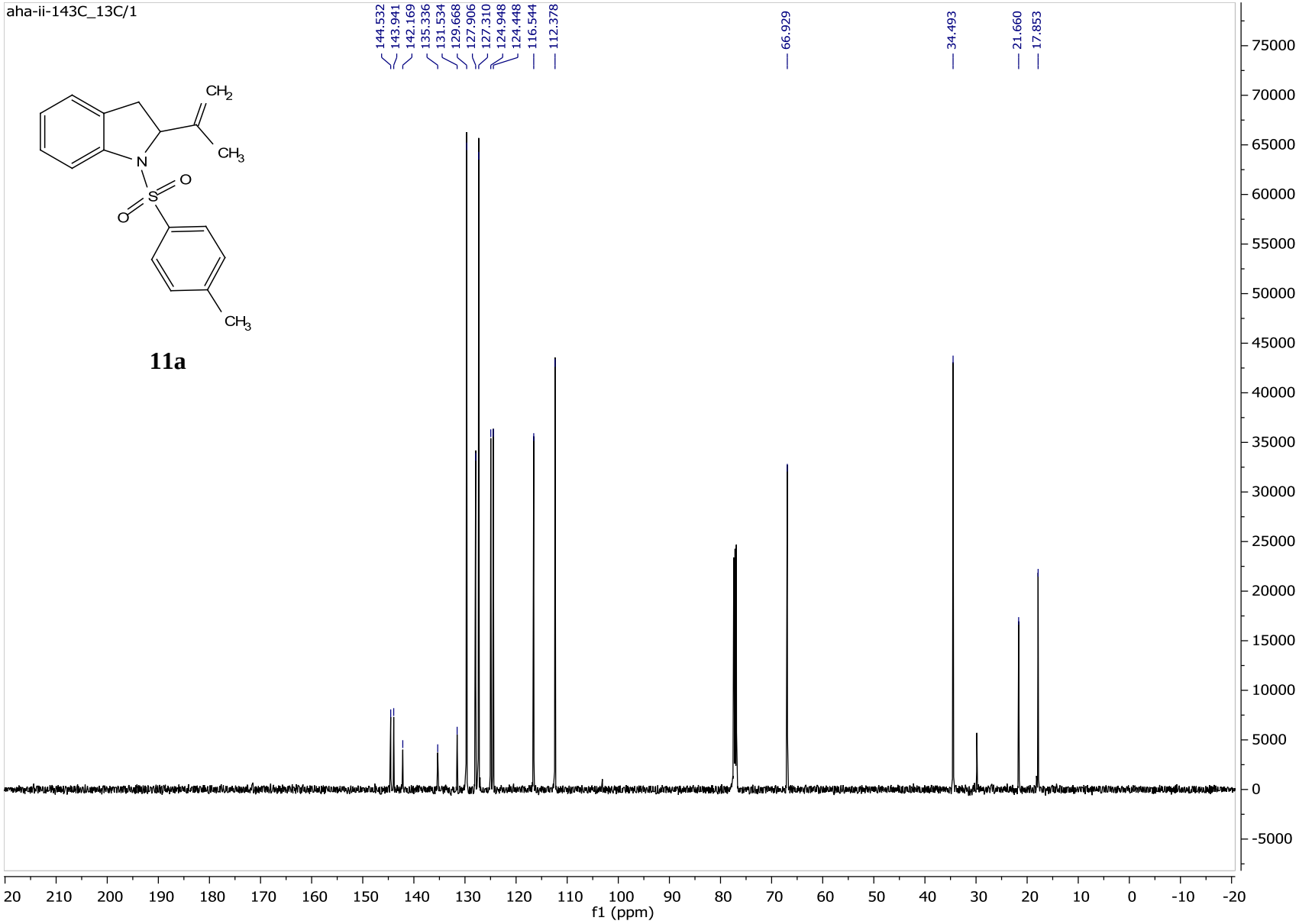
aha-ii-143C_13C/1
144.532
143.941
142.169
135.336
131.534
129.668
127.906
127.310
124.948
124.448
116.544
112.378
66.929
34.493
21.660
17.853
CH2
CH3
N
O
S
O
CH3
11a
f1 (ppm)

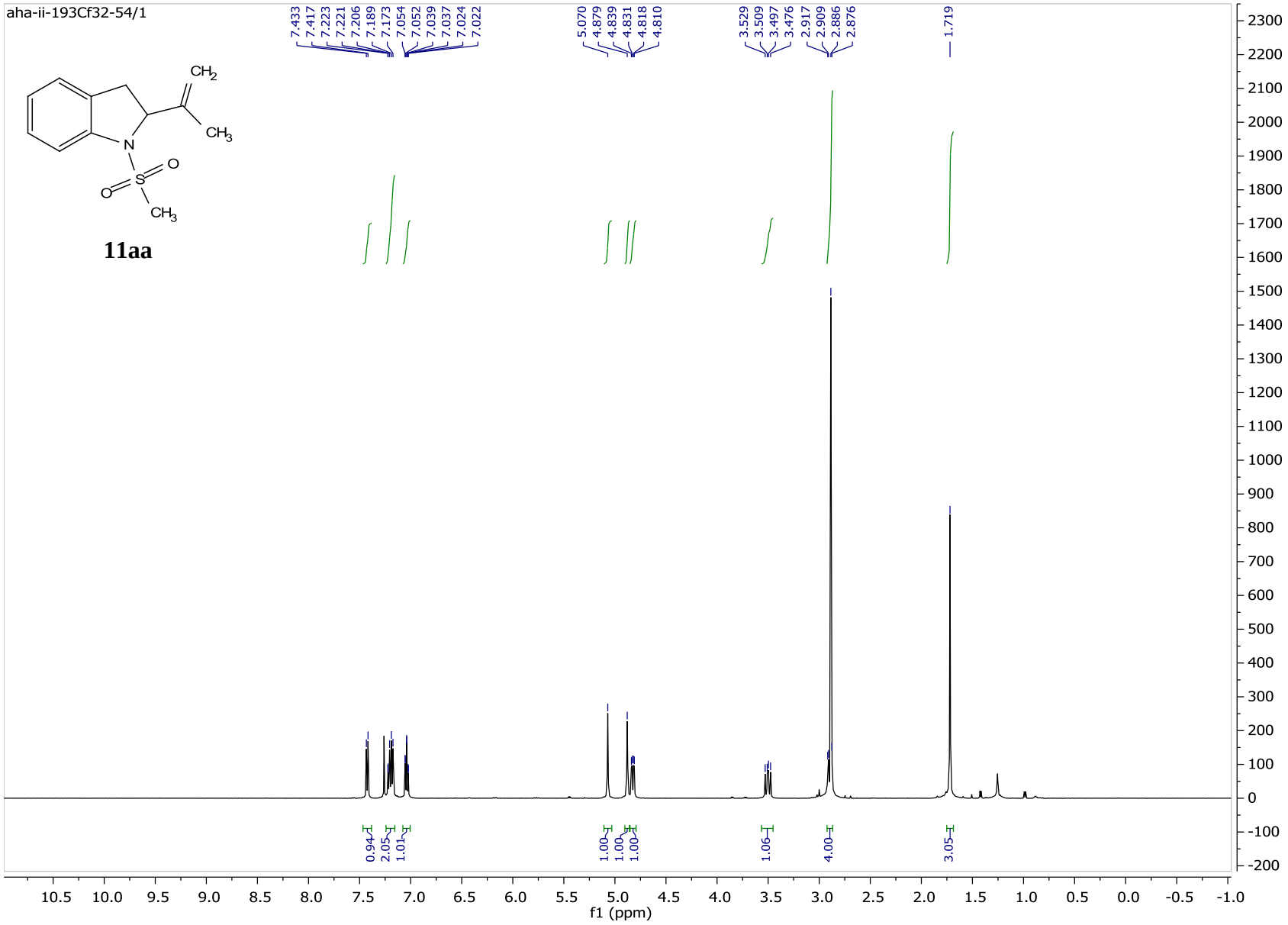
aha-ii-193Cf32-54/1
7.433
7.417
7.223
7.221
7.206
7.189
7.173
7.054
7.052
7.039
7.037
7.024
7.022
5.070
4.879
4.839
4.831
4.818
4.810
3.529
3.509
3.497
3.476
2.917
2.909
2.886
2.876
1.719
CH2
CH3
N
S
O
O
CH3
11aa
0.94
2.05
1.01
1.00
1.00
1.00
1.06
4.00
3.05
f1 (ppm)

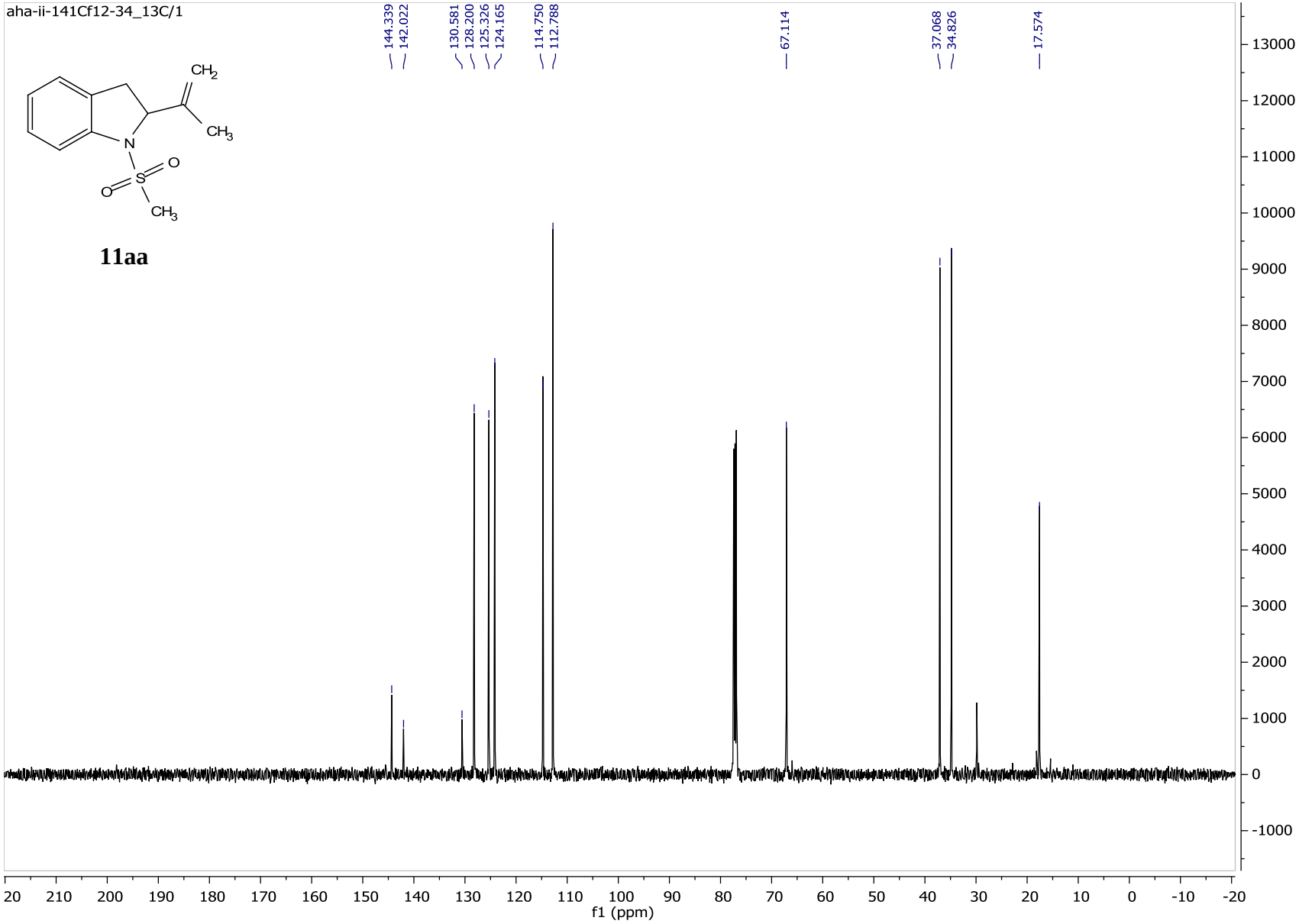
aha-ii-141Cf12-34_13C/1
144.339
142.022
130.581
128.200
125.326
124.165
114.750
112.788
67.114
37.068
34.826
17.574
CH2
CH3
N
S
O
O
CH3
11aa
13000
12000
11000
10000
9000
8000
7000
6000
5000
4000
3000
2000
1000
0
-1000
20 210 200 190 180 170 160 150 140 130 120 110 100 90 80 70 60 50 40 30 20 10 0 -10 -20
f1 (ppm)

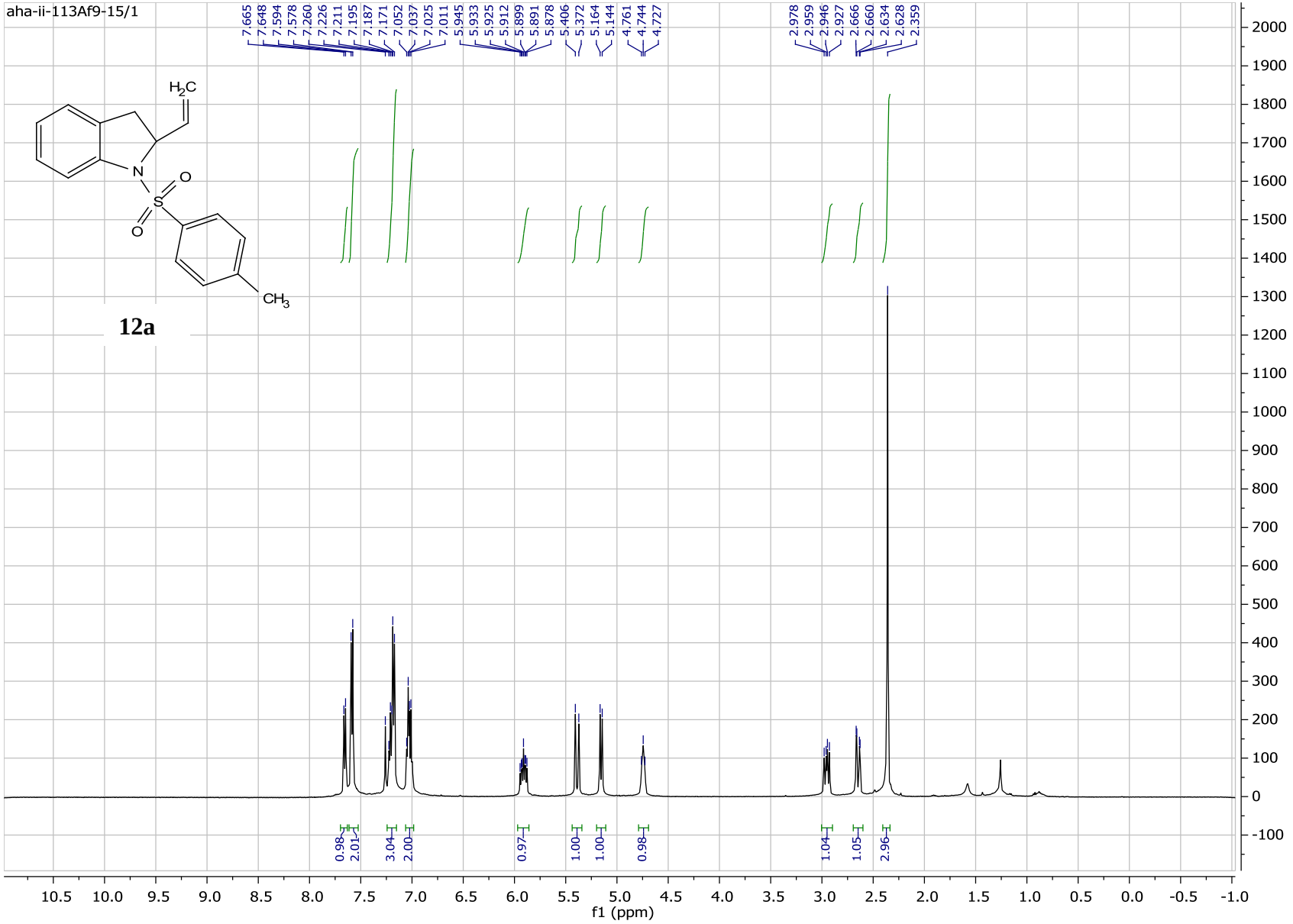
aha-ii-113Af9-15/1
7.665
7.648
7.594
7.578
7.260
7.226
7.211
7.195
7.187
7.171
7.052
7.037
7.025
7.011
5.945
5.933
5.925
5.912
5.899
5.891
5.878
5.406
5.372
5.164
5.144
4.761
4.744
4.727
2.978
2.959
2.946
2.927
2.666
2.660
2.634
2.628
2.359
H2C
N
O
S
O
CH3
12a
0.98
2.01
3.04
2.00
0.97
1.00
1.00
0.98
1.04
1.05
2.96
f1 (ppm)

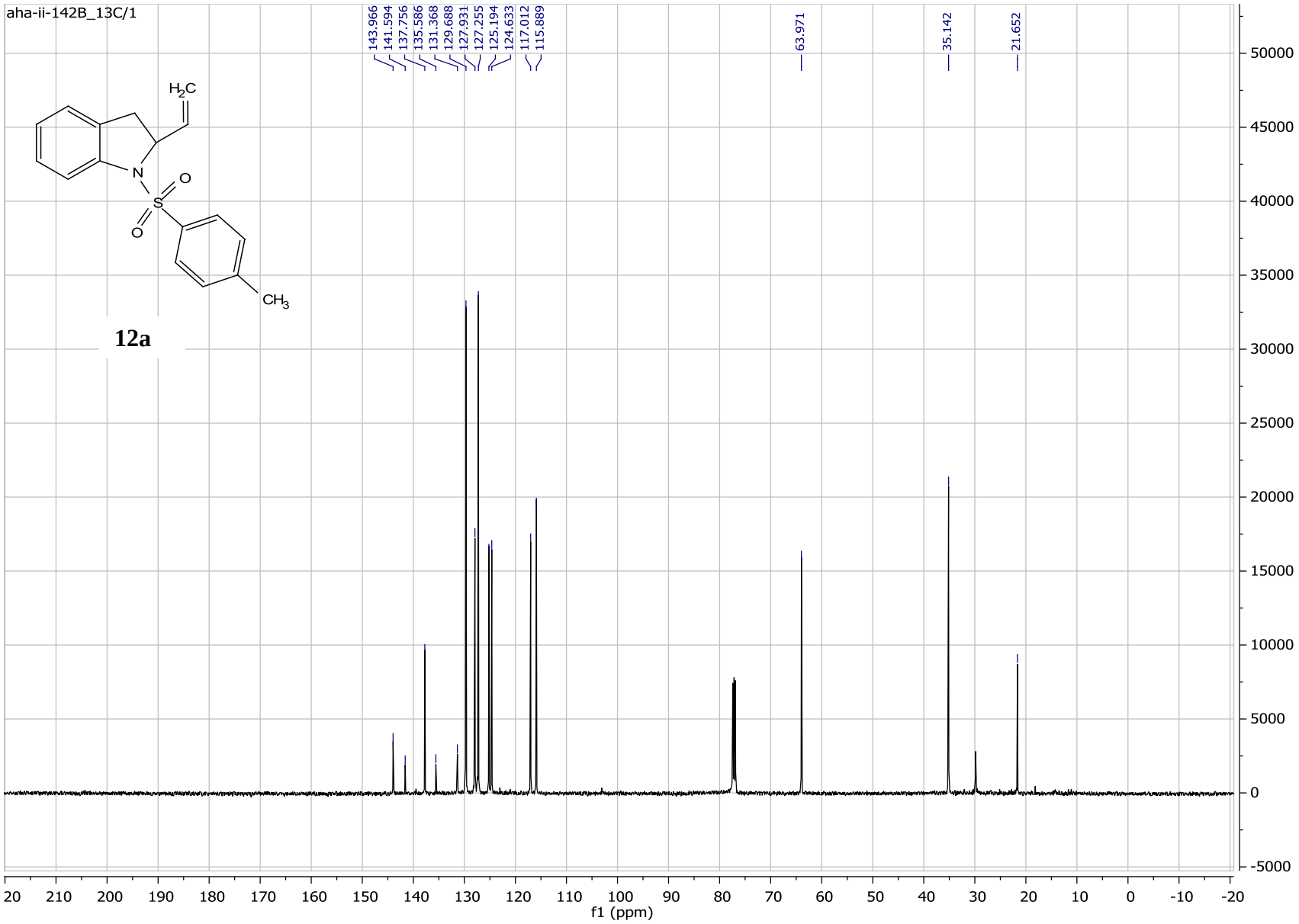
aha-ii-142B_13C/1
143.966
141.594
137.756
135.586
131.368
129.688
127.931
127.255
125.194
124.633
117.012
115.889
63.971
35.142
21.652
H2C
N
O
S
O
CH3
12a
50000
45000
40000
35000
30000
25000
20000
15000
10000
5000
0
-5000
20 210 200 190 180 170 160 150 140 130 120 110 100 90 80 70 60 50 40 30 20 10 0 -10 -20
f1 (ppm)

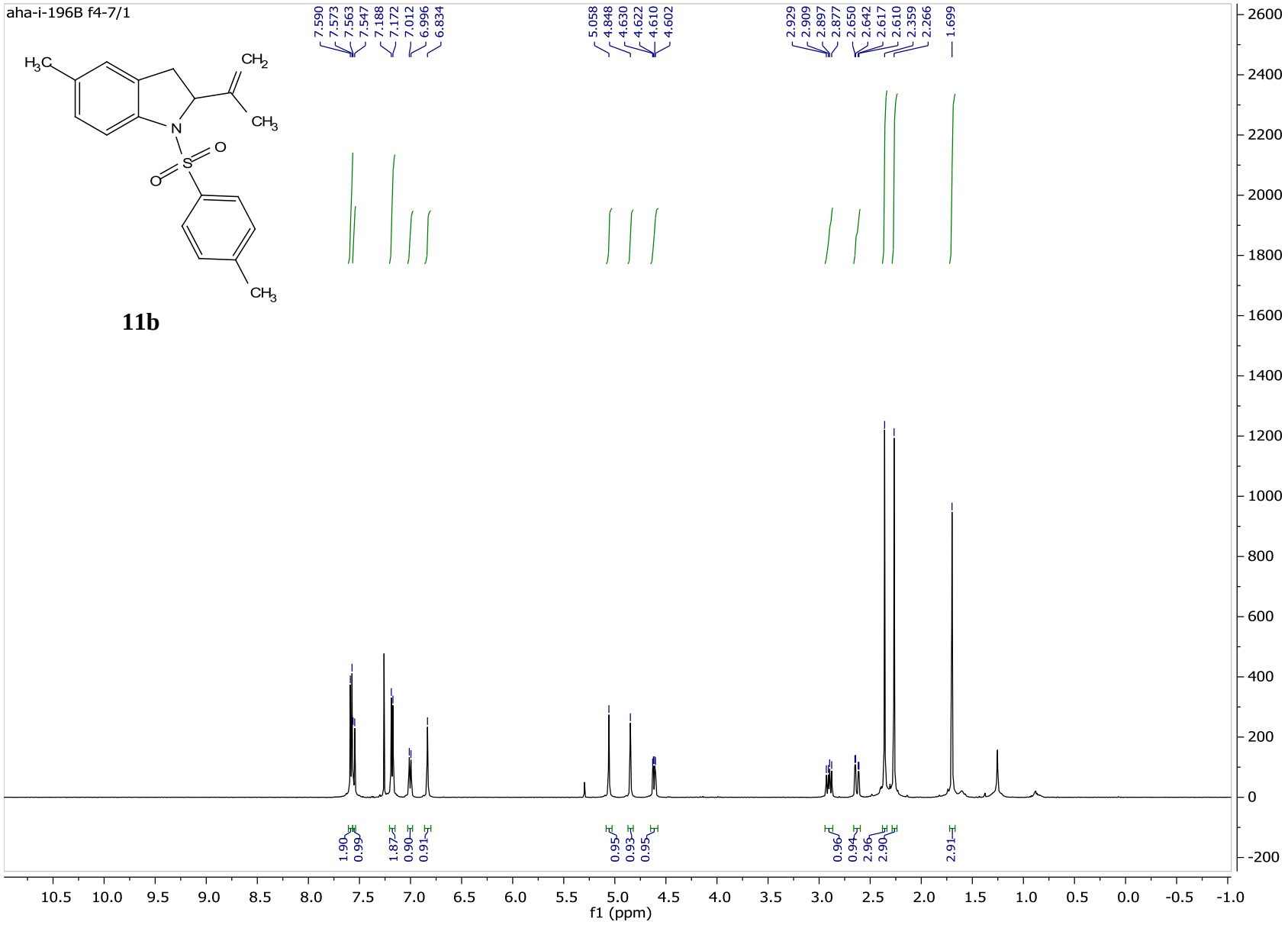
aha-i-196B f4-7/1
7.590
7.573
7.563
7.547
7.188
7.172
7.012
6.996
6.834
5.058
4.848
4.630
4.622
4.610
4.602
2.929
2.909
2.897
2.877
2.650
2.642
2.617
2.610
2.359
2.266
1.699
1.90
0.99
1.87
0.90
0.91
0.95
0.93
0.95
0.96
0.94
2.96
2.90
2.91
f1 (ppm)

11b

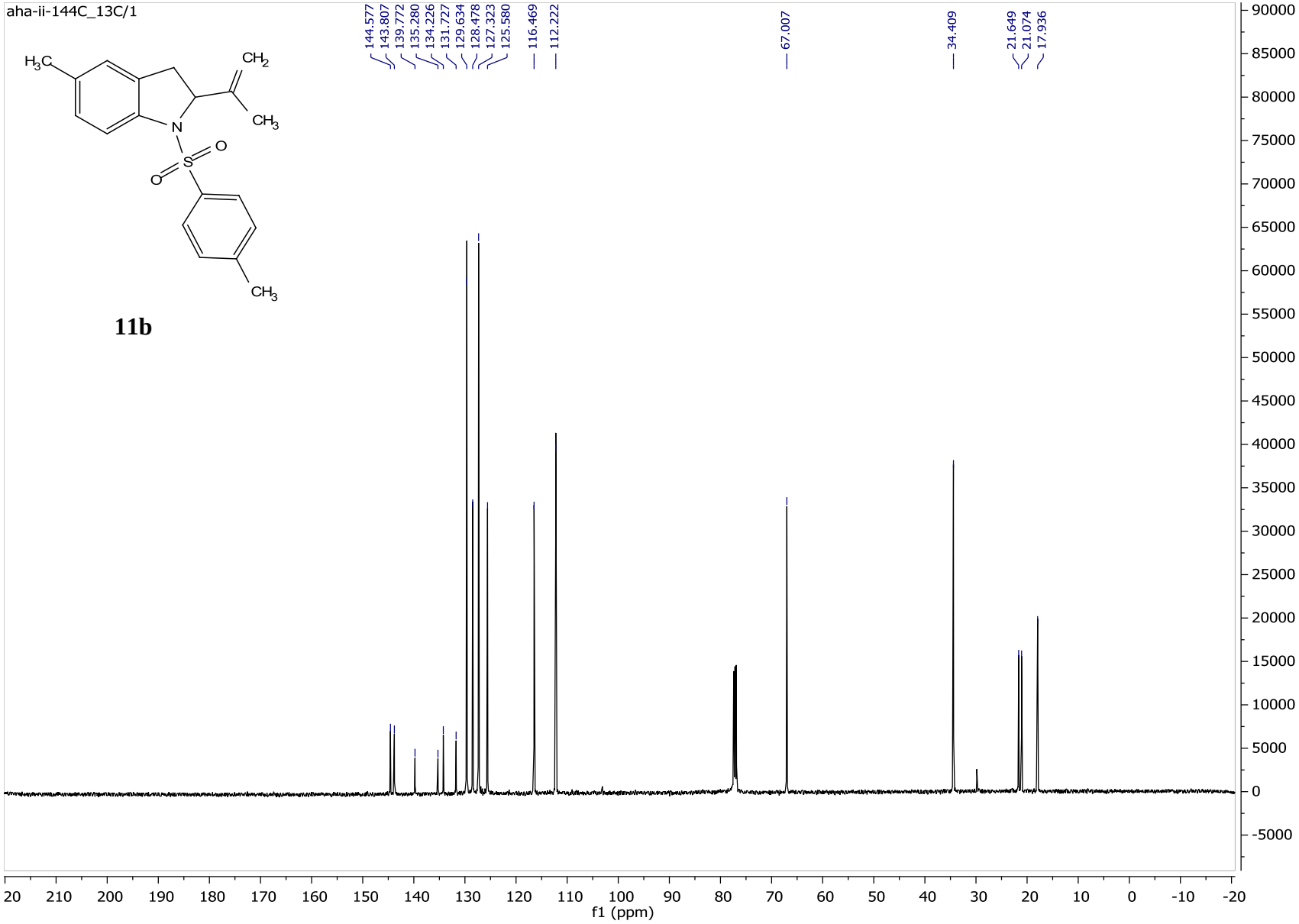
aha-ii-144C_13C/1
144.577
143.807
139.772
135.280
134.226
131.727
129.634
128.478
127.323
125.580
116.469
112.222
67.007
34.409
21.649
21.074
17.936
H3C
CH2
CH3
N
S
O
O
CH3
11b
f1 (ppm)

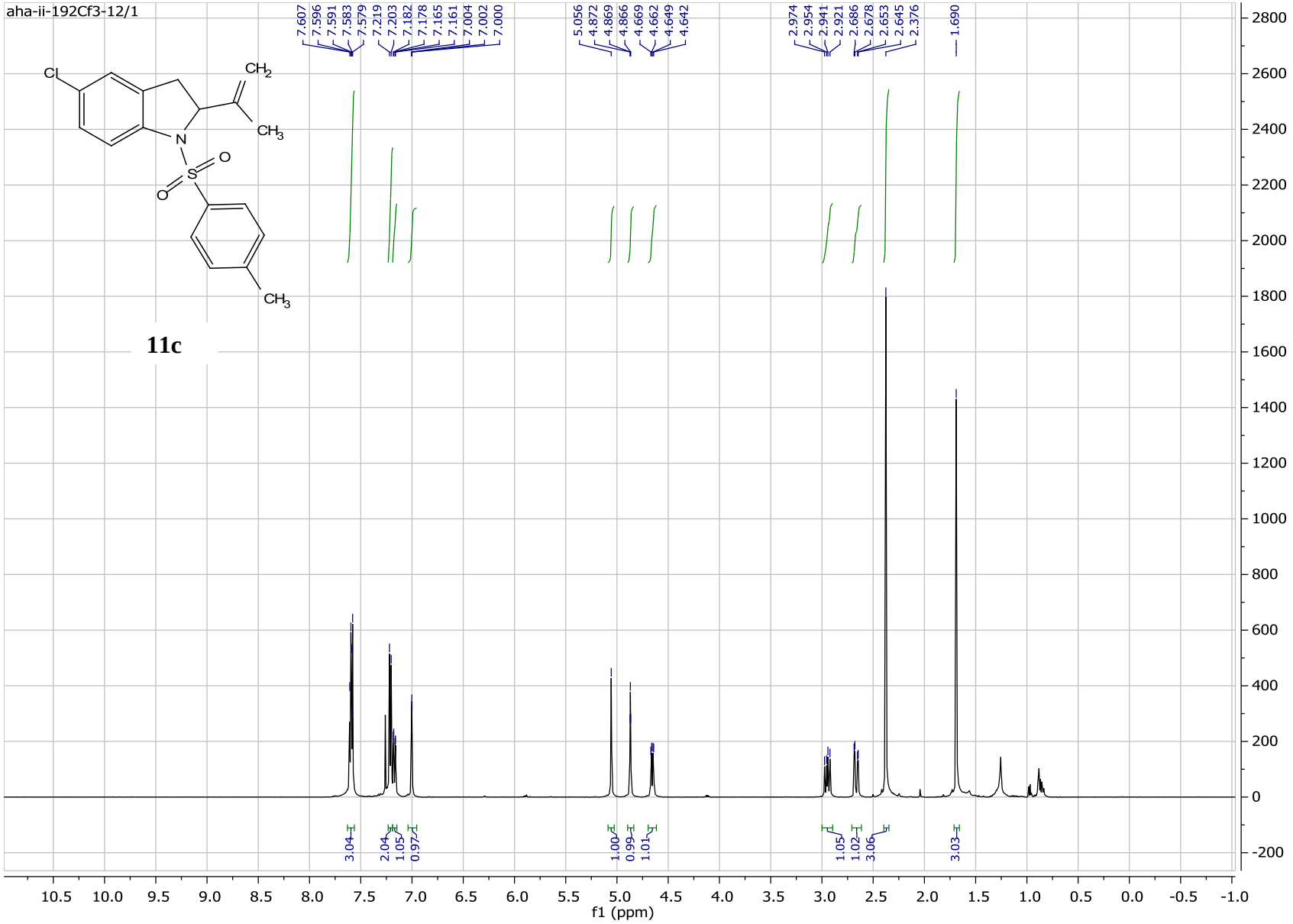
aha-ii-192Cf3-12/1
11c
7.607
7.596
7.591
7.583
7.579
7.219
7.203
7.182
7.178
7.165
7.161
7.004
7.002
7.000
5.056
4.872
4.869
4.866
4.669
4.662
4.649
4.642
2.974
2.954
2.941
2.921
2.686
2.678
2.653
2.645
2.376
1.690
3.04
2.04
1.05
0.97
1.00
0.99
1.01
1.05
1.02
3.06
3.03
f1 (ppm)

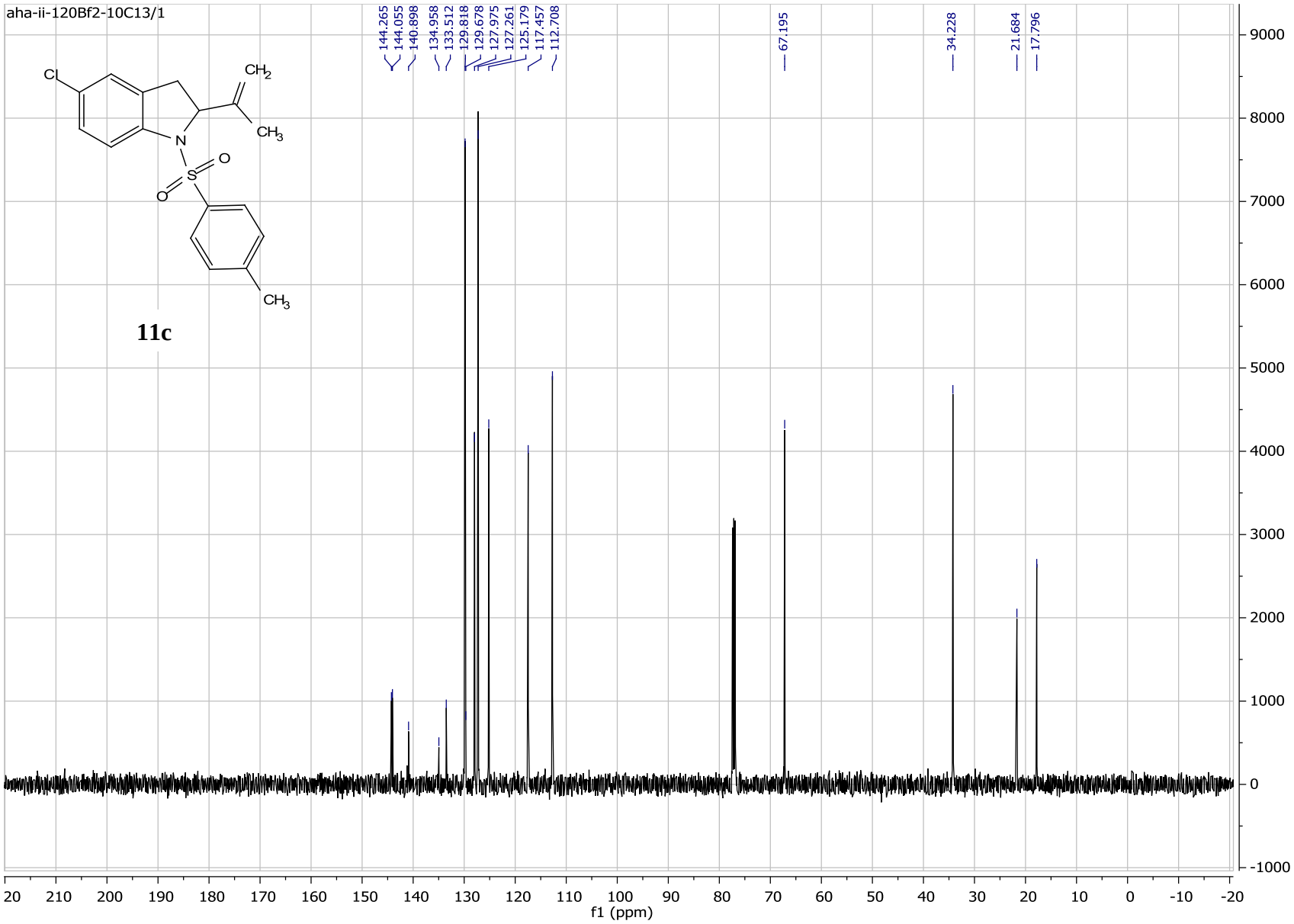
aha-ii-120Bf2-10C13/1
144.265
144.055
140.898
134.958
133.512
129.818
129.678
127.975
127.261
125.179
117.457
112.708
67.195
34.228
21.684
17.796
Cl
CH2
CH3
N
O
S
O
CH3
11c
f1 (ppm)

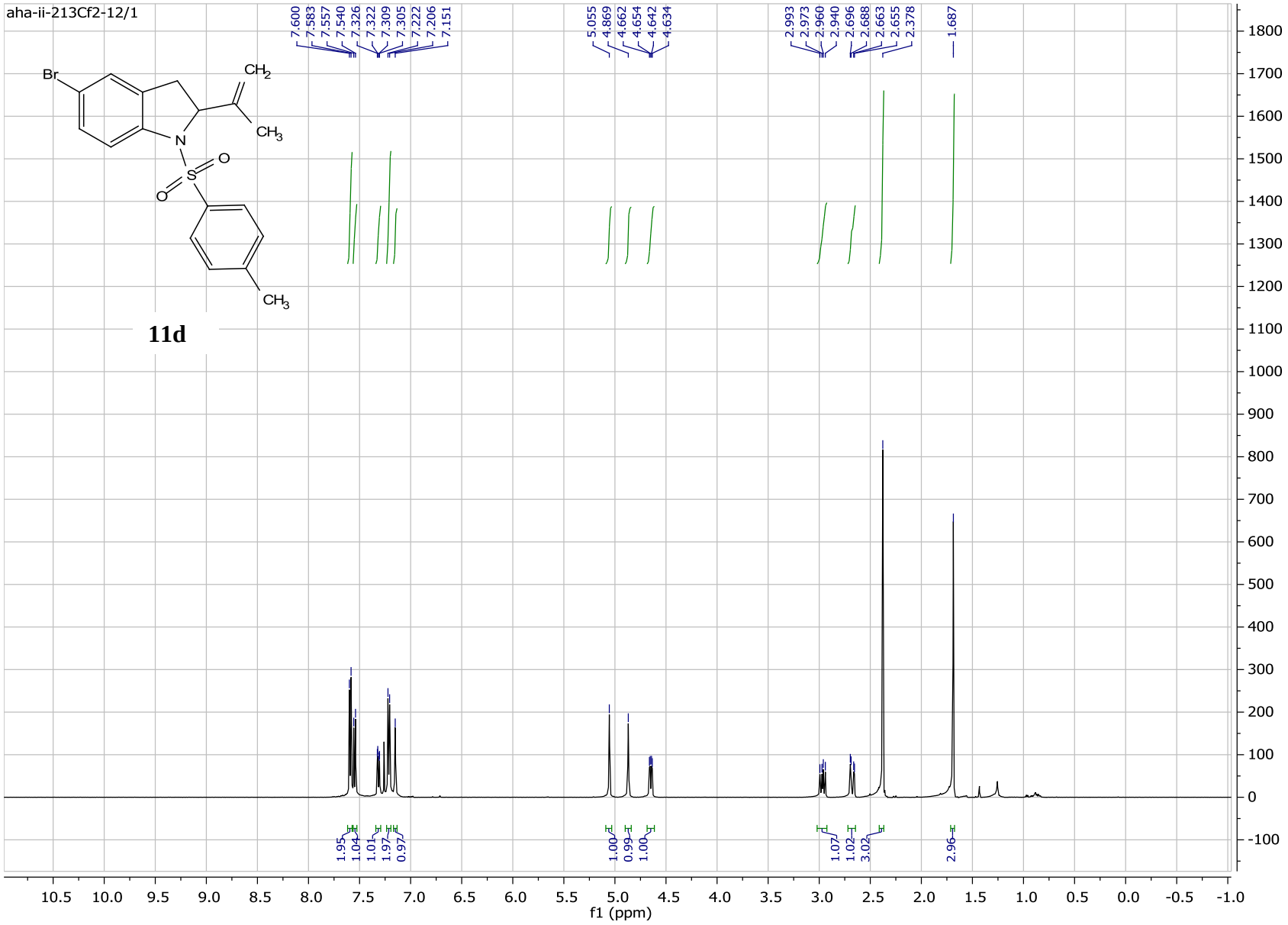
aha-ii-213Cf2-12/1
Br
CH2
CH3
N
O
S
O
CH3
11d
7.600
7.583
7.557
7.540
7.326
7.322
7.309
7.305
7.222
7.206
7.151
5.055
4.869
4.662
4.654
4.642
4.634
2.993
2.973
2.960
2.940
2.696
2.688
2.663
2.655
2.378
1.687
1.95
1.04
1.01
1.97
0.97
1.00
0.99
1.00
1.07
1.02
3.02
2.96
f1 (ppm)

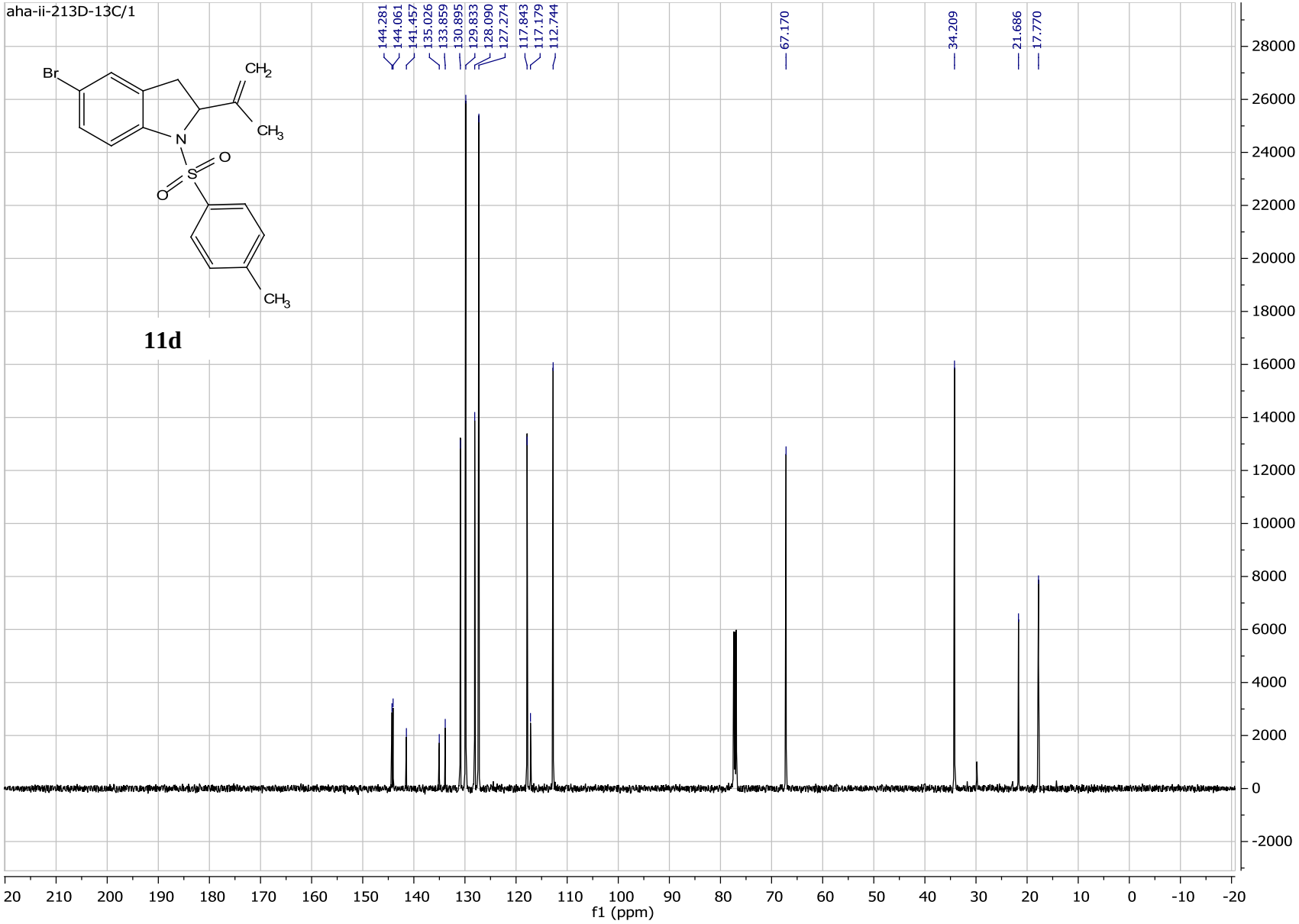
aha-ii-213D-13C/1
144.281
144.061
141.457
135.026
133.859
130.895
129.833
128.090
127.274
117.843
117.179
112.744
67.170
34.209
21.686
17.770
Br
CH2
CH3
N
S
O
O
CH3
11d
f1 (ppm)

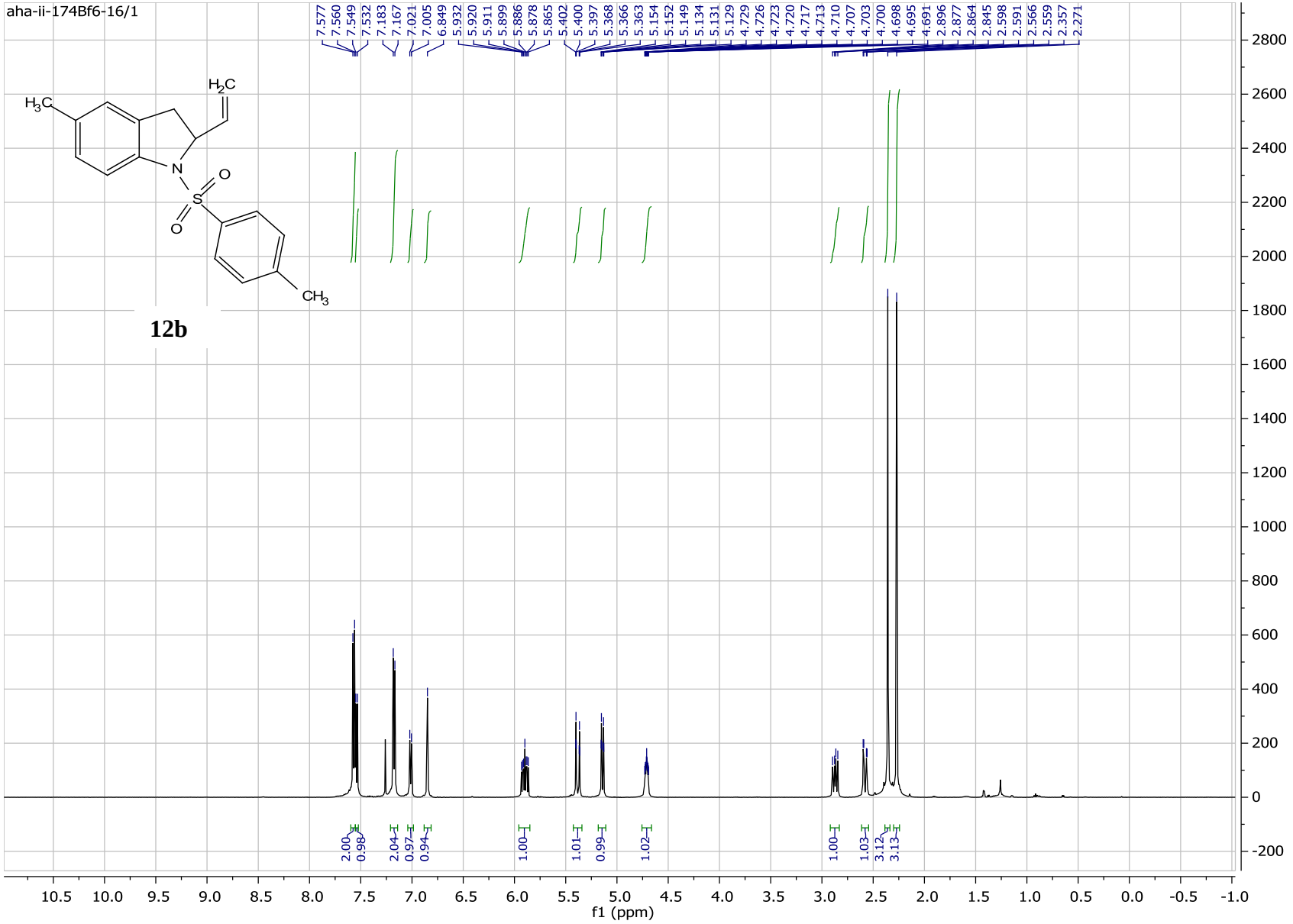
aha-ii-174Bf6-16/1
7.577
7.560
7.549
7.532
7.183
7.167
7.021
7.005
6.849
5.932
5.920
5.911
5.899
5.886
5.878
5.865
5.402
5.400
5.397
5.368
5.366
5.363
5.154
5.152
5.149
5.134
5.131
5.129
4.729
4.726
4.723
4.720
4.717
4.713
4.710
4.707
4.703
4.700
4.698
4.695
4.691
2.896
2.877
2.864
2.845
2.598
2.591
2.566
2.559
2.357
2.271
H3C
H2C
N
S
O
O
CH3
12b
2.00
0.98
2.04
0.97
0.94
1.00
1.01
0.99
1.02
1.00
1.03
3.12
3.13
f1 (ppm)

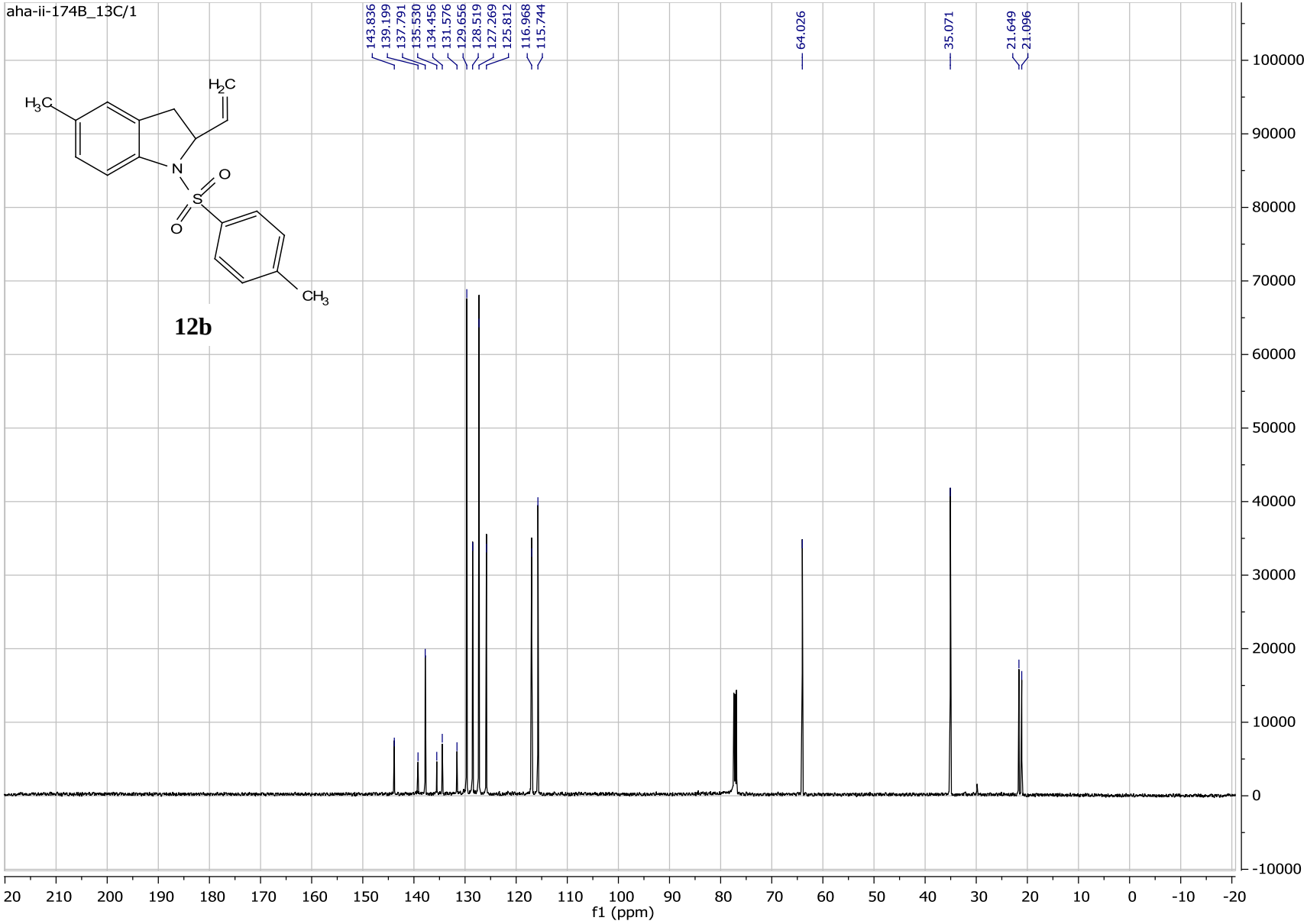
aha-ii-174B_13C/1
143.836
139.199
137.791
135.530
134.456
131.576
129.656
128.519
127.269
125.812
116.968
115.744
64.026
35.071
21.649
21.096
H3C
H2C
N
O
S
O
O
CH3
12b
f1 (ppm)

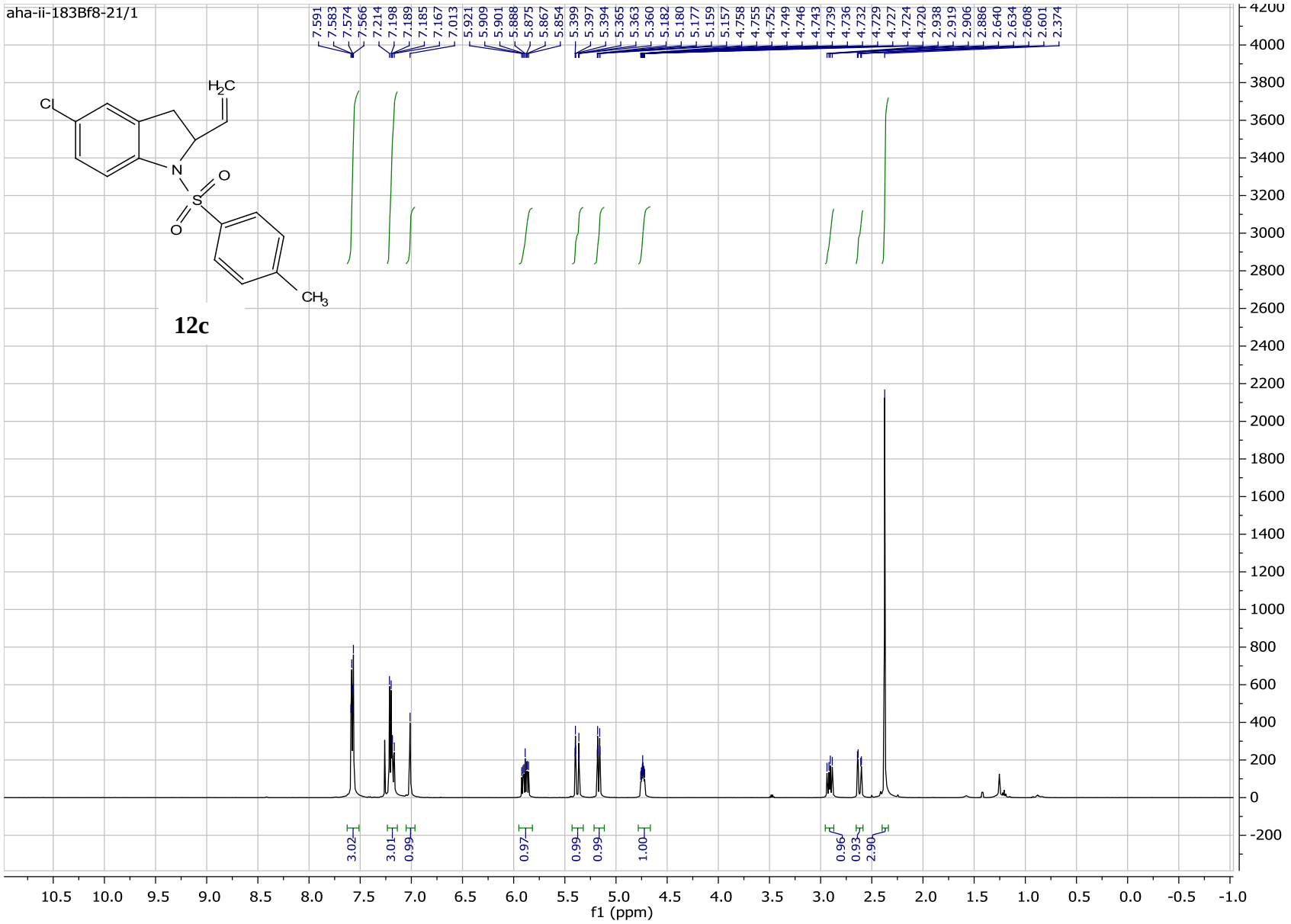
aha-ii-183Bf8-21/1
7.591
7.583
7.574
7.566
7.214
7.198
7.189
7.185
7.167
7.013
5.921
5.909
5.901
5.888
5.875
5.867
5.854
5.399
5.397
5.394
5.365
5.363
5.360
5.182
5.180
5.177
5.159
5.157
4.758
4.755
4.752
4.749
4.746
4.743
4.739
4.736
4.732
4.729
4.727
4.724
4.720
2.938
2.919
2.906
2.886
2.640
2.634
2.608
2.601
2.374
Cl
H2C
N
O
S
O
O
CH3
12c
3.02
3.01
0.99
0.97
0.99
0.99
1.00
0.96
0.93
2.90
f1 (ppm)

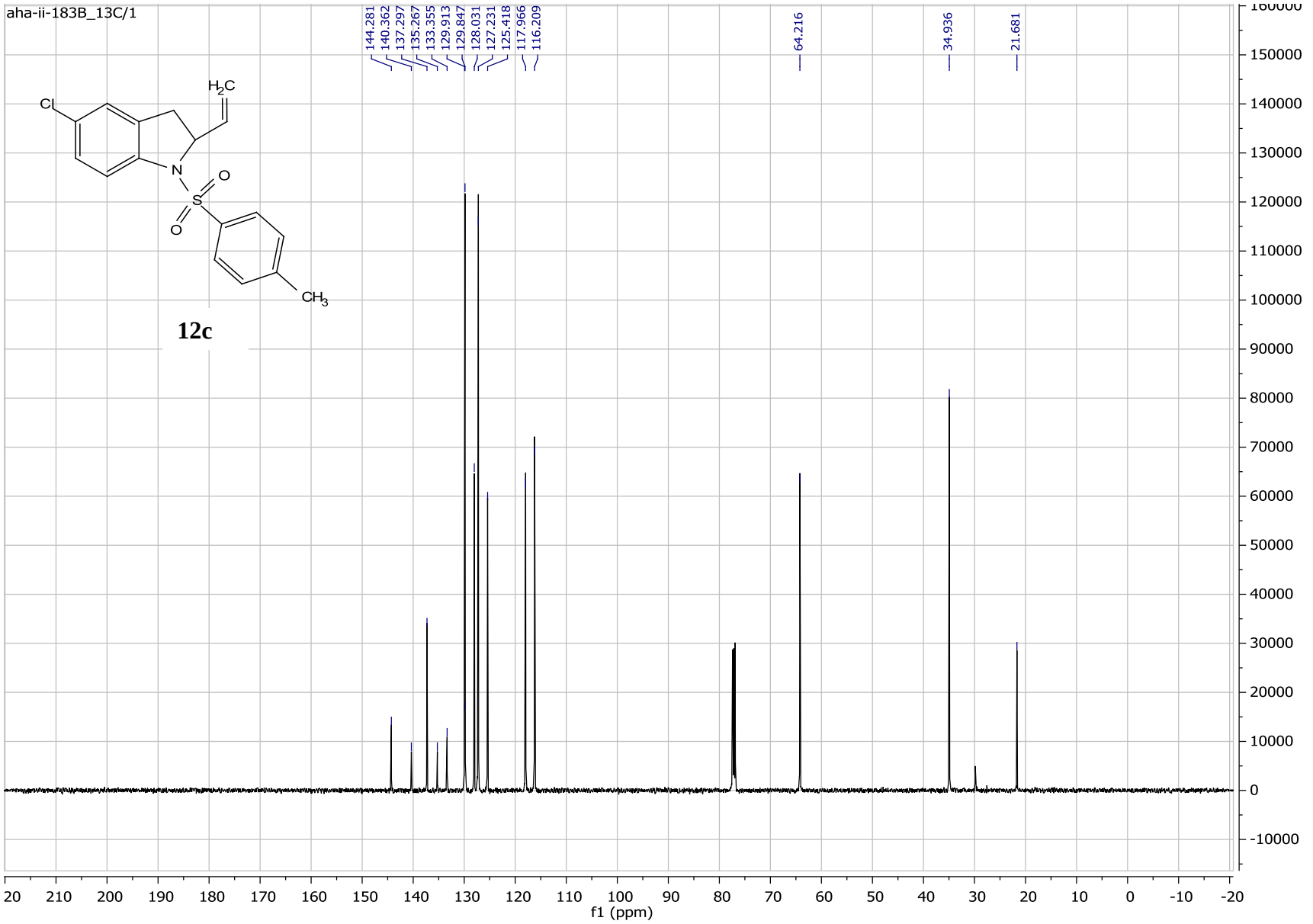
aha-ii-183B_13C/1
144.281
140.362
137.297
135.267
133.355
129.913
129.847
128.031
127.231
125.418
117.966
116.209
64.216
34.936
21.681
Cl
H2C
N
O
S
O
O
CH3
12c
f1 (ppm)

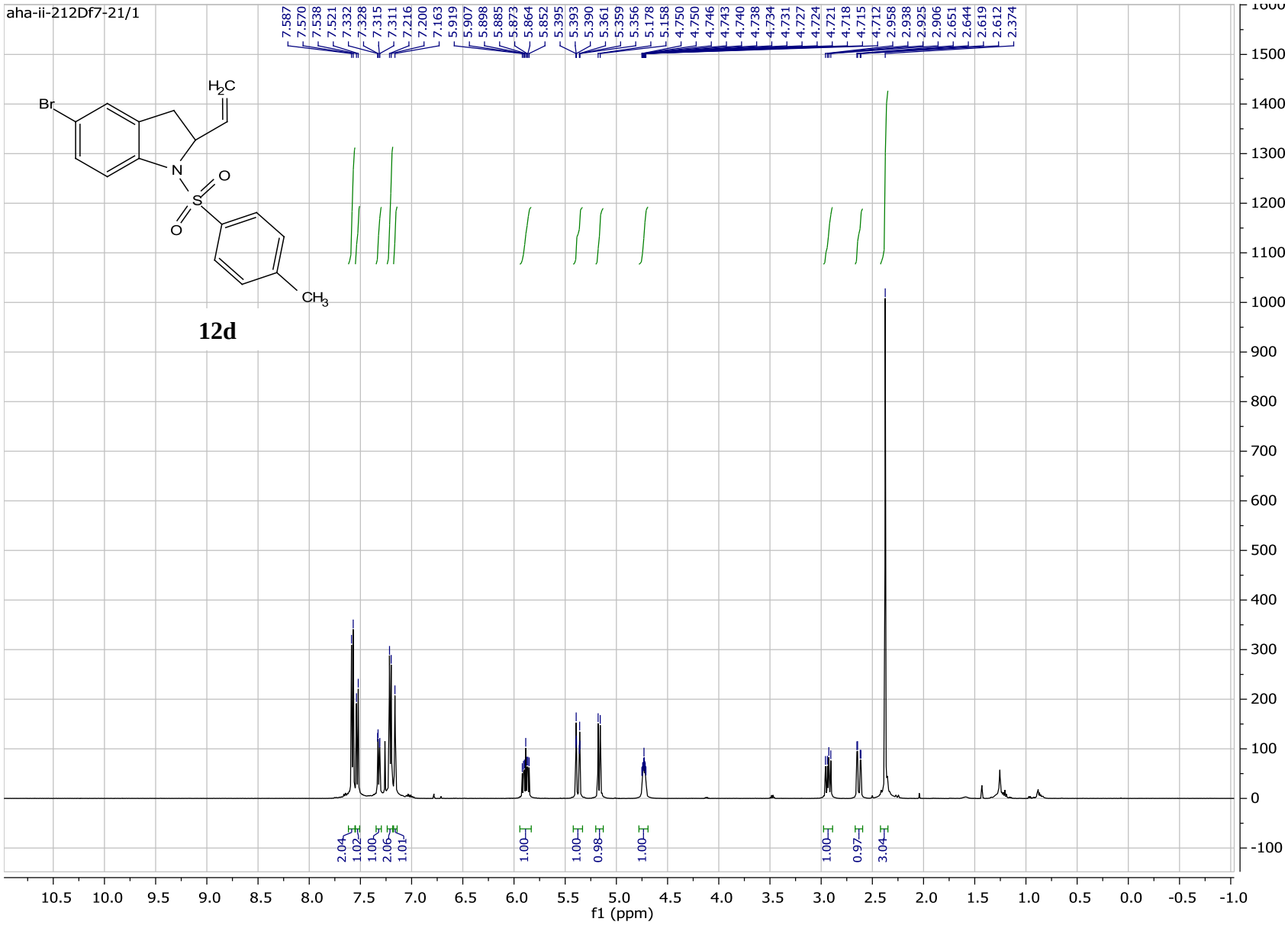
aha-ii-212Df7-21/1
7.587 7.570 7.538 7.521 7.332 7.328 7.315 7.311 7.216 7.200 7.163 5.919 5.907 5.898 5.885 5.873 5.864 5.852 5.395 5.393 5.390 5.361 5.359 5.356 5.178 5.158 4.750 4.750 4.746 4.743 4.740 4.738 4.734 4.731 4.727 4.724 4.721 4.718 4.715 4.712 2.958 2.938 2.925 2.906 2.651 2.644 2.619 2.612 2.374
Br
H2C
N
O
S
O
O
CH3
12d
2.04 1.02 1.00 2.06 1.01 1.00 1.00 0.98 1.00 1.00 0.97 3.04
f1 (ppm)

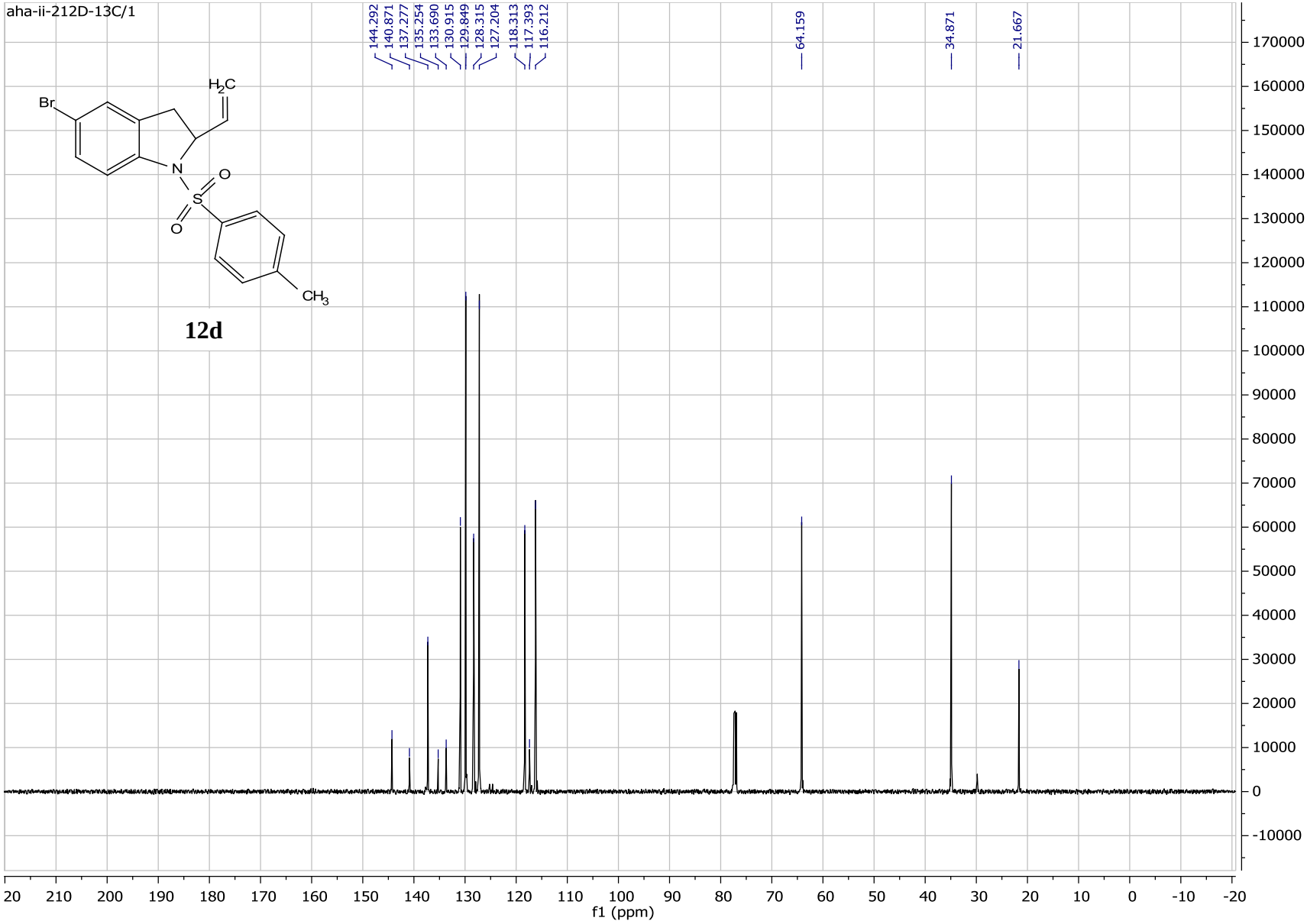
aha-ii-212D-13C/1
144.292
140.871
137.277
135.254
133.690
130.915
129.849
128.315
127.204
118.313
117.393
116.212
64.159
34.871
21.667
Br
H2C
N
O
S
O
CH3
12d
f1 (ppm)

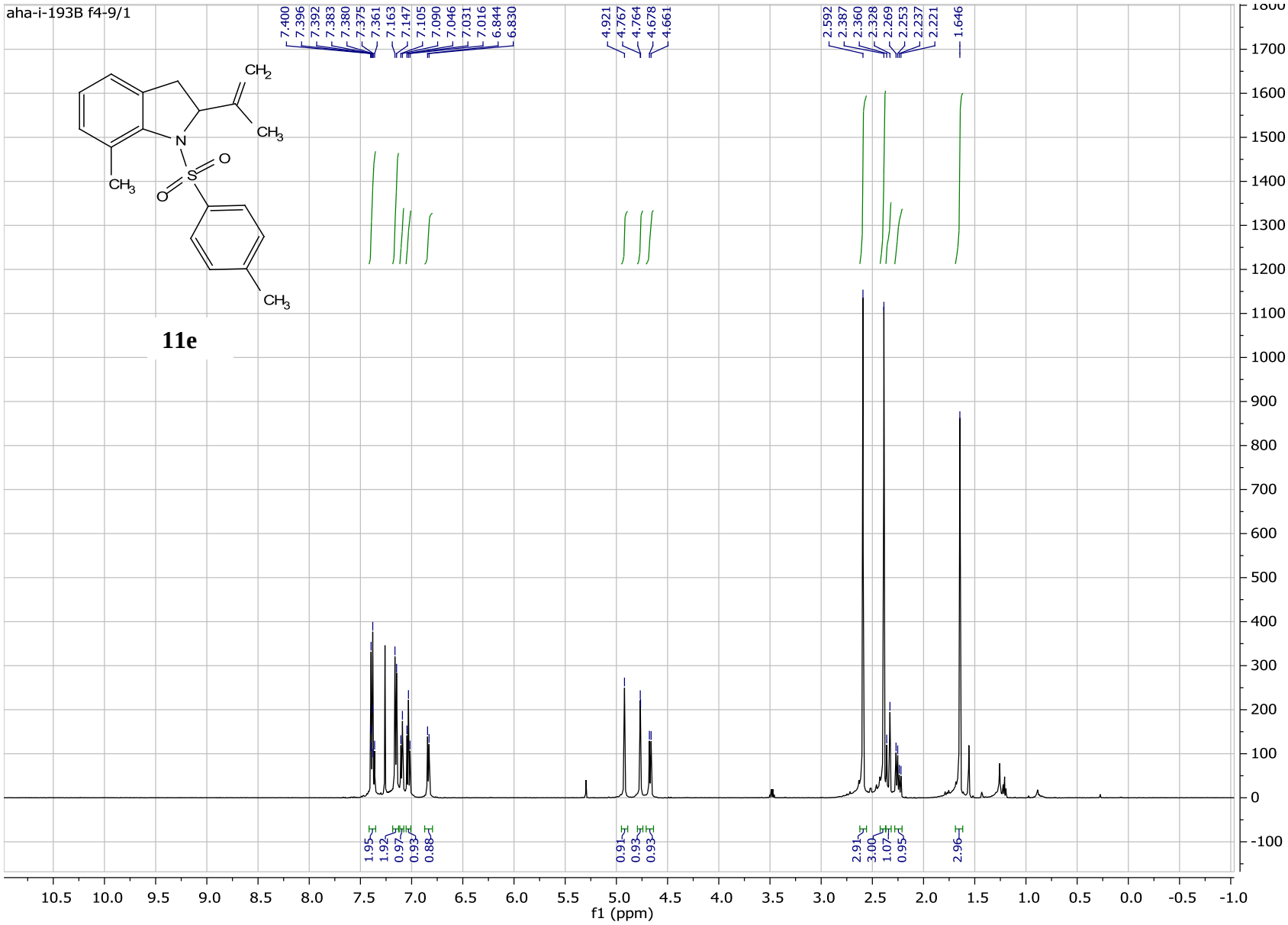
aha-i-193B f4-9/1
7.400
7.396
7.392
7.383
7.380
7.375
7.361
7.163
7.147
7.105
7.090
7.046
7.031
7.016
6.844
6.830
4.921
4.767
4.764
4.678
4.661
2.592
2.387
2.360
2.328
2.269
2.253
2.237
2.221
1.646
CH2
CH3
N
S
O
O
CH3
CH3
11e
1.95
1.92
0.97
0.93
0.88
0.91
0.93
0.93
2.91
3.00
1.07
0.95
2.96
f1 (ppm)

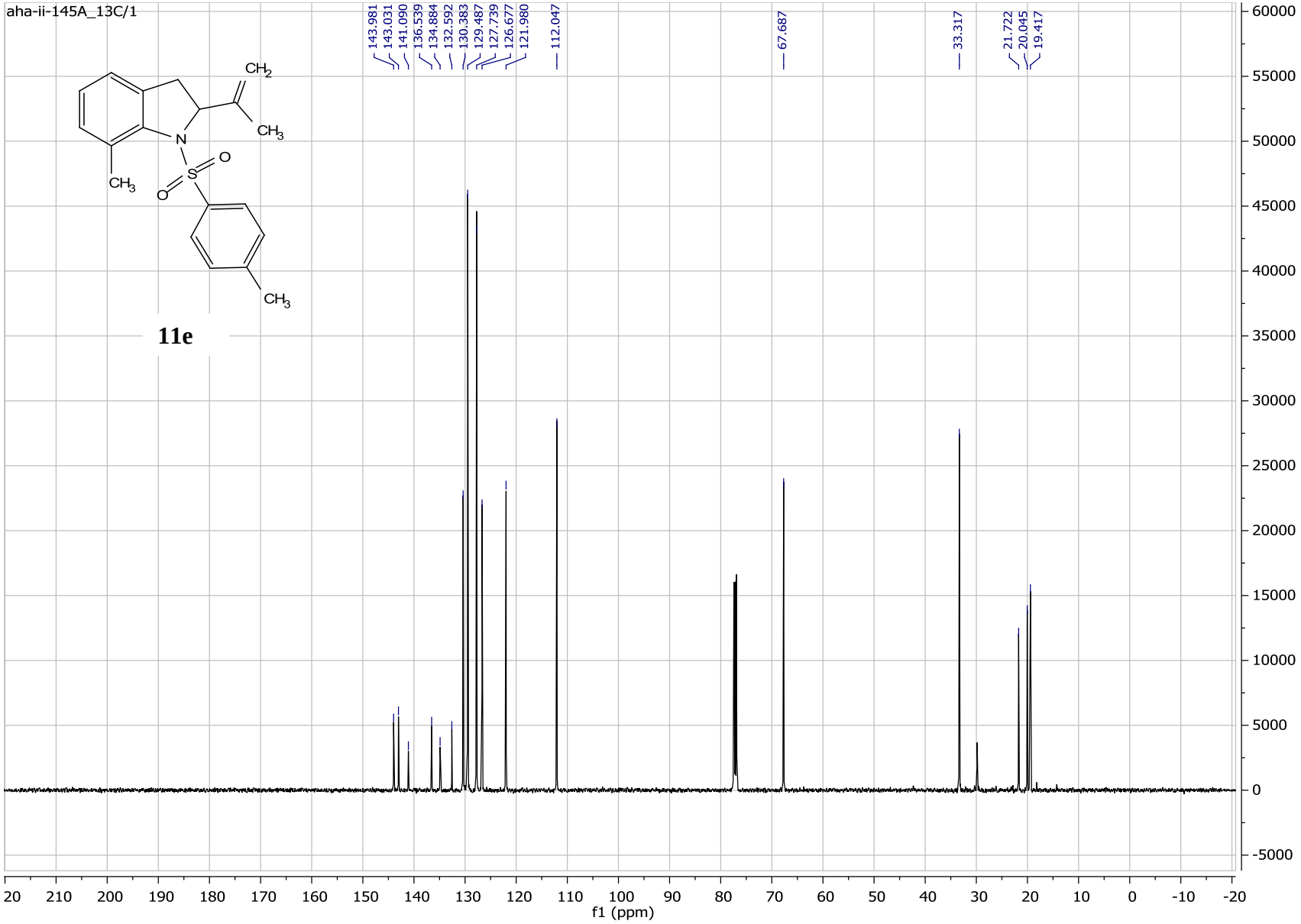
aha-ii-145A_13C/1
143.981
143.031
141.090
136.539
134.884
132.592
130.383
129.487
127.739
126.677
121.980
112.047
67.687
33.317
21.722
20.045
19.417
CH2
CH3
N
S
O
O
CH3
CH3
11e
f1 (ppm)

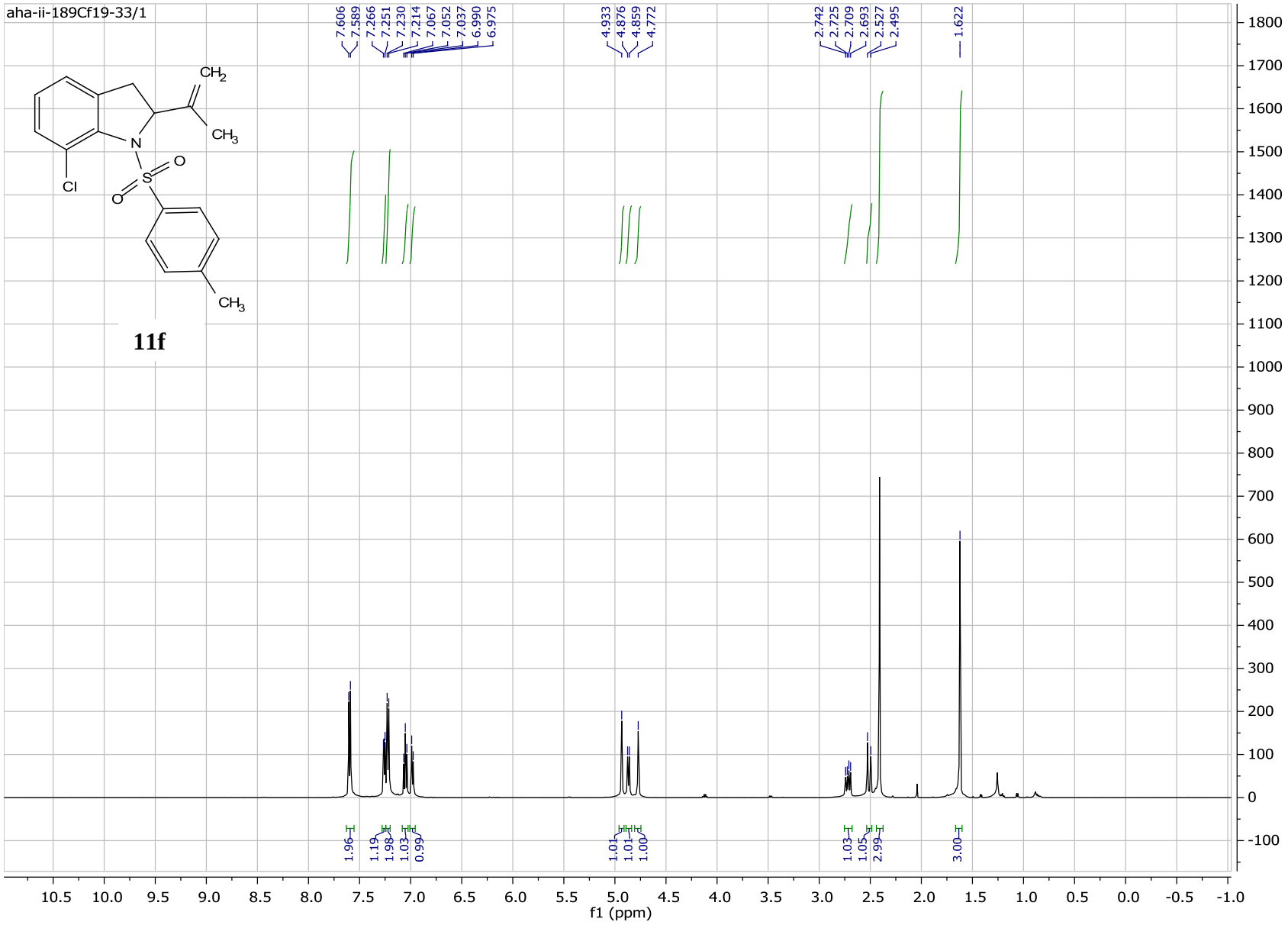
aha-ii-189Cf19-33/1
7.606
7.589
7.266
7.251
7.230
7.214
7.067
7.052
7.037
6.990
6.975
4.933
4.876
4.859
4.772
2.742
2.725
2.709
2.693
2.527
2.495
1.622
CH2
CH3
N
S
O
O
Cl
CH3
11f
1.96
1.19
1.98
1.03
0.99
1.01
1.01
1.00
1.03
1.05
2.99
3.00
f1 (ppm)

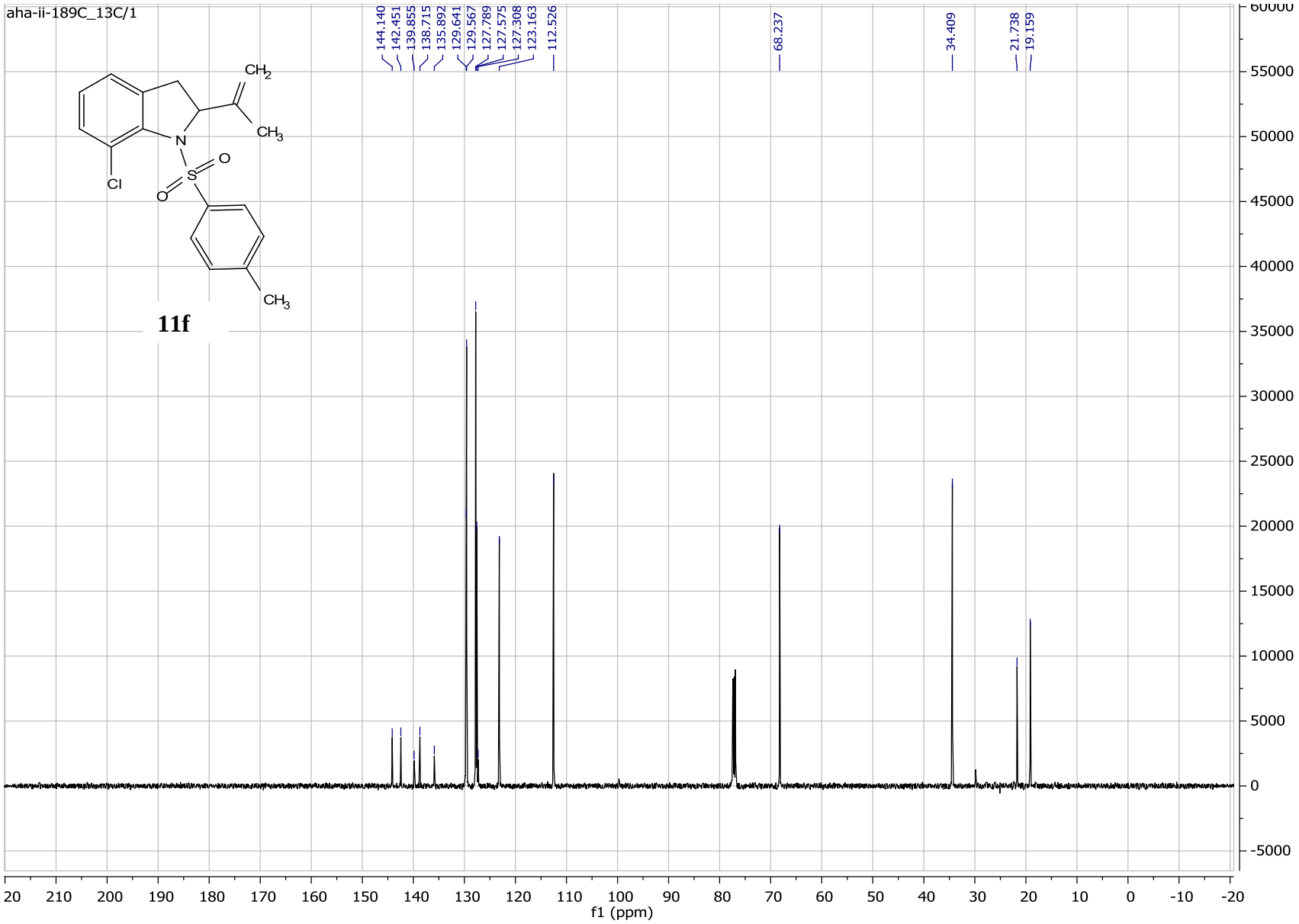
aha-ii-189C_13C/1
144.140
142.451
139.855
138.715
135.892
129.641
129.567
127.789
127.575
127.308
123.163
112.526
68.237
34.409
21.738
19.159
CH2
CH3
N
O
S
O
Cl
CH3
11f
60000
55000
50000
45000
40000
35000
30000
25000
20000
15000
10000
5000
0
-5000
20 210 200 190 180 170 160 150 140 130 120 110 100 90 80 70 60 50 40 30 20 10 0 -10 -20
f1 (ppm)

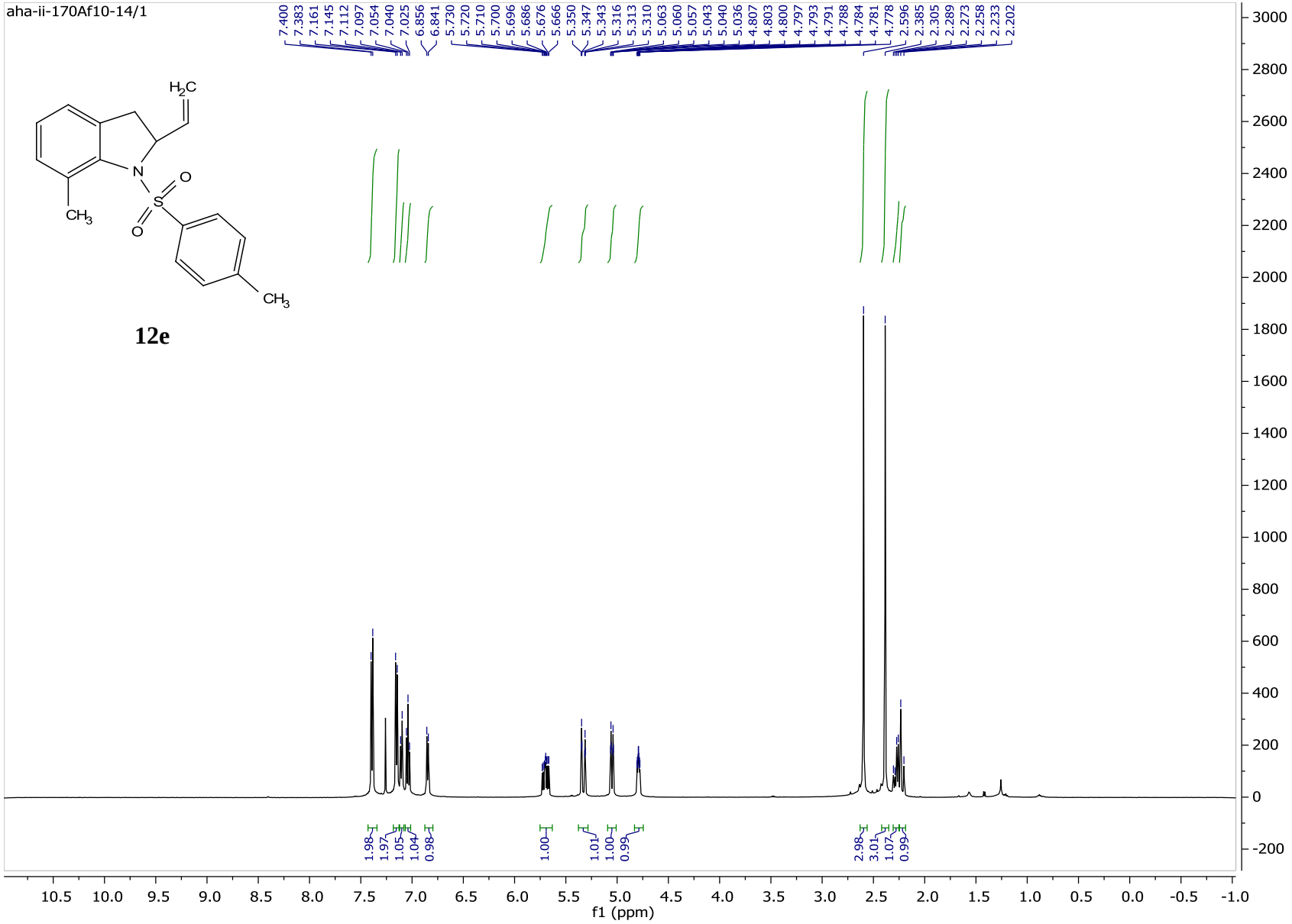
aha-ii-170Af10-14/1
7.400
7.383
7.161
7.145
7.112
7.097
7.054
7.040
7.025
6.856
6.841
5.730
5.720
5.710
5.700
5.696
5.686
5.676
5.666
5.350
5.347
5.343
5.316
5.313
5.310
5.063
5.060
5.057
5.043
5.040
5.036
4.807
4.803
4.800
4.797
4.793
4.791
4.788
4.784
4.781
4.778
2.596
2.385
2.305
2.289
2.273
2.258
2.233
2.202
H2C
N
O
S
O
CH3
CH3
12e
1.98
1.97
1.05
1.04
0.98
1.00
1.01
1.00
0.99
2.98
3.01
1.07
0.99
f1 (ppm)

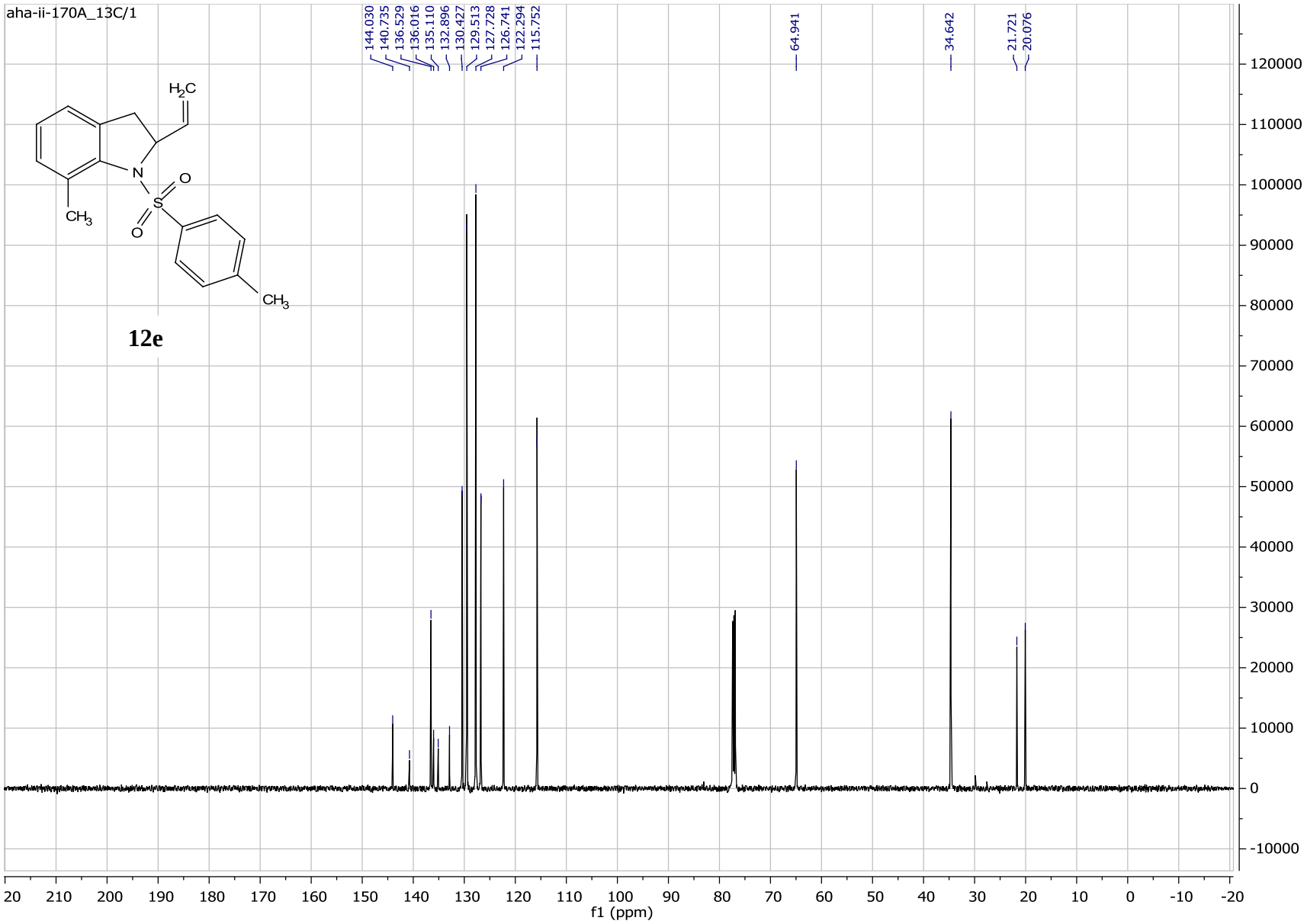
aha-ii-170A_13C/1
144.030
140.735
136.529
136.016
135.110
132.896
130.427
129.513
127.728
126.741
122.294
115.752
64.941
34.642
21.721
20.076
H2C
N
O
S
O
CH3
CH3
12e
f1 (ppm)

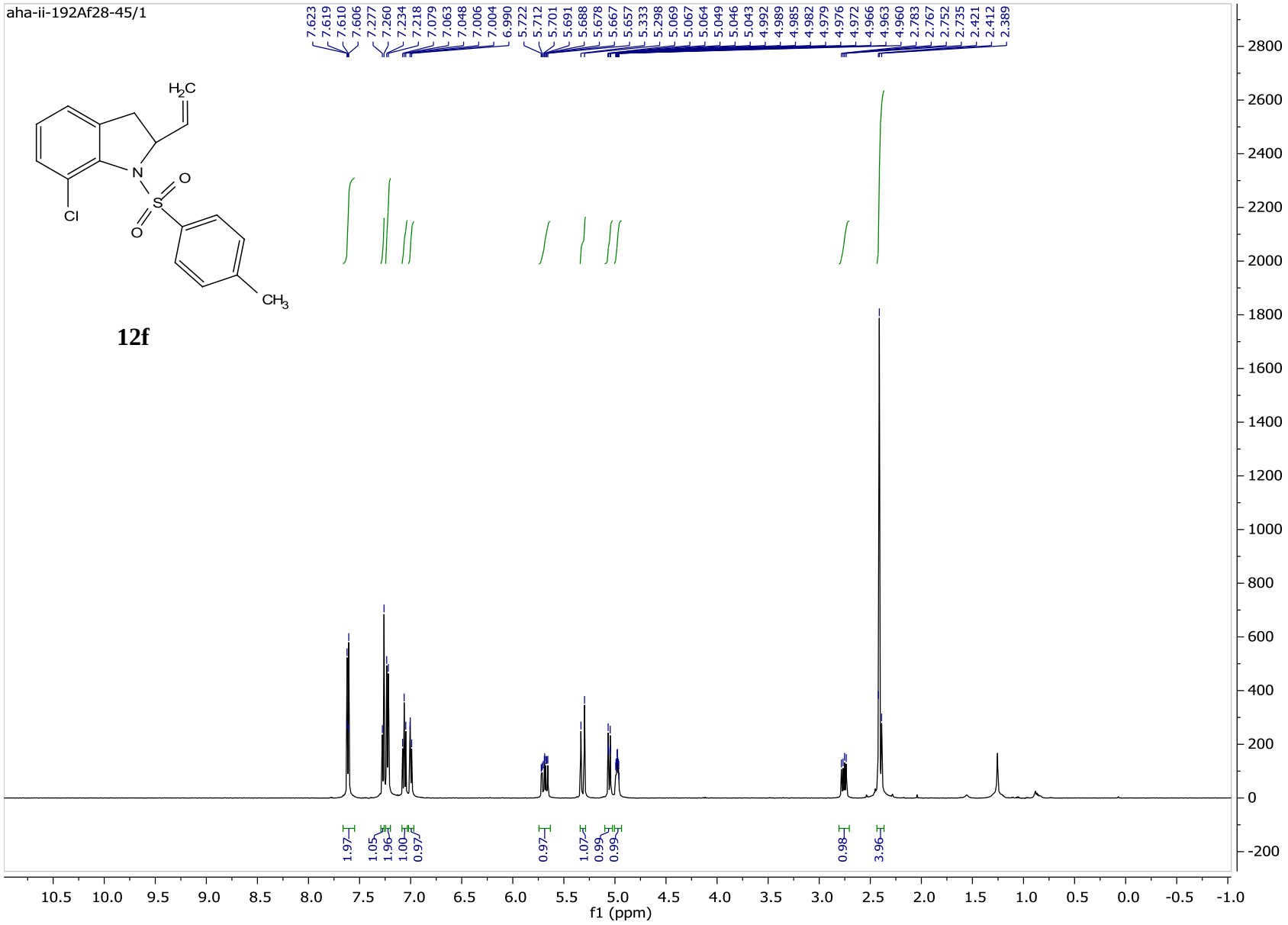
aha-ii-192Af28-45/1
7.623
7.619
7.610
7.606
7.277
7.260
7.234
7.218
7.079
7.063
7.048
7.006
7.004
6.990
5.722
5.712
5.701
5.691
5.688
5.678
5.667
5.657
5.333
5.298
5.069
5.067
5.064
5.049
5.046
5.043
4.992
4.989
4.985
4.982
4.979
4.976
4.972
4.966
4.963
4.960
2.783
2.767
2.752
2.735
2.421
2.412
2.389
H2C
N
O
S
O
Cl
CH3
12f
1.97
1.05
1.96
1.00
0.97
0.97
1.07
0.99
0.99
0.98
3.96
f1 (ppm)

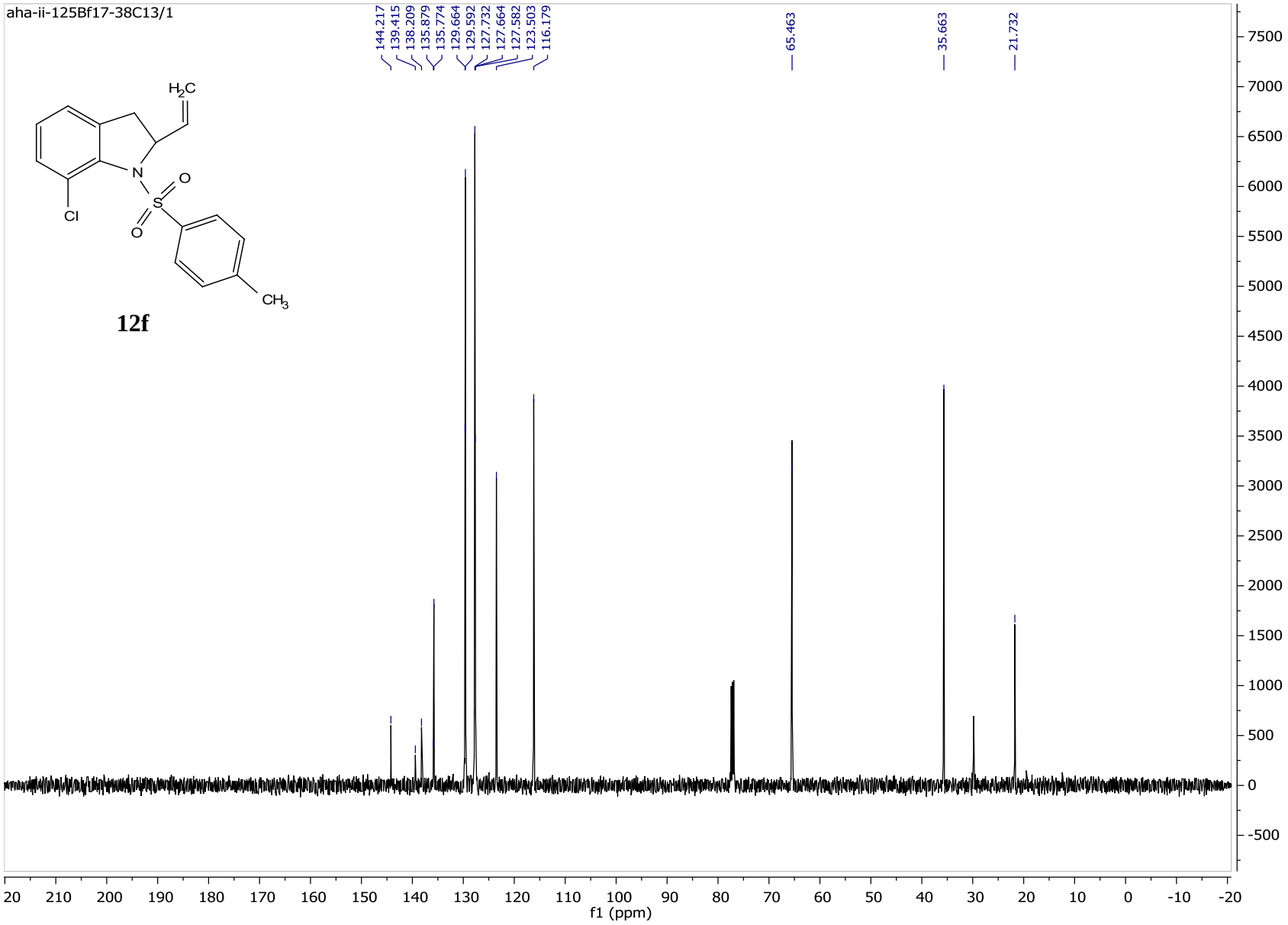
aha-ii-125Bf17-38C13/1
144.217
139.415
138.209
135.879
135.774
129.664
129.592
127.732
127.664
127.582
123.503
116.179
65.463
35.663
21.732
H2C
N
O
S
O
Cl
CH3
12f
f1 (ppm)

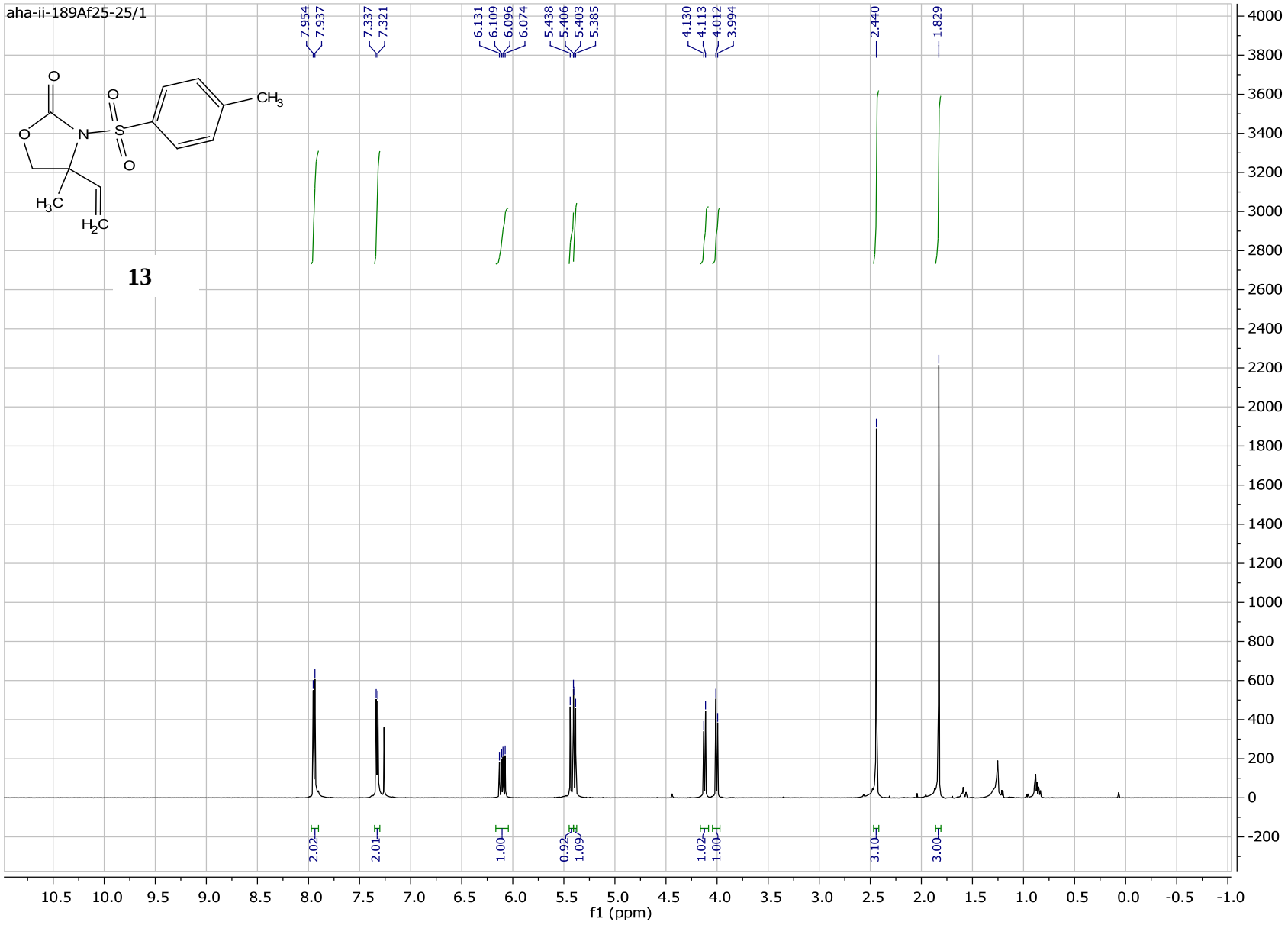
aha-ii-189Af25-25/1
7.954
7.937
7.337
7.321
6.131
6.109
6.096
6.074
5.438
5.406
5.403
5.385
4.130
4.113
4.012
3.994
2.440
1.829
CH3
H3C
H2C
13
2.02
2.01
1.00
0.92
1.09
1.02
1.00
3.10
3.00
f1 (ppm)

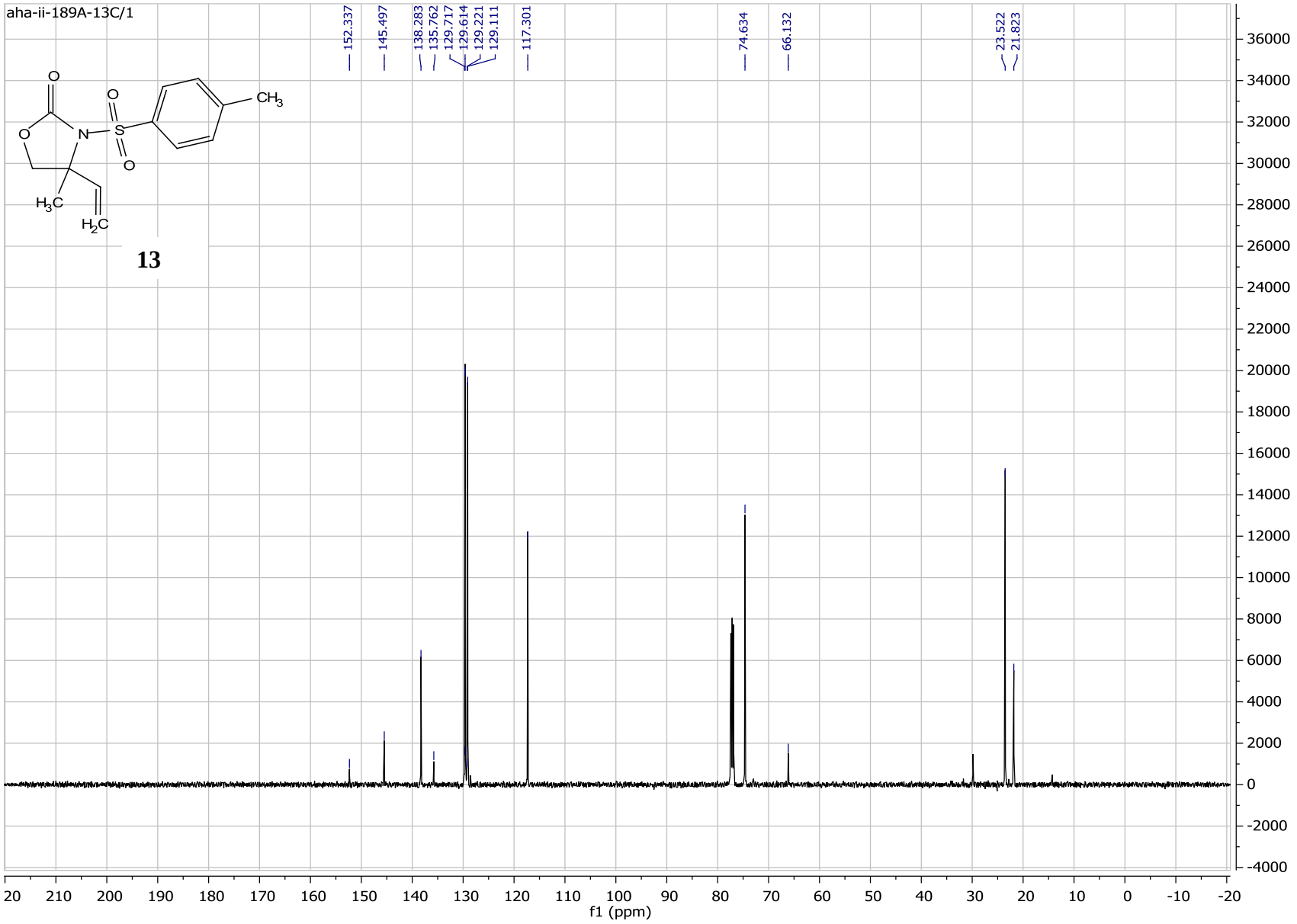
aha-ii-189A-13C/1
152.337
145.497
138.283
135.762
129.717
129.614
129.221
129.111
117.301
74.634
66.132
23.522
21.823
CH3
H3C
H2C
13
f1 (ppm)

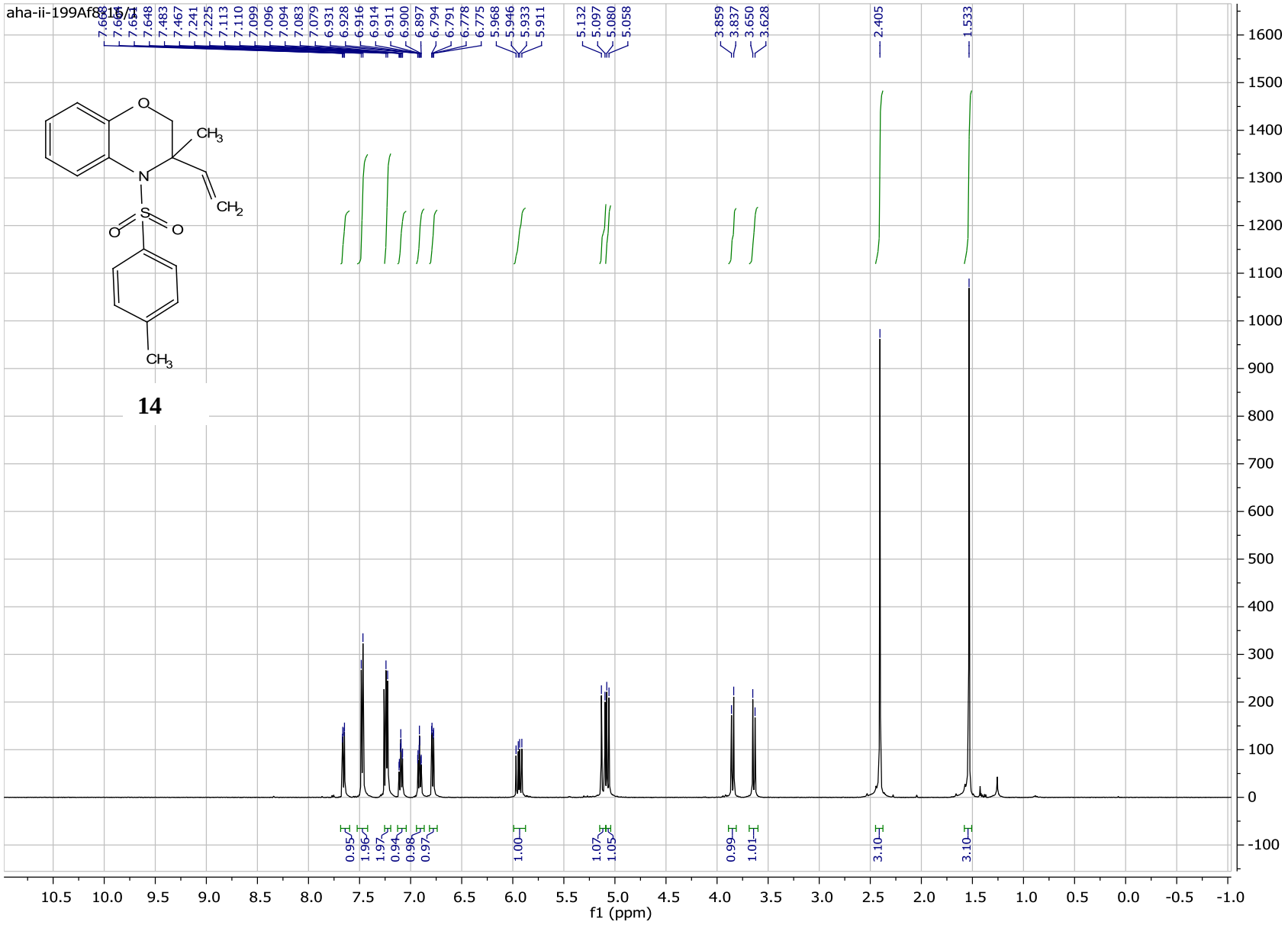
aha-ii-199Af8516/1
7.683
7.667
7.651
7.648
7.483
7.467
7.241
7.225
7.113
7.110
7.099
7.096
7.094
7.083
7.079
6.931
6.928
6.916
6.914
6.911
6.900
6.897
6.794
6.791
6.778
6.775
5.968
5.946
5.933
5.911
5.132
5.097
5.080
5.058
3.859
3.837
3.650
3.628
2.405
1.533
O
CH3
N
S
O
O
CH2
CH3
14
0.95
1.96
1.97
0.94
0.98
0.97
1.00
1.07
1.05
0.99
1.01
3.10
3.10
f1 (ppm)

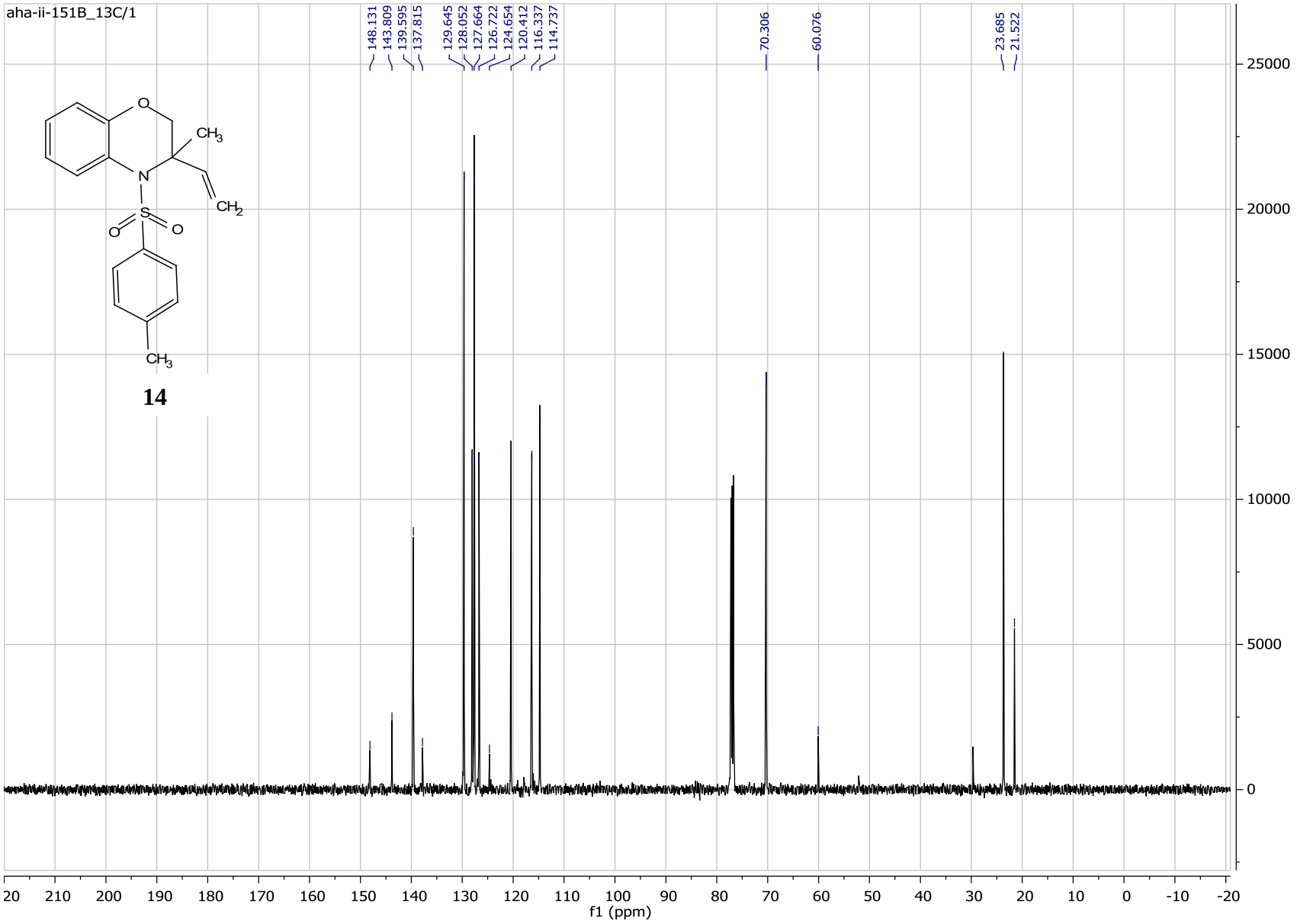
aha-ii-151B_13C/1
148.131
143.809
139.595
137.815
129.645
128.052
127.664
126.722
124.654
120.412
116.337
114.737
70.306
60.076
23.685
21.522
O
CH3
N
S
O
O
CH2
CH3
14
25000
20000
15000
10000
5000
0
20 210 200 190 180 170 160 150 140 130 120 110 100 90 80 70 60 50 40 30 20 10 0 -10 -20
f1 (ppm)

aha-iii-140Bf13-22.1.fid

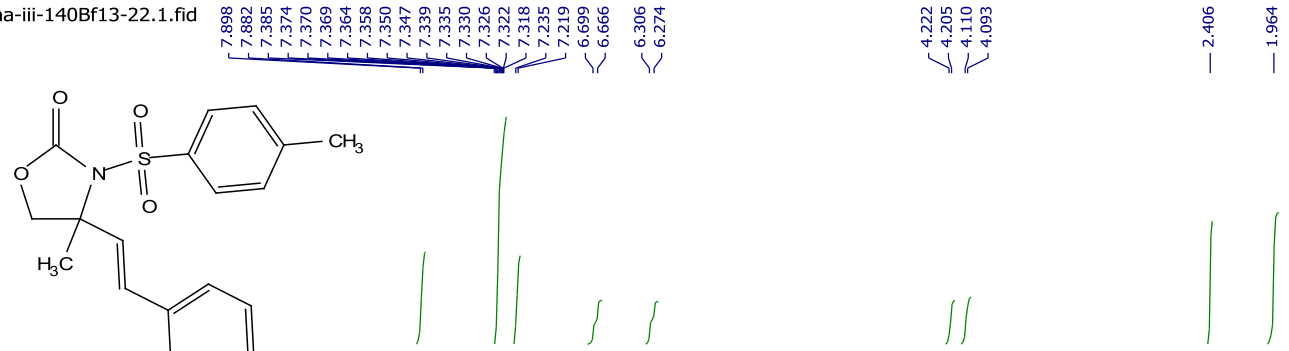

17

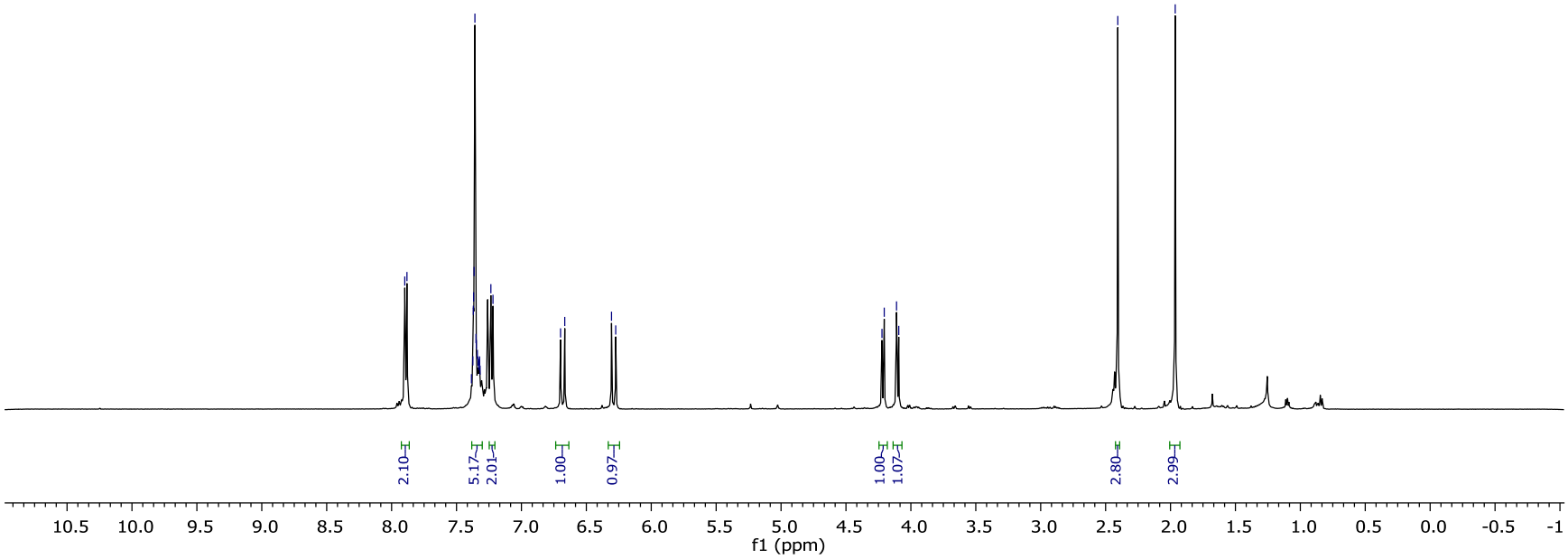

aha-iii-140B_13C.1.fid

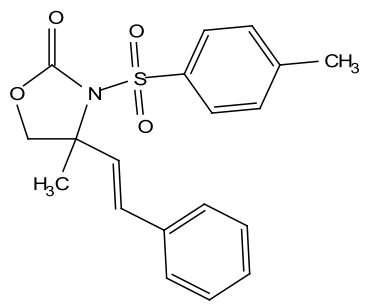

17

aha-iii-18Aflush1.1.fid

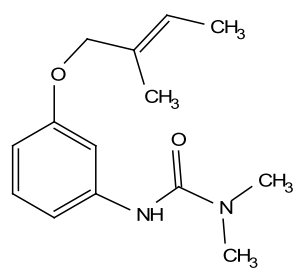

21

aha-iii-18Aflush_13C.1.fid

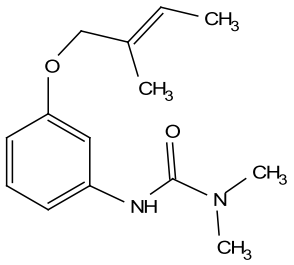

21

159.771
155.696
140.499
131.882
129.503
123.395
111.856
109.918
106.243
74.173
36.605
13.788
13.409

f1 (ppm)

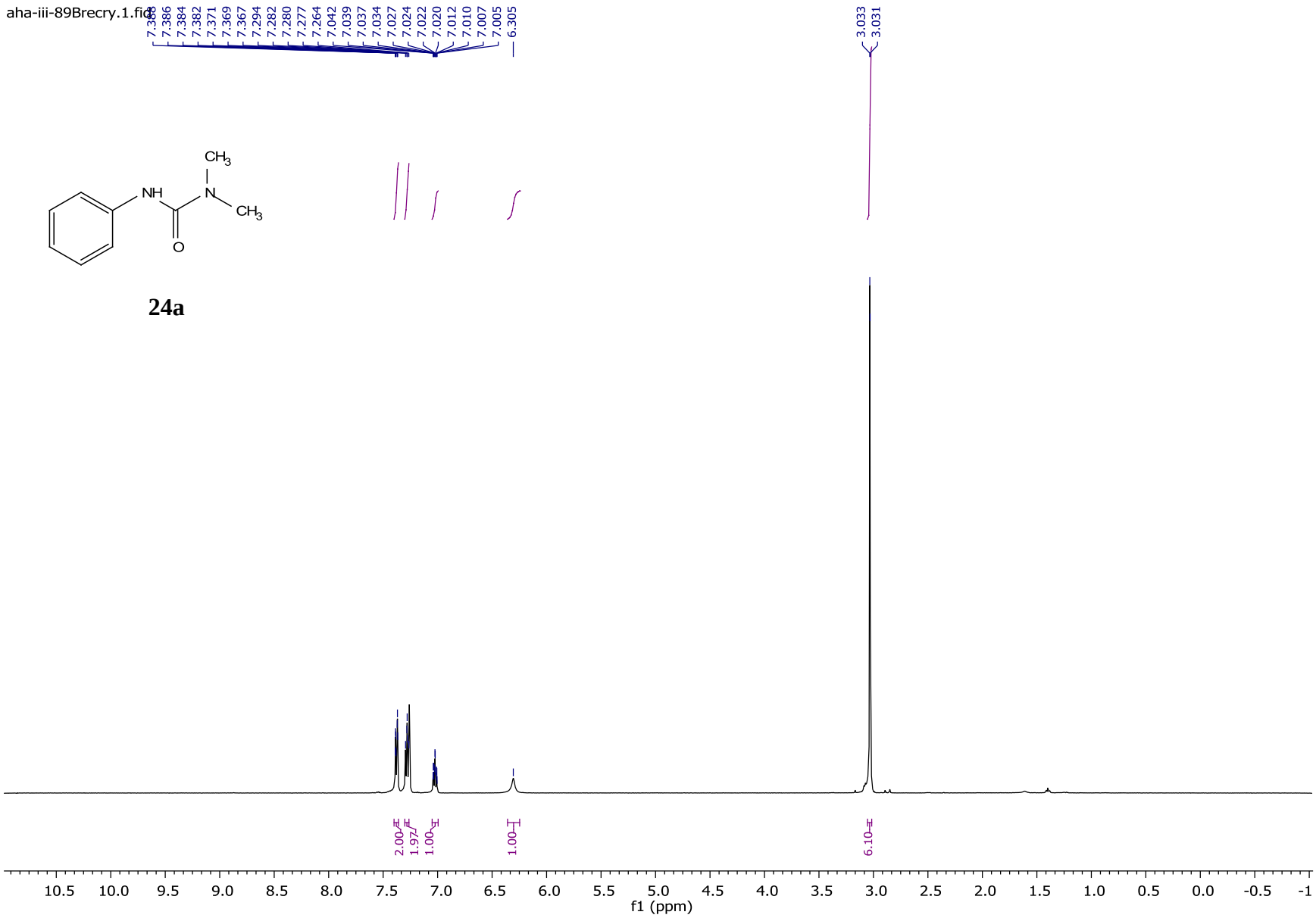
aha-iii-89Brecry.1.fid
7.388
7.386
7.384
7.382
7.371
7.369
7.367
7.294
7.282
7.280
7.277
7.264
7.042
7.039
7.037
7.034
7.027
7.024
7.022
7.020
7.012
7.010
7.007
7.005
6.305
3.033
3.031
CH3
NH
N
CH3
O
2.00
1.97
1.00
1.00
6.10
10.5
10.0
9.5
9.0
8.5
8.0
7.5
7.0
6.5
6.0
5.5
5.0
4.5
4.0
3.5
3.0
2.5
2.0
1.5
1.0
0.5
0.0
-0.5
-1
f1 (ppm)

24a

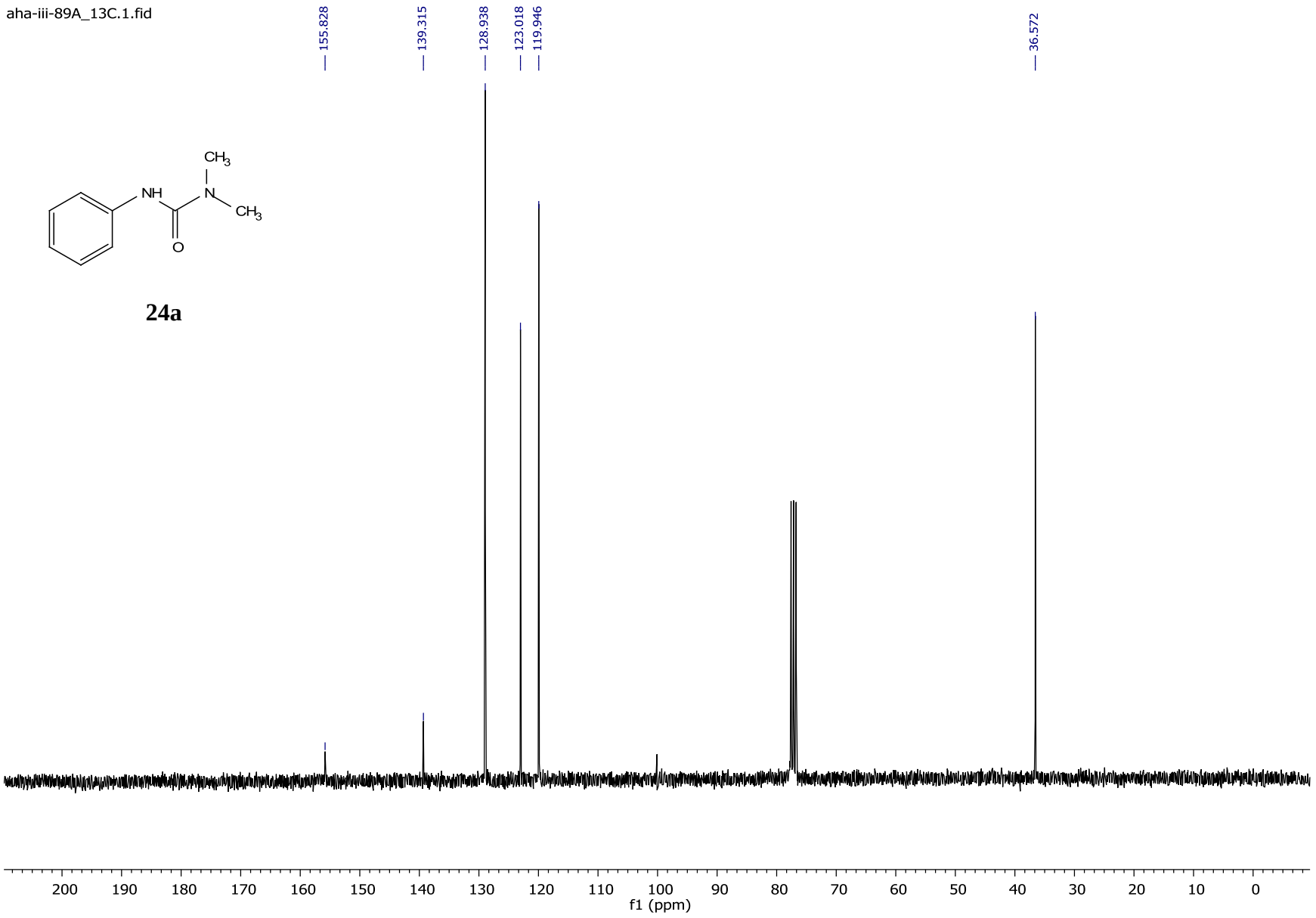
aha-iii-89A_13C.1.fid
155.828
139.315
128.938
123.018
119.946
36.572
NH
N
CH3
CH3
O
24a
200
190
180
170
160
150
140
130
120
110
100
90
80
70
60
50
40
30
20
10
0
f1 (ppm)

aha-iii-42Brecrys.1.fid

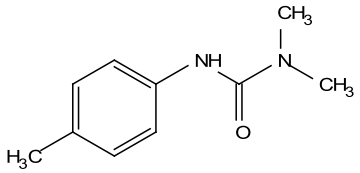

24b

aha-iii-42B_13C.1.fid

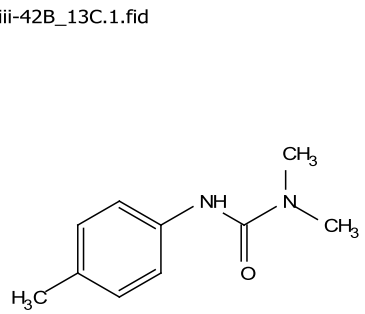

24b

aha-iii-65Af22-55a.1.fid

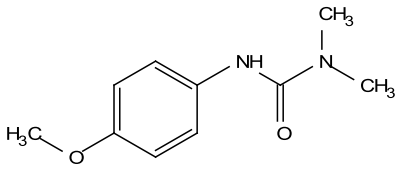

24c

aha-iii-123A_13C.1.fid

156.324
155.833
132.341
122.379
114.139
55.612
36.533

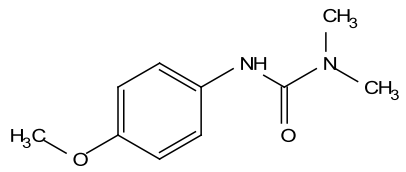

24c

aha-iii-88Af37-flush.1.fid

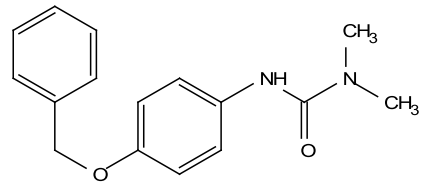

24d

aha-iii-88A_13C.1.fid

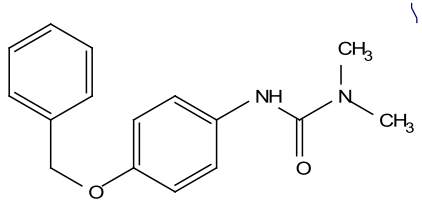

24d

aha-iii-68Drecry1.1.fid

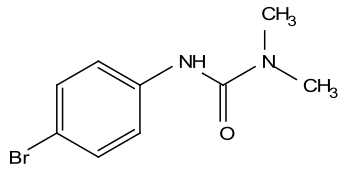

24e

aha-iii-68D_13C.1.fid

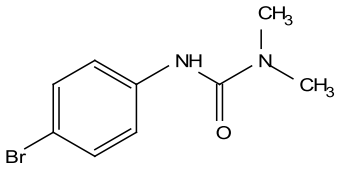

24e

aha-iii-110B.1.fid

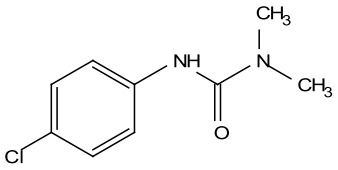

24f

aha-iii-110B_13Cx.1.fid

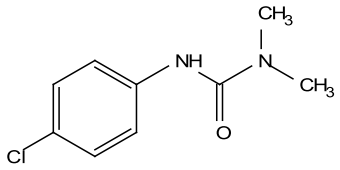

24f

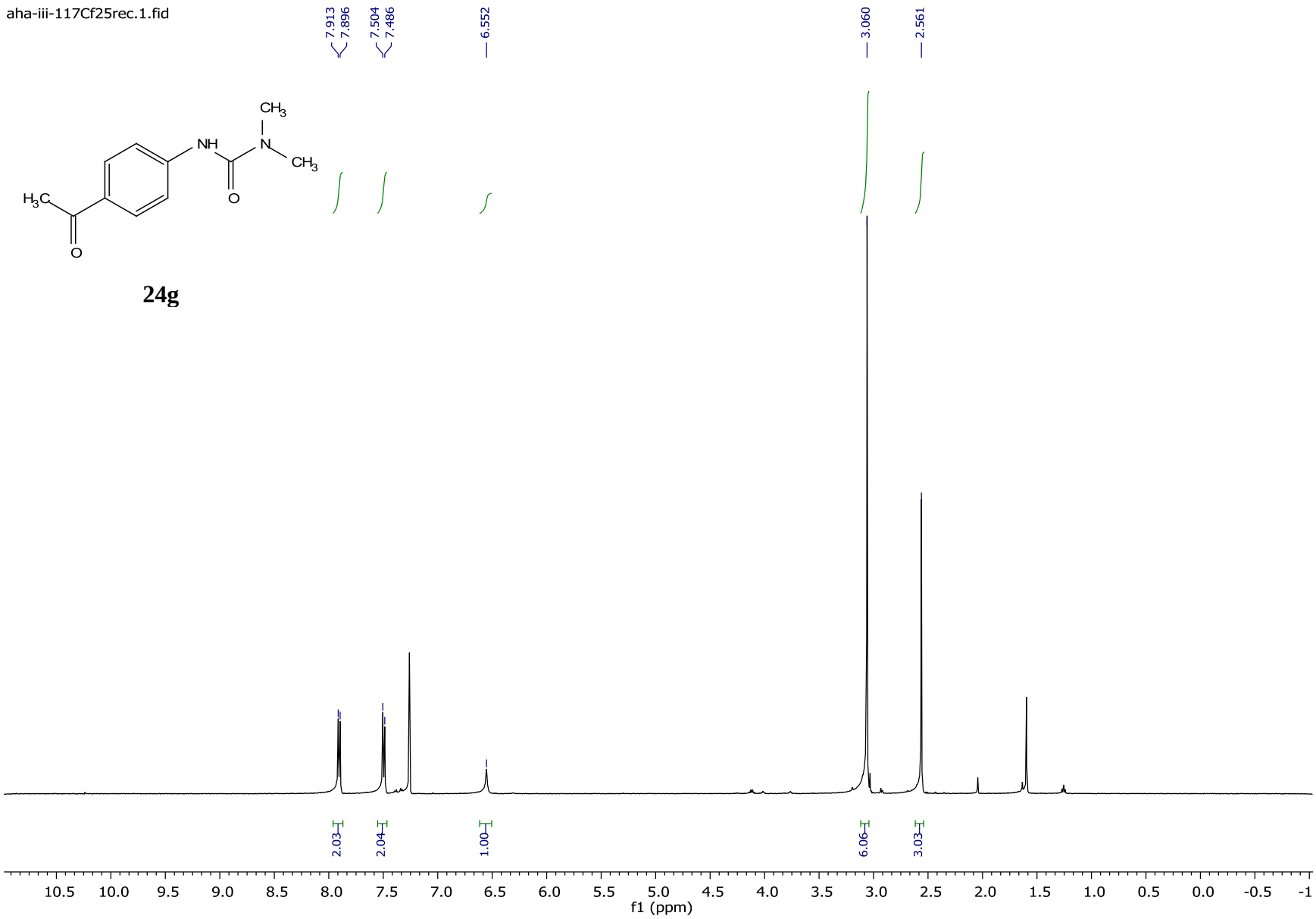
aha-iii-117Cf25rec.1.fid
7.913
7.896
7.504
7.486
6.552
3.060
2.561
CH3
NH
N
CH3
H3C
O
O
2.03
2.04
1.00
6.06
3.03
10.5 10.0 9.5 9.0 8.5 8.0 7.5 7.0 6.5 6.0 5.5 5.0 4.5 4.0 3.5 3.0 2.5 2.0 1.5 1.0 0.5 0.0 -0.5 -1
f1 (ppm)

24g

aha-iii-11[illegible]C_13C.1.fid

197.194
155.122
144.101
131.620
129.811
118.489
36.651
26.497

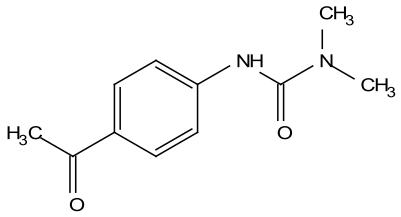

24g

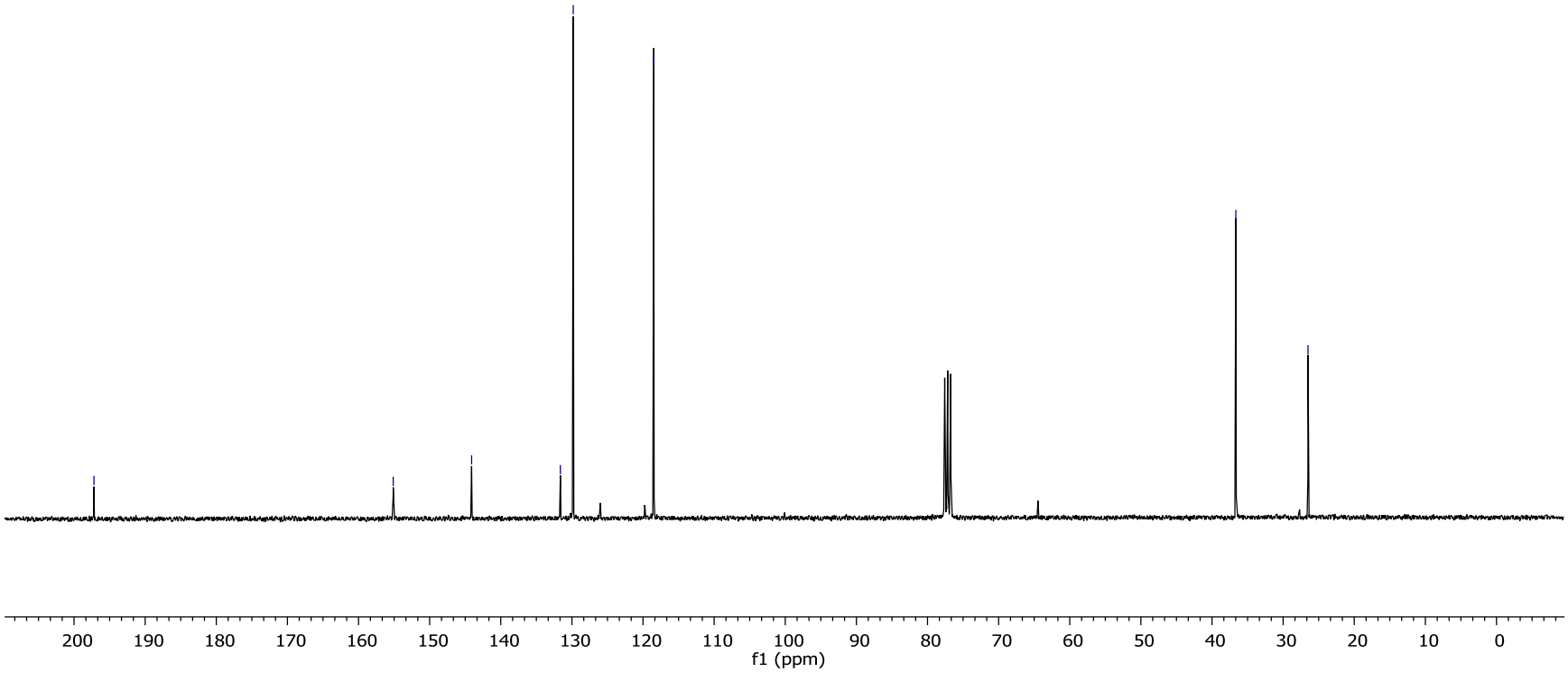

aha-iii-108Af38-64.1.fid

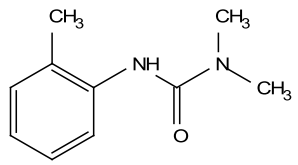

24h

aha-iii-108A_13C.1.fid

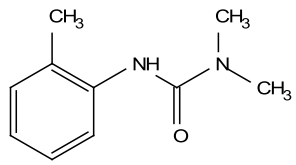

24h

aha-iii-84Bf15-40.1.fid

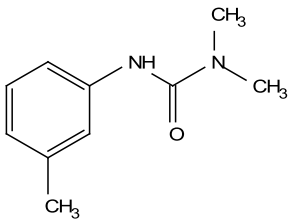

24i

aha-iii-84B_13C.1.fid

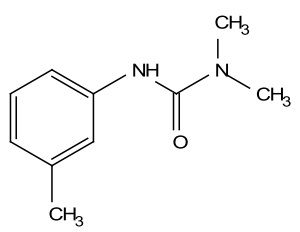

24i

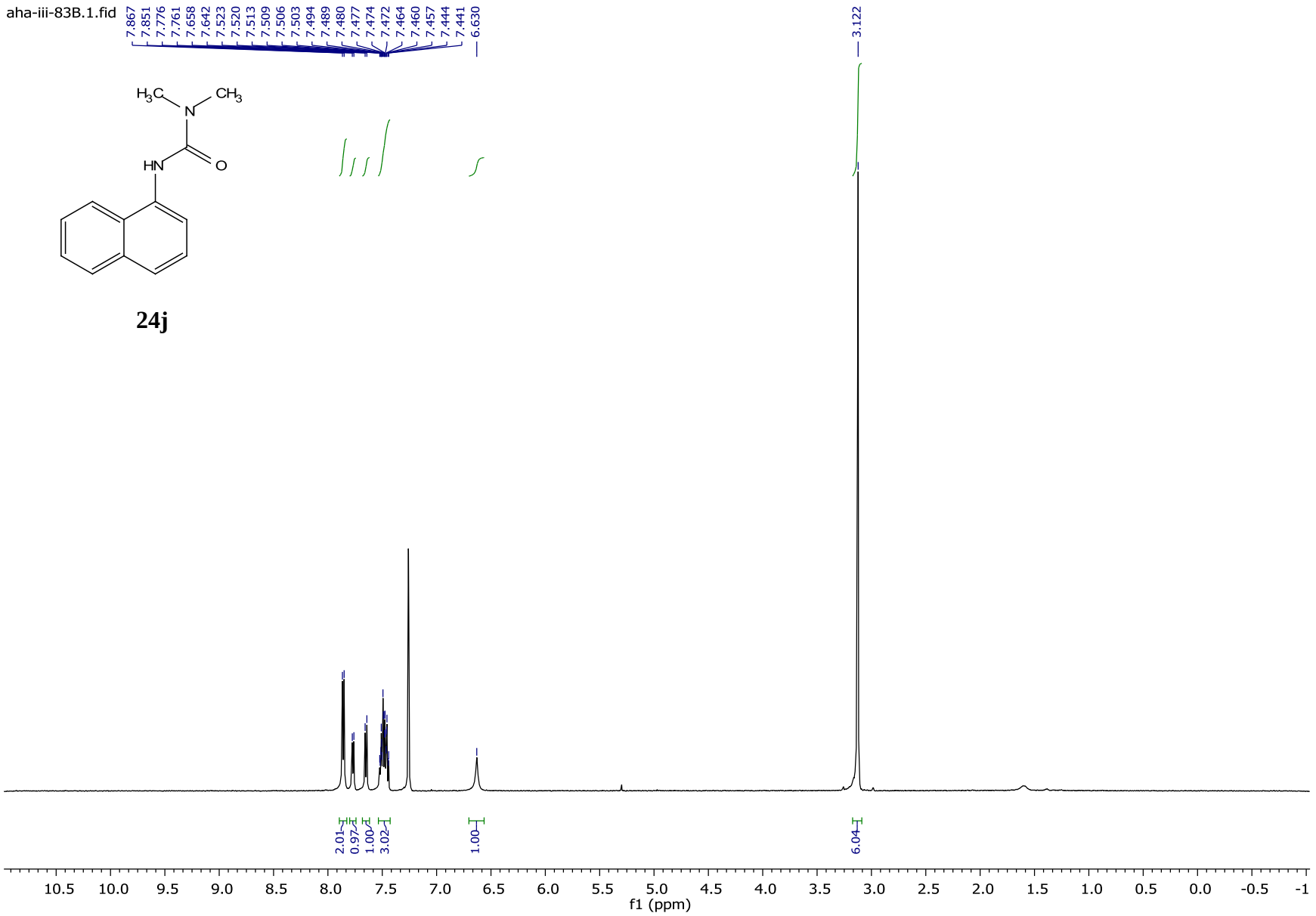
aha-iii-83B.1.fid
7.867
7.851
7.776
7.761
7.658
7.642
7.523
7.520
7.513
7.509
7.506
7.503
7.494
7.489
7.480
7.477
7.474
7.472
7.464
7.460
7.457
7.444
7.441
6.630
3.122
H3C
N
CH3
HN
O
2.01
0.97
1.00
3.02
1.00
6.04
10.5
10.0
9.5
9.0
8.5
8.0
7.5
7.0
6.5
6.0
5.5
5.0
4.5
4.0
3.5
3.0
2.5
2.0
1.5
1.0
0.5
0.0
-0.5
-1
f1 (ppm)

24j

aha-iii-83B_13C.1.fid

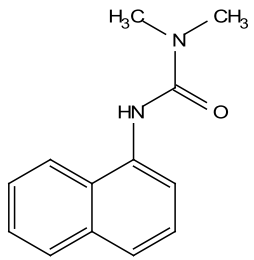

24j

aha-iii-131Af12-51.1.fid

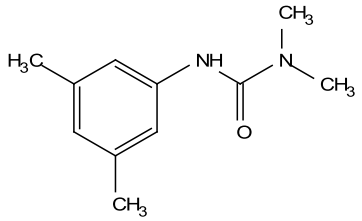

24k

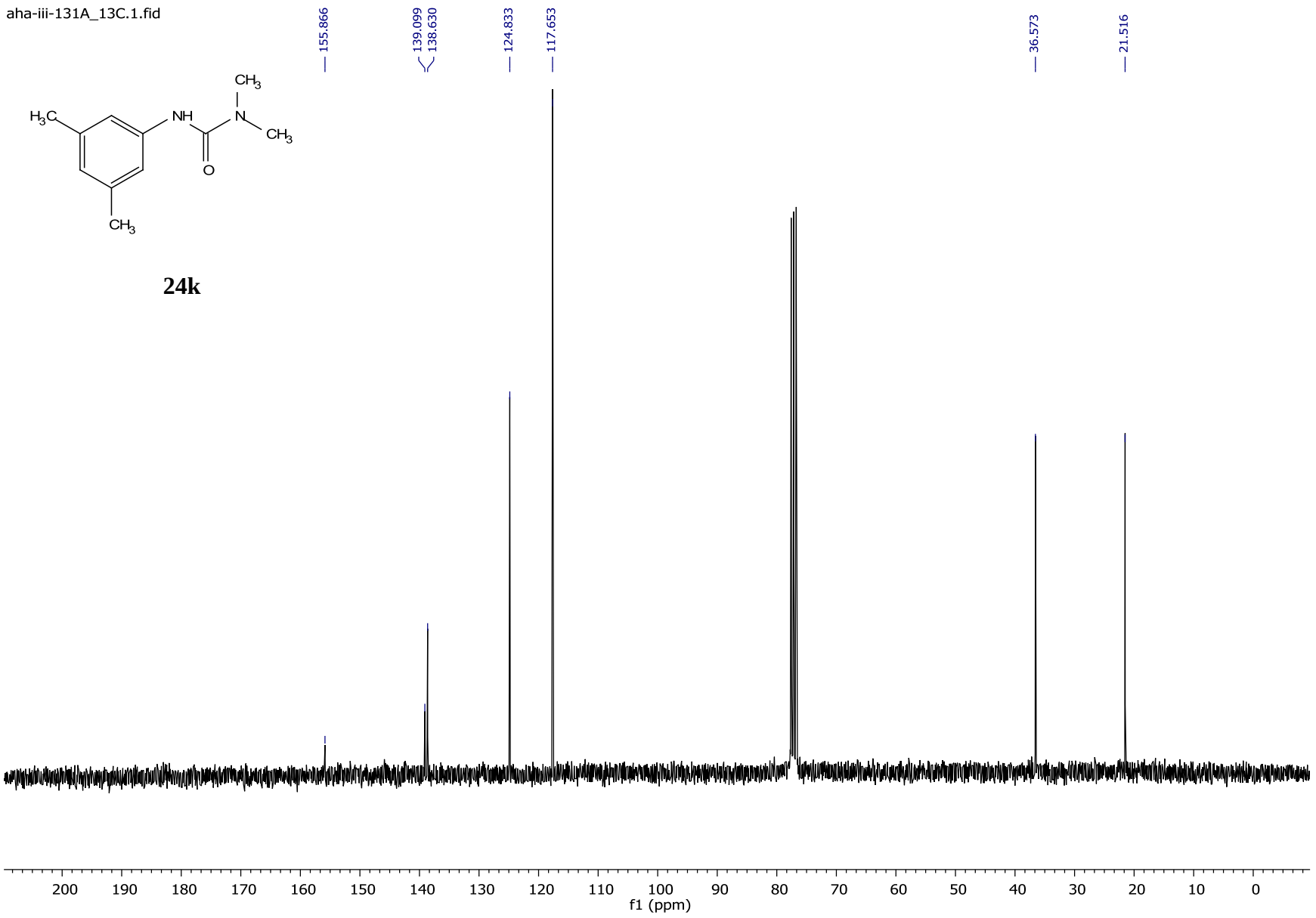
aha-iii-131A_13C.1.fid
155.866
139.099
138.630
124.833
117.653
36.573
21.516
CH3
H3C
NH
N
CH3
O
CH3
24k
200
190
180
170
160
150
140
130
120
110
100
90
80
70
60
50
40
30
20
10
0
f1 (ppm)

aha-iii-105Bf16-56.1.fid

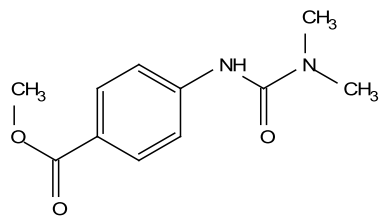

24l

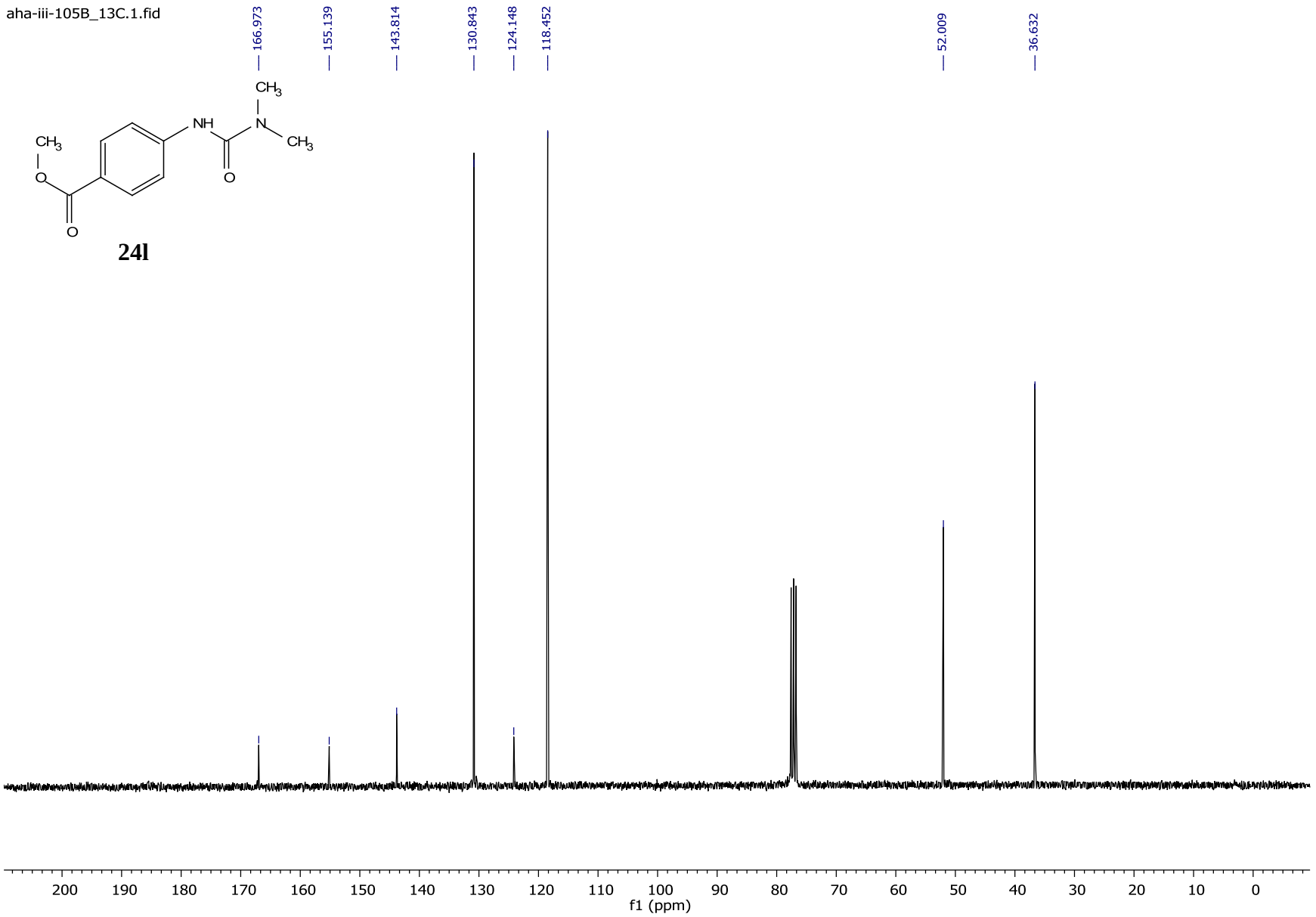
aha-iii-105B_13C.1.fid
166.973
155.139
143.814
130.843
124.148
118.452
52.009
36.632
CH3
NH
N
CH3
CH3
O
O
O
24l
200
190
180
170
160
150
140
130
120
110
100
90
80
70
60
50
40
30
20
10
0
f1 (ppm)

aha-iii-52Af20-55.1.fid

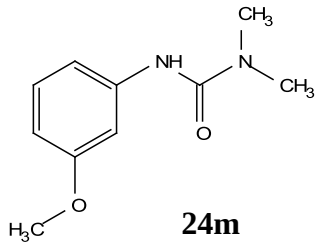

24m

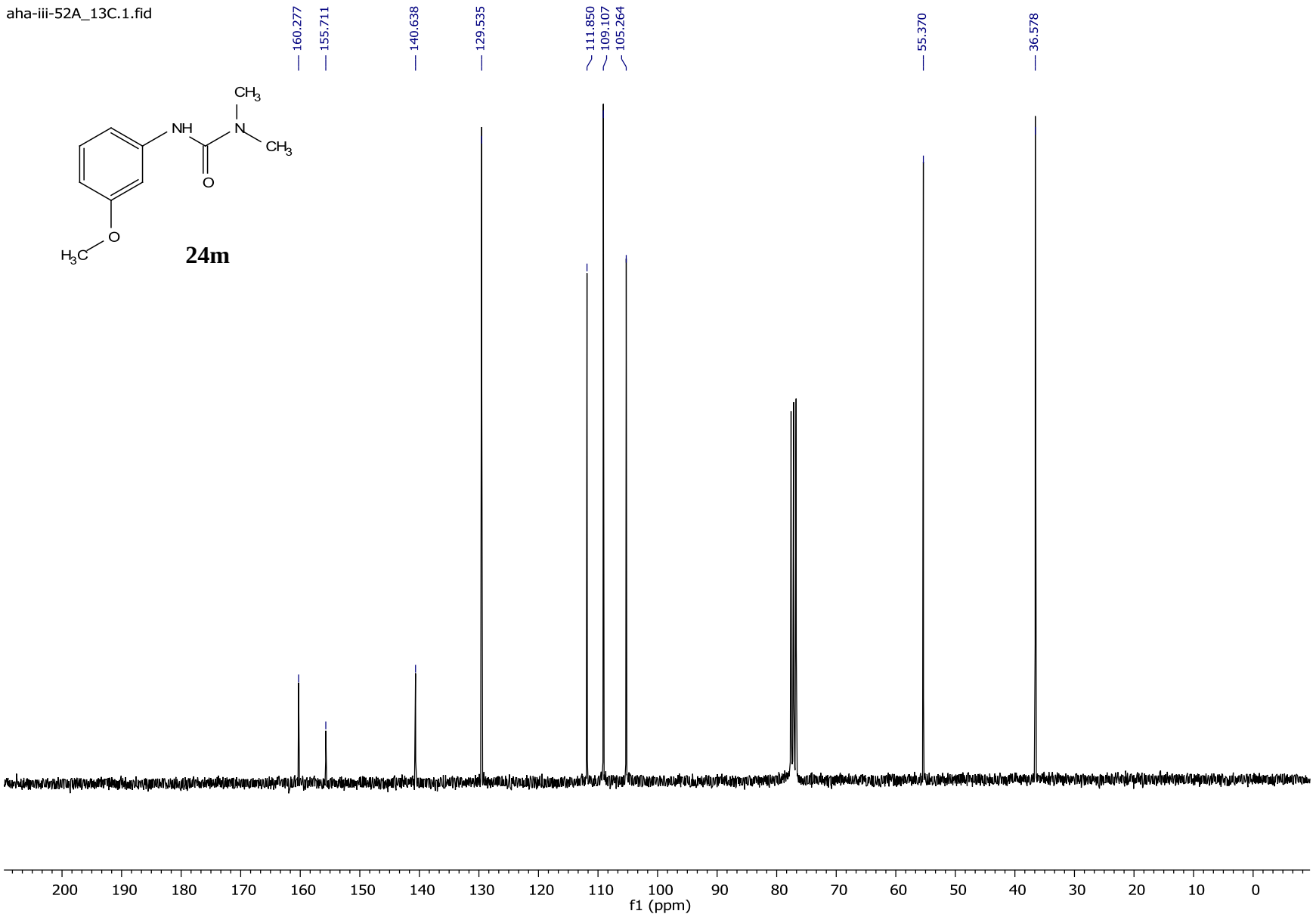
aha-iii-52A_13C.1.fid
160.277
155.711
140.638
129.535
111.850
109.107
105.264
55.370
36.578
NH
N
CH3
CH3
O
O
H3C
24m
200
190
180
170
160
150
140
130
120
110
100
90
80
70
60
50
40
30
20
10
0
f1 (ppm)

aha-iii-115Bf20-42.1.fid

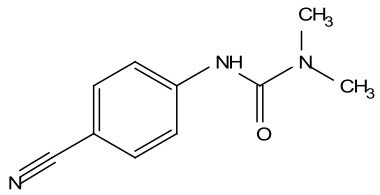

24n

aha-iii-115B_13C.1.fid

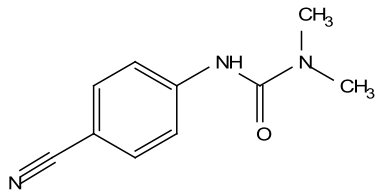

24n

aha-iii-109Brecry.1.fid

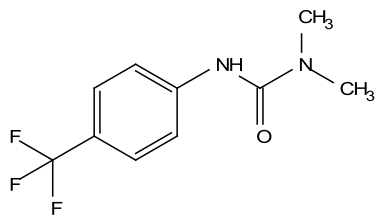

24o

aha-iii-109B_13C.1.fid

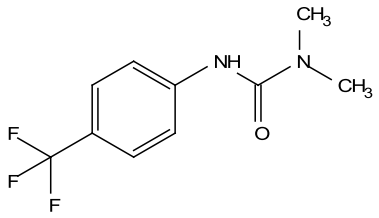

24o

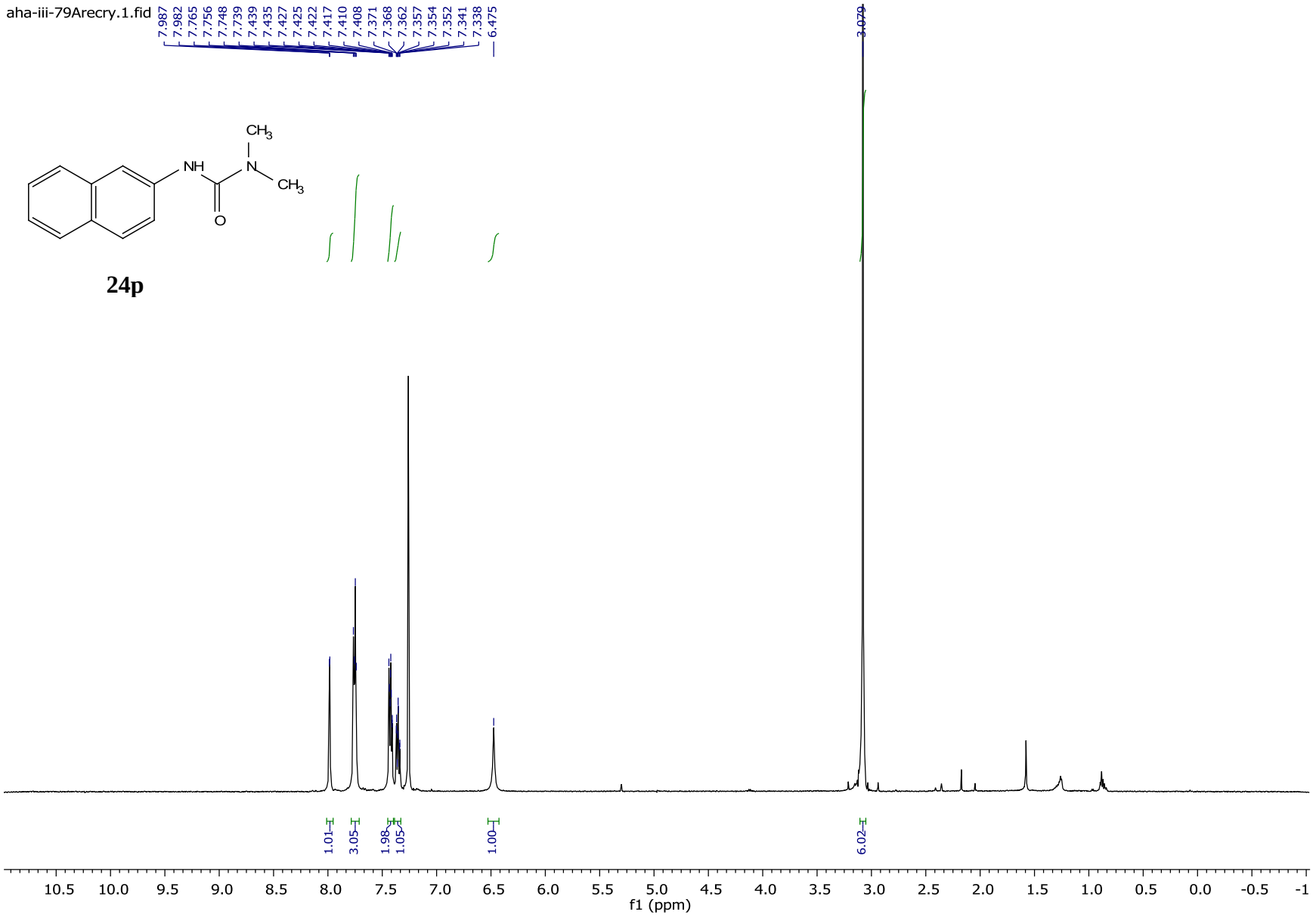
aha-iii-79Arecry.1.fid
7.987
7.982
7.765
7.756
7.748
7.739
7.439
7.435
7.427
7.425
7.422
7.417
7.410
7.408
7.371
7.368
7.362
7.357
7.354
7.352
7.341
7.338
6.475
3.079
CH3
NH
N
CH3
O
1.01
3.05
1.98
1.05
1.00
6.02
10.5
10.0
9.5
9.0
8.5
8.0
7.5
7.0
6.5
6.0
5.5
5.0
4.5
4.0
3.5
3.0
2.5
2.0
1.5
1.0
0.5
0.0
-0.5
-1
f1 (ppm)

24p

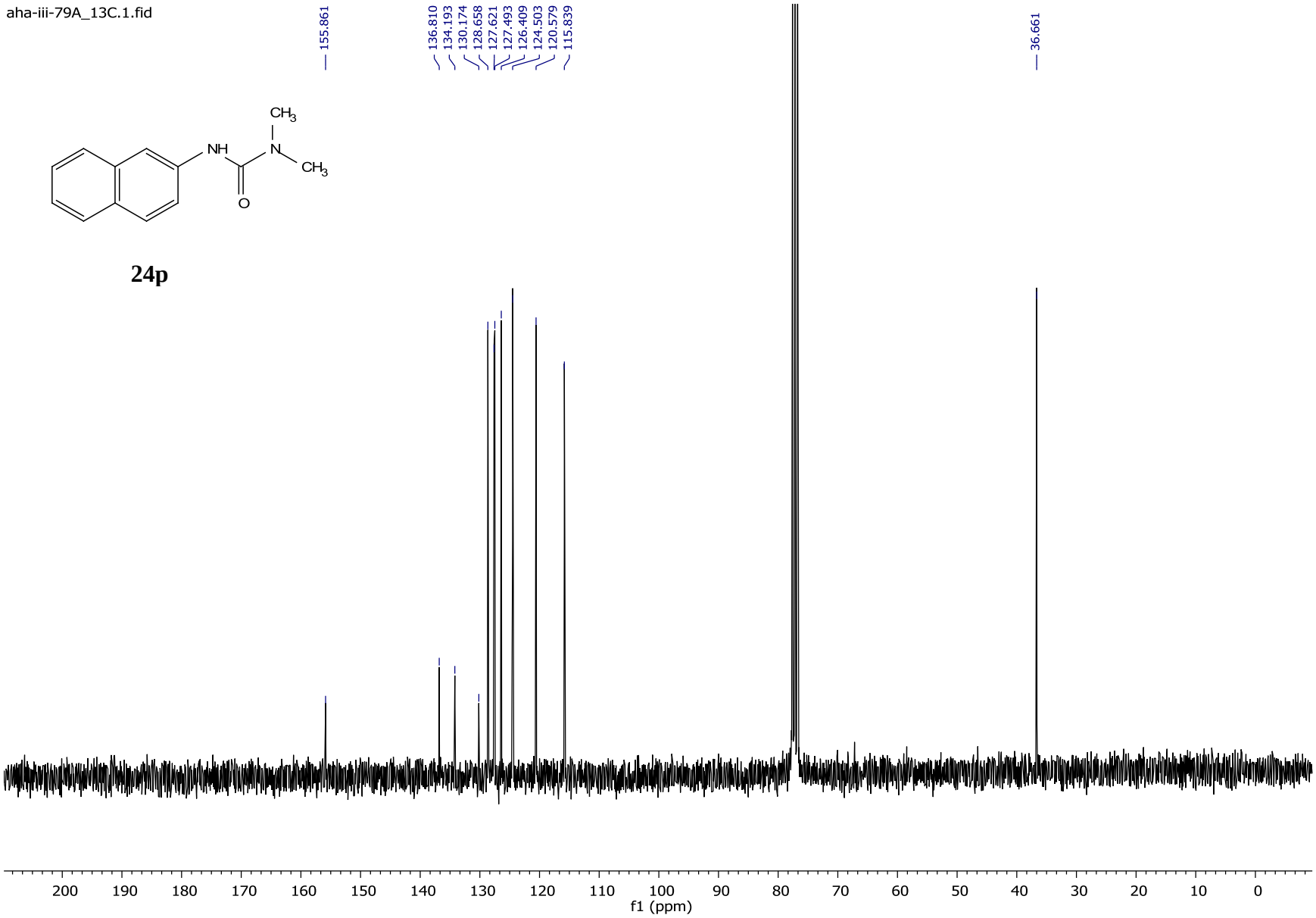
aha-iii-79A_13C.1.fid
155.861
136.810
134.193
130.174
128.658
127.621
127.493
126.409
124.503
120.579
115.839
36.661
NH
N
CH3
CH3
O
f1 (ppm)

24p

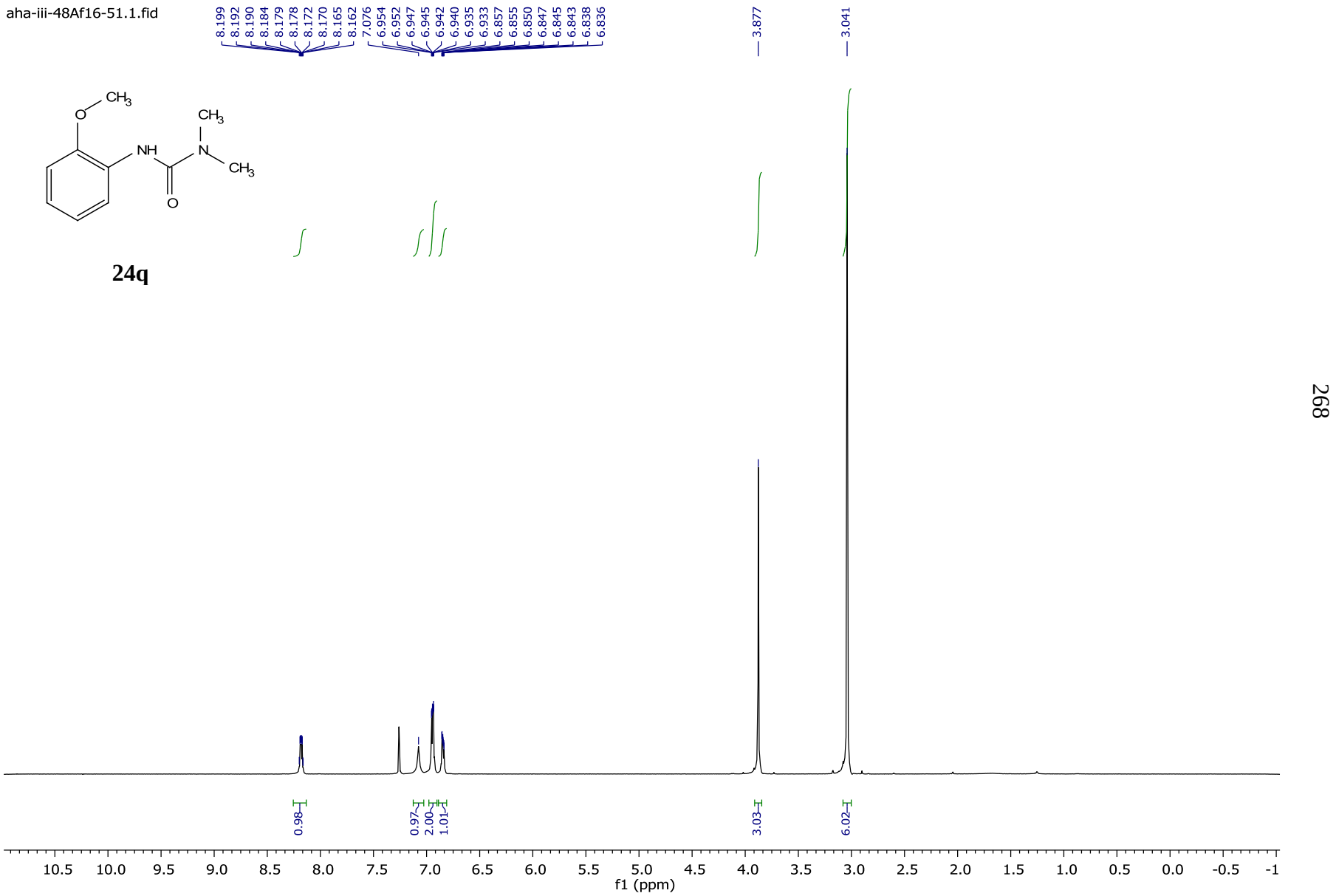
aha-iii-48Af16-51.1.fid
8.199
8.192
8.190
8.184
8.179
8.178
8.172
8.170
8.165
8.162
7.076
6.954
6.952
6.947
6.945
6.942
6.940
6.935
6.933
6.857
6.855
6.850
6.847
6.845
6.843
6.838
6.836
3.877
3.041
O
CH3
NH
N
CH3
CH3
O
0.98
0.97
2.00
1.01
3.03
6.02
10.5
10.0
9.5
9.0
8.5
8.0
7.5
7.0
6.5
6.0
5.5
5.0
4.5
4.0
3.5
3.0
2.5
2.0
1.5
1.0
0.5
0.0
-0.5
-1
f1 (ppm)

24q

aha-iii-48A_13C.1.fid

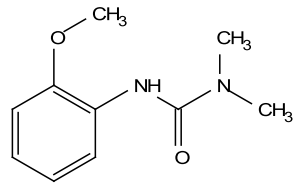

24q

aha-iii-83A.1.fid

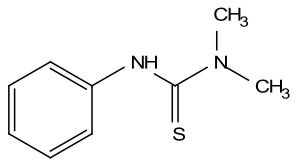

24r

aha-iii-83A_13C.1.fid

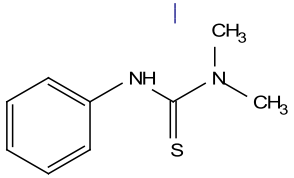

24r

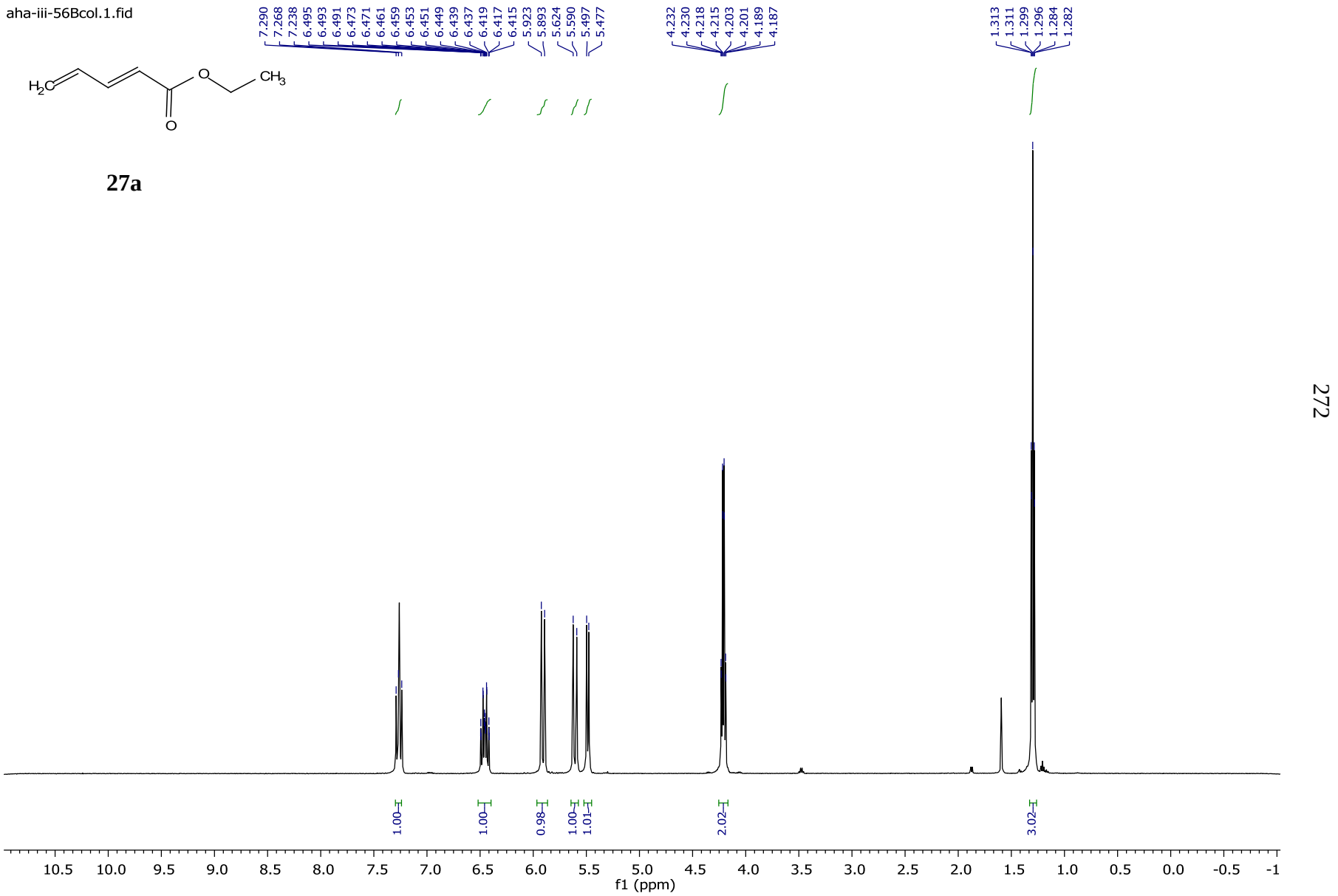
aha-iii-56Bcol.1.fid
7.290
7.268
7.238
6.495
6.493
6.491
6.473
6.471
6.461
6.459
6.453
6.451
6.449
6.439
6.437
6.419
6.417
6.415
5.923
5.893
5.624
5.590
5.497
5.477
4.232
4.230
4.218
4.215
4.203
4.201
4.189
4.187
1.313
1.311
1.299
1.296
1.284
1.282
H2C
O
O
CH3
1.00
1.00
0.98
1.00
1.01
2.02
3.02
10.5
10.0
9.5
9.0
8.5
8.0
7.5
7.0
6.5
6.0
5.5
5.0
4.5
4.0
3.5
3.0
2.5
2.0
1.5
1.0
0.5
0.0
-0.5
-1
f1 (ppm)

27a

aha-iii-94C_13C.1.fid

167.001
144.765
134.907
125.615
122.388
60.542
14.431

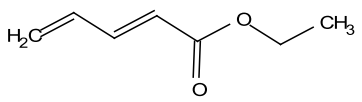

27a

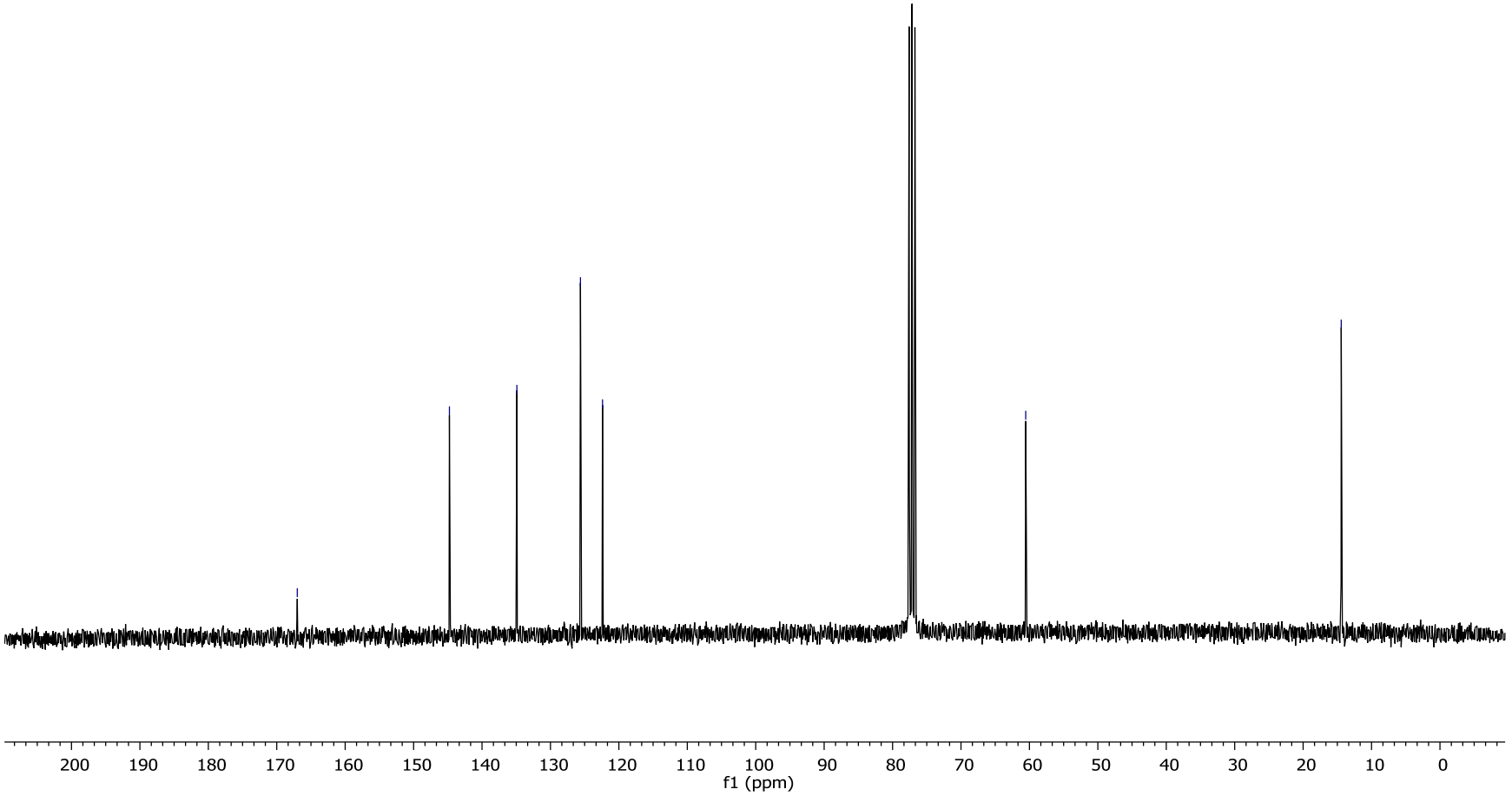

aha-iii-135C.1.fid

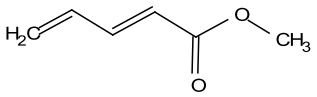

27b

aha-iii-135C_13C.1.fid

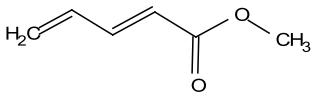

27b

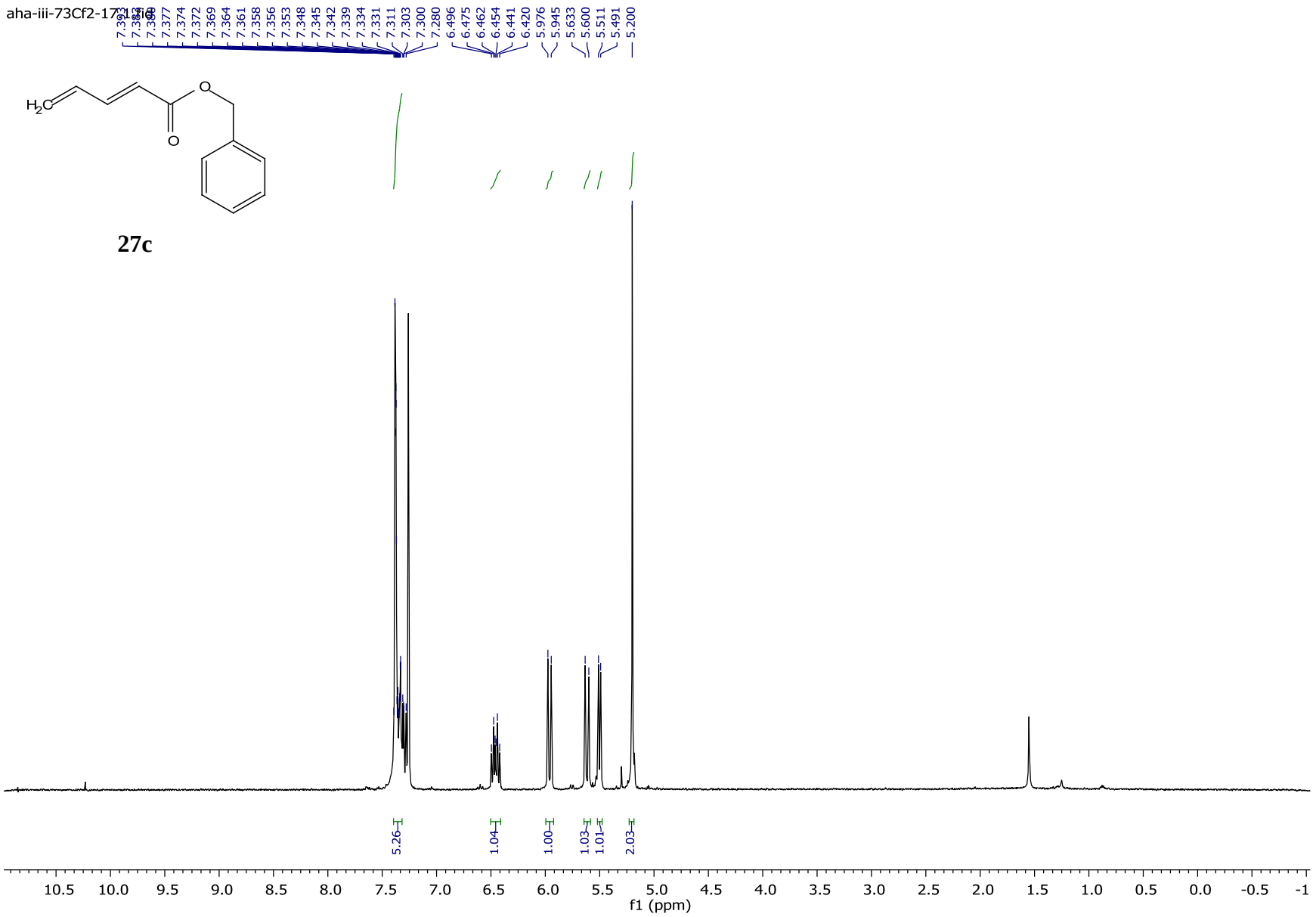
aha-iii-73Cf2-17-1H
7.391
7.386
7.382
7.377
7.374
7.372
7.369
7.364
7.361
7.358
7.356
7.353
7.348
7.345
7.342
7.339
7.334
7.331
7.311
7.303
7.300
7.280
6.496
6.475
6.462
6.454
6.441
6.420
5.976
5.945
5.633
5.600
5.511
5.491
5.200
H2C
O
O
5.26
1.04
1.00
1.03
1.01
2.03
10.5
10.0
9.5
9.0
8.5
8.0
7.5
7.0
6.5
6.0
5.5
5.0
4.5
4.0
3.5
3.0
2.5
2.0
1.5
1.0
0.5
0.0
-0.5
-1
f1 (ppm)

27c

aha-iii-120A_13Cx.1.fid

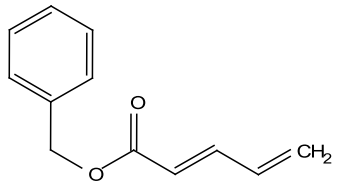

27c

aha-iii-114Bf12-40.1.fid

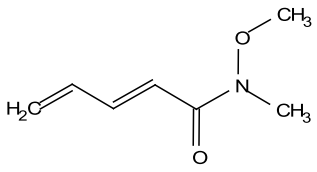

29

aha-iii-114B_13Cx.1.fid

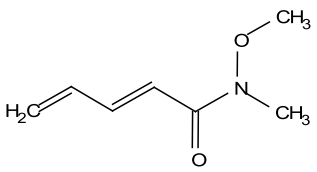

29

aha-iii-49Bf9-21.1.fid

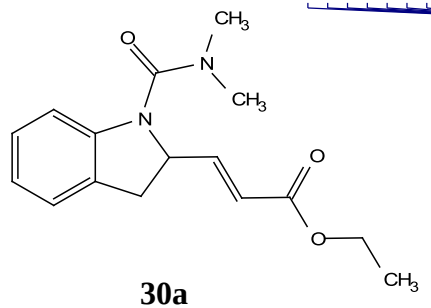

30a

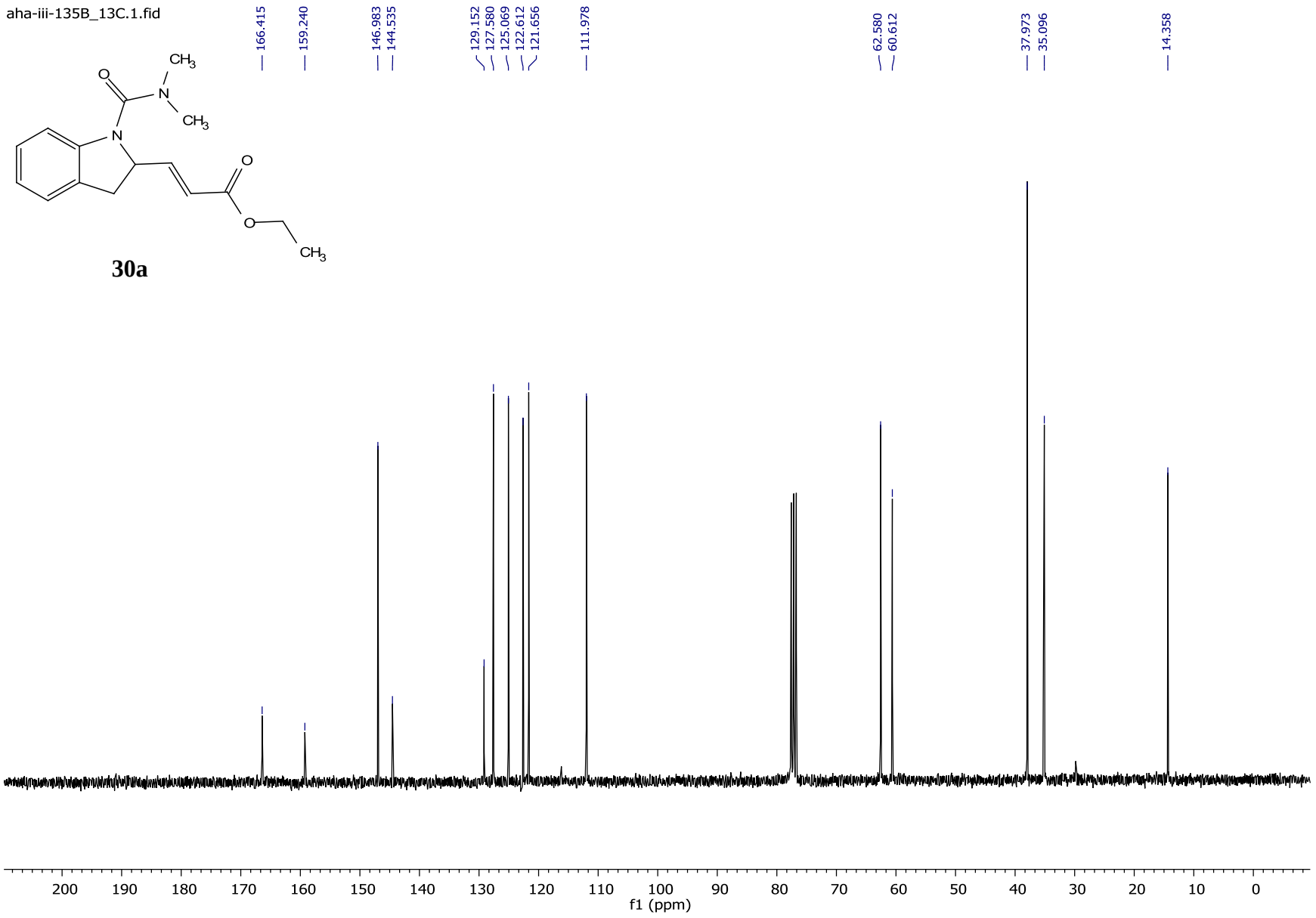
aha-iii-135B_13C.1.fid
166.415
159.240
146.983
144.535
129.152
127.580
125.069
122.612
121.656
111.978
62.580
60.612
37.973
35.096
14.358
f1 (ppm)

30a

aha-iii-58Df11-21.1.fid

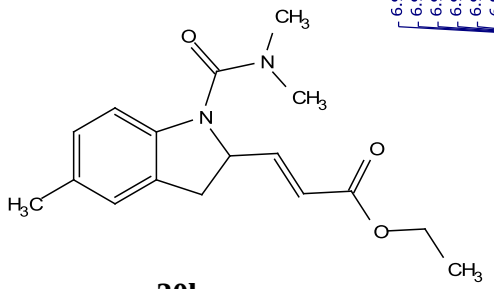

30b

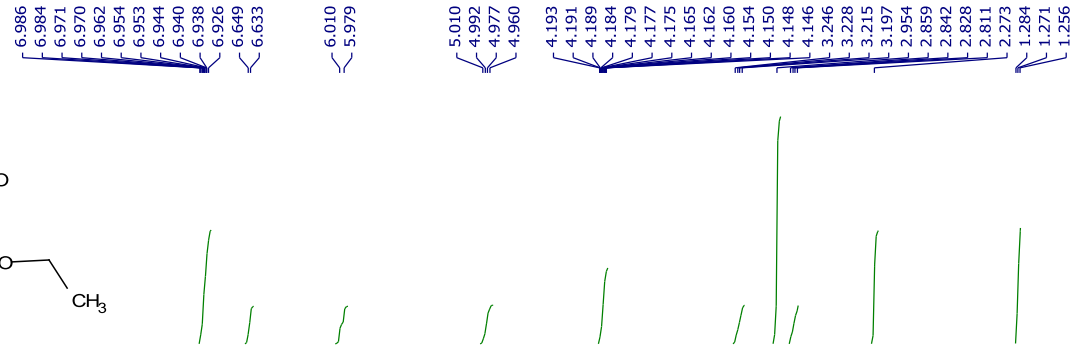

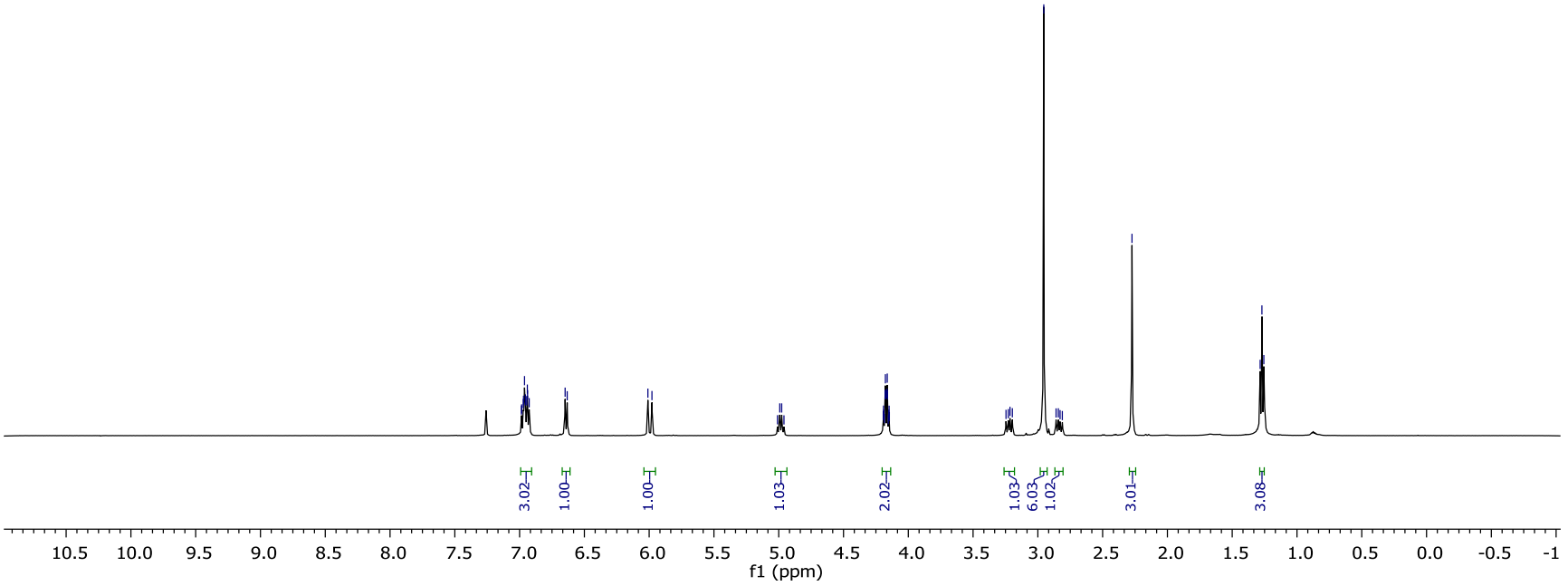

aha-iii-130A_13C.1.fid

166.448
159.431
147.152
142.139
131.196
129.295
127.836
125.828
122.413
111.864
62.608
60.575
38.022
35.069
20.874
14.355

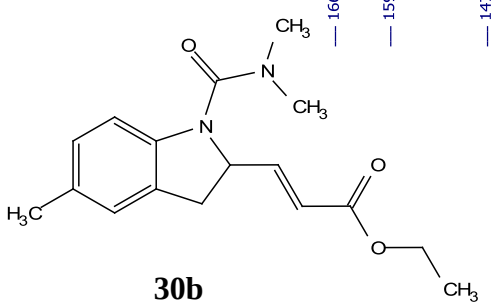

30b

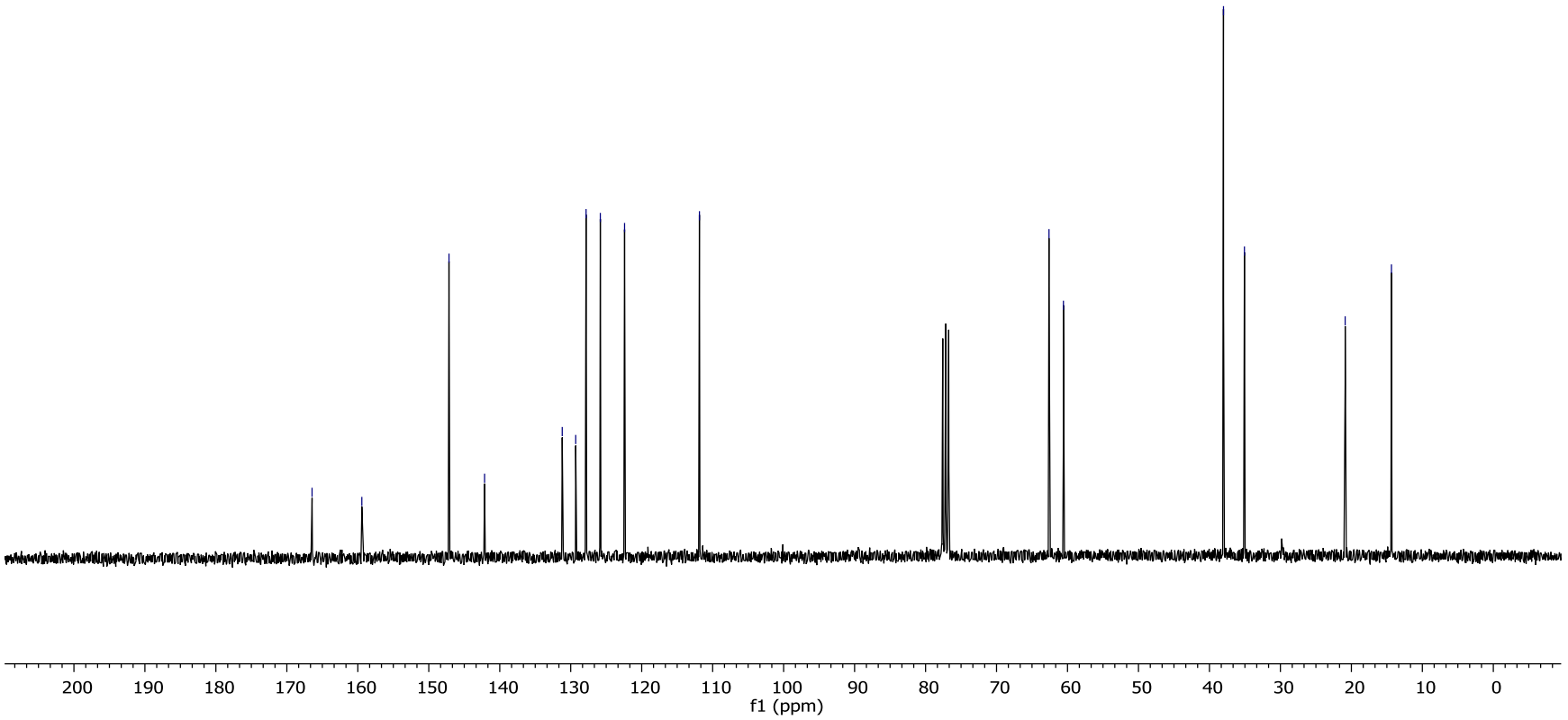

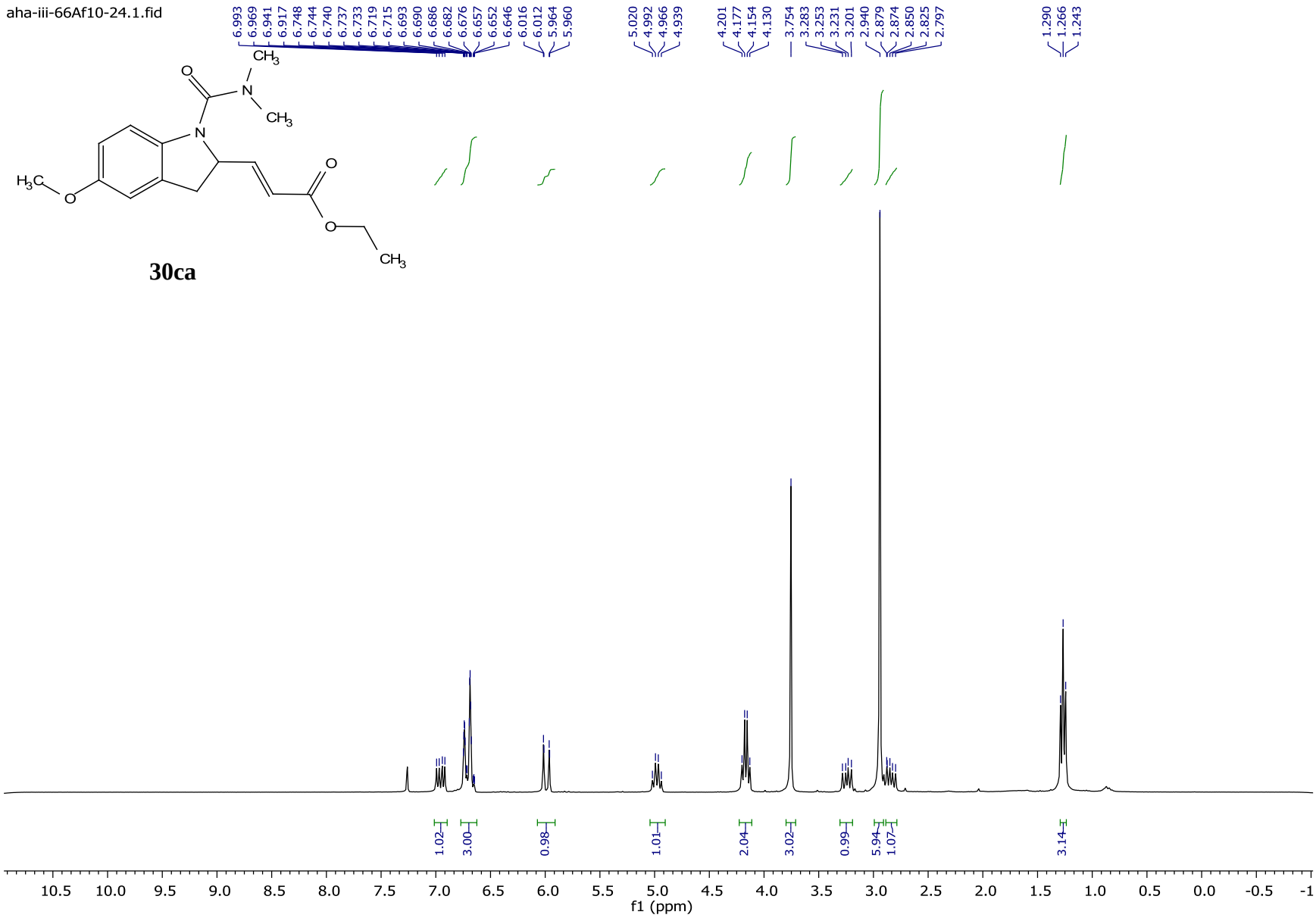
aha-iii-66Af10-24.1.fid
6.993
6.969
6.941
6.917
6.748
6.744
6.740
6.737
6.733
6.719
6.715
6.693
6.690
6.686
6.682
6.676
6.657
6.652
6.646
6.016
6.012
5.964
5.960
5.020
4.992
4.966
4.939
4.201
4.177
4.154
4.130
3.754
3.283
3.253
3.231
3.201
2.940
2.879
2.874
2.850
2.825
2.797
1.290
1.266
1.243
CH3
N
CH3
O
N
O
H3C
O
O
CH3
30ca
1.02
3.00
0.98
1.01
2.04
3.02
0.99
5.94
1.07
3.14
10.5
10.0
9.5
9.0
8.5
8.0
7.5
7.0
6.5
6.0
5.5
5.0
4.5
4.0
3.5
3.0
2.5
2.0
1.5
1.0
0.5
0.0
-0.5
-1
f1 (ppm)

aha-iii-66C_13C.1.fid

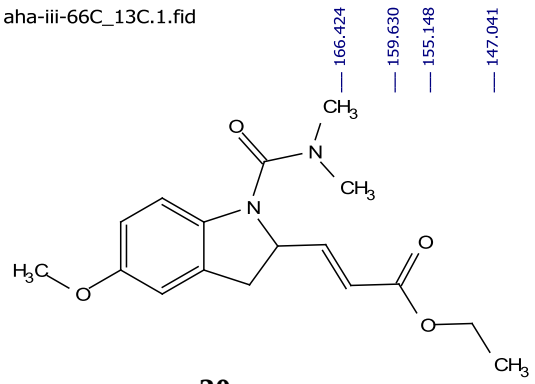

30ca

aha-iii-73Bf15-26.1.fid

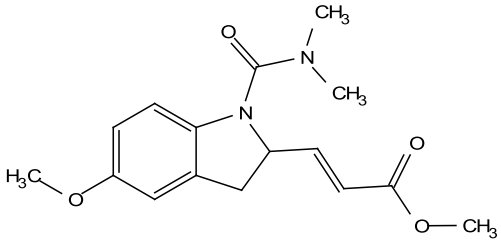

30cb

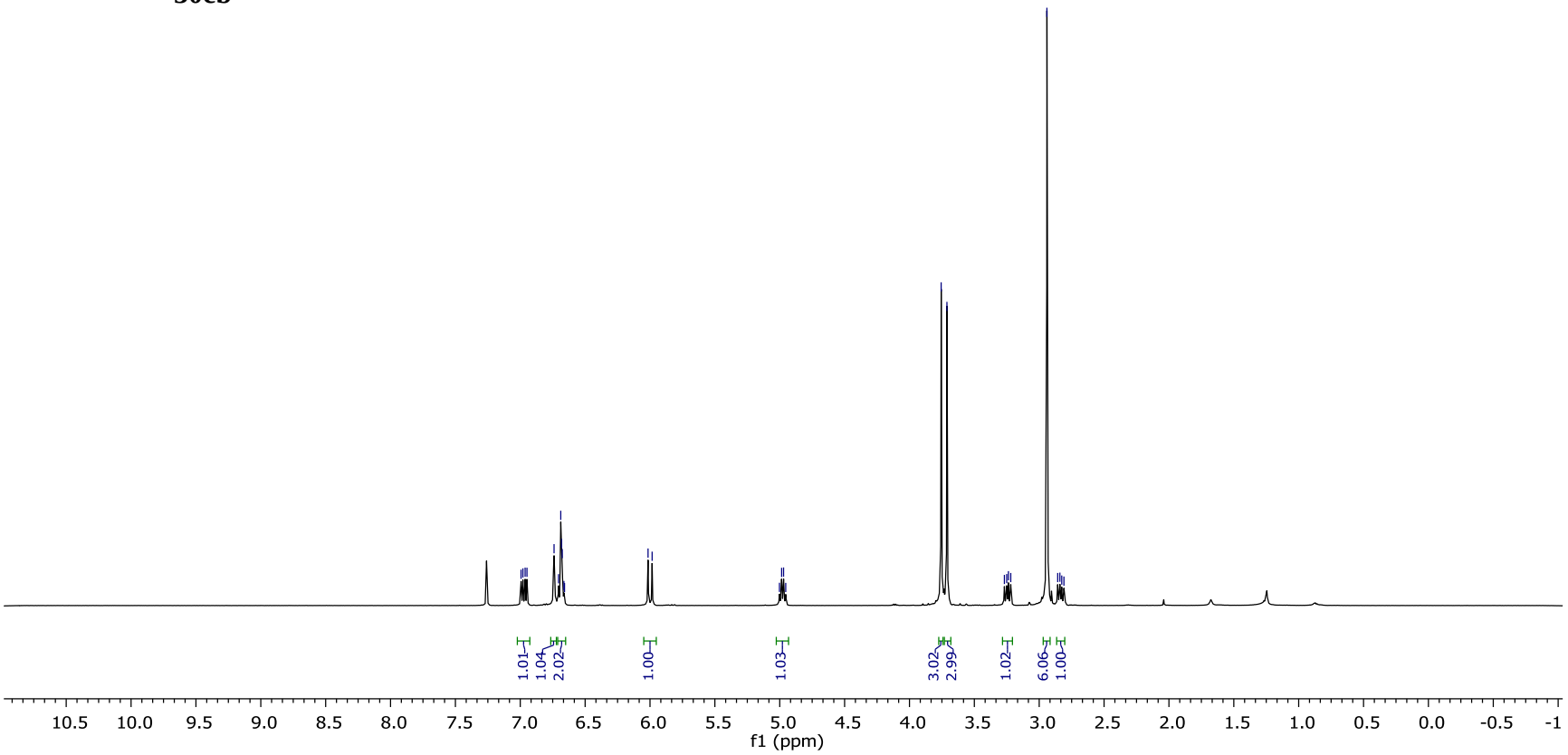

aha-iii-73B_13C.1.fid

166.831
159.604
155.168
147.413
138.049
130.586
121.946
112.756
112.208
111.644
62.640
55.890
51.730
38.088
35.276

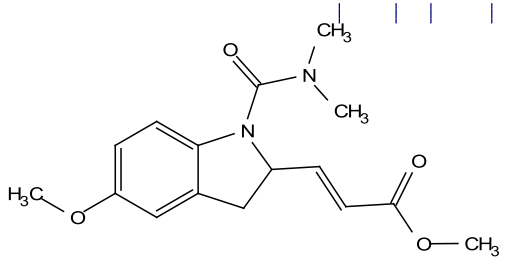

30cb

aha-iii-91Df8-14.1.fid

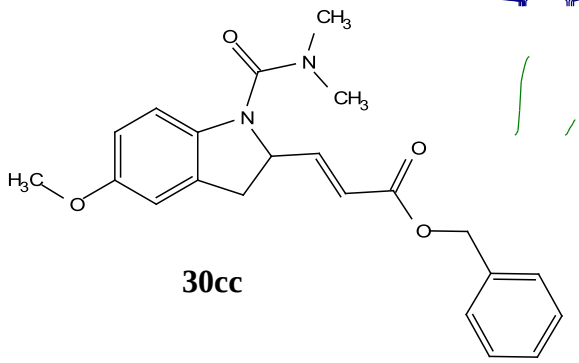

30cc

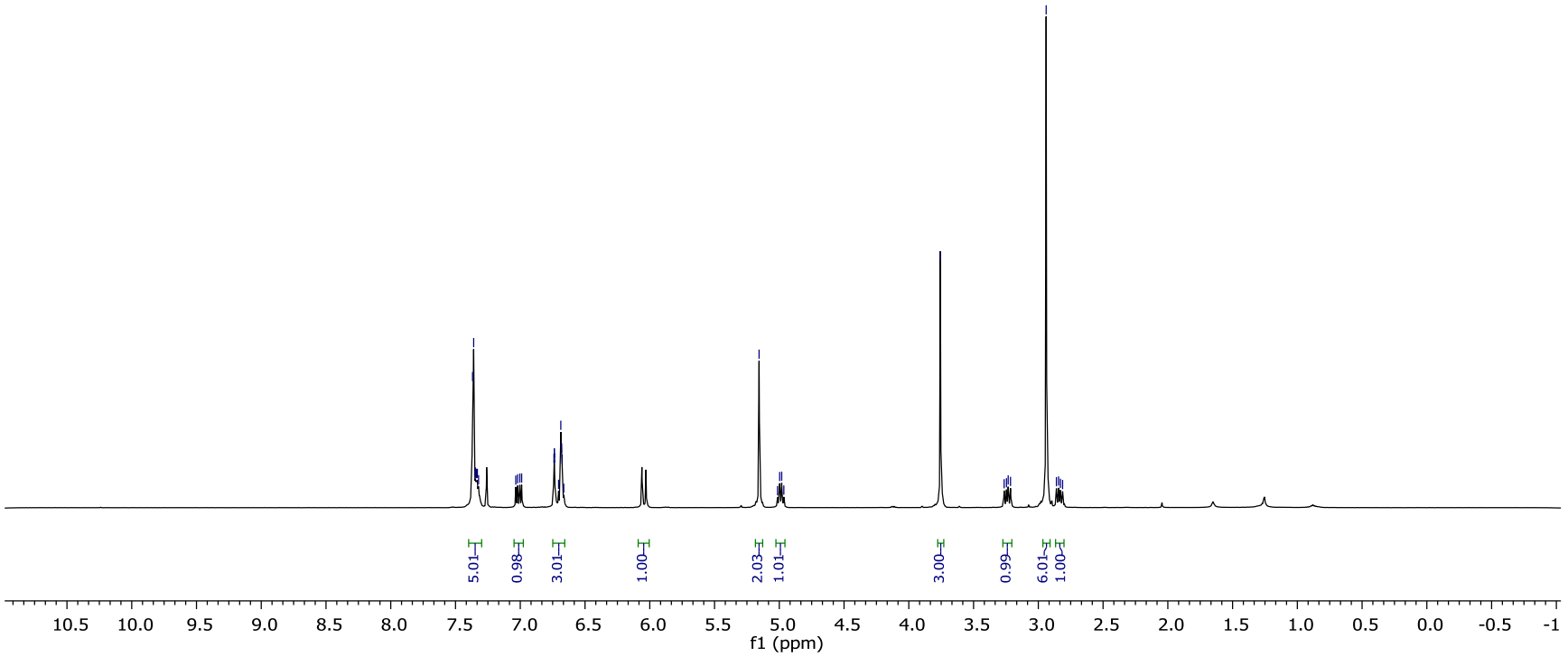

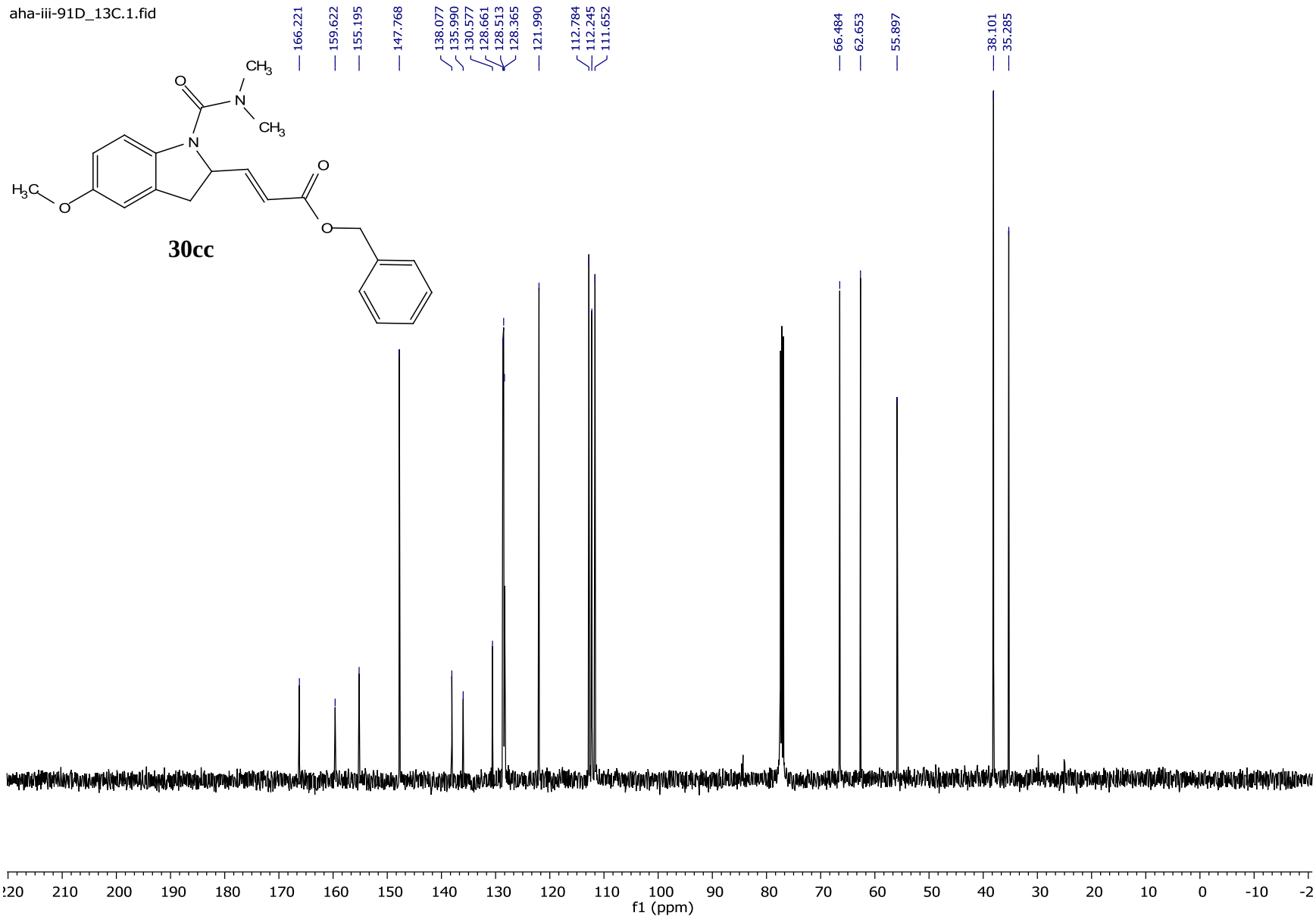
aha-iii-91D_13C.1.fid
166.221
159.622
155.195
147.768
138.077
135.990
130.577
128.661
128.513
128.365
121.990
112.784
112.245
111.652
66.484
62.653
55.897
38.101
35.285
30cc
f1 (ppm)

aha-iii-136Cf17-42.1.fid

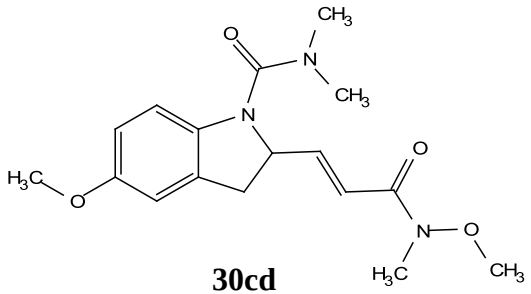

30cd

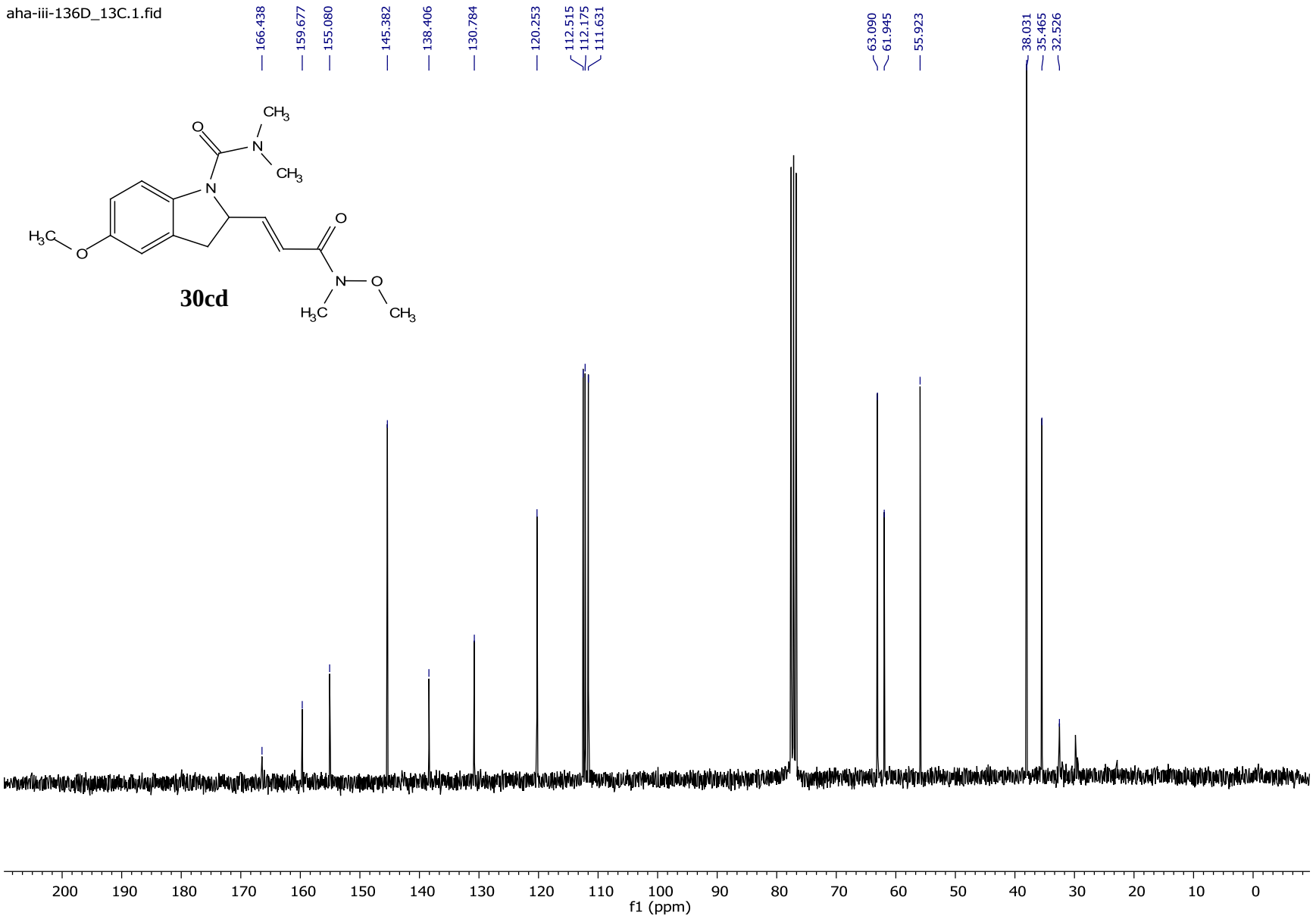
aha-iii-136D_13C.1.fid
166.438
159.677
155.080
145.382
138.406
130.784
120.253
112.515
112.175
111.631
63.090
61.945
55.923
38.031
35.465
32.526
30cd
f1 (ppm)

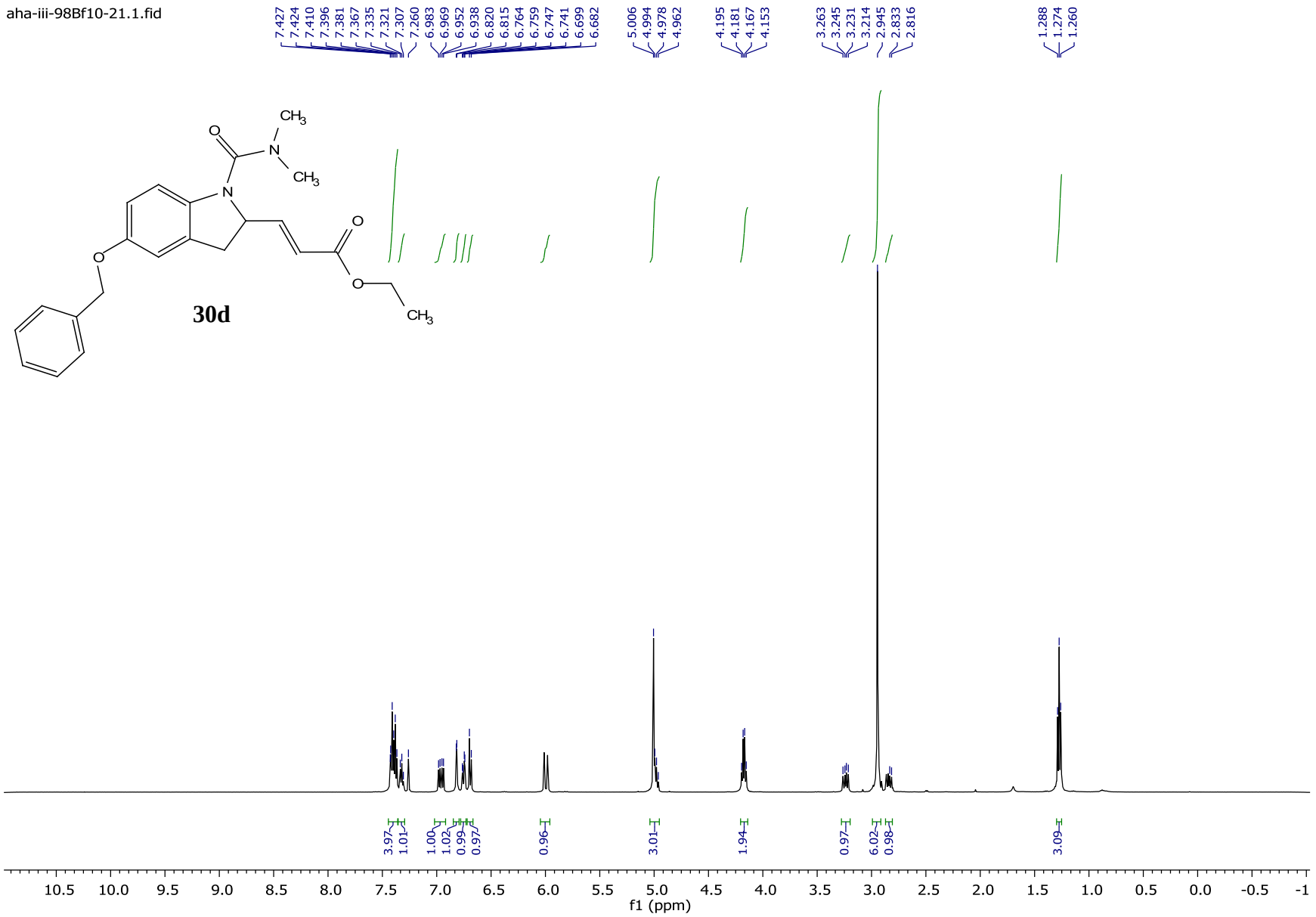
aha-iii-98Bf10-21.1.fid
7.427
7.424
7.410
7.396
7.381
7.367
7.335
7.321
7.307
7.260
6.983
6.969
6.952
6.938
6.820
6.815
6.764
6.759
6.747
6.741
6.699
6.682
5.006
4.994
4.978
4.962
4.195
4.181
4.167
4.153
3.263
3.245
3.231
3.214
2.945
2.833
2.816
1.288
1.274
1.260
30d
3.97
1.01
1.00
1.02
0.99
0.97
0.96
3.01
1.94
0.97
6.02
0.98
3.09
f1 (ppm)

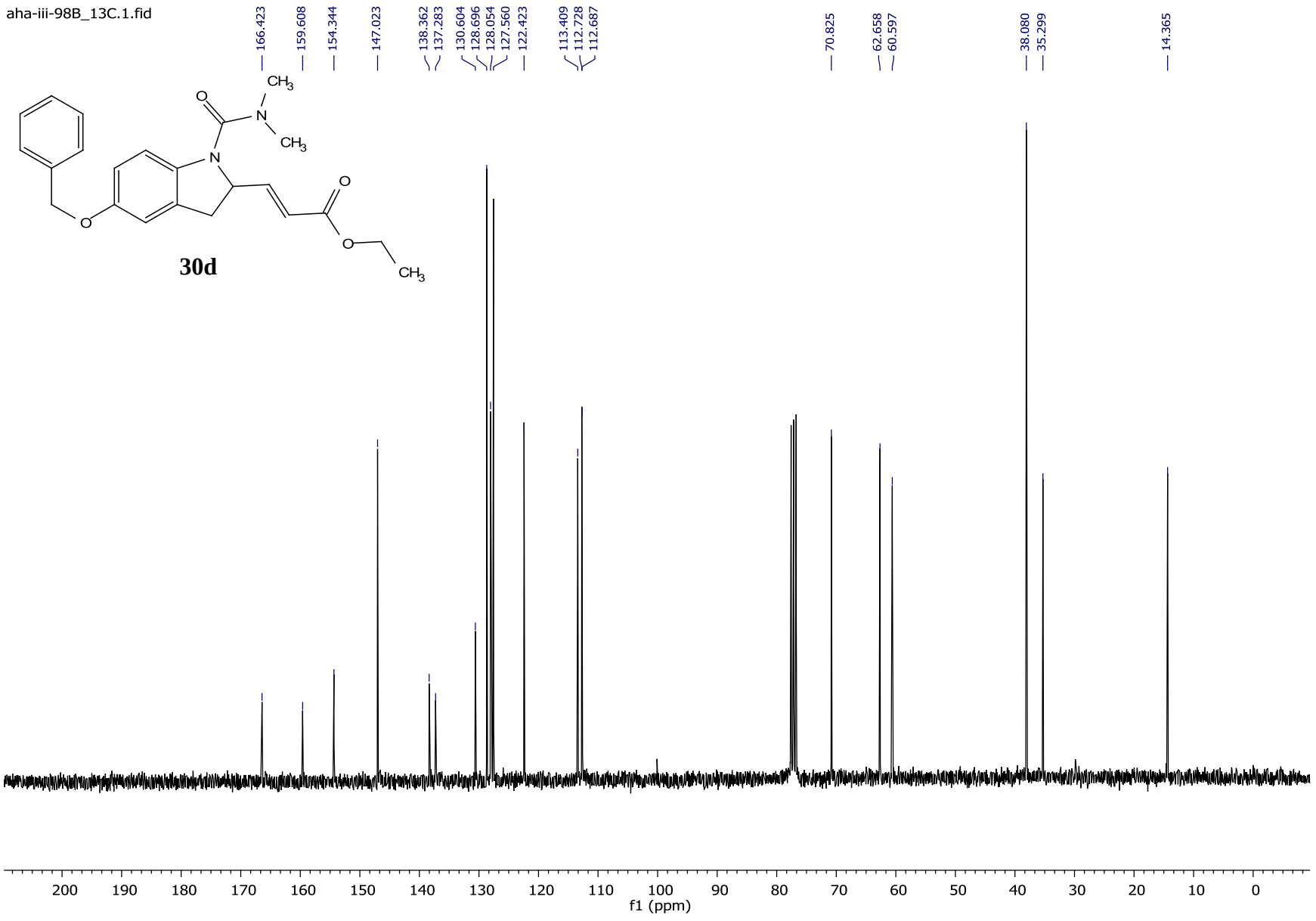
aha-iii-98B_13C.1.fid
166.423
159.608
154.344
147.023
138.362
137.283
130.604
128.696
128.054
127.560
122.423
113.409
112.728
112.687
70.825
62.658
60.597
38.080
35.299
14.365
30d
f1 (ppm)

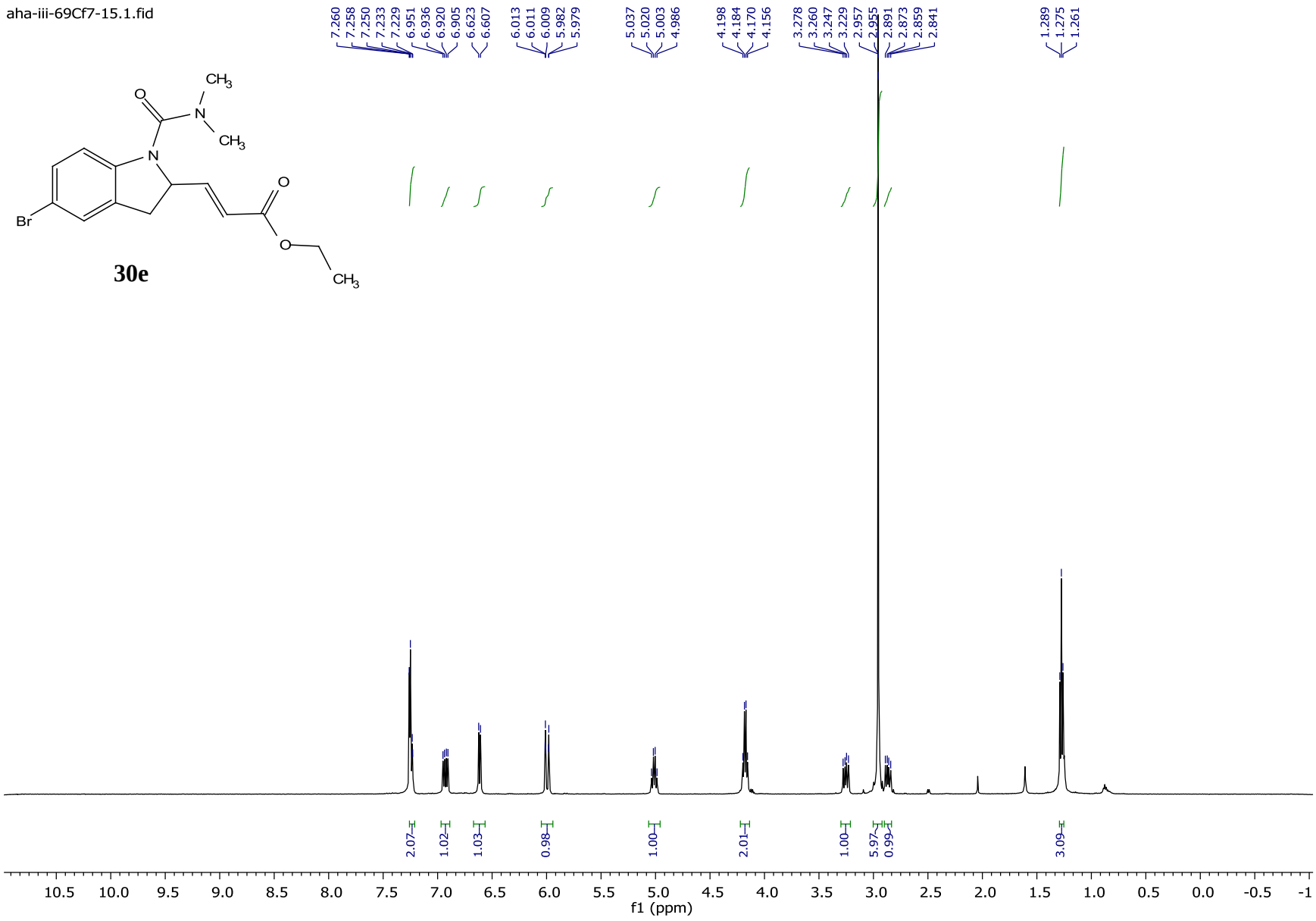
aha-iii-69Cf7-15.1.fid
7.260
7.258
7.250
7.233
7.229
6.951
6.936
6.920
6.905
6.623
6.607
6.013
6.011
6.009
5.982
5.979
5.037
5.020
5.003
4.986
4.198
4.184
4.170
4.156
3.278
3.260
3.247
3.229
2.957
2.955
2.891
2.873
2.859
2.841
1.289
1.275
1.261
O
N
CH3
CH3
N
Br
O
O
CH3
30e
2.07
1.02
1.03
0.98
1.00
2.01
1.00
5.97
0.99
3.09
10.5
10.0
9.5
9.0
8.5
8.0
7.5
7.0
6.5
6.0
5.5
5.0
4.5
4.0
3.5
3.0
2.5
2.0
1.5
1.0
0.5
0.0
-0.5
-1
f1 (ppm)

aha-iii-130C_13C.1.fid

166.268
158.880
146.194
143.737
131.458
130.385
128.142
122.994
113.812
113.403
62.740
60.722
37.966
34.796
14.355

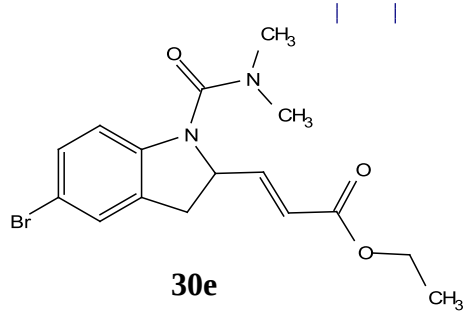

30e

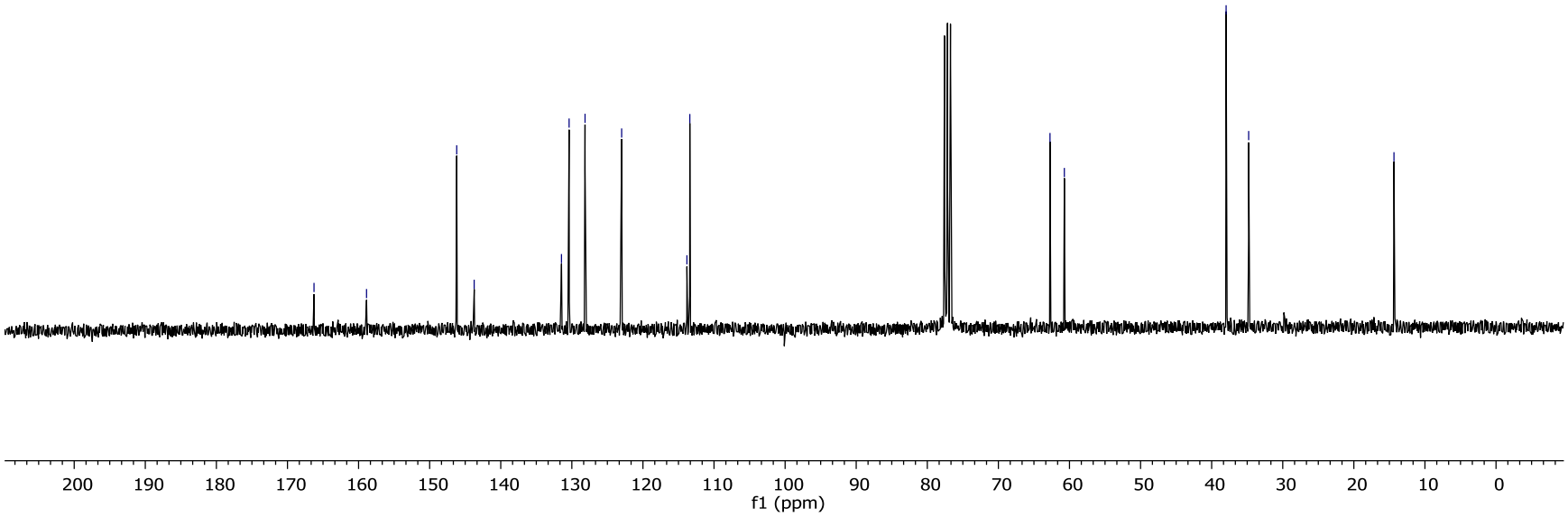

aha-iii-113Bf6-11.1.fid

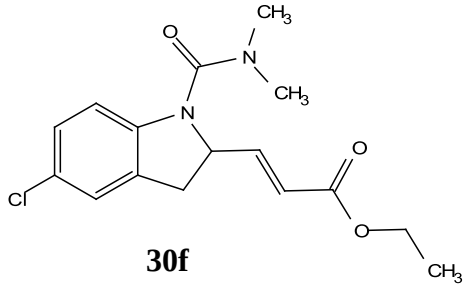

30f

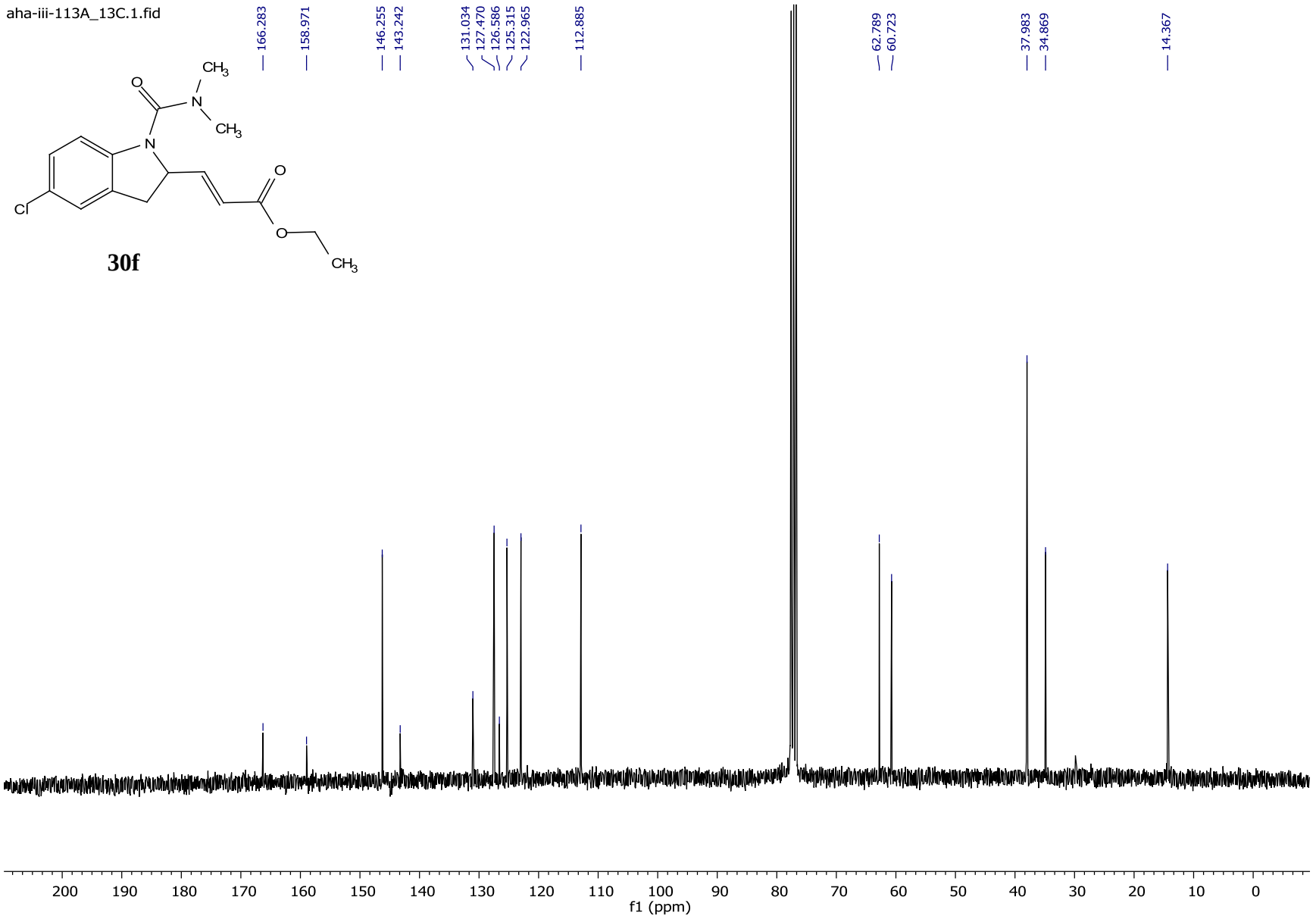
aha-iii-113A_13C.1.fid
166.283
158.971
146.255
143.242
131.034
127.470
126.586
125.315
122.965
112.885
62.789
60.723
37.983
34.869
14.367
30f
f1 (ppm)

aha-iii-119Af13-19.1.fid

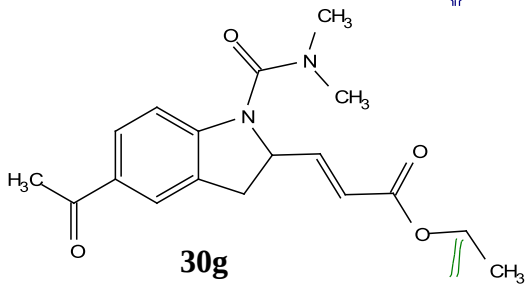

30g

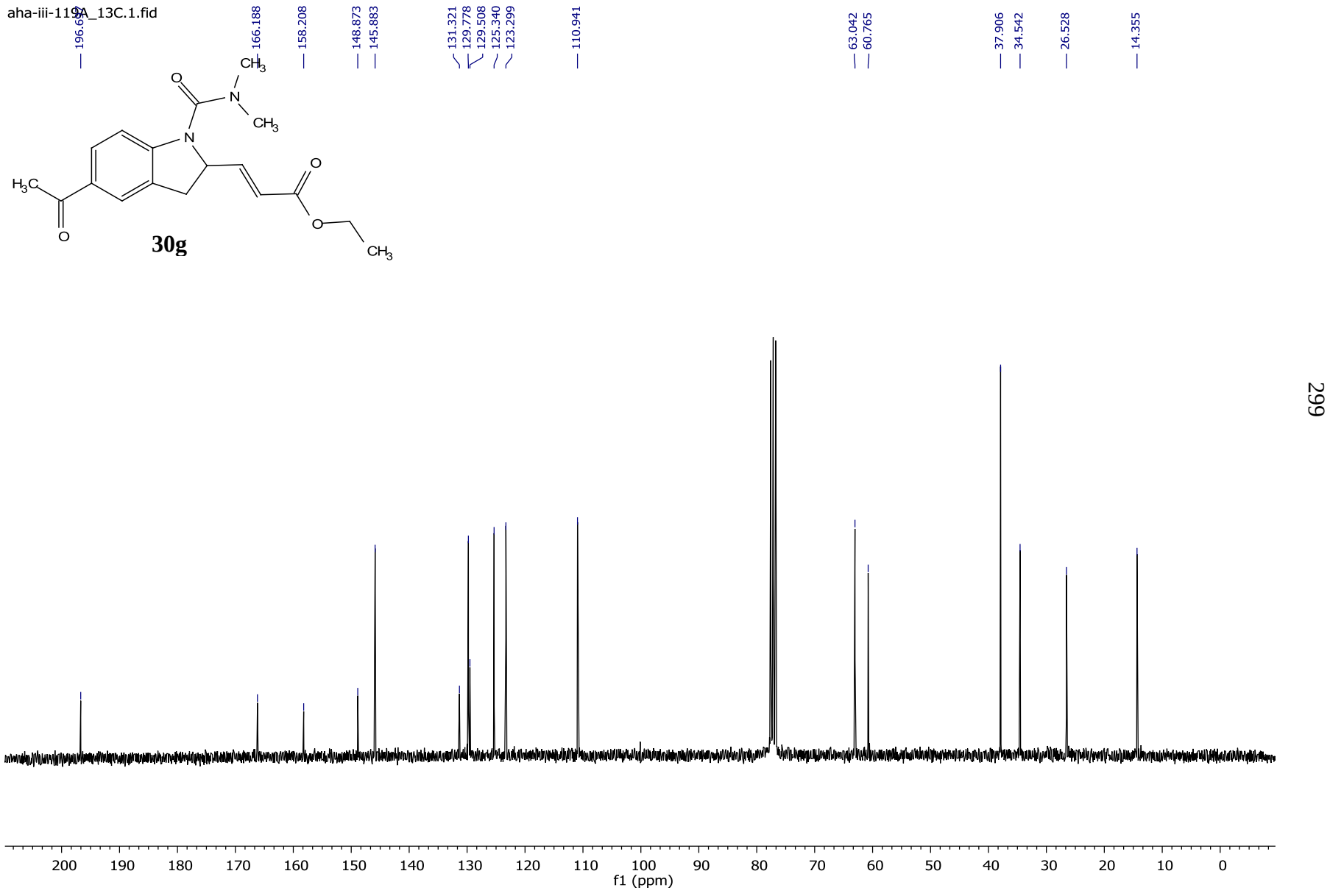
aha-iii-119A_13C.1.fid
196.694
166.188
158.208
148.873
145.883
131.321
129.778
129.508
125.340
123.299
110.941
63.042
60.765
37.906
34.542
26.528
14.355
30g
f1 (ppm)

aha-iii-128Df19-25a.1.fid

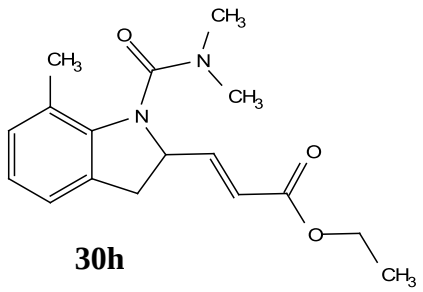

30h

aha-iii-128D_13C.1.fid

166.349
161.055
147.322
143.659
131.302
129.509
128.171
124.428
122.296
121.236
64.189
60.741
38.249
36.961
18.511
14.334

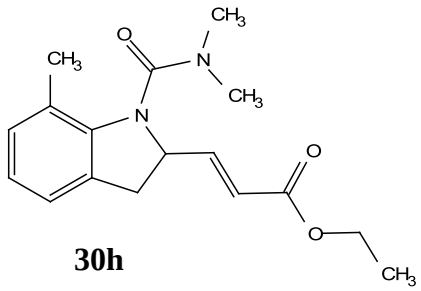

30h

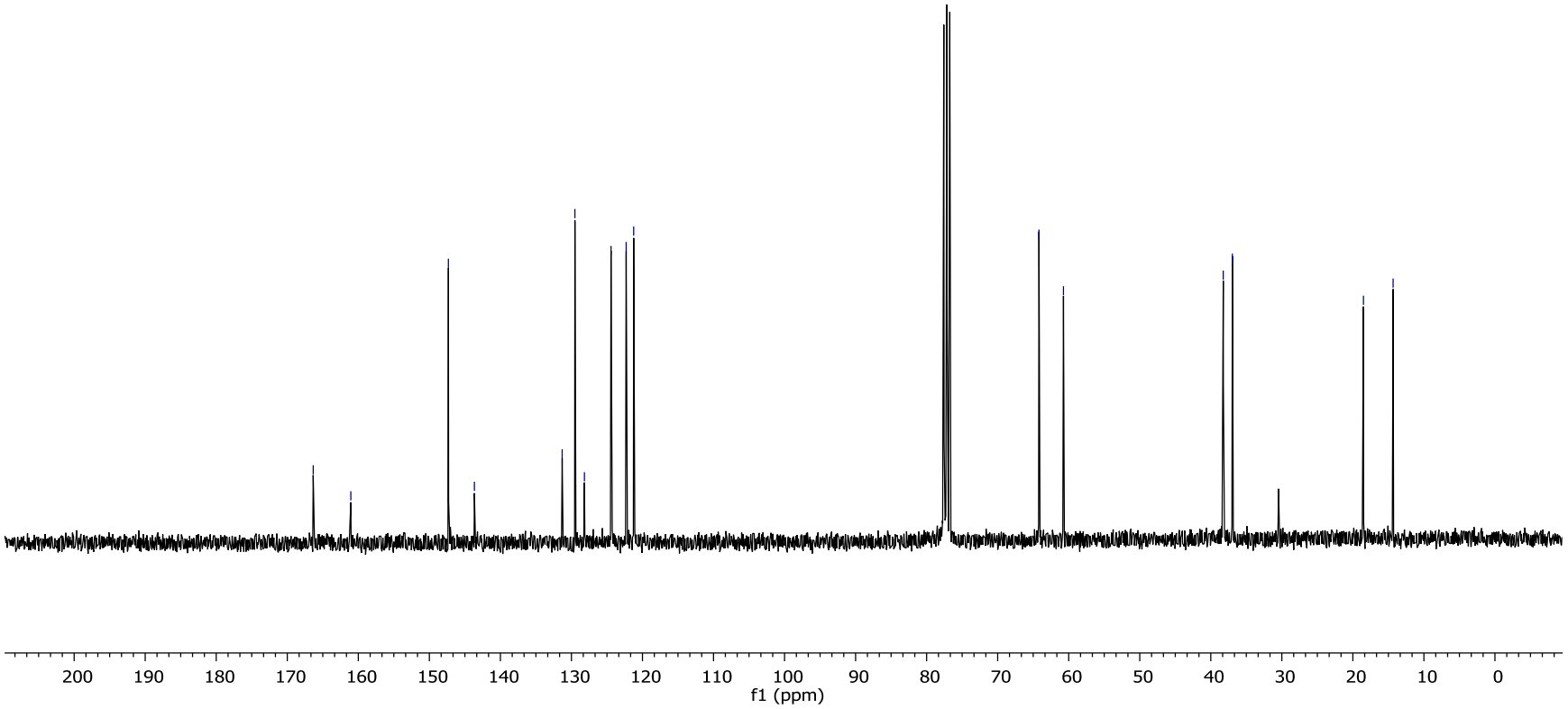

aha-iii-95Af9-21.1.fid

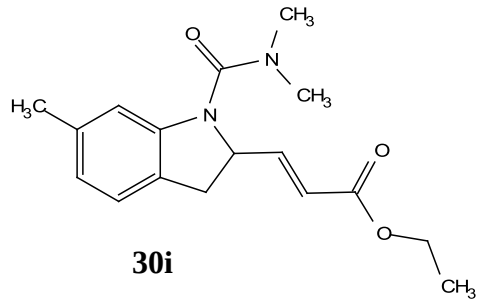

30i

aha-iii-128A_13C.1.fid

166.444
159.295
147.098
144.621
137.461
126.205
124.682
122.440
122.292
116.143
112.909
62.849
60.588
37.997
34.771
21.885
14.342

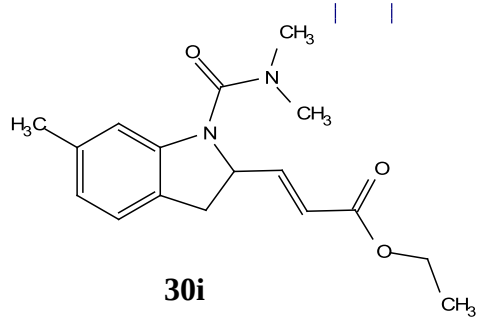

30i

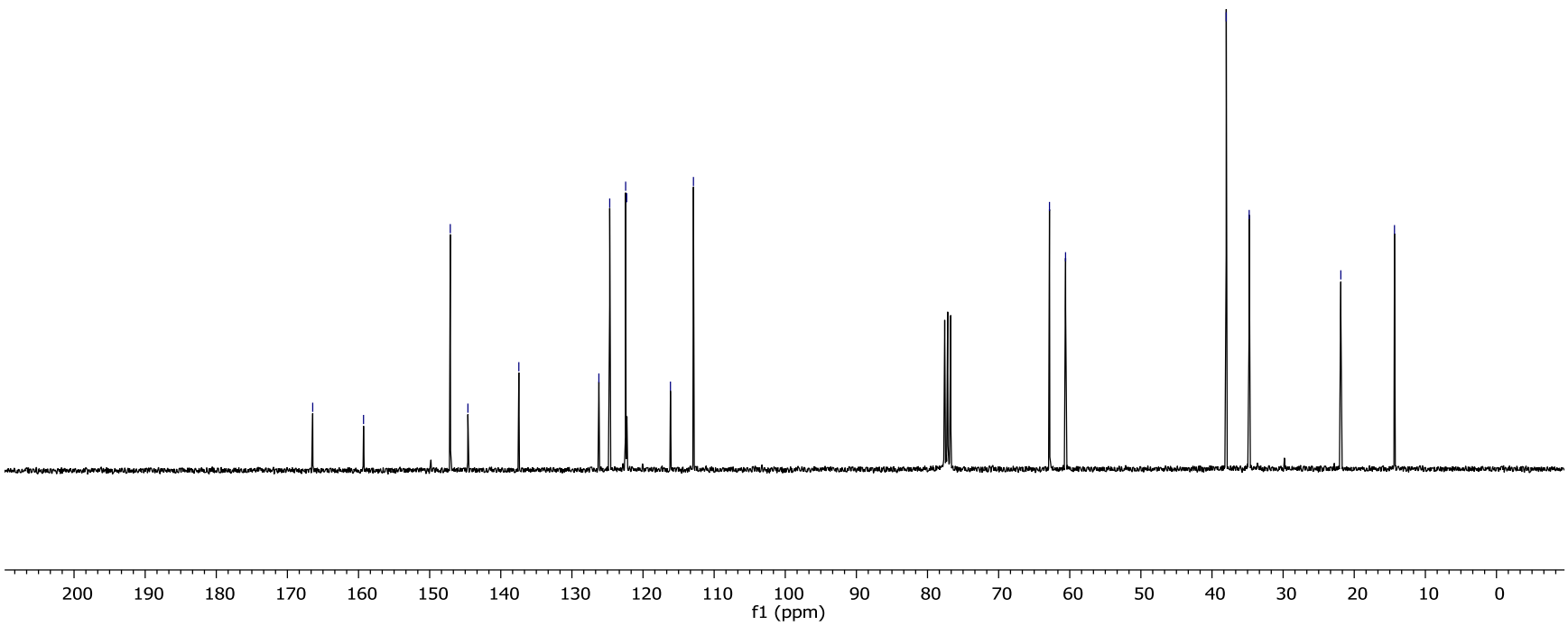

aha-iii-86Af14-26b.1.fid

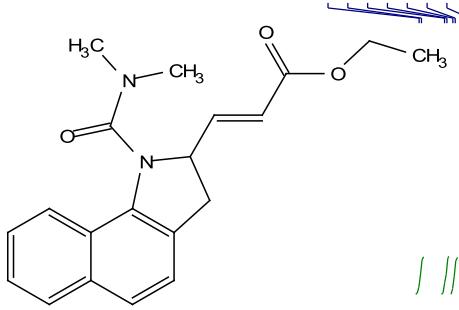

30j

aha-iii-86A_13Cx.1.fid

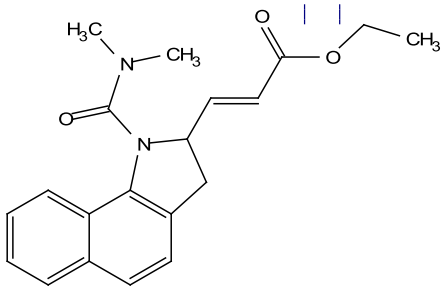

166.342 161.822 147.157 140.582 133.792 128.563 127.572 126.115 125.445 125.351 125.251 123.445 122.753 121.251 64.971 60.705 38.311 37.435 14.274

30j